

**ACTIVATION AND CAPTURE OF CARBON DIOXIDE AND
CARBON DISULFIDE BY N-CONTAINING COMPOUNDS**

by

Mary Trisha Cabacungan Ang

A thesis submitted to the Department of Chemistry
In conformity with the requirements for
the degree of Doctorate of Philosophy

Queen's University
Kingston, Ontario, Canada
(November, 2013)

Copyright © Mary Trisha Cabacungan Ang, 2013

Abstract

The interaction between carbon dioxide (CO₂) and N-compounds such as 1,8-diazobicyclo[5.4.0]undec-7-ene (DBU) has been extensively studied in the Jessop Lab. Carbon disulfide (CS₂) is the sulfur congener of CO₂, although it exhibits different reactivity with N-containing compounds. This thesis presents the search for zwitterionic CO₂-switchable polarity solvents, new and general reactivity of CS₂ with amidines and guanidines, and attempts at using CO₂ as a carbonyl source in the synthesis of nitrogen containing compounds.

In the second chapter, the reactions of CO₂ with various diamines are described. Spectroscopic methods and X-ray crystallography determined the structure of a solid zwitterionic carbamate salt of CO₂ and *N,N'*-dimethyl-1,3-propanediamine. The polarity of the liquid zwitterionic carbamate salt formed with *N,N,N'*-trimethyl-1,3-propanediamine was measured using UV-Vis and the solvatochromic dye Nile red; its polarity was comparable to previous switchable polarity systems. The CO₂ gravimetric uptake of the liquid zwitterionic carbamate salt was 28%, far greater than other solvents for the capture and release of CO₂.

In the third chapter, it was found that a variety of products can be accessed depending on the structure of the N-base (cyclic or acyclic) upon reaction of the base with CS₂ at room temperature. The reaction of CS₂ with cyclic amidines produced a cyclic trithioanhydride structure, forming a new C-C bond at a sp²-carbon *beta* to the imino nitrogen centre. When an amidine was acyclic it led to cleavage and formation of isothiocyanates in near quantitative yields. When a N-base had a N-H bond, CS₂ can insert, forming a dimer in the presence of dichloromethane.

In the fourth chapter, preliminary investigations are ascribed for synthesis of α -amino acids, amides, and ureas. Carboxylation of ketimines was detected, although the formed carboxylates from a variety of ketimines readily decomposed. Isomerization products of two ketimines were generated with DBU and CO₂. Lewis acid catalysts were implemented towards

the amidation of benzoylacetic acid and synthesis of ureas. Amidation of benzoylacetic acid did not occur in the presence of Lewis acid catalysts and CO₂. Formation of a cyclic tetraalkylurea was afforded in low yields by the use of a diamine, CO₂ and Lewis acid catalysts.

Acknowledgements

Even to the smallest degree, all the people in the Department of Chemistry at Queen's I have crossed paths with have influenced me in some particular way on this journey. First, thank you Philip for the opportunity to work in your lab throughout these years along with your unwavering patience, encouragement, and guidance. You have tempered me to be an innovative researcher and I can only hope to be akin to you in research. I also would not have an appreciation for wildlife and cricket if it were not for you!

I would like to thank my peers at the beginning of my journey at Queen's. Thank you Sean, Elize, and Ying, from the very beginning, and even now, you selflessly encouraged, supported, and helped me. Ying, no matter the time frame in between our conversations, we always manage to pick up where we left off, you are such a dear friend of mine. Then there is Darrell, Alaina, Amy and Vanessa, you guys continue to guide and keep me on track, whether on track for research or enjoying the niceties of life.

Without the help of staff, I would not have been able to find precedence in my chemistry. Ruiyao aside from being an excellent X-ray crystallographer, you have always been there for support and useful conversations. Lyndsay, Igor, Robin and Tom...I love you guys. Dr. Sauriol, thank you for helping me with the NMR facilities and for your useful insight. Annette, I'm sure a lot of people thank you, but you are the one that keeps all us grad students in order! Thank you to my readers, Dr. David Zechel and Dr. Donal Macartney and my examining committee members, Dr. Suning Wang, Dr. Brian Amsden, and Dr. Paul Ragogna.

I would like to thank the people in the middle of my journey. Tobias, Tamara, and Michael, you are the trio of people that kept me going and always managed to provide sustenance. Tamara, you always manage to make me laugh, even in difficult times, you are a kindred spirit who has unlimited generosity. Brian, Keith, Joanne, and Edmond, I am still very much your young padawan, you knew me from when I was a wee undergrad, and I am very

fortunate to have your advice throughout this journey. Brian, my brother, honest, protective, and incredibly patient with me! Joanne, my sister, you continue to be an influential person in my life who inspires me to explore new things. Dave Farrar and Scott Browning, thank you for taking a chance on a budding chemist back at U of T. It was a fun and valuable learning experience to be under your supervision.

I would like to thank the people that helped mold me as a person in life and in chemistry. Stephen, this journey would not have been a good one without you in it. You are an insightful and thoughtful person who motivated and supported me by your hard-working yet quiet nature. LoriAnne, I love you! I have known you for twenty-two years and I do not think I would have made it through without you by my side, encouraging me along the way, keeping me grounded and helping me focus on the goals that I aspire to. Ryan, you breathed new life into me. There have been some difficult times leading up to the close of this journey and it was you that has been there for me, helping me through it. You are patient, kind, compassionate, and generous with your time and efforts. I would not have had such meaningful times outside of Chernoff Hall if it was not for your benevolent nature. I appreciate everything you have done for me and I cherish the time that we share.

Lastly, I would like to thank my family for their unending support and love. First I would like to thank my cousins that are closest to me, my buddies, Ning and Mei, who are positive influences in my life. My grandparents that are with me in spirit, Trinidad and Bienvenido Cabacungan and Thai Khun and Chai Luan Lim Ang, it was their teachings and wisdom that led me to where I am today. I hope that I make them proud.

Thank you Hazel, Patrick and Marc, my siblings, you keep me together. Hazel my bold, courageous, and artistic sister, I am ever grateful to have you in my corner and for feeding my soul starting from an early age with art and music. Patrick, a teacher of science, and by the way a great guitar player, I aspire to be as knowledgeable as you are and as a result I learn from you

every day. Marc, you embody the teachings of the poem *Invictus*, I find shelter in your strength. I would like to thank my mom who keeps us siblings together. Mom, it was you that made every effort to ensure that your children were able to have a stable, happy and wholesome life. I am grateful for all that you have given me and I am proud to have you as my mother.

Statement of Originality

(Required only for Division IV Ph.D.)

I hereby certify that all of the work described within this thesis is the original work of the author.

Any published (or unpublished) ideas and/or techniques from the work of others are fully acknowledged in accordance with the standard referencing practices.

(Mary Trisha Cabacungan Ang)

(November, 2013)

Table of Contents

Abstract.....	ii
Acknowledgements.....	iv
Statement of Originality.....	vii
List of Figures.....	xii
List of Schemes.....	xvi
List of Tables.....	xxi
List of Abbreviations.....	xxii
Chapter 1 Introduction.....	1
1.1 Carbon Dioxide Sources.....	1
1.1.1 Strategies to Cope with the Carbon Dioxide Output.....	1
1.1.2 CO ₂ Capture and Storage.....	2
1.2 CO ₂ Utilization.....	5
1.2.1 The Physical Properties of CO ₂ for use in Industry.....	5
1.2.2 Industrial use of CO ₂ as a C1 Source.....	6
1.3 The Use of CO ₂ Under Ambient to Near Ambient Conditions.....	8
1.3.1 Activation of CO ₂ Without Using Metals.....	8
1.3.2 CO ₂ as a Trigger to Elicit a Physico-Chemical Change.....	14
1.4 Amidines and Guanidines for CO ₂ Activation and Utilization.....	19
1.4.1 The Importance of Design and Development for CO ₂ Adsorption.....	19
1.4.2 The Elusive CO ₂ Adduct with 1,8-Diazobicyclo[5.4.0]undec-7-ene (DBU).....	20
1.4.3 First Isolated CO ₂ Adduct with a Guanidine.....	24
1.5 Scope of Thesis.....	29
1.6 References.....	31
Chapter 2 The Search for Zwitterionic Switchable-Polarity Solvents.....	36
2.1 Introduction.....	36
2.1.1 Two-Component Switchable Polarity Solvents with Base/Alcohol Mixtures.....	36
2.1.2 Secondary Amines as One-Component SPS.....	39
2.1.3 SPS for Reaction Media, Extraction and CO ₂ Capture Agents.....	40
2.1.4 Drawbacks of Base/Alcohol and Secondary Amine SPS.....	41
2.2 Zwitterionic SPS for CO ₂ Capture.....	43
2.2.1 Zwitterionic SPS.....	43
2.2.2 Alkanolamidines and Alkanolguanidines for CO ₂ Capture.....	45

2.2.3 Alkanolamines for use as Zwitterionic Switchable Solvents	48
2.2.4 Secondary Diamines for SPS and CO ₂ Capture	51
2.3 Results and Discussion	51
2.3.1 Investigation of Secondary Diamines as Switchable Polarity Solvents	51
2.3.2 A Diamine Containing one Secondary and one Tertiary Amine	55
2.4 Conclusion and Future Considerations	57
2.5 Experimental Methods	59
2.5.1 General Considerations	59
2.5.2 IR Spectroscopic Data for the Bases Before and After CO ₂ Treatment.....	60
2.5.3 Gravimetric Uptake of CO ₂ by <i>N,N,N'</i> -Trimethyl-1,3-propanediamine (2-18b).....	60
2.5.4 Polarity Measurement of <i>N,N,N'</i> -Trimethyl-1,3-propanediamine (2-18b).....	61
2.5.5 Spectroscopic Data for Diamines Without (Species a) and With (Species b) CO ₂	61
2.6 References.....	64
Chapter 3 Unexpected Reactivity of CS ₂ with N-Containing Compounds.....	67
3.1 Introduction.....	67
3.2 Results and Discussion	77
3.2.1 Reaction of CS ₂ and Cyclic Amidines	77
3.2.2 Further Reactivity of Cyclic Amidine 3-3 with CS ₂	82
3.2.3 Reaction of CS ₂ with Cyclic Amidines Possessing an N-H Bond	86
3.2.4 Methylation and Ring Opening of Cyclic Trithioanhydride 3-1a.....	89
3.2.5 Reaction of CS ₂ and Acyclic Amidines and an Acyclic Guanidine.....	94
3.2.6 Reaction of CS ₂ with Acyclic Guanidine that Features an Imino N-H Bond	97
3.2.7 Reaction of CS ₂ with Related N-Containing Compounds	100
3.3 Conclusions and Future Considerations.....	105
3.4 Experimental Methods	107
3.4.1 General Considerations	107
3.4.2 General Procedure for the Synthesis of Cyclic Trithioanhydrides.....	107
3.4.3 General Procedure for Growing the Crystals of the Cyclic Trithioanhydrides.....	108
3.4.4 Spectroscopic Data for Cyclic Trithioanhydrides 3-1a, 3-2a, 3-3a, and H ₂ S salt of 3-3	108
3.4.5 Procedure for the Synthesis of 3-1b and 3-1c	109
3.4.6 Synthesis of Compounds 3-4a and Proposed 3-4x.....	111
3.4.7 General Procedure for the Synthesis of 3-8	112
3.4.8 Synthesis of 3-9a and 3-10.....	112

3.4.9 Synthesis of 3-13b and Spectroscopic Data of Proposed 3-14a.....	113
3.5 References.....	114
Chapter 4 CO ₂ as a Carbonyl Source for N-Containing Compounds	117
4.1 General Introduction	117
4.1.1 CO ₂ Fixation for the Synthesis of β -Hydroxycarboxylic Acids.....	117
4.2 Towards the Synthesis of α -Amino Acids	121
4.2.1 Introduction to <i>N</i> -Alkylidenes and Their use in a Mannich-type Reaction	121
4.2.2 Correlating the Methods from the Jessop Lab and Kobayashi Lab	123
4.2.3 Results and Discussion: Preliminary Studies with Ketimine 4-10.....	127
4.2.4 Other Ketimine Candidates Towards the Synthesis of α -Amino Acids.....	132
4.3 Preliminary Study of the Amidation of Benzoylactic Acid	135
4.3.1 Synthesis of Amides and the use of Lewis Acid Catalysts for Amidation	135
4.3.2 Results and Discussion: Attempted Amidation of Benzoylactic Acid.....	138
4.4 Lewis Acid Catalysts for the Formation of Ureas.....	142
4.4.1 Synthesis of Ureas and the Search to Overcome the High Energy Barrier.....	142
4.4.2 Results and Discussion: Investigation of Amidation Catalysts for Urea Synthesis	145
4.4.3 Investigation of Amidation Catalysts for the Synthesis of Tetraalkylureas using a Diamine.....	148
4.5 Conclusions and Future Considerations.....	151
4.5.1 Investigation of Ketimines towards the Synthesis of α -Amino Acids	151
4.5.2 Investigation of Lewis Acid Catalysts for Amidation of Benzoylactic Acid.....	153
4.5.3 Investigation of Lewis Acid Catalysts for Synthesis of Ureas.....	154
4.6 Experimental Methods	155
4.6.1 General Considerations	155
4.6.2 Synthesis of Ketimines	155
4.6.3 General Procedures for the Carboxylation of Ketimines using Various Bases and CO ₂	157
4.6.4 Attempted Amidation of Benzoylactic Acid.....	160
4.6.5 Formation of Dialkylureas Using the Amidation Catalysts MIBA and ZrCl ₄	160
4.6.6 Formation of Cyclic Urea with <i>N,N'</i> -Dimethyl-1,3-propanediamine Using MIBA or ZrCl ₄	161
4.7 References.....	162
Chapter 5 Conclusions and Future Work.....	166
5.1 The Search for Zwitterionic SPS	166

5.2 Unexpected Reactivity of CS ₂ with N-Containing Compounds	167
5.3 CO ₂ as a Carbonyl Source for N-Containing Compounds	169
5.4 Closing Remarks	172
5.5 References	173
Appendix A X-ray Crystallography Data	174
Appendix B NMR Spectra of Compounds	244

List of Figures

Figure 1.1. Industrial organic syntheses using CO ₂ .	8
Figure 1.2. Resonance structures of <i>N, N'</i> -disubstituted-2-methylene imidazoline	10
Figure 1.3. Peralkylated amidines and guanidines, acyclic and cyclic.	20
Figure 1.4. Proposed DBU-CO ₂ zwitterionic adduct.	21
Figure 1.5. DBU bicarbonate salt.	21
Figure 1.6. [DBUH] ⁺ [HCO ₃] ⁻ .	22
Figure 1.7. View of the TBD bicarbonate salt dimer. Displacement ellipsoids are drawn at 50% probability level. Only the position of the disordered C6 is represented.	24
Figure 1.8. Molecular structure of the TBD-CO ₂ zwitterionic adduct. Displacement ellipsoids are drawn at the 50% probability level.	25
Figure 1.9. Top: Molecular structure of [TBNH] ⁺ [HCO ₃] ⁻ . Bottom: molecular structure of [TBDH] ⁺ [HCO ₃] ⁻ . Displacement ellipsoids are drawn at the 50% probability level.	28
Figure 2.1. Molecular structure of [DBUH][O ₂ COMe]. Displacement ellipsoids for non-hydrogen atoms are shown at the 50% probability level and H atoms are represented by circles of arbitrary size.	37
Figure 2.2. Starting from left: COSBOL, CS ₂ BOL, and SO ₂ BOL salts.	38
Figure 2.3. Molecular structure of [DBUH ⁺][S ₂ COCH ₂ Ph]. Displacement ellipsoids for non-hydrogen atoms are shown at the 50% probability level and H atoms are represented by circles of arbitrary size.	38
Figure 2.4. A comparison of the polarity ranges of several SPS (white circles indicate the low-polarity form, black circles indicate the high polarity form). The scale is the λ _{max} for Nile red solvatochromic dye dissolved in the solvent. Select traditional solvents are indicated above the scale for comparison ([bmim]PF ₆ = 1-butyl-3-methylimidazolium hexafluorophosphate).	40
Figure 2.5. Single-component CO ₂ BOLs with amidines and guanidines as the core (2-4 – 2-8) and an IL mixture (2-9) for CO ₂ capture.	46

Figure 2.6. Alkanolamines for CO ₂ capture: (A) industrial chemical absorbents, (B) pressure-swing physical sorbents, (C) sterically hindered chemical absorbents.	50
Figure 2.7. Diamine candidates for zwitterionic switchable polarity solvents.	52
Figure 2.8. Molecular structure and extended network of 2-11b and CO ₂ . Displacement ellipsoids for non-H atoms are shown at 50% probability level.	58
Figure 2.9. A comparison of the polarity ranges of several SPS (white circles indicate the low-polarity form, black circles indicate the high polarity form). The scale is the λ_{\max} for Nile red solvatochromic dye dissolved in the solvent. Select traditional solvents are indicated above the scale for comparison ([bmim]PF ₆ = 1-butyl-3-methylimidazolium hexafluorophosphate). Polarity change of 2-18 illustrated.	57
Figure 3.1. Starting from left: COSBOL salt, CS ₂ BOL salt, and SO ₂ BOL salt.	68
Figure 3.2. One of the two independent 3-1a molecular structures isolated in the Jessop Lab with ellipsoids drawn at 50 % probability level.	72
Figure 3.3. Molecular structure of acetamidine thiocarbamate and protonated acetamidine.	75
Figure 3.4. Cyclic amidines.	77
Figure 3.5. Molecular structure of 3-2a . Displacement ellipsoids for non-H atoms are shown at the 50% probability level and H atoms are represented by circles of arbitrary size.	78
Figure 3.6. Molecular structure of 3-3a : major conformer A (~53%) and minor conformer B (~47%). Displacement ellipsoids for non-H atoms are shown at the 50% probability level and H atoms are represented by circles of arbitrary size.	80
Figure 3.7. Molecular structure of hydrogen sulfide salt of 3-3 , isolated as a by-product from the synthesis of 3-3a . Displacement ellipsoids for non-H atoms are shown at the 50% probability level and H atoms are represented by circles of arbitrary size.	81
Figure 3.8. Molecular structure of 3-3b . Displacement ellipsoids for non-H atoms are shown at the 50% probability level and H atoms are represented by circles of arbitrary size.	83
Figure 3.9. Molecular structure of bicarbonate salt formed with 3-3 . Displacement ellipsoids for non-H atoms are shown at the 50% probability level and H atoms are	83

represented by circles of arbitrary size.

Figure 3.10. Molecular structure and unit cell packing of **3-3c**. Displacement ellipsoids for non-H atoms are shown at the 50% probability level and H atoms are represented by circles of arbitrary size. 85

Figure 3.11. 2-Ethyl-2-imidazoline **3-4**. 86

Figure 3.12. Molecular structure of **3-4a**. Displacement ellipsoids for non-H atoms are shown at the 50% probability level and H atoms are represented by circles of arbitrary size. 97

Figure 3.13. Molecular structure of **3-1b**. Displacement ellipsoids for non-H atoms are shown at the 50% probability level and H atoms are represented by circles of arbitrary size. 90

Figure 3.14. Stacked ^1H NMR spectra, 400 MHz, in CD_2Cl_2 at room temperature. Top spectrum: **3-1a**, middle spectrum: proposed ring-opened structure, and bottom spectrum: after bubbling CO_2 through solution of proposed ring-opened structure. 92

Figure 3.15. Molecular structure of **3-1c**. Displacement ellipsoids for non-H atoms are shown at the 50% probability level and H atoms are represented by circles of arbitrary size. 93

Figure 3.16. Molecular structure of *N,N,N',N'*-tetramethylthiourea. Displacement ellipsoids for non-H atoms are shown at the 50% probability level and H atoms are represented by circles of arbitrary size. 96

Figure 3.17. Molecular structures of **3-9a** and **3-10**. Displacement ellipsoids for non-H atoms are shown at the 50% probability level. 99

Figure 3.18. N-Containing compounds featuring a methylene *beta* to the nitrogen centre towards the formation of a cyclic trithioanhydride. 2-Ethyl-2-oxazoline (v) is also designated as **3-14**. 101

Figure 3.19. Molecular structure of **3-13b**. Displacement ellipsoids for non-H atoms are shown at the 50% probability level and H atoms are represented by circles of arbitrary size. 103

Figure 3.20. Proposed mixture of the unknown yellow precipitate from the reaction of **3-14** and CS_2 . 104

Figure 4.1. pK _a (DMSO) scale of select substrates: those in the dotted area are not carboxylated in the presence of DBU and CO ₂ .	119
Figure 4.2. The structures of DBU (4-1), TMGN (4-2), bis(1-methyl-4,5-dihydroimidazol-2-yl)methane (4-3a), and 2,2'-bis(1-methyl-4,5-dihydroimidazol-2-yl)propane (4-3b).	120
Figure 4.3. Tautomerization of 4-3a .	120
Figure 4.4. Ketimines with pK _a 's (DMSO): <i>N</i> -diphenylmethylene-protected α -aminotoluene 4-10 and <i>N</i> -fluorenylidene-protected α -aminotoluene 4-11 .	125
Figure 4.5. <i>N</i> -(diphenylmethylene)-aminoacetonitrile 4-18 .	132
Figure 4.6. Drawing of zwitterionic <i>N,N</i> -dimethyl-1,3-propanediamine CO ₂ -adduct.	148
Figure 5.1. From left: TBD-CO ₂ adduct, cyclic trithioanhydride of DBU, proposed DBU-CO ₂ adduct.	168
Figure 5.2. Illustration correlating CO ₂ as a carbonyl source to the three areas of research: 1) synthesis of α -amino acids, 2) amidation of benzoylacetic acid, and 3) synthesis of ureas.	169

List of Schemes

Scheme 1.1. Azaphosphatranes for the synthesis of cyclic carbonates.	9
Scheme 1.2. Catalytic carboxylative cyclization of propargylic alcohols with CO ₂ and a NHO. Select examples taken from the work of Lu and co-workers.	11
Scheme 1.3. Synthesis of methanol <i>via</i> hydrosilylation of CO ₂ using a catalytic amount of an NHC under ambient conditions.	12
Scheme 1.4. Catalytic reduction of CO ₂ with a phosphine-borane to give CH ₃ OBcat.	13
Scheme 1.5. Two of the many known switchable hydrophilicity solvents (SHS). The hydrophobic form is on the left while the hydrophilic form is on the right.	15
Scheme 1.6. “Switchable water.” On the left, the aqueous solution has uncharged base B , a lower ionic strength. On the right, after addition of CO ₂ the bicarbonate salt of B is made, forming a solution of higher ionic strength. The <i>n</i> denotes the number of sites that can be protonated in the amine or polyamine base B .	17
Scheme 1.7. The switching of anionic surfactants in aqueous solution. The structure on the left will stabilize emulsions while the structure on the right is too insoluble in water to stabilize emulsions.	18
Scheme 1.8. Long-chain amidines serve as demulsifiers in the absence of CO ₂ and as emulsion-stabilizing surfactants in the presence of CO ₂ .	19
Scheme 1.9. Deuteration of 4'-methoxyacetophenone in CDCl ₃ at room temperature with select examples of bases used for the study.	27
Scheme 2.1. DBU and alcohol switchable-polarity solvent.	36
Scheme 2.2. Guanidines and alcohol switchable solvent system.	37
Scheme 2.3. Reactivity of secondary and primary amines with CO ₂ .	39
Scheme 2.4. Amidine and amine combination as SPS.	42
Scheme 2.5. Siloxated ethanolamines.	44
Scheme 2.6. Comparison of SPS systems, top: two- and single-component base/alcohol, bottom: secondary amines and diamines, (~~~~) represents linker.	45
Scheme 2.7. Alkanolamidines and alkanolguanidines for CO ₂ capture.	46
Scheme 2.8. Formation of 8-membered ring with alkanol-guanidine and CO ₂ .	52
Scheme 2.9. Addition of CO ₂ to 2-11 to form zwitterionic salt 2-11b .	54

Scheme 2.10. Addition of CO ₂ to 2-18 to form zwitterionic salt 2-18b .	55
Scheme 3.1. Preparation of amidinium dithiocarbamates.	69
Scheme 3.2. Proposed mechanism for the thermolysis of an amidinium dithiocarbamate.	70
Scheme 3.3. Proposed mechanism for the reaction of DBU and CS ₂ .	71
Scheme 3.4. Hydrothermal reaction forming a cyclic trithioanhydride from diamino-benzene and CS ₂ .	73
Scheme 3.5. Formation of the first reported cyclic trithioanhydride where thionation is done on a chloride derivative of 1,8-naphthalic anhydride using Lawesson's reagent (LR) in refluxing conditions.	73
Scheme 3.6. Formation of a cyclic trithioanhydride ring with CS ₂ and phenylisothiocyanate.	74
Scheme 3.7. Synthesis of cyclic trithioanhydrides, 4-arylthiazolidene-2,5-dithiones (top) and 1,3-thiazine-2,6-dithiones (bottom).	74
Scheme 3.8. Reaction of acetamidine and CS ₂ forming dithiocarbamates.	75
Scheme 3.9. Representation of the reaction of guanidine and CS ₂ at three different conditions: path a) in acetone at -18 °C, path b) in acetone at 50 °C, and path c) in ethanol at 20 °C.	76
Scheme 3.10. Preparation of cyclic trithioanhydrides 3-2a .	78
Scheme 3.11. Preparation of cyclic trithioanhydride 3-3a .	79
Scheme 3.12. Synthesis of 3-4a , with proposed yellow precipitate structure 3-4x .	88
Scheme 3.13. Resonance of 3-1a exhibiting the nucleophilic character of conjugated sulfur atom.	89
Scheme 3.14. Methylation of 3-1a with iodomethane forming 3-1b .	89
Scheme 3.15. Proposed mechanism of sodium hydroxide reacting with 3-1a to a ring-opened structure.	90
Scheme 3.16. Proposed mechanism following the addition of a nucleophile to 3-1a .	92

Scheme 3.17. Proposed mechanism for the formation of 3-1c . Dashed box represents the proposed counterion exchange by crystal growth of 3-1c by slow evaporation in dichloromethane.	
Scheme 3.18. Acyclic amidines 3-5 – 3-7 reacted with CS ₂ forming <i>N,N</i> -dimethylthioacetamide 3-8 and alkylated isothiocyanates.	95
Scheme 3.19. Proposed mechanism for the formation of thiourea formed from pentaalkylated guanidine.	96
Scheme 3.20. Reaction of 1,1,3,3-tetramethylguanidine 3-9 and CS ₂ in the presence of sodium hydroxide.	98
Scheme 3.21. Reaction of CS ₂ and 3-9 in the presence of CH ₂ Cl ₂ and hexanes to give 3-9a and 3-10 .	99
Scheme 3.22. Formation of <i>N,N</i> -Dialkyldithiocarbamates with secondary amines, CS ₂ , and dichloromethane.	100
Scheme 3.23. Reaction of ketone Mannich bases with CS ₂ .	102
Scheme 3.24. Synthesis of dithiocarbamate methyl ester from 4-ethyl-2-isopropyl-4,5-dihydrooxazole.	103
Scheme 4.1. Carboxylation of ketones followed by asymmetric hydrogenation.	118
Scheme 4.2. Removal of amino protecting groups under acidic conditions followed by hydrolysis of the nitrile yielding the 1,2-diaminocarboxylic acid.	123
Scheme 4.3. Top reaction: Mannich-type reaction developed by Kobayashi and co-workers. Bottom reaction: carboxylation of acetophenone with CO ₂ developed by the Jessop Lab.	124
Scheme 4.4. Proposed synthesis using ketimines 4-10 and 4-11 in the presence of DBU and CO ₂ for the synthesis of an amino acid.	126
Scheme 4.5. Synthetic strategies for the α -amino acids from α -amino sulfone.	127
Scheme 4.6. Synthesis of 4-10 using benzophenone and benzylamine with trifluoroborate etherate under Dean Stark conditions.	127

Scheme 4.7. Reaction conditions used towards the carboxylation of 4-10 using DBU for a base a pressure of CO ₂ .	128
Scheme 4.8. Attempted carboxylation of 4-10 with DBU and CO ₂ which lead to the isolation of isomerized product 4-17 .	129
Scheme 4.9. Deprotonation of 4-10 with DBU to give imine/enamine tautomerization about α - and α' -carbon atoms.	129
Scheme 4.10. Attempts to isolate carboxylated product of 4-10 by two methods: 1) reduction of imine by NaBH ₄ and 2) addition of iodomethane or benzylbromide to esterify carboxylate.	131
Scheme 4.11. Synthesis of ketimines that feature 9-fluorenylidene as an imino protecting group.	133
Scheme 4.12. Deprotonation with <i>n</i> -BuLi and addition of CO ₂ .	134
Scheme 4.13. Direct amide bond formation by reaction of a free carboxylic acids and amines.	136
Scheme 4.14. Direct amidation of phenylacetic acid with benzylamine with various arylboronic acids with isolated amide product yields.	137
Scheme 4.15. Formation and proposed amidation of benzoylacetic acid with amidation catalysts MIBA and ZrCl ₄ .	139
Scheme 4.16. Attempted amidation of benzoylacetic acid with ideal reaction conditions reported for MIBA and ZrCl ₄ as amidation catalysts.	140
Scheme 4.17. Summary for the synthesis of tetraalkylated ureas (cyclic or acyclic) from either direct thermal dehydration or with stoichiometric activation.	142
Scheme 4.18. Above: synthesis of tetraalkylated ureas using a Pd-catalyst and stoichiometric amount of triphenylphosphine. Below: two-step method developed in the Jessop Lab for the synthesis of tetraalkylated ureas using CO ₂ and CCl ₄ .	143
Scheme 4.19. Proposed synthesis of ureas by initial formation of carbamates using i) secondary amines and equivalent of base (B = DBU) and ii) primary amines, where MIBA or ZrCl ₄ would catalyze the reaction.	144

- Scheme 4.20.** Excerpt from proposed reaction mechanism of cyclic urea from CO₂ and ethylenediamine by CeO₂ reported by Tomishige and co-workers. 145
- Scheme 4.21.** Formation of dibenzylurea starting from benzylamine and CO₂ under 180 °C and 50 bar of CO₂ in absence of solvent. Yield of dibenzylurea calculated from ¹H NMR spectra. 146
- Scheme 4.22.** Attempts to prepare dialkylureas by initial formation of carbamate salts from amines and 1 bar of CO₂ followed by addition of 10 mol% MIBA or ZrCl₄. Piperidine was also tried without success. 146
- Scheme 4.23.** Formation of dibenzylurea using high temperature and pressure in the presence of ZrCl₄ as a catalyst. Yield of dibenzylurea is approximated from ¹H NMR spectra. 147
- Scheme 4.24.** Proposed synthesis and mechanism using *N,N'*-dimethyl-1,3-propanediamine for the synthesis of cyclic urea in the presence of a Lewis acid catalyst. A base can either be added or it can be *in situ* (Base). 149
- Scheme 4.25.** Proposed synthesis of an α -amino acid with diphenylphosphinyl-amine and CO₂. 153
- Scheme 5.1.** Formation of zwitterionic species with CO₂ with a secondary diamine (R = H) and a diamine containing both secondary and tertiary nitrogen centres (R = CH₃). 167

List of Tables

Table 1.1. The worldwide capacity of potential CO ₂ storage reservoirs.	4
Table 2.1. CO ₂ -uptake by select SPS systems.	48
Table 4.1. Stereoselective Mannich-type reactions of <i>N</i> -fluorenylidene-protected α -amino-acetonitrile (4-4) reported by Kobayashi's group.	122
Table 4.2. Solution colours of after addition of <i>n</i> -BuLi and addition of CO ₂ for the investigated ketimines that have a diphenylmethylene (Ph ₂ C-) or 9-fluorenylidene (9-flu-) protecting-group (PG).	134
Table 4.3. Attempts at the formation of cyclic urea starting from <i>N,N'</i> -dimethyl-1,3-propanediamine. All reaction conditions yielded trace amounts (<10%) of cyclic urea.	150

List of Abbreviations

Å	angstrom(s)
AMP	2-amino-2-methyl-1-propanol
atm	atmosphere
ATR	attenuated total reflectance
β	beta
Bcat	catecholborane
BINAP	2,2'-bis(diphenylphosphino)-1,1'-binaphthyl
[bmim]PF ₆	1-butyl-3-methylimidazolium hexafluorophosphate
BOL	binding organic liquid
br	broad
<i>n</i> -BuLi	<i>n</i> -butyllithium
C	carbon
CCS	carbon capture and storage
cat.	catalyst
CFC	chlorofluorocarbon
¹³ C{ ¹ H} NMR	carbon-13 nuclear magnetic resonance proton-decoupled
COSY	correlation spectroscopy
cP	centipoise
18-crown-6	1,4,7,10,13,16-hexaoxacyclooctadecane
DBN	1,5-diazabicyclo[4.3.0]non-5-ene
DBU	1,8-diazabicyclo[5.4.0]undec-7-ene
d	doublet
dd	doublet of doublets

DEA	diethanolamine
DFT	density functional theory
DIPEA	<i>N,N'</i> -diisopropyl-ethanolamine
2-DMAM-PrOH	2-(dimethylamino)-2-methyl-1-propanol
DMAN	<i>N,N,N',N'</i> -tetramethyl-1,8-naphthalenediamine
DMEA	<i>N,N'</i> -dimethylethanolamine
DMF	dimethylformamide
DMSO	dimethylsulfoxide
DPP	diphenylphosphinyl
DSFs	deep saline-filled sedimentary formations
ee	enantiomeric excess
EI	electron impact
EOR	enhanced oil recovery
equiv	equivalents
ESI	electrospray ionization
FLP	frustrated Lewis pair
FT	fourier transform
GC	gas chromatography
Gt	gigaton
h	hour(s)
HRMS	high resolution mass spectrometry
HSQC	heteronuclear single quantum correlation
Hz	hertz
IL	ionic liquid
Ile	isoleucine

IR	infrared
KO ^t Bu	potassium <i>tert</i> -butoxide
LDA	lithium diisopropylamide
Leu	leucine
m	multiplet
M	molarity
MDEA	<i>N</i> -methyldiethanolamine
Me	methyl
MEA	monoethanolamine
MeCN	acetonitrile
MeOH	methanol
min	min(s)
MIBA	5-methoxy-2-iodophenylboronic acid
mmol	millimole(s)
mol	mole(s)
MPa	megapascal
M.S.	molecular sieves
MTBD	7-methyl-1,5,7-triazabicyclo[4.4.0]dec-5-ene
m/z	mass to charge ratio
N	normality
NHC	<i>N</i> -heterocyclic carbene
NHO	<i>N</i> -heterocyclic olefin
Nile red	9-diethylamino-5-benzo[<i>a</i>]phenoxazinone
nm	nanometer
NMR	nuclear magnetic resonance

ov	overlap
p	pentet
PEG	polyethylene glycol
Ph	phenyl
PMDBD	3,3,6,9,9-pentamethyl-2,10-diazobicyclo-[4.4.0]dec-1-ene
[pmIm]Br	1-methyl-3-pentylimidazolium bromide
ppm	parts per million
Pr	propyl
Pro	proline
q	quartet
quint	quintet
R	alkyl or aryl group
RT	room temperature
s	singlet
SBA-15	Santa Barbara amorphous type material
salen	2,2'-ethylenebis(nitrilomethylidene)diphenol
scCO ₂	supercritical carbon dioxide
sec	second(s)
sep	septet
SHS	switchable hydrophilicity solvent(s)
SO _x	sulfur oxide
SPS	switchable polarity solvent(s)
STP	standard temperature and pressure
SW	switchable water
t	triplet

TBAE	2-[(1,1-dimethylethyl)amino]-ethanol
TBAP	1-[(1,1-dimethylethyl)amino]-2-propanol
TBD	1,5,7-triazabicyclo[4.4.0]dec-5-ene
TBN	1,4,6-triazabicyclo[3.4.0]non-4-ene
THF	tetrahydrofuran
TMG	1,1,3,3-tetramethylguanidine
TMGN	1,8-bis(tetramethylguanidino)naphthalene
TMP	2,2,6,6-tetramethylpiperidine
TMS	tetramethylsilane
TOF	turnover frequency
TON	turnover number
UV	ultraviolet
Vis	visible
wt.	weight

Chapter 1

Introduction

1.1 Carbon Dioxide Sources

1.1.1 Strategies to Cope with the Carbon Dioxide Output

Carbon dioxide (CO₂) is a non-toxic, abundant, and economical material. Thus, CO₂ fixation and sequestration from the atmosphere has become a competitive field.¹ Carbon dioxide is a greenhouse gas and considered to be the greatest contributor to global warming.² There is an excess of 115 ppm by volume of CO₂ in the atmosphere with respect to the pre-industrial value of 270 ppm, amounting to about 900 Gt of CO₂. The largest of the CO₂ emitters comes from power generation and heat production from fossil fuel combustion.

There is a need to address the imbalance between the amount of CO₂ emitted every year *versus* the amount of CO₂ consumed or sequestered by human activities. Progress in how CO₂ is captured and stored, and the use of CO₂ as a chemical feedstock would help to address the above imbalance. Even improved methods for CO₂ usage may not lead to a reduction in the amount of CO₂ produced. To cause a reduction in CO₂ emissions there are certain rules that have to apply:³

- 1) new processes must reduce the overall CO₂ emissions, not just appear to consume CO₂ in the balanced reaction equation,
- 2) be less energy- and material-intensive with respect to the process it aims to replace,
- 3) employ safer and eco-friendly working conditions, and
- 4) be economically viable.

1.1.2 CO₂ Capture and Storage

Carbon capture and storage (CCS) technologies are promising for the reduction of CO₂ emissions in the near-term.⁴ The design and development of current and novel ways in which to capture CO₂ from flue gas streams is an intense area of research. Two methods that are considered suitable for industry are post-combustion CO₂ capture using amine solvents and calcium looping technologies.

Scrubbing with aqueous amine solutions is a well known technology for CO₂ capture on a large scale and is used across several industries. CO₂ is contacted with aqueous amine solutions; the amine solvent reacts reversibly with CO₂ and forms water-salts. This method is well suited for dilute and low pressure CO₂ streams.

A well-studied reagent for aqueous amine solutions is monoethanolamine (MEA).⁵ Other comparable solvents are 2-amino-2-methyl-1-propanol (AMP), secondary amines such as diethanolamine (DEA), and tertiary amines such as methyldiethanolamine (MDEA). MEA is a conventionally used amine reagent since it exhibits rapid CO₂ absorption at low pressure, and it forms a stable carbamate species.⁴

However, there are disadvantages associated with using MEA in aqueous amine solutions, such as corrosion and degradation products that form after the amine is in contact with the flue stream. The packing material that is used for the solution stream of MEA could have the potential to form metal salts after prolonged exposure.⁶⁻⁸ The amine is susceptible to degradation by O₂, SO_x, and CO₂ in addition to being prone to thermal degradation. While MEA can form a stable carbamate species with CO₂, upon the regeneration step a small fraction of carbamate can further react to form 2-oxazolidone that can react with MEA to form N-(2-hydroxyethyl)-ethylenediamine.⁹ It is also known that some degradation products of amines include amides and aldehydes as well as nitrosamines, which are known to be carcinogenic.¹⁰

The non-volatility of ionic liquids (ILs) has made them an attractive substitute for amine sorbents, in that there is no loss of solvent into the gas stream, thus facilitating the capture of CO₂.¹¹ In addition to the low volatility, ILs have a broad range of liquid temperature and high thermal and chemical stability. A drawback that is associated with ILs is that they normally have a higher viscosity than most conventional solvents. High viscosities can hamper the uptake of CO₂ and be detrimental to the thermal regeneration cycle, needing more energy to release CO₂. There is also a higher economic and environmental cost for the preparation and purification of ILs in comparison to the conventional amine sorbents.

Corrosion is a drawback that is associated with the two types of liquid sorbents mentioned above. Avoiding corrosion can be achieved by using solid sorbents for the capture of CO₂. In general there are two types of dry sorbents, those that are amine based, and those that are alkali (earth) metal-based sorbents. Silica, activated carbon, and SBA-15¹² are generally used as the base for dry amine sorbents. Syntheses of such dry amine sorbents requires a lot of expensive material, including the use of large amounts of solvents. Calcium oxide (CaO) is a well-studied alkali metal-based dry sorbent, which at high temperatures can reversibly react with CO₂ to form carbonate CaCO₃ in the absence of water.¹³ The use of CaO can be seen as an attractive solid sorbent for pre- and post-combustion processes. However, a decrease in reactivity is seen over a number of cycles due to the degradation in structure of the CaO, where there is a change in pore shape, pore shrinkage, and grain growth that is a result of heating CaO.¹³

Following CO₂ capture, CO₂ must be sequestered to avoid or delay emission into the atmosphere. There are three natural sites into which CO₂ can be disposed following its capture and storage: deep geological sequestration, mineral carbonation, or ocean storage.¹⁴ Geological sequestration will be described further as an example for CO₂ sequestration.

Three geological formations have been recognized as major potential CO₂ sinks following the capture, regeneration cycle, and transport of CO₂: deep saline-filled sedimentary

formations (DSFs), depleted oil and natural gas reservoirs, and unmineable coal-beds. These suitable formations are more than 800 m deep, have a thick and extensive seal and porosity that can facilitate large volumes of CO₂ at high flow rates without the need of high pressure for injection.¹⁵ For North American capacity, DSFs could accommodate between 900 and 3300 Gt C, oil and gas reservoirs ~80 Gt C, and coal-beds 150 Gt C.¹⁶ Table 1 lists the worldwide capacities for potential CO₂ storage reservoirs.

Table 1.1. The worldwide capacity of potential CO₂ storage reservoirs.¹⁷ Ocean and land-based sites together contain an enormous capacity for storage of CO₂.^a

Sequestration option	Worldwide capacity^b
Ocean	1,000s GtC
DSFs	100s – 1000s GtC
Depleted oil and gas reservoirs	100s GtC
Coal seams	10s – 100s GtC
Terrestrial	10s GtC
Utilization	<1 GtC/yr

^aWorldwide total anthropogenic carbon emissions are ~7 GtC per year (1 GtC = 1 billion metric tons of carbon equivalent).

^bOrders of magnitude estimates.

The feasibility of CO₂ to fill these reservoirs is dependent on the miscibility of the fluid it replaces in the pores of the geological formations. Water and oil are the typical species found in these pores. Under the conditions for sequestration, CO₂ is immiscible with water and miscible and sometimes immiscible with oil. Water is present in all geological formations and some of it will remain in the reservoir even with the introduction of CO₂. How CO₂ will occupy the water laden pores is dependent on the pressure and rate at which CO₂ enters this formation. Even with the injection of CO₂ into such geological reservoirs, there is the risk of CO₂ leakage. Geologic and oceanic injection of CO₂ only delays the release of CO₂, although in some cases the delay

could be for a geologically significant time period. Monitoring of this leakage would be imperative for public and environmental concerns.

Improvements to methods for CO₂ capture and storage are still needed. While there are a variety of methods that were developed to capture CO₂, CO₂ emissions remain overwhelming and far higher than the preindustrial levels. Even the sequestration techniques in development to trap CO₂ into geological formations still could not cope with the amount of CO₂ emitted. Coal-fired power plants emit about 8 million tons of CO₂ annually, which means 10 million cubic meters of CO₂, as a supercritical fluid, would need to be sequestered per year.¹⁶ The sheer volume of CO₂ cannot be contained.

1.2 CO₂ Utilization

1.2.1 The Physical Properties of CO₂ for use in Industry

CO₂ is a gas under ambient conditions, though by varying temperature and pressure to CO₂ alone or in the presence of a solvent, supercritical CO₂ (scCO₂), liquid CO₂ and CO₂-expanded liquids can be formed respectively. Supercritical CO₂ and CO₂-expanded liquids have made headway into the industry where their utilities are based on the change on the physical characteristics of CO₂. While the use of gaseous CO₂, scCO₂, and CO₂-expanded liquids does not result in CO₂ fixation and may not contribute to the reduction in CO₂ emission, it can be seen that they might have a role in reducing the amount of materials used for a given industrial process. The reduction in the amount of materials needed, thus making a process more energy efficient would contribute to CO₂ emission avoidance. The disposal/recycling of CO₂, scCO₂, and CO₂-expanded liquids is more energy efficient than conventional solvents. In an industrial process, the main burden to the financial cost and the environment is the use and remediation of solvents for that process. As a result, researchers strive towards the reduction of solvent usage and replacement with benign alternatives.

Gaseous CO₂, scCO₂, and CO₂-expanded liquids all have a target area in which each 'physical' state of CO₂ is used. CO₂ in the gaseous state has precedence in the food industry.¹⁹ CO₂ is a benign gas and can be used as a protective one, for food preservation and even in fire extinguishers.²⁰ Within enhanced oil recovery (EOR), the application of CO₂-expanded liquids leads to reducing the viscosity of the oil in order to facilitate the transport of oil through porous rock of the reservoir.²¹ Currently, the use of scCO₂ in industry is for extraction.²² It is used in the decaffeination of coffee, extraction of soybeans and hops, recovery of active materials in the pharmaceutical industry, extraction of fats and ethereal oils in the cosmetic industry, and the extraction of spices, aromas, and essences in the food industry.²² Aside from the different states of CO₂ mentioned above, solid CO₂ or dry ice is used in refrigeration mainly for railcars or trailers, to replace the use of toxic CFCs to combat the greenhouse effect as well as the ozone depletion effect.²³

1.2.2 Industrial use of CO₂ as a C1 Source

While CO₂ is an abundant and renewable carbon source, there are only a few industrial processes that utilize CO₂ as a C1 source. Since CO₂ is in the most oxidized state of carbon, perhaps the biggest challenge in establishing CO₂ in industry is overcoming its high stability and thus activation of CO₂ is crucial. One way to activate CO₂ is to recognize the electron deficiency of the carbonyl carbon and that CO₂ is readily attracted to nucleophiles and electron donating groups. CO₂ can be seen as a weak Lewis acid or 'anhydrous carbonic acid',²⁴ and as a result it can rapidly react with basic compounds. Without the use of strong nucleophiles and electron donating groups, the use of a catalyst is necessary to facilitate the formation of a stable product with CO₂. CO₂ is not used extensively as a source of carbon in current laboratory and industrial practices. As a result, much research has gone into the field of CO₂ transformations that uses CO₂ as a raw substrate in order to negate the use of other C1 sources that are otherwise highly toxic, such as phosgene or CO.²⁵

There are four general ways in which to overcome the high stability of CO₂: 1) use high-energy starting materials such as hydrogen, unsaturated compounds, small-membered ring compounds, and organometallics, 2) choose oxidized low-energy synthetic targets such as organic carbonates, 3) shift the equilibrium to the product side by removing a particular compound, 4) supply physical energy such as light or electricity.²⁵ Selecting the appropriate reactions can lead to a negative Gibb's free energy of reaction.²⁶

As a reactant in industry, CO₂ is used in the synthesis of salicylic acid, cyclic carbonates, methanol and urea (Figure 1.1).²⁵ Phenols are converted from their sodium or potassium salt to carboxylic acids with the reaction of CO₂. The practical synthesis is the Kolbe-Schmitt reaction which heats the sodium salt in an autoclave with CO₂; the acid is recovered with sulfuric acid. Salicylic acid, an intermediate in the production of acetylsalicylic acid, is synthesized by this process.^{22,24} Cyclic carbonates are formed by epoxides and CO₂ in the presence of ammonium halides. The formation of five-membered cyclic carbonates (ethylene and propylene carbonate) from CO₂ has been in industry since the 1950s. Cyclic carbonates can be further reacted with amines or ammonia to form carbamates. The carbamates can then be converted into polyurethane, a material that has high commercial value.²² Methanol is produced commercially from synthesis gas using natural gas or coal that mainly contains CO and H₂ with a small amount of CO₂. Methanol is used as a precursor for other useful products such as dimethyl ether.⁴ The production of urea by using CO₂ is carried out in two steps at elevated pressure (150 to 250 bar) and temperature (150 to 200 °C). Formation of ammonium carbamate from ammonia and CO₂ is the first step and the second step is the dehydration of the carbamate to urea.

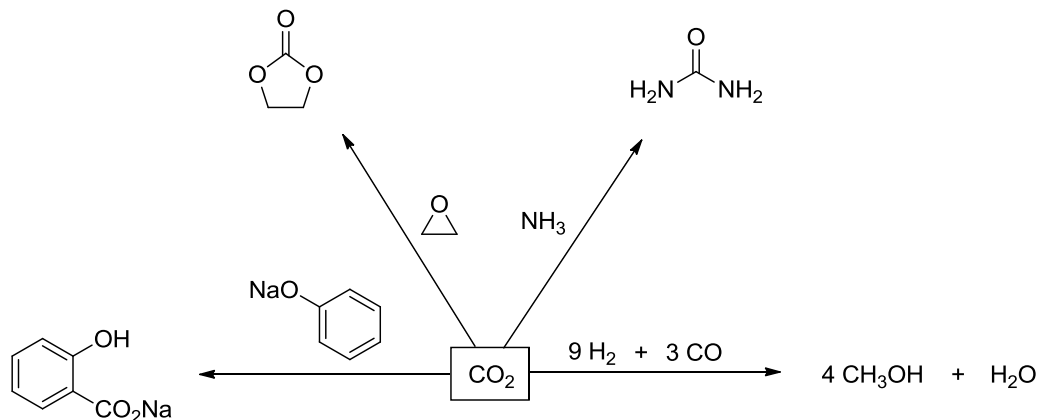


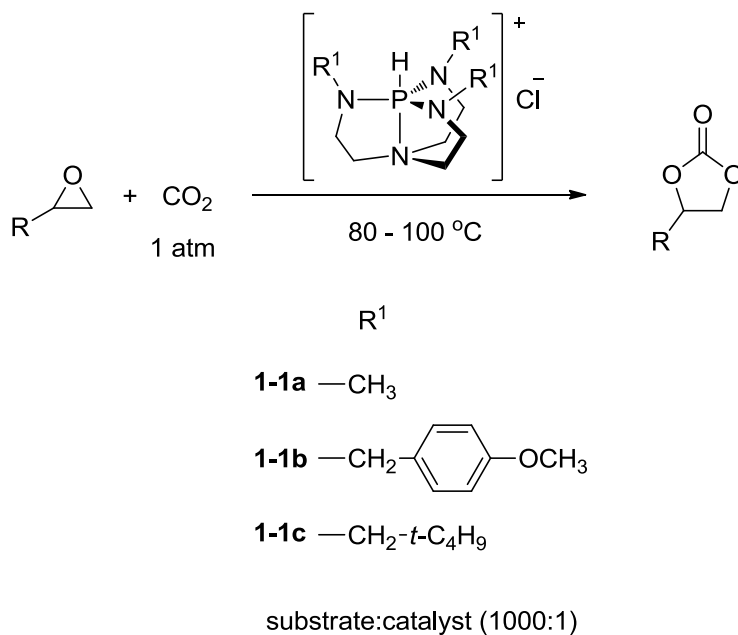
Figure 1.1. Industrial organic syntheses using CO₂.²⁵

1.3 The Use of CO₂ Under Ambient to Near Ambient Conditions

1.3.1 Activation of CO₂ Without Using Metals

A push towards the activation of CO₂ in a ‘metal-free’ environment could be a direct way to circumvent the use of precious metals. The use of transition metals for the activation of CO₂ at ambient to near ambient conditions has precedence in the laboratory and in industry.²⁷ However, with the impending shortage of such precious metals other reservoirs for precious metals have been proposed such as mining near-Earth asteroids.²⁸ Organocatalysis is the acceleration of chemical reactions with a substoichiometric amount of an organic compound which does not contain a metal atom.²⁹ Organocatalysts bear abundant elements such as nitrogen, oxygen, carbon, and hydrogen. While there are several examples of organocatalysts for use in organic transformations,²⁹ to date there are a limited number of examples where organocatalysts directly use CO₂ as a C1 source in an organic transformation at ambient or near ambient conditions.^{32,33,36,45} These recent reports demonstrate the formation of the value-added products that were discussed in the previous section that are formed from CO₂ and challenge the established methods to synthesize them in industry.

Over the past few decades, there have been a number of catalysts developed for the synthesis of carbonates, and recently, the same synthesis has been re-visited under the guise of a metal-free environment. While typically ammonium and phosphonium salts or alkali metal halides are used as homogenous catalysts for the synthesis of acyclic carbonates, recent examples include $\text{ZnBr}_2(\text{pyridine})_2$ ³⁰ and salen complexes such as Cr-salen-Cl/base.³¹ However in most cases, additives and/or cocatalysts in addition to solvents are needed. In contrast, Dufaud and co-workers investigated three azaphosphatranes for the synthesis of cyclic carbonates from CO_2 and epoxides (Scheme 1.1).³² When styrene oxide is used as a substrate, the formation of cyclic carbonate is afforded at temperatures of 80 – 100 °C, with a substrate-to-catalyst ratio of 1000:1 and solventless conditions. Steric bulk around the phosphorus centre contributed to the activity of the catalyst. The bulky *neo*-pentyl azaphosphatrane **1-1c** was the most stable and active species; its reactivity lasted over a course of four days with styrene oxide as a substrate and gave turn-over number (TON) over 500. In contrast, the catalytic reactivity of *p*-methoxybenzyl-substituted azaphosphatrane **1-1b** decreased over the four day period.



Scheme 1.1. Azaphosphatranes for the synthesis of cyclic carbonates.³²

Lu and co-workers used a N-heterocyclic olefin (NHO) for CO₂ activation for the catalytic cyclization of propargylic olefins giving α -alkylidene cyclic carbonates.³³ It was previously known that N-heterocyclic carbenes (NHCs) can activate CO₂ to form imidazolium carboxylates.^{34,35} The N-heterocyclic olefin has the ability to stabilize a positive charge through aromatization of the heterocyclic ring and the terminal carbon of the olefin is electronegative (Figure 1.2). The isolated NHO-CO₂ adducts have a C_{CO₂} – C_{NHO} bond that is in the range of 1.55 – 1.57 Å, that is significantly longer than a C_{CO₂} – C_{NHC} bond of NHC-CO₂ adducts. Under mild temperatures and pressures, in some cases room temperature and 1 atm of CO₂, the catalytic use of a NHO-CO₂ adduct afforded the cyclic carbonates in good yields (Scheme 1.2).

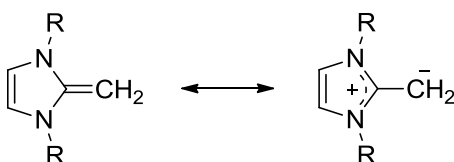
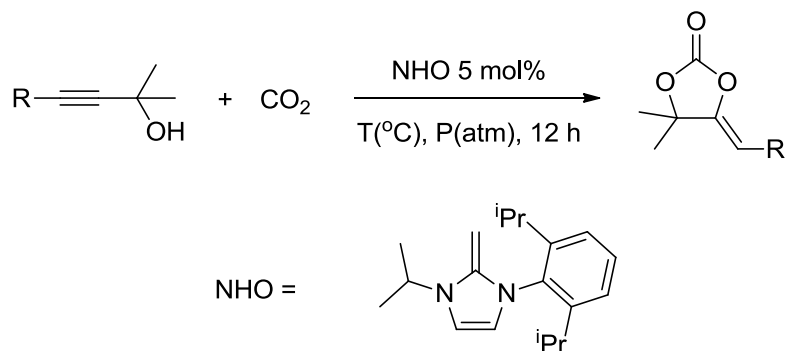


Figure 1.2. Resonance structures of *N, N'*-disubstituted-2-methylene imidazoline.³³



Entry	R	T (°C)	P (atm)	yield (%) ^a
1	Ph	50	20	76
2	Ph	60	20	93
3	Ph	60	40	94
4 ^b	3-pyridyl	60	20	90
5 ^b	3-pyridyl	25	1	42

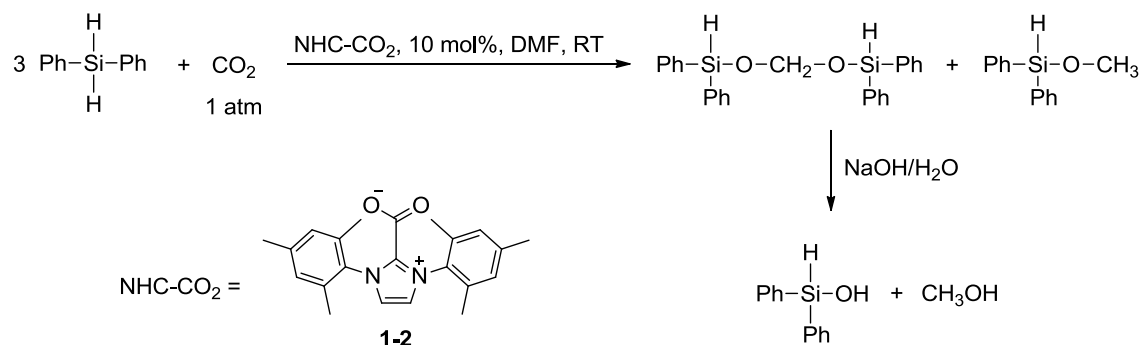
^aIsolated yield, ^b0.5 mL CH₂Cl₂

Scheme 1.2. Catalytic carboxylative cyclization of propargylic alcohols with CO₂ and a NHO. Select examples taken from the work of Lu and co-workers.³³

The reduction of CO₂ could lead it to being a more important C1 source for the production of methanol. Industrially, the production of methanol starts from synthesis gas that is comprised of CO, H₂ with a small amount of CO₂. An alternative method to negate the use of toxic CO to produce methanol would be a valuable process. Ying and co-workers reported the synthesis of methanol by first reducing CO₂ with a silane by using a stable carboxylated carbene organocatalyst (**1-2**, Scheme 1.3).³⁶ What Ying and co-workers envisioned is the use of a hydrosilane in the reaction to act as a hydride donor to the activated carbon dioxide, reducing CO₂ ultimately to methoxide. By using the stable NHC catalyst, CO₂ was converted to methanol

under mild conditions and dry air that contained a low concentration of CO₂ was even used as a feedstock. Hydrolysis of the CO₂-reduction product was done using an aqueous solution of NaOH after a 24 h period, where methanol was produced in over 90% yield based on the silane through characterization by GC with the use of an external standard.

Systems that use transition-metals for hydrosilylation of CO₂ are limited by moisture and air sensitivity, as well as the low activities of the catalysts. Even with a low NHC loading of 0.05 mol%, the reactivity was better than that of the organometallic reagents. Under ambient conditions the turnover number (TON) and turnover frequency (TOF) reached 1840 and 25.5 h⁻¹, respectively. In contrast, ruthenium catalysts achieved values of 78 – 400 and 2.8 – 17 h⁻¹, TON and TOF respectively, at elevated temperatures and high CO₂ pressures (40 atm).³⁷⁻³⁹

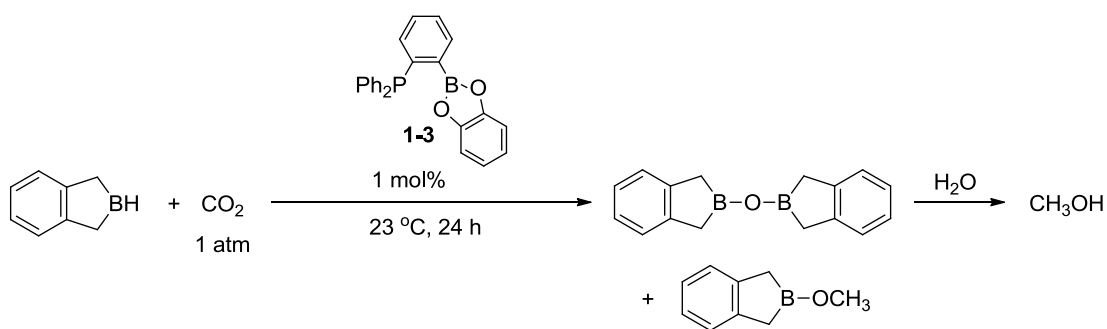


Scheme 1.3. Synthesis of methanol *via* hydrosilylation of CO₂ using a catalytic amount of an NHC under ambient conditions.³⁵

The above methods do circumvent the use of toxic CO, though hydrosilanes are more valuable than methanol. The volumes of hydrosilanes required to produce the industrial amount of methanol would inevitably lead to more waste and financial cost associated to remediate such waste. Silanes are also highly water sensitive, which would lead to a cumbersome industrial process in comparison to the conventional method of producing methanol.

Aside from using silanes in the presence of organocatalysts, hydroboranes can be used for the reduction of CO₂.⁴⁰ Frustrated Lewis pairs (FLPs), which were pioneered by Stephan and

Erker,⁴¹ have been shown to stoichiometrically activate CO₂.⁴² From this, researchers were able to demonstrate the reduction of CO₂ in the presence of boranes, albeit in stoichiometric quantities.⁴³ Piers and co-workers demonstrated the catalytic reduction of CO₂ to methane using a robust TMP/B(C₆F₅)₃ (TMP = 2,2,6,6-tetramethylpiperidine) catalyst with Et₃SiH though it gave limited turnovers.⁴⁴ A very recent report of Fontaine and co-workers looked at aryl bridged phosphine-boranes for the catalytic reduction of CO₂.⁴⁵ Among the phosphine-boranes Fontaine and co-workers noted that, phosphine borane **1-3** (Scheme 1.4) was not previously reported. It was found that under ambient pressure and a temperature of 70 °C with a loading of **1-3** at 1 mol%, the reduction of CO₂ is afforded generating TOFs up to 973 h⁻¹ and TONs up to 2,950. Interestingly, while there is no observable formation of a FLP-CO₂ adduct, Fontaine and co-workers note that CO₂ is also an ambiphilic molecule, having an electrophilic carbon and nucleophilic oxygens, that does not require significant bonding interaction with the ambiphilic **1-3** to undergo reduction with hydroboranes. They also concluded that once the initial reduction occurs, the following reductions occur readily to generate CH₃OBR₂.



Scheme 1.4. Catalytic reduction of CO₂ with a phosphine-borane to give CH₃OBcat.⁴⁵

The design and development of organocatalysts for the activation of CO₂ towards value-added products is a growing area of research. Transition-metal catalysts have proven to be useful for the activation of CO₂ for industrially relevant materials, even with an ambient pressure of

CO₂.³⁶ However moisture and air sensitivity, as well as the scarcity and the price of metals used in most such transition-metal catalysts are significant concerns.

1.3.2 CO₂ as a Trigger to Elicit a Physico-Chemical Change

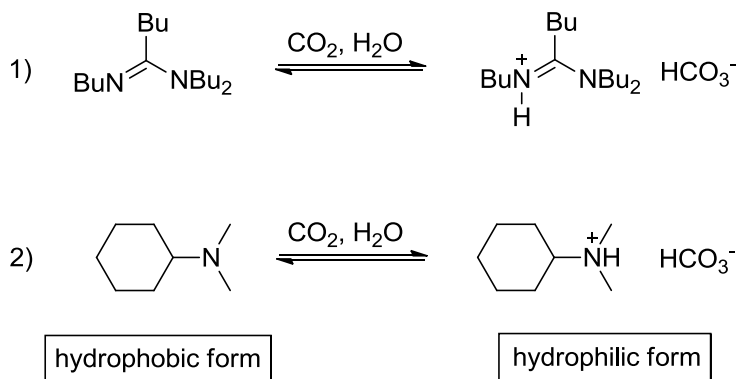
Solvents are considered the highest contributor to the waste in many industrial processes. During a chemical industrial process, there is no single solvent that can address all the needs for the different reaction and separation stages. Therefore a process will typically use at least one solvent per stage. Because of this, thousands of liters of waste solvent are produced. The ideal situation would be to have one solvent that can be used in all stages of an industrial process. Having one solvent as opposed to several different solvents will inevitably mean less solvent waste. This can be a daunting task in industry and in the chemical laboratory. In order to have one solvent for all tasks would mean changing the physical or chemical behaviour of a solvent at any given moment.

Switching the properties of a solvent requires the application of a trigger. Addition of chemical triggers, such as acids or oxidants, are undesirable because they are normally used in stoichiometric quantities and can build up in the system after each cycle. The build-up of these would lead to more environmental and economic cost for their disposal. The ideal situation would be to have a single trigger that is inexpensive, benign, and that can be easily removed and preferably reused. Having a single trigger that can be easily applied and removed while changing the character of a single solvent multiple times during a chemical process, would reduce waste and financial cost and lead to a sustainable system.

Jessop and co-workers have developed various solvent systems that use CO₂ as a single trigger to change polarity, hydrophilicity, or ionic strength.⁴⁶ In almost all of the solvent systems, CO₂ is applied at ambient pressure and the removal of CO₂ can be done by bubbling inert gas into solution or heating the solvent to 60 °C. The application and removal of CO₂ can be done over more than one cycle; thus these are fully reversible switchable solvents. Switchable

hydrophilicity solvents, switchable water, and switchable surfactants will be discussed further here, while switchable polarity solvents and their CO₂ capturing ability will be discussed in the Introduction section of Chapter 2.

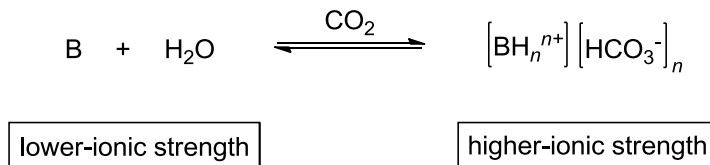
Changing the hydrophilicity of a solvent circumvents the need for distillation in a chemical process. While distillation is often used to remove solvent from a product, the energy requirement is high and the use of a volatile solvent is needed. The use of volatile solvents leads to drawbacks such as flammability, vapour emissions, smog formation, and health impacts by inhalation. Switchable hydrophilicity solvents (SHS) that have been developed in the Jessop group are normally (in the absence of CO₂) hydrophobic and sparingly miscible in water, thus forming a biphasic mixture. Upon the addition of CO₂, the solvents become hydrophilic and completely soluble in water (Scheme 1.5).^{47,48} SHS can be used as just another low-polarity solvent like hexane, but is unusual because it can be removed with carbonated water without the use of distillation.



Scheme 1.5. Two of the many known switchable hydrophilicity solvents (SHS). The hydrophobic form is on the left while the hydrophilic form is on the right.⁴⁶

The ionic strength of “switchable water”, an aqueous solution of an amine or polyamine, can be altered by using CO₂ as a trigger. Increasing the ionic strength of any aqueous solution, normally achieved by adding salt, will destabilize an emulsion, suspension, or foam. However,

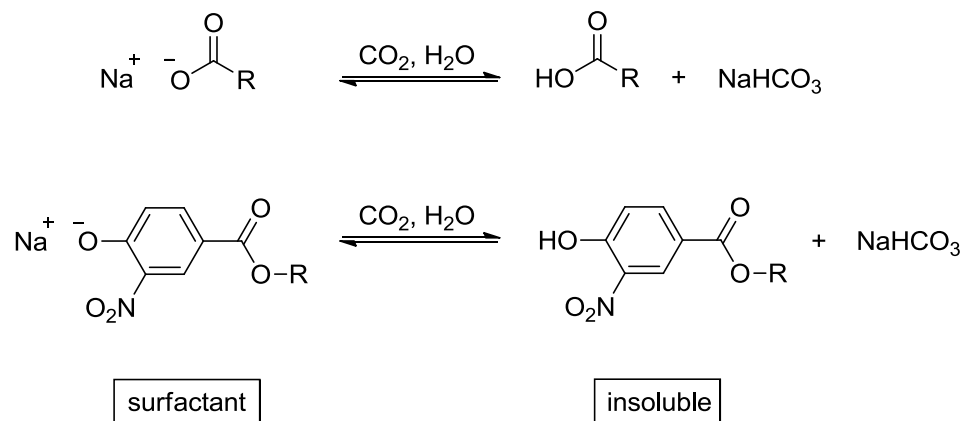
the energy, economic, and environmental costs associated with disposal and recycling of the salt solution are high; thus the addition of salt is generally avoided. If water contains a neutral amine or polyamine base, it has an ionic strength that is low but not zero because of the dissociation of water. Upon the addition of CO₂, the formation of the ammonium bicarbonate salt raises the ionic strength of the aqueous solution, while removal of CO₂ reverts to the original ionic strength of solution (Scheme 1.6). This reversibility in ionic strength by the addition of CO₂ to an aqueous solution of organic base is the operating principle of the aqueous solvent known as switchable water (SW).⁴⁹ A change in the ionic strength of a solution can affect the solubility of compounds in that solution. For instance, the increase in ionic strength can separate compounds out of a solution that would normally be soluble in a solution with a lower ionic strength. THF is completely miscible with water. Upon the addition of CO₂ to water containing THF and some SW base, the formation of bicarbonate salt increases the ionic strength of solution and decreases the miscibility of THF thus forcing it out of solution.⁴⁹ SW can also be used to destabilize emulsions and suspensions. Finely suspended clay particles settle out rapidly from water in the presence of a SW base and CO₂. Having one of these two species present in the water, whether it is SW base or CO₂, is not nearly as effective at promoting clay settling. The higher ionic strength of the SW solution destabilizes the suspension by causing a dramatic drop in the zeta potential.^{50,51}



B = amine or polyamine

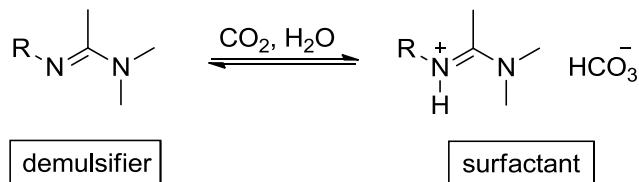
Scheme 1.6. “Switchable water.” On the left, the aqueous solution has uncharged base **B**, a lower ionic strength. On the right, after addition of CO₂ the bicarbonate salt of **B** is made, forming a solution of higher ionic strength. The *n* denotes the number of sites that can be protonated in the amine or polyamine base **B**.⁴⁶

Emulsions and suspensions are necessary in some industrial processes, such as the production of latex suspensions. The preparation of latex polymer suspensions requires the formation of a stable emulsion, while a stable suspension for the shipment and storage of the polymer is necessary. Jessop and co-workers developed switchable surfactants, where CO₂ is used as a trigger for both anionic and cationic surfactants.^{52,53} The addition of CO₂ can either stabilize or destabilize the emulsion with the cationic or anionic surfactants, respectively that is originally formed by the charged species. The addition of CO₂ to water for the re-protonation of soap (sodium alkanoates) has been known for a long time.⁵⁴ In the Jessop lab, formation of an emulsion with long-tail carboxylates and phenolates was reversible with CO₂ addition and removal (Scheme 1.7).



Scheme 1.7. The switching of anionic surfactants in aqueous solution. The structure on the left will stabilize emulsions while the structure on the right is too insoluble in water to stabilize emulsions (R = long alkyl chain).^{55,56}

Recyclable CO₂-triggered switchable cationic surfactants having either an amidine⁵² or guanidine⁵⁷ head-group with a long alkyl chain were developed in the Jessop lab. Addition of CO₂ to these solvents formed bicarbonate salts that stabilize emulsions and suspensions, where removal of CO₂ would revert the species to the neutral form and no longer stabilize emulsions or suspensions (Scheme 1.8). Switchable surfactants that have a guanidine head-group^{53,57} have greater basicity and heat of protonation, so that the surfactant can be used at higher temperatures, though removal of CO₂ is more difficult than from a surfactant that has an amidine head-group. The removal of CO₂ ruins the ability of the surfactant to stabilize the emulsion, switching back to the neutral form of the amidine.



Scheme 1.8. Long-chain amidines serve as demulsifiers in the absence of CO₂ and as emulsion-stabilizing surfactants in the presence of CO₂.⁴⁶

1.4 Amidines and Guanidines for CO₂ Activation and Utilization

1.4.1 The Importance of Design and Development for CO₂ Adsorption

As previously discussed, CO₂ is an attractive C1 building block because it is non-toxic, benign and there is plenty of it. While the production of recyclable CO₂ per year is 6.8 Gt at point sources⁵⁹ there are a limited number of examples where CO₂ is used in industry and even at the lab-scale towards the synthesis of useful products. Within the laboratory, much attention has been paid to the development of metal-containing catalysts for the activation and utilization of CO₂. In comparison, the number of examples of the catalytic activation of CO₂ without using metals, are sparse. To further the applicability of activating CO₂ without metals, there needs to be a deeper understanding of CO₂ and its interaction with organic compounds leading to the design and development of such organic compounds to achieve reactivity of the CO₂ molecule.

One of the most-well researched processes of CO₂ capture is based on chemically reversible CO₂ fixation by primary and secondary amines at ambient temperature to give ammonium carbamates, and CO₂ release from the ammonium carbamates upon heating. Water and alkoxides also add to CO₂ to produce compounds with a carboxyl or carboxylate group. Reacting the formed species with CO₂ further with electrophiles leads to the formation of organic carbonates and carbamates. However, the formation of carbamate requires two stoichiometric equivalents of amines for CO₂ fixation and a high temperature for release.⁶⁰ Currently, there are a

limited number of routes to access CO₂ as a C1 building block and include use of substoichiometric quantities of reagents.

1.4.2 The Elusive CO₂ Adduct with 1,8-Diazobicyclo[5.4.0]undec-7-ene (DBU).

While much attention has been paid to the development of metal-containing catalysts, there have been many examples of reactions of CO₂ that are promoted by bases. Peralkylated amidine and guanidine bases (Figure 1.3), that can either be acyclic or cyclic, have been used as catalysts for reactions involving the use of CO₂.^{61,63,65a-c} These bases are effective in promoting various reactions including the hydrogenation of CO₂ to formic acid,⁶² the carboxylation of methylene compounds with CO₂,⁶³ and various coupling reactions of CO₂.⁶⁴ The catalytic activity of these bases is, in many cases, associated with their proton-transfer activity. There are examples where hindered amidine and guanidine bases are used in nucleophilic catalysis where the formation of an intermediate base-CO₂ adduct is integral to the catalytic system^{65a-c} and sometimes used to explain why amidines are promoters in catalysis.^{65d-e}

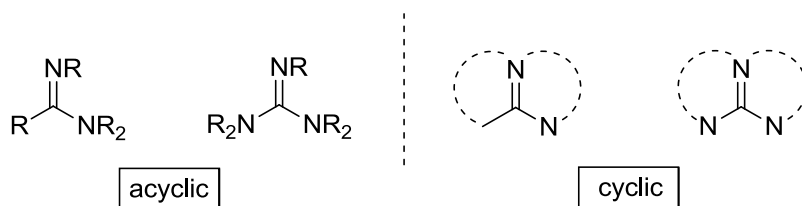


Figure 1.3. Peralkylated amidines and guanidines, acyclic and cyclic.

The use of amidines and guanidines, for reversible CO₂ fixation and release processes is considered more attractive than the use of primary or secondary amines, since the CO₂ fixation requires one equivalent of the amidine and the CO₂ release proceeds readily at low temperature.⁶¹ Understanding the behaviour and formation of the proposed zwitterionic structure (Figure 1.4) that is formed between an amidine and CO₂ would provide further information for the design and

development of other compounds that could efficiently utilize CO₂. The formation of a zwitterionic CO₂ species is one explanation as to why the activation of CO₂ is afforded by the non-nucleophilic amidines.

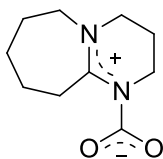


Figure 1.4. Proposed DBU-CO₂ zwitterionic adduct.

A zwitterionic adduct made by exposing liquid DBU to CO₂ was first reported by Iwatani and co-workers and was identified by IR and elemental analysis but they and subsequent researchers failed to dry their solvents and DBU.⁶⁶ Perez and co-workers supported the carbamic nature of the zwitterion, although in an attempt to crystallize the zwitterionic DBU-CO₂ adduct, a amidinium bicarbonate salt structure was isolated instead. The authors attributed the bicarbonate to reaction of the zwitterion with adventitious water during the crystallization process⁶⁷ (Figure 1.5). While a DBU-CO₂ adduct has not been unambiguously detected, Endo and co-workers have repeatedly claimed the formation of the zwitterionic CO₂-adduct.^{68b-d}

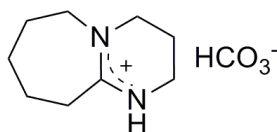


Figure 1.5. DBU bicarbonate salt.⁶⁹

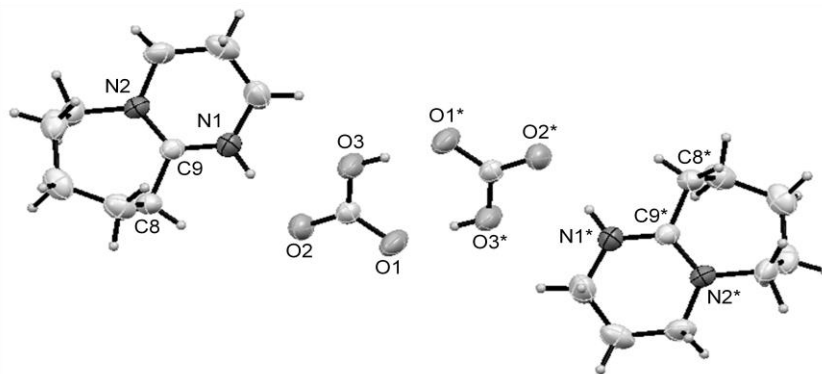


Figure 1.6. [DBUH]⁺[HCO₃]⁻.⁶⁷

Spectroscopic studies were done by Jessop and co-workers on the interaction between DBU and CO₂ to clarify the role of water in product formation.⁶⁹ Their results did not support the formation of a stable zwitterionic adduct between DBU and CO₂ either in the presence or absence of water. Evidence from IR and NMR spectra suggested that the product that previous researchers had observed was a bicarbonate salt and not a DBU-CO₂ adduct. A solid precipitate formed when CO₂ was exposed to the wet DBU. The IR spectrum of the solid sample in KBr showed a band at 1644 cm⁻¹ similar to that reported by Iwatani and co-workers (1640 cm⁻¹)⁶⁶ but was attributed by Jessop and co-workers to protonated DBU rather than a DBU-CO₂ adduct. Additionally, a band at 836 cm⁻¹ was similar to the out-of-plane bending mode for the bicarbonate ion of KHCO₃ at 835 cm⁻¹.⁷⁰ Furthermore the ¹H and ¹³C NMR spectra were consistent with protonated DBU and not a DBU-CO₂ adduct. A peak at 161.1 ppm in the ¹³C NMR spectrum, attributed by other researchers to the zwitterionic DBU-CO₂ adduct, was found to be similar in shift to the bicarbonate ion of KHCO₃ (160.4 ppm in D₂O).⁷¹ Exposing CO₂ to dry neat DBU or DBU in dry solvent did not form a white precipitate. Thus, it was demonstrated that the failure of prior researchers to dry their DBU and solvents caused the formation of the white precipitation of the white solid, amidinium bicarbonate salt, which they mistakingly believed to be the zwitterionic DBU-CO₂

adduct. The results do not support the notion that a stable and isolable zwitterionic adduct between DBU and CO₂ forms either in the presence or absence of water.

A way to detect a possible DBU-CO₂ adduct would be through *in-situ* IR spectroscopy. There has been research examining the IR spectra of several bases in the presence of CO₂, with CO₂ dissolved in more than thirty-five organic solvents.⁷² The frequencies and bandwidths of the $\nu_3(\text{CO}_2)$ (asymmetric stretch) and $\nu_2(\text{CO}_2)$ (bend) were investigated. The bending mode of CO₂ changes and even separates into two bands in solutions of tertiary amides, tertiary amines and DMSO. The bending modes that appear at lower wavenumbers were assigned to CO₂-N-electron donor complexes. The change and split in the bending vibration was attributed to the nucleophile's lone pair directed to the CO₂ carbon atom. This report provided some evidence that a CO₂-adduct with DBU is possible.

Following the report from the Jessop lab, more recent articles have described the use of anhydrous conditions to study the release and capture of CO₂ by the use of solid and liquid state ¹³C NMR spectroscopy. González and co-workers studied the capture and release of CO₂ by amidines 1,5-diazabicyclo[4.3.0]non-5-ene (DBN) and 3,3,6,9,9-pentamethyl-2,10-diazobicyclo[4.4.0]dec-1-ene (PMDBD) using ¹³C solid-state NMR.⁷³ Specifically with DBN, the solid-state ¹³C NMR analysis showed that two DBN-CO₂ products formed, one that was suggested to be stable bicarbonate and the other unstable carbamate. The formation of carbamate is favoured in dry DBN, though in the presence of water it decomposes to form bicarbonate. Endo and co-workers investigated small monocyclic amidines which fixed CO₂ quantitatively under dry conditions where the bicarbonates were afforded after hydrolysis of the zwitterionic structures.⁶¹ They found by extensive solution ¹³C and ¹H NMR studies, that zwitterionic adduct formation with CO₂ was reversible and in equilibrium faster than the NMR time scale.⁶¹ Using the same dry conditions, Endo and co-workers did not observe the same equilibrium with DBU and DBN; they concluded that neither amidine could effectively trap CO₂.

1.4.3 First Isolated CO₂ Adduct with a Guanidine

Villiers and co-workers reported the first isolated adduct of CO₂ and a neutral nitrogen base, 1,5,7-triazabicyclo[4.4.0]dec-5-ene (TBD),⁷⁴ which supports the notion of the elusive zwitterionic DBU-CO₂ adduct. Before the isolation of the zwitterionic adduct, Villiers and co-workers isolated the bicarbonate salt of TBD in either THF or acetonitrile in the presence of ambient moisture (Figure 1.7). Colourless crystals of the bicarbonate salt formed after the suspension was heated under reflux. Under strictly anhydrous conditions, diffusion of CO₂ in a THF solution containing TBD led to the immediate formation of an off-white precipitate that was the isolated TBD-CO₂ adduct (Figure 1.8).⁷⁴ Colourless crystals were grown after the suspension was heated at 70 °C in a CO₂ atmosphere. Loss of CO₂ could be achieved by heating the crystals or powder of TBD-CO₂ to 40 °C under vacuum. ¹H NMR spectra in THF-*d*₈ revealed that in the presence of CO₂, the equilibrium shifted towards the complete formation of the CO₂ adduct. In the solid state, hydrogen bonding is important; three intermolecular CH...O hydrogen bonds are formed between the CO₂ moiety and three neighbouring TBD-CO₂ adducts. With the intramolecular O...H hydrogen bond, the oxygen participates in two hydrogen bonds, thus an induced stacking in the solid state is observed between TBD-CO₂ adducts. DBU-CO₂ has yet to be detected and if this adduct were to be isolated, it would not have the stability of TBD-CO₂.

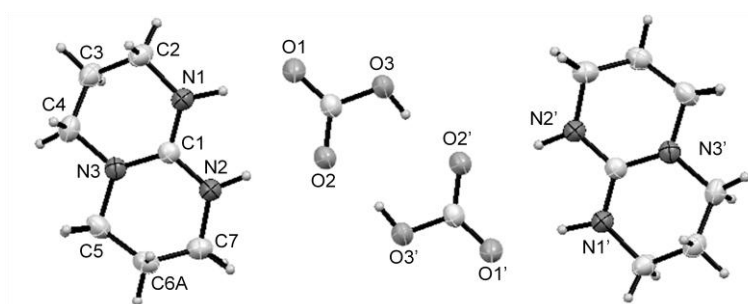


Figure 1.7. View of the TBD bicarbonate salt dimer. Displacement ellipsoids are drawn at 50% probability level. Only the position of the disordered C6 is represented.⁷⁴

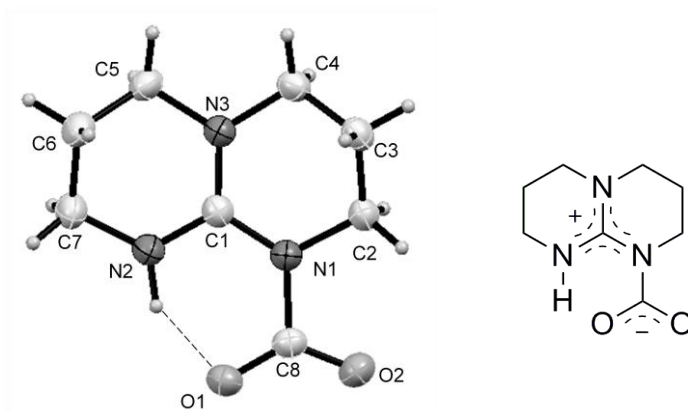
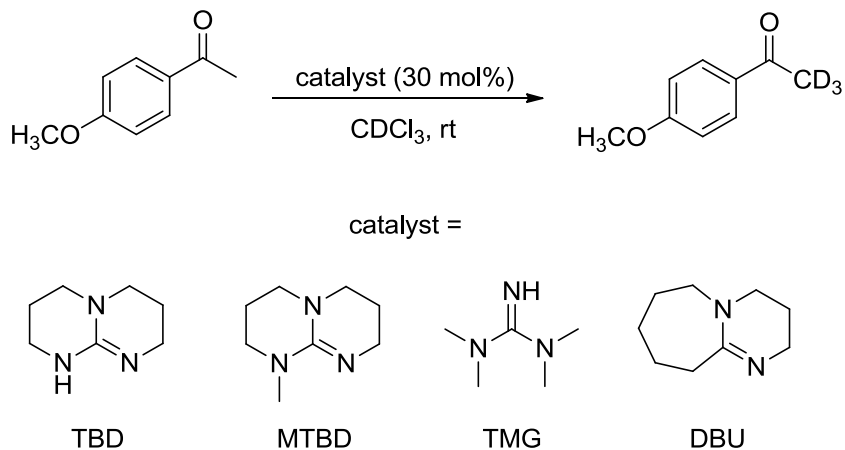


Figure 1.8. Molecular structure of the TBD-CO₂ zwitterionic adduct. Displacement ellipsoids are drawn at the 50% probability level.⁷⁴

The TBD-CO₂ adduct is the first zwitterionic species isolated with CO₂ and a guanidine base. There are some key structural aspects of the guanidine that facilitated the formation of such a CO₂ adduct. The guanidine structure features three nitrogen atoms, as opposed to one or two nitrogen atoms that are found in an amine or amidine respectively. Delocalization about the three nitrogen atoms in the protonated guanidine (or the CO₂ adduct) adds to the overall basicity of the guanidine structure. Additionally, the bound CO₂ molecule participates in an intramolecular hydrogen bond with the neighbouring N-H site. Villiers and co-workers studied the TBD-CO₂ structure further by looking at solution and solid state density functional theory (DFT) calculations. Villiers and co-workers found that only some interactions are present in the solid state. For example, three intermolecular hydrogen CH^{δ+}⋯O hydrogen bonds (with H^{δ+}⋯O in the range of 2.50 – 2.55 Å) are formed between the CO₂ moiety and three neighbouring TBD-CO₂ adducts.⁷⁴

The structure and electronics of TBD are noteworthy in that studies have shown that its hydrogen bonding can in part contribute to the reactivity of TBD for catalytic reactions. Prior to the isolation of the TBD-CO₂ adduct, Waymouth and co-workers described the hydrogen-bonding capability of TBD as an asset of the guanidine base.⁷⁵ TBD was a more active catalyst than 7-

methyl-1,5,7-triazabicyclo[4.4.0]dec-5-ene (MTBD) or DBU for lactide polymerization and catalyzes the ring-opening polymerization of δ -valerolactone and ϵ -caprolactone under conditions where MTBD and DBU are inactive.⁷⁵ The pK_{aH} of TBD (TBDH⁺, $pK_a = 26$), MTBD (MTBDH⁺, $pK_a = 25$), and DBU (DBUH⁺, $pK_a = 24$) in THF⁷⁶ are different, however their differences in activity implies that their basicity cannot be the only criterion to predict their catalytic activity. It was further determined by Waymouth and co-workers with mechanistic and theoretical studies that TBD can act both as a general base/H-bond donor and a nucleophile for transacylation reactions.⁷⁵ Mioskowski and co-workers looked at TBD and other bases for the H/D exchange for acidic substrates at room temperature.⁷⁷ On the basis of NMR studies, Mioskowski and co-workers proposed that TBD acts as a fast deuterium transfer catalyst with CDCl₃ and a ketone due to the labile proton on TBD. While TMG contains a potential labile N-H like that of TBD, there was no observed H/D exchange in CDCl₃ by ¹H NMR spectroscopy. The basicity of TBD is one order higher than MTBD. A methyl group of MTBD is in place of the N-H found on TBD, the deuterium exchange activity decreases. After 0.5 h, deuteration of 4'-methoxyacetophenone was low (9%) when MTBD was used as a catalyst, in comparison to the deuteration that is done with TBD as a catalyst (92%). DBU gave moderate deuteration of 4'-methoxyacetophenone in CDCl₃ at room temperature following 64 h (62%) (Scheme 1.9).



Scheme 1.9. Deuteration of 4'-methoxyacetophenone in CDCl_3 at room temperature with select examples of bases used for the study.⁷⁷

The structure of TBD and its capability for hydrogen bonding is apart from other similar guanidine structures.⁷⁴ The molecular structure of the bicarbonate salt of TBD that was isolated by Villiers and co-workers acts as an illustration of the hydrogen-bonding capability of TBD. Villiers and co-workers determined that while the dimeric structure of the bicarbonate salt is identical to that adopted by the amidinium bicarbonate $[\text{PMDBDH}]^+[\text{HCO}_3]^-$,⁷³ it does not match that of other guanidinium bicarbonates, $[\text{C}(\text{NH}_2)_3][\text{HCO}_3]^-$ ^{78a} and $[\text{TBNH}]^+[\text{HCO}_3]^-$ (TBN = 1,4,6-triazabicyclo[3.4.0]non-4-ene)^{78b}, where the guanidine hydrogen bonds to one or two bicarbonate anions respectively. In particular comparing the molecular structure of $[\text{TBNH}]^+[\text{HCO}_3]^-$ to that of $[\text{TBDH}]^+[\text{HCO}_3]^-$ (Figure 1.9) shows how the hydrogen bonding of TBN differs from that of TBD. The molecular structures of the bicarbonate salt of TBD and TBN contain two bicarbonate anion. The bonding of the dimerized bicarbonate is different among the two guanidines. In the $[\text{TBD}]^+[\text{HCO}_3]^-$ structure, the hydrogen bonding is distributed about two nitrogen sites and two of the oxygen atoms of a bicarbonate anion, while in $[\text{TBN}]^+[\text{HCO}_3]^-$ the hydrogen bonding is distributed between one nitrogen site and one oxygen atom of a bicarbonate anion. Villiers and

co-workers also note that the extended structures of the two guanidinium bicarbonates, $[\text{C}(\text{NH}_2)_3][\text{HCO}_3^-]$ and $[\text{TBNH}]^+[\text{HCO}_3^-]$, exist as infinite hydrogen-bonded chains where the cations alternate between either one or two bicarbonate anions.

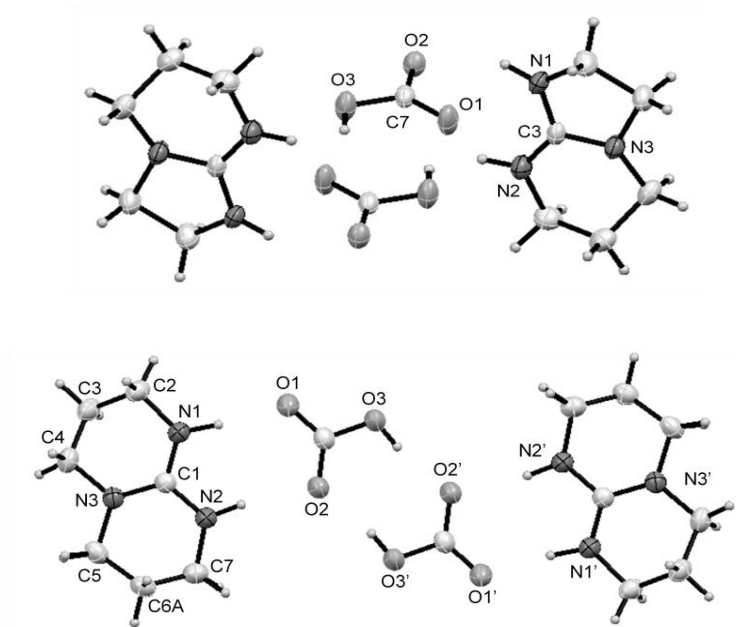


Figure 1.9. Top: Molecular structure of $[\text{TBNH}]^+[\text{HCO}_3^-]$.^{78b} Bottom: molecular structure of $[\text{TBDH}]^+[\text{HCO}_3^-]$.⁶⁴ Displacement ellipsoids are drawn at the 50% probability level.

The combination of studies from various researchers illustrates the nucleophilicity and hydrogen-bonding capability of TBD, thus relating to its reactivity with CO_2 . The insight into the reactivity of TBD provides information that could be important to the reactivity of other bases with CO_2 . The combined effort to investigate the reactivity of a single base, while the purposes for each author varied, is serendipitous. The information that was gathered could be useful for the design and development of other amidine- and guanidine-based substrates for CO_2 fixation and organocatalysts for CO_2 insertion.

Nucleophilicity and hydrogen-bonding capability could be inherent in other N-compounds studied within our lab, namely DBU. There is something that is inherent in the DBU structure which makes it an efficient base or organocatalyst for the activation of CO₂. Labile hydrogens could be accessible from the DBU-backbone that provide enough stabilization for the apparent DBU-CO₂ adduct, similar to either the intramolecular or intermolecular H-bonding interaction that stabilizes the TBD-CO₂ adduct.

1.5 Scope of Thesis

The objective of the thesis is the investigation of small molecule activation, of carbon dioxide and carbon disulfide for fixation and insertion into substrates that do not contain a metal centre. While DBU and alkylated acetamidines and guanidines have been implemented for various applications in the Jessop lab, there is still a search for other amidines and guanidines that would either be comparable or superior to the established N-containing bases we have used so far.

Within this thesis each chapter will begin with an introduction, outlining the various theoretical aspects and literature examples pertaining to the work that follows.

The second chapter will be an investigation of novel zwitterionic species created from secondary diamines and CO₂ in the search for new switchable polarity solvents. The initial survey will focus on secondary diamines that have various substituent groups on each nitrogen atom. The molecular structure of a diamine and CO₂, determined by X-ray crystallography, will represent the overall reactivity of the secondary diamines that are investigated by CO₂. Followed by the above investigation, an asymmetric diamine will be studied that contains one secondary nitrogen atom and one tertiary nitrogen atom. It will be clear that while there is only one example of a zwitterionic switchable polarity solvent, the gravimetric uptake of CO₂ of this compound is also exciting for the purposes of CO₂ capture.

The third chapter will describe the activation of carbon disulfide (CS₂), a small molecule that is isovalent to CO₂, by N-containing bases. While CS₂ is a toxic reagent, its sorption from

flue gas streams and utilization in organic synthesis is scientifically interesting both on its own and as an analogue to CO₂ chemistry. From the investigation of a previously reported reactivity of CS₂ and DBU, other amidines and guanidines were investigated where CS₂ reacts in a similar fashion or in an unforeseen manner depending on whether the structure of the N-containing compound is cyclic or acyclic in structure. What is common in the reactivity is C-H activation of the various N-bases. The majority of the chapter will focus on the isolated structures determined by X-ray crystallography, because NMR spectroscopy does not give intuitive information as to the structure of these new compounds. Secondly, further reactivity of formed amidine sulfur containing compounds will be demonstrated. The reactivity of CS₂ with N-containing compounds is strikingly different than what is observed with CO₂ at room temperature, although these results may provide further insight into the reactivity of CO₂ with related N-containing compounds.

The fourth chapter is multifaceted and emphasizes on the partnership of DBU and CO₂. It is divided into three areas of study that lead from a method developed in the Jessop lab for the synthesis of β-ketocarboxylic acids, from ketones, DBU, and CO₂: 1) whether the above process is feasible for the synthesis of α-amino acids starting from ketimines, 2) whether amidation of β-benzoylactic acid, which is made from the above method, can occur by the use of a boronic acid catalyst and 3) the eventual lead-up to investigate the same boronic acid catalyst for the formation of tetraalkylated ureas. These studies can act as a stepping stone to the creation of cheaper syntheses for useful industrial products and without use of toxic reagents.

1.6 References

- 1) Hammond, G. P.; Akwe, S. S. O. *Int. J. Energy Res.* **2007**, *31*, 1180 – 1201.
- 2) Stewart C, Hessami M. *Energy Convers. Manage.* **2005**, *46*, 403 – 420.
- 3) Aresta, M. *Carbon Dioxide as Chemical Feedstock*; Wiley –VCH, Weinheim, 2010, pp. 8 – 9.
- 4) H. Yang, H.; Xu, Z.; Fan, M.; Gupta, R.; Slimane, R. B.; Bland, A. E.; Wright, I. J. *Environ. Sci.* **2008**, *20*, 14 – 27.
- 5) Bello, A.; Idem, R.O. *Ind. Eng. Chem. Res.* **2005**, *44*, 945 – 969.
- 6) Kennard, M.L.; Meisen, A. *Hydrocarbon Process. Int. Ed.* **1982**, *59*, 103 – 106.
- 7) Chakma, A.; Meisen, A. *J. Chromatogr. A* **1988**, *457*, 287 – 297.
- 8) Chakma, A.; Meisen, A. *Can. J. Chem. Eng.* **1997**, *75*, 861 – 871.
- 9) Kohl, A. L.; Riesenfeld, F. C. *Gas Purification*; 2nd edn. Gulf Publishing Company, Houston, 1974.
- 10) Renard, J.J.; Calidonna, S. E.; Henley, M. V. *J. Hazard. Mater.* **2004**, *108*, 29 – 60.
- 11) MacDowell, N.; Florin, N.; Buchard, A. Hallett, J.; Galindo, A.; Jackson, G.; Adjiman, C. S.; Williams, C. K.; Shah, N.; Fennell, P. *Energy Environ. Sci.* **2010**, *3*, 1645 – 1669.
- 12) Shannon, M. S.; Bara, J. E. *Sep. Sci. Technol.* **2012**, *47*, 178 – 188.
- 13) Harlick, P. J. E.; Sayari, A. *Ind. Eng. Chem. Res.* **2007**, *46*, 446 – 458.
- 14) MacKenzie, A.; Granatstein, D. L.; Anthony, E. J.; Abanades. J. C. *Energy Fuels* **2007**, *21*, 920 – 6.
- 15) Benson, S. M.; Cole, D. R. *Elements* **2008**, *4*, 325 – 331.
- 16) DOE (Department of Energy). Carbon Sequestration Atlas of the United States and Canada Online. National Energy and Technology Laboratory, Morgantown, WV, http://www.netl.doe.gov/technologies/carbon_seq/refshelf/atlasIII (accessed Oct 5, 2013).
- 17) Herzog, H. J. *Environ. Sci. Technol.* **2001**, *35*, 148A – 153A.
- 18) Li, L.; Zhao, N.; Wei, W.; Sun, Y. *Fuel* **2013**, *108*, 112 – 130.
- 19) Chen, Y.; Brown, P. H.; Hu, K.; Black, R. M.; Prior, R. L.; Ou, B.; Chu, Y.-F. *J. Food Sci.* **2011**, *76*, H182 – 186.
- 20) Aresta, M.; Forti, G. Eds. *Carbon Dioxide as a Source of Carbon*; NATO ASI Series, D; Reidel: Dordrecht, The Netherlands, 1987.
- 21) Todd, M. R.; Grand, G. W. *Energy Convers. Mgmt* **1993**, *34*, 1157 – 1164.
- 22) Xiaoding, X.; Moulijn, J. A. *Energy Fuels* **1996**, *10*, 305 – 325.
- 23) Steiner, R. W. *Chem. Eng.* **1993**, *100*, 114 – 119.

- 24) Sakakura, T.; Choi, J.-C.; Yasuda, H. *Chem. Rev.* **2007**, 2365 – 2387.
- 25) Mikkelsen, M.; Jørgensen, M.; Krebs, F. C. *Energy Environ. Sci.* **2010**, 3, 43 – 81.
- 26) Olah, G. A.; Goeppert, A.; Prakash, G. K. S. *J. Org. Chem.* **2009**, 74, 487 – 498.
- 27) Riduan, S. N.; Zhang, Y. *Dalton Trans.* **2010**, 39, 3347 – 3357.
- 28) Hasnain, Z.; Lamb, C. A.; Ross, S. D. *Acta Astronautica* **2012**, 81, 523 – 531.
- 29) Dalko, P. I.; Moisan, L. *Angew. Chem. Int. Ed.* **2004**, 43, 5138 – 5175.
- 30) Kim, H. S.; Kim, J. J.; Lee, B. G.; Jung, O. S.; Jang, H. G.; Kang, S. O. *Angew. Chem. Int. Ed.* **2000**, 39, 4096 – 4098.
- 31) Alvaro, M.; Baleizao, C.; Das, D.; Carbonell, E.; García, H. *J. Catal.* **2004**, 228, 254 – 258.
- 32) Chatelet, B.; Joucla, L.; Dutasta, J.-P.; Martinez, A.; Szeto, K. C. *J. Am. Chem. Soc.* **2013**, 135, 5348 – 5351.
- 33) Wang, Y.-B.; Wang, Y.-M.; Zhang, W.-Z.; Lu, X.-B. *J. Am. Chem. Soc.* **2013**, 135, 11996 – 12003.
- 34) J. D. Holbrey, W. M. Reichert, I. Tkatchenko, E. Bouajila, O. Walter, I. Tommasi, R. D. Rogers, *Chem. Commun.* **2003**, 28 – 29.
- 35) H. A. Duong, T. N. Tekavec, A. M. Arif, J. Louie, *Chem. Commun.* **2004**, 112 – 113.
- 36) Riduan, S. N.; Zhang, Y.; Ying, J. Y. *Angew. Chem. Int. Ed.* **2009**, 48, 3322 – 3325.
- 37) Deglmann, P.; Ember, E.; Hofman, P.; Pitter, S.; Walter, O. *Chem. Eur. J.* **2007**, 13, 2864 – 2879.
- 38) Jansen, A.; Görls, H.; Pitter, S. *Organometallics* **2000**, 19, 135.
- 39) Jansen, A.; Pitter, S. *J. Mol. Catal. A* **2004**, 217, 41 – 45.
- 40) a) Ménard, G.; Stephan, D. W. *J. Am. Chem. Soc.* **2010**, 132, 1796 – 1797. b) Ashley, A. E.; Thompson, A. L.; O'Hare, D. *Angew. Chem. Int. Ed.* **2009**, 48, 9839 – 9843.
- 41) Momming, C.; Otten, M.; Kehr, E. G.; Fröhlich, R.; Grimme, S.; Stephan, D. W.; Erker, G. *Angew. Chem. Int. Ed.* **2009**, 48, 6643–6646.
- 42) Peuser, I.; Neu, R. C.; Zhao, X.; Ulrich, M.; Schirmer, B.; Tannert, J. A.; Kehr, G.; Fröhlich, R.; Grimme, S.; Erker, G.; Stephan, D. W. *Chem. Eur. J.* **2011**, 17, 9640 – 9650.
- 43) (a) Boudreau, J.; Courtemanche, M.-A.; Fontaine, F.-G. *Chem. Commun.* **2011**, 47, 11131 – 11133. (b) Appelt, C.; Westenberg, H.; Bertini, F.; Ehlers, A. W.; Sloatweg, J. C.; Lammertsma, K.; Uhl, W. *Angew. Chem. Int. Ed.* **2011**, 50, 3925 – 3928.
- 44) Berkefeld, A.; Piers, W. E.; Parvez, M. *J. Am. Chem. Soc.* **2010**, 132, 10660 – 10661.

- 45) Courtemanche, M.-A.; Légaré, M.-A.; Maron, L.; Fontaine, F.-G. *J. Am. Chem. Soc.* **2013**, *135*, 9326 – 9329.
- 46) Jessop, P. G.; Mercer, S. M.; Heldebrant, D. J. *Energy Environ. Sci.* **2012**, *5*, 7240 – 7253.
- 47) Jessop, P. G.; Phan, L.; Carrier, A.; Robinson, S.; Dürr, C. J.; Harjani, J.R. *Green Chem.* **2010**, *12*, 809 – 814.
- 48) Jessop, P. G.; Kozycz, L.; Rahami, Z. G.; Schoenmakers, D.; Boyd, A. R.; Wechsler, D.; and Holland, A. M. *Green Chem.* **2011**, *13*, 619 – 623.
- 49) Mercer, S. M.; Jessop, P. G. *ChemSusChem* **2010**, *3*, 467 – 470.
- 50) Lau, Y.Y., M. Sc. Thesis, Queen's University, 2010.
- 51) Chen, C.-S.; Lau, Y. Y.; Mercer, S. M.; Robert, T.; Horton, J. H.; Jessop, P. G. *ChemSusChem* **2013**, *6*, 132 – 140.
- 52) Liu, Y.; Jessop, P. G.; Cunningham, M.; Eckert, C. A.; Liotta, C. L. *Science*, **2006**, *313*, 958 – 960.
- 53) Jessop, P. G. US Patent Application, 11/599,623, 2006.
- 54) Lottermoser, *Trans. Faraday Soc.* **1935**, *31*, 200 – 204.
- 55) Liang, C., M. Sc. Thesis, Queen's University, 2010.
- 56) Ceschia, E., M. Sc. Thesis, Queen's University, 2010.
- 57) Scott, L. M.; Robert, T.; Harjani, J. R.; Jessop, P. G. *RSC Advances* **2012**, *2*, 4925 – 4931.
- 58) Tracking industrial energy efficiency and CO₂ emissions, International Energy Agency, Paris, France, **2007**.
- 59) a) Benson, E. E.; Kubiak, C. P.; Sathrum, A. J.; Smieja, J. M. *Chem. Soc. Rev.* **2009**, *38*, 89–99; b) Wang, W.; Wang, S. P.; Ma, X.B.; Gong, J. L. *Chem. Soc. Rev.* **2011**, *40*, 3703 – 3727.
- 60) (a) George, M.; Weiss, R. G. *J. Am. Chem. Soc.* **2001**, *123*, 10393 – 10394. ; (b) Carretti, E.; Dei, L.; Baglioni, P.; Weiss, R. G. *J. Am. Chem. Soc.* **2003**, *125*, 5121 – 5129.; (c) Dell'Amico, D. B.; Calderazzo, F.; Labella, L.; Marchetti, F.; Pampaloni, G. *Chem. Rev.* **2003**, *103*, 3857 – 3898.; (d) Blasucci, V.; Dilek, C.; Huttenhower, H.; John, E.; Llopis-Mestre, V.; Pollet, P.; Eckert, C. A.; Liotta, C. L. *Chem. Commun.* **2009**, 116 – 118.
- 61) a) Zhang, X.; Jia, Y.-B.; Lu, X.-B.; Li, B.; Wang, H.; Sun, L.-C. *Tetrahedron Lett.* **2008**, *49*, 6589 – 6592. b) Cota, I.; Medina, F.; Sueiras, J. E.; Tichit, D. *Tetrahedron Lett.* **2011**, *52*, 385 – 387. c) Yang, Z.-Z.; Li, Y.-N.; Wei, Y.-Y.; He, L.-N. *Green Chem.* **2011**, *13*,

- 2351 – 2353. d) Aoyagi, N.; Furusho, Y.; Sei, Y.; Endo, T. *Tetrahedron* **2013**, *69*, 5476 – 5480.
- 62) Corr, M.J.; Gibson, K. F.; Kennedy, A. R.; Murphy, J. A. *J. Am. Chem. Soc.*, **2009**, *131*, 9174 – 9175.
- 63) a) Waldman, T. E.; McGhee, W. *J. Chem. Soc. Chem. Commun.* **1994**, 957 – 958. b) McGhee, W.; Pan, Y.; Riley, D. P. *J. Chem. Soc., Chem. Commun.* **1994**, 699 – 700. c) McGhee, W.; Riley, D. *J. Org. Chem.* **1995**, *60*, 6205 – 6207.
- 64) a) Guiducci, A. E.; Boyd, C. L.; Mountford, P. *Organomet.* **2006**, *25*, 1167 – 1187. b) Shi, M.; Xu, Y.-M.; Zhao, G.-L.; Wu, X.-F. *Eur. J. Org. Chem.* **2002**, 3666 – 3679.
- 65) a) Haruki, E.; Arakawa, M.; Matsumura, M.; Otsuji, Y.; Imoto, E. *Chem. Lett.* **1974**, 427 – 428. b) McGhee, W.; Riley, D. *J. Org. Chem.* **1995**, *60*, 6205 – 6207. c) Mizuno, T.; Okamoto, N.; Ito, T.; Miyata, T. *Tetrahedron Lett.* **2000**, *41*, 1051 – 1053. d) Dinsmore, C. J.; Mercer, S. P.; *Org. Lett.* **2004**, *6*, 2885 – 2888. e) Kishimoto, Y.; Ogawa, I. *Ind. Eng. Chem. Res.* **2004**, *43*, 8155 – 8162. f) Paddock, R. L.; Hiyama, Y.; McKay, J. M.; Nguyen, S. T. *Tetrahedron Lett.* **2004**, *45*, 2023 – 2026.
- 66) Iwatani, M.; Kudo, K.; Sugita, N.; Takezaki, Y. *Sekiyu Gakkaishi*, **1978**, *21*, 290.
- 67) Pérez, E. R.; Santos, R. H. A.; Gambardella, M. T. P.; de Macedo, L. G. M.; Rodrigues-Filho, U. P.; Launay, J. C.; Franco, D. W. *J. Org. Chem.* **2004**, *69*, 8005 – 8011.
- 68) a) Pérez, E. R.; da Silva, M. O.; Costa, V. C.; Rodrigues-Filho, U.P.; Franco, D. W. *Tetrahedron Lett.* **2002**, *43*, 4091 – 4093. b) Endo, T.; Nagai, D.; Monma, T.; Yamaguchi, H.; Ochiai, B. *Macromolecules* **2004**, *37*, 2007 – 2009. c) Barkakaty, B.; Morino, K.; Sudo, A.; Endo, T. *Green Chem.* **2010**, *12*, 42 – 44. d) Ochiai, B.; Yokota, K.; Fujii, A.; Nagai, D.; Endo, T. *Macromolecules*, **2008**, *41*, 1229 – 1236.
- 69) Heldebrant, D. J.; Jessop, P. G.; Thomas, C. A.; Eckert, C. A.; Liotta, C. L. *J. Org. Chem.* **2005**, *70*, 5335 – 5338.
- 70) Bernitt, D. L.; Hartman, K. O.; Hisatsune, I. C. *J. Chem. Phys.* **1965**, *42*, 3553 – 3558.
- 71) Benetollo, F.; Bertani, R.; Ganis, P.; Pace, G.; Pandolfo, L.; Zanotto, L. *J. Organomet. Chem.* **2002**, *642*, 64 – 70.
- 72) a) Dobrowolski, J. Cz.; Jamróz, M. H. *J. Mol. Struct.* **1992**, *275*, 211 – 219. b) Meredith, J. C.; Johnston, K. P.; Seminario, J. M.; Kazarian, S. G.; Eckert, C. A. *J. Phys. Chem.*, **1996**, *100*, 10837 – 10848.
- 73) Pereira, F. S.; da Silva Agostini, D. L.; do Espírito Santo, R. D.; de Azevedo, E. R.; Bonagamba, T. J.; Job, A. E.; González, E. R. P. *Green Chem.* **2011**, *13*, 2146 – 2153.

- 74) Villiers, C.; Dognon, J.-P.; Pollet, R.; Thuéry, P.; Ephritikhine, M. *Angew. Chem. Int. Ed.* **2010**, *49*, 3465 – 3468.
- 75) Kiesewetter, M. K.; Scholten, M. D.; Kirn, N.; Weber, R. L.; Hedrick, J. L.; Waymouth, R. M. *J. Org. Chem.* **2009**, *74*, 9490 – 9496.
- 76) Kaljurand, I.; Kütt, A.; Sooväli, L.; Rodima, T.; Mäemets, V.; Leito, I.; Koppel, I. A. *J. Org. Chem.* **2005**, *70*, 1019 – 1028.
- 77) Sabot, C.; Kumar, K. A.; Antheaume, C.; Mioskowski, C. *J. Org. Chem.* **2007**, *72*, 5001 – 5004.
- 78) a) D. A. Baldwin, L. Denner, T. J. Egan, A. J. Markwell, *Acta Crystallogr. Sect. C* **1986**, *42*, 1197 – 1199; b) F. A. Cotton, C. A. Murillo, X. Wang, C. C. Wilkinson, *Inorg. Chem.* **2006**, *45*, 5493 – 5500.

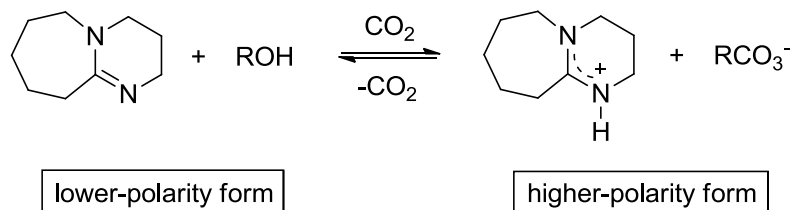
Chapter 2

The Search for Zwitterionic Switchable-Polarity Solvents

2.1 Introduction

2.1.1 Two-Component Switchable Polarity Solvents with Base/Alcohol Mixtures

Switchable polarity solvents (SPS) that have been developed in the Jessop lab have can be applicable for industry-scale reactions. Each SPS offers two polarities, and can switch between the two using CO₂ as trigger. CO₂ is preferred as a trigger because it is inexpensive, benign and can be easily removed. The original SPS that was published by our group was a two-component system, consisting of DBU and an alcohol (Scheme 2.1).¹ Switching from the ionic form (higher polarity) back to the neutral form (lower polarity) is triggered by removal of CO₂ which can be easily achieved by either bubbling an inert gas into the solution or heating the solution to 60 °C.



Scheme 2.1. DBU and alcohol switchable-polarity solvent.¹

The molecular structure of DBU in the presence of methanol and CO₂ was determined *via* X-ray crystallography. The molecular structure shows the alkylcarbonate anion hydrogen bonding to the protonated nitrogen centre of DBU (Figure 2.1).^{1b}

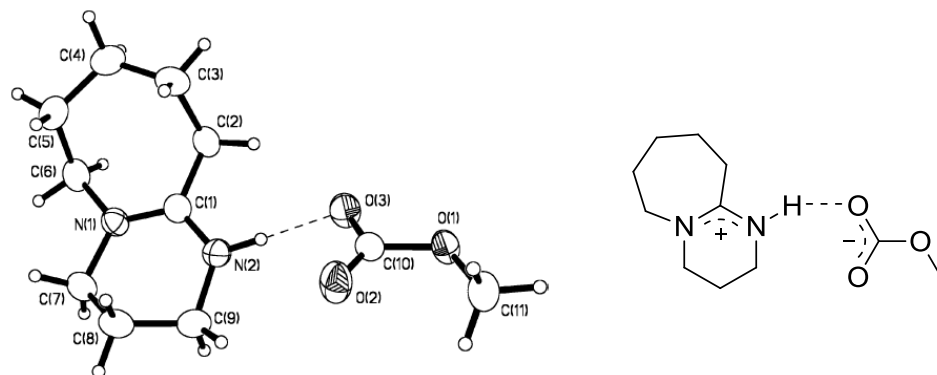
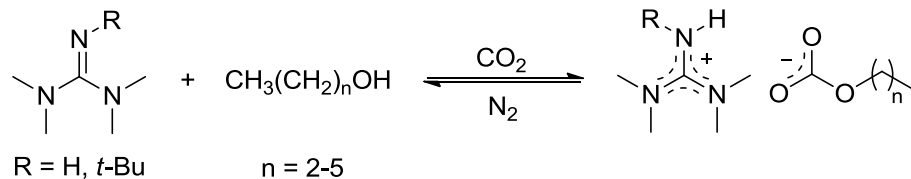


Figure 2.1. Molecular structure of [DBUH][O₂COMe]. Displacement ellipsoids for non-hydrogen atoms are shown at the 50% probability level and H atoms are represented by circles of arbitrary size.^{1b}

From this, Jessop and co-workers have been able to demonstrate that other similar mixtures of a base, such as an amidine or guanidine, and an alcohol – could serve as SPS. Alkylcarbonic acids that result from attack of the alcohol on CO₂ could be reversibly trapped as liquid alkylcarbonate salts when in the presence of amidines or guanidines.^{1b,2a-c} A tetraalkylated and pentaalkylated guanidine shown below, exhibits the same reactivity as that of the two component system DBU/alcohol (Scheme 2.2). Not only can these mixtures be used as switchable solvents but they can also be used as solvents for CO₂ capture and release; when used for that purpose, they are called CO₂-binding organic liquids (CO₂BOLs) rather than SPS.



Scheme 2.2. Guanidines and alcohol switchable solvent system.^{3a-c}

Similar reactivity is likely to extend to other Lewis acidic gases that are isovalent to CO₂, such as COS and CS₂. Both COS and CS₂ have a central electrophilic carbon and exhibit the same reactivity as CO₂ in the presence of both DBU and an alcohol, resulting in the formation of analogous structures, COSBOL and CS₂BOL (Figure 2.2).^{2c} Sulfur dioxide (SO₂) which is chemically different from CO₂, COS, and CS₂, nevertheless showed similar reactivity forming the SO₂BOL, where the reactivity was attributed to the electrophilic sulfur atom (Figure 2.2). X-ray crystallography determined the molecular structure of the product from the reaction of CS₂, DBU, and benzyl alcohol (Figure 2.3).^{2c} The reverse reaction to remove such Lewis acid gases was afforded by thermolysis at temperatures above that to remove CO₂, a range between 100 – 150 °C. Base/alcohol combinations reversibly bind CO₂, COS, and CS₂.

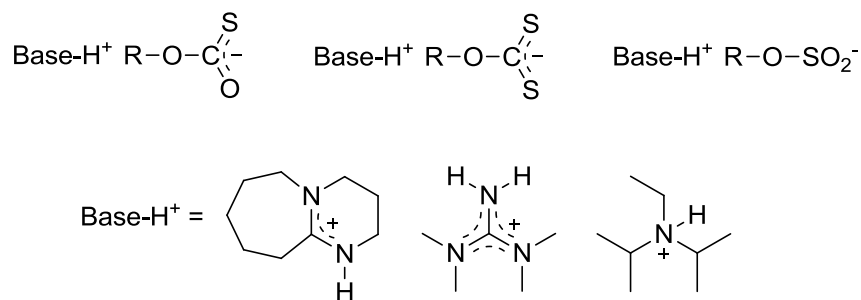


Figure 2.2. Starting from left: COSBOL, CS₂BOL, and SO₂BOL salts.^{2c}

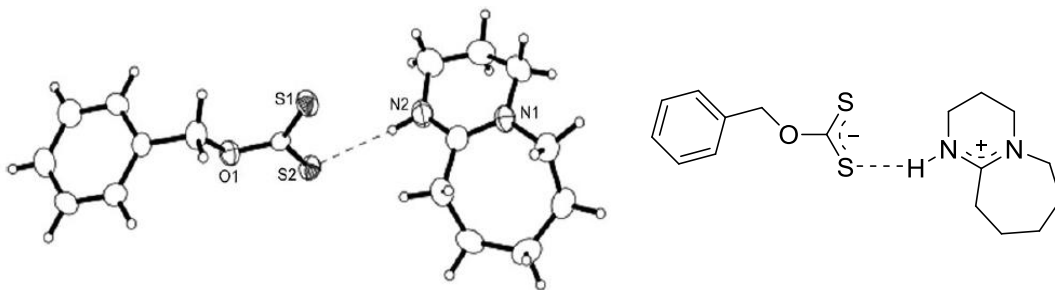
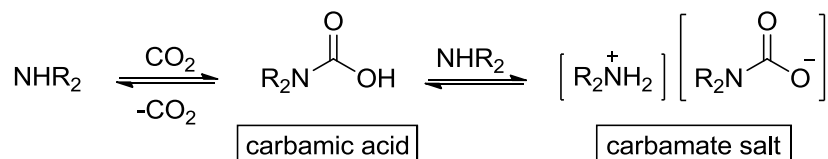


Figure 2.3. Molecular structure of [DBUH⁺][S₂COCH₂Ph]. Displacement ellipsoids for non-hydrogen atoms are shown at the 50% probability level and H atoms are represented by circles of arbitrary size.^{2c}

2.1.2 Secondary Amines as One-Component SPS

Carbamate salts *via* carbamic acids can be formed from the reaction of primary or secondary amines with CO₂ (Scheme 2.3).⁴ Most liquid primary amines such as alkylamines,^{5b,6} allylamine,^{7a} piperidine,⁸ pyrrolidine,⁸ and benzylamine^{7b} form solid carbamate salts in the presence of CO₂; therefore, these amines would not be useful as SPS.



Scheme 2.3. Reactivity of secondary and primary amines with CO₂.⁴

Some secondary amines can act as single-component SPSs, where the amine is both the proton donor and proton acceptor. It was found that CO₂ can trigger four liquid secondary amines in their lower polarity form (namely *N*-ethyl-*N*-butylamine, *N*-methyl-*N*-propylamine, dipropylamine, and benzylmethylamine) into higher polarity liquid carbamate salts, showing that these amines can serve as SPS.⁴ To switch back to the low polarity neutral form, CO₂ can be thermally removed from the liquid carbamate salts by heating the viscous carbamate liquid to 60 °C and purging it with N₂.

SPS offer two polarities, swinging back and forth between the two by the addition and removal of CO₂, though SPS that provides a larger polarity swing would broaden the utility of SPS in an industrial process. The polarities of some SPS in their lower and higher polarity forms have been measured by use of a solvatochromic probe, Nile red. The wavelength or maximum absorbance of a solution of the dye changes towards longer wavelength in the visible spectrum if the solvent increases in polarity. The UV shift is recorded before and after the addition of CO₂; the change in wavelengths gives a representation of the polarity swing. Figure 2.4 shows a range of wavelengths and therefore polarity ranges afforded by some of the secondary amines and

base/alcohol systems in comparison to some conventional solvents. Base/alcohol systems in their non-polar form are close to that of chloroform. Secondary amine SPS cover lower polarity ranges since primary and secondary amines are generally less polar than alcohols.

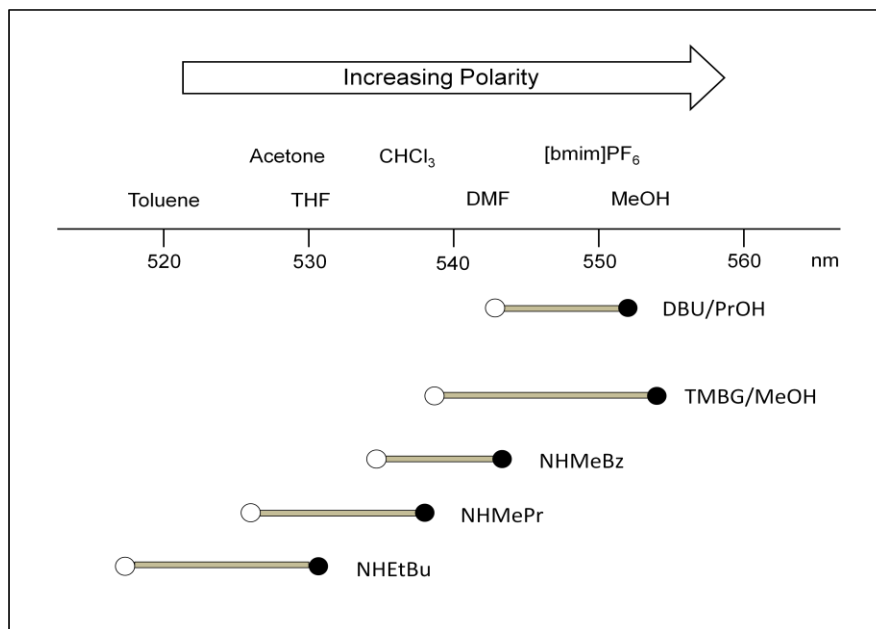


Figure 2.4. A comparison of the polarity ranges of several SPS (white circles indicate the low-polarity form, black circles indicate the high polarity form). The scale is the λ_{\max} for Nile red solvatochromic dye dissolved in the solvent. Select traditional solvents are indicated above the scale for comparison ($[\text{bmim}]\text{PF}_6$ = 1-butyl-3-methylimidazolium hexafluorophosphate).⁴

2.1.3 SPS for Reaction Media, Extraction and CO₂ Capture Agents

A solvent having the ability to change from one polarity to another, afforded by a single trigger, have several avenues of applications. The earliest examples of SPS have been demonstrated to be useful as reaction media,^{1b,4 9-10} for extraction,^{11,12} and for CO₂ capture.^{2,3} In the following paragraphs SPS used as reaction media and for extraction will be briefly discussed emphasizing on early examples of SPS to illustrate the play on solubility, while more recent examples of SPS for CO₂ capture will be discussed in Section 2.2.

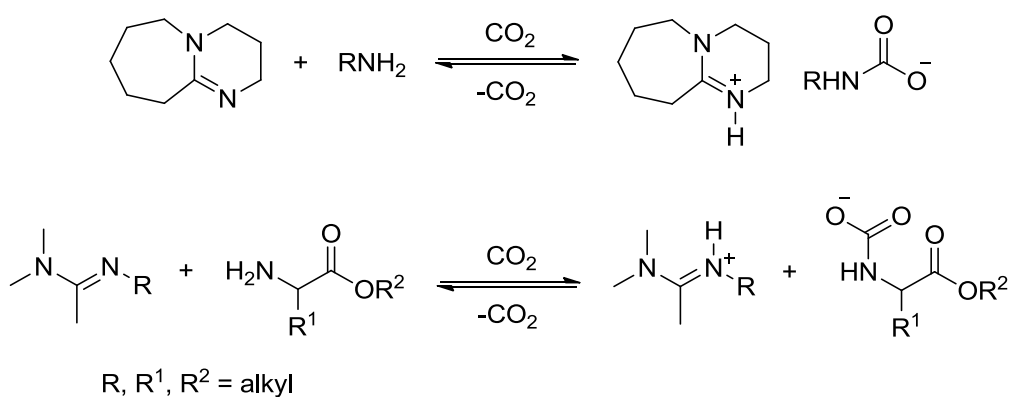
A change in polarity is a clear advantage for post-reaction separations. Depending on the characteristics of the chosen SPS, the product or catalyst in the SPS will either remain soluble or become insoluble when the solvent polarity is triggered to change. One SPS (DBU/1-propanol mix) has been used as the reaction medium, in its low polarity form, for the polymerization of styrene. The solvent in its high polarity form precipitates the polymer.^{1b} An extension of the above method is by Darensbourg and co-workers that were able to separate a Cr-catalyst from their polycarbonate by using a SPS (*N*-ethyl-*N*-butylamine).⁴ Prior to this, post-polymerization, the Darensbourg group would add HCl to cleave the Cr-catalyst from the polymer. With the use of the above SPS, the formation of the carbamic acid facilitated cleavage and liberation of the active Cr-catalyst from the polymer, where the catalyst can be reused.⁴ The solubility of product or catalyst in a SPS has been extended to other useful organic transformations.^{9,10}

As an extraction medium, SPS have been shown to extract oil from dry soybeans¹¹ and freeze-dried algae.¹² For the extraction of soybean oil, methylbenzylamine and DBU/alcohol mixtures were able to extract oil from soybeans.¹¹ Sartorì and co-workers used DBU/alcohol mixtures for the extraction of lipids and fatty acids from algae.¹² In particular, the DBU/1-octanol was able to extract 16% by weight of lipids from freeze-dried algae, more than the conventionally used *n*-hexane which extracted 7.8% by weight. It was found that the DBU/1-octanol system was sensitive to water, where the system needed to be dried prior to CO₂ addition in order to prevent formation of solid bicarbonate salt of DBU.

2.1.4 Drawbacks of Base/Alcohol and Secondary Amine SPS

The earliest examples of SPS that afford a polarity change triggered by CO₂ have clear advantages as reaction media^{1b,4, 9-10} and for extraction,^{11,12} but there are some disadvantages that need to be addressed. These disadvantages include, small polarity swing, water sensitivity, high volatility, and low robustness.

The amidine/alcohol and guanidine/alcohol SPS have some limitations that may inhibit their use in industry. These two-component systems are water-sensitive, in the sense that the presence of water promotes the formation of solid bicarbonate salt which is thermodynamically preferred over the alkylcarbonate salt. The bicarbonate salt is a solid, which is not a desirable characteristic for a solvent. While the bicarbonate salt is not a problem if the water is in large excess (the salt is water-soluble), the formation of the salt is problematic in situations where water is not in large excess. To prevent the formation of bicarbonate, the amidine or guanidine must be dried before use. One method to address the water-sensitivity issue was exchanging the alkylcarbonate anions for carbamate anions. When amidine/amine or guanidine/amine mixtures are used as SPS, carbamate salts are formed which are thermodynamically more stable than bicarbonate and alkylcarbonate salts (Scheme 2.4, top scheme).⁵ It was shown by Weiss and coworkers⁵ that an amidine/primary amine SPS is less water sensitive than an amidine/alcohol SPS. They further demonstrated that a chiral SPS can be generated by employing amino acids as the amine component (Scheme 2.4, bottom scheme).^{5b}



Scheme 2.4. Amidine and amine combination as SPS.

The secondary amines or some of the alcohols partnered with amidines or guanidines in SPS are somewhat volatile, so that after removal of CO₂, switching back to the lower polarity

form, the component ratio has changed, which diminishes the recyclability of the SPS. In an industrial process, controlling the base/alcohol ratio could be cumbersome. There are many secondary amines that are of a lower molecular weight and gave liquid carbamate salts, such as ethylmethanamine, diethanamine, and methylpropylamine. These secondary amines of lower molecular weight would not be useful as SPS in industry since these amines are very volatile.

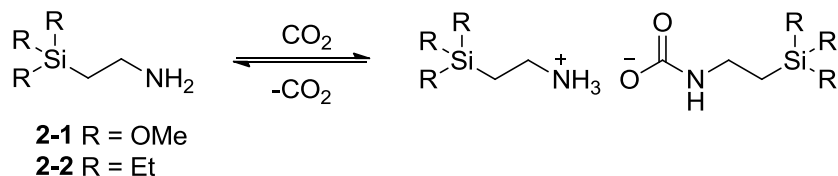
There are financial, environmental, and health costs associated with the use of a volatile solvent in an industrial process. The volatility of a compound directly affects the solvent concentration and having to add fresh solvent to a process is cumbersome, costly, and contributes to waste. Flammability is partnered with volatility; the use of very flammable reagents would create an unsafe work environment. In addition, some of the amine and amidine or guanidine/alcohol mixtures are subject to decomposition due to hydrolysis. Secondary amine SPS have the advantage over base/alcohol systems in that they are less water sensitive, though they are more flammable.

2.2 Zwitterionic SPS for CO₂ Capture

2.2.1 Zwitterionic SPS

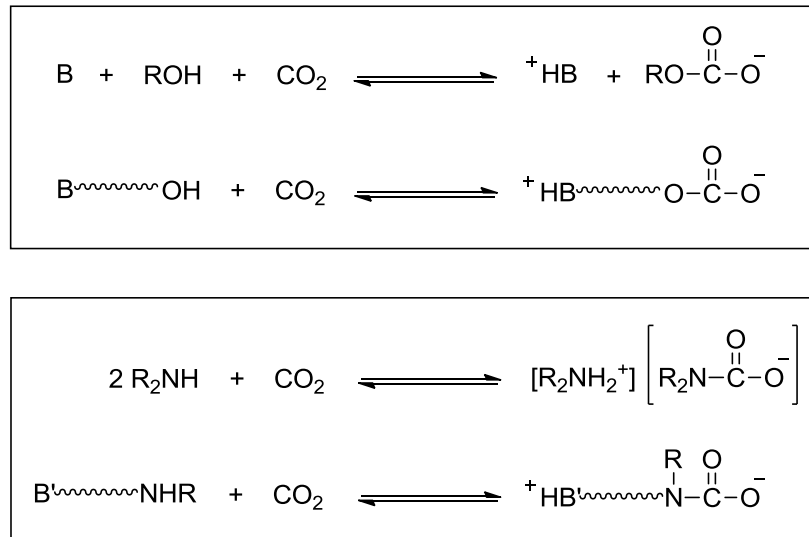
The first generation SPS consisted of one CO₂-binding group (the alcohol or one equivalent of amine) and a base (amidine or guanidine or a second equivalent of secondary amine) and the capability for these systems to capture CO₂ varied. Jessop and co-workers have been able to demonstrate that amidine or guanidine/alcohol mixtures could reversibly capture and release CO₂, in addition these liquids exhibited high gravimetric CO₂ capacity.^{2a-c} Some of the base/alcohol systems would not be industrially viable due to the volatility of the organic bases and alcohols. Carbamate SPS are more appealing for CO₂ capture since they are less water sensitive and in some cases are cheaper than base/alcohol SPS. Primary amines as single-component carbamate systems were later developed by Eckert and Liotta's group where siloxylated ethanamines, like the one shown in Scheme 2.5, were able to reversibly capture CO₂

from flue gas.^{9a} At high temperatures, the CO₂ stripping would lead to the hydrolysis of Si-O linkages. Eckert and Liotta have improved their system by synthesizing trialkylsilylpropylamines with more robust Si-C bonds.^{9b}



Scheme 2.5. Siloxated ethanolamines.⁹

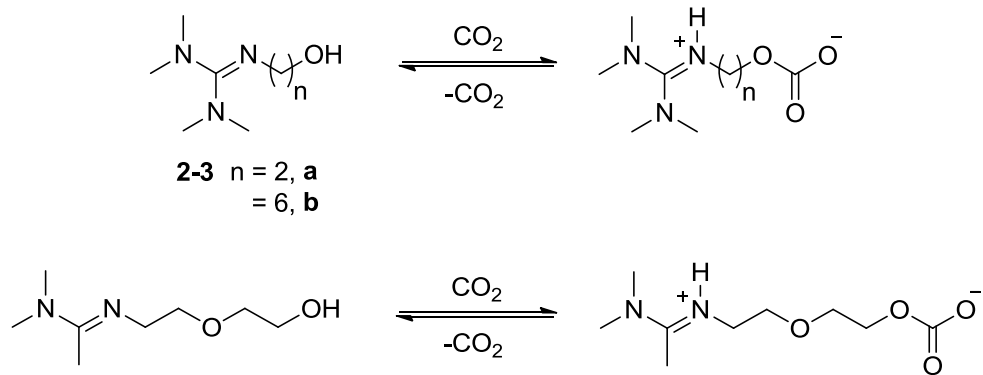
Incorporating the CO₂-binding group and a basic functional group into one molecule would create as a single-component SPS based upon the two-component base/alcohol SPS. By incorporating amine and alcohol into the same molecule, the addition of CO₂ creates a zwitterionic species in solution. The addition of CO₂ creates a negatively charged alkylcarbonate group and a positively charged nitrogen centre (Scheme 2.5). Single-component SPS derived from alkanolamidines, alkanolguanidines, and diamines have the potential to address the disadvantages that are associated with amine and base/alcohol SPS, as described in the previous section. Diamines have lower volatility and are more robust than secondary amine SPS. They are also less water sensitive, like secondary amines, in contrast to the base/alcohol SPS.



Scheme 2.6. Comparison of SPS systems, top: two- and single-component base/alcohol, bottom: secondary amines and diamines, (---) represents linker.

2.2.2 Alkanolamidines and Alkanolguanidines for CO₂ Capture

Alkanolamidines and alkanolguanidines were concurrently developed by Heldebrant and co-workers¹³ that have an alcohol and base incorporated into one molecule and form switchable zwitterionic species upon the addition of CO₂ (Scheme 2.7). Upon the addition of CO₂ an increase in solution viscosity (>2000 cP) is observed due to the formation of the corresponding alkylcarbonate salts. The species were non-volatile, although because of the high viscosity the diffusion of CO₂ through the material is low and as a result lower CO₂ uptake is observed in comparison to the two-component base/alcohol mixtures.



Scheme 2.7. Alkanolamidines and alkanolguanidines for CO₂ capture.¹³

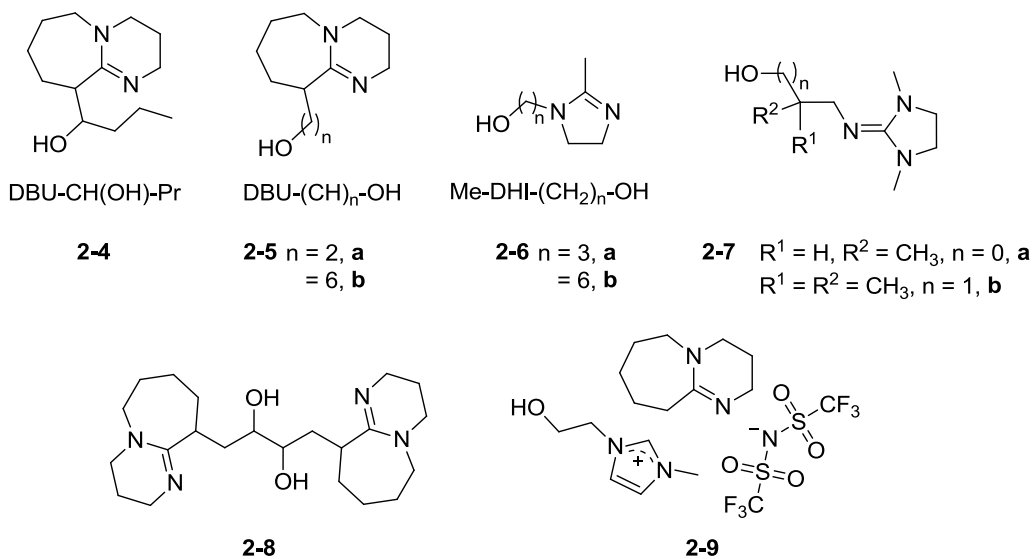


Figure 2.5. Single-component CO₂BOLs with amidines and guanidines as the core (**2-4** – **2-8**) and an IL mixture (**2-9**) for CO₂ capture.^{3c}

Heldebrant and co-workers synthesized single-component systems that contain a cyclic amidine or guanidine with an aliphatic alcohol chain (Figure 2.5, **2-4** – **2-7**).^{3b} It was found that under anhydrous conditions the original base/alcohol two-component systems exhibit greater CO₂ uptake than the single-component systems. The lower amount of CO₂ uptake was attributed to the higher viscosity of the single-component systems, which makes it difficult for CO₂ to diffuse through the material. Once the viscosity of the linear alcohol-functionalized **2-5** was lowered by

heating to 60 °C and applying a pressure under 0.34 MPa for 3 h, a five-fold increase in CO₂ uptake was observed.^{3b} In contrast, the branched alcohol-functionalized **2-4** was the least reactive towards CO₂. This observation parallels the low reactivity of CO₂ with the dual-component system of secondary alcohols and strong bases, where steric encumbrance is attributed to this interaction.^{1b} The low viscosity five-membered cyclic amidine single-component, **2-6** exhibits higher CO₂ uptake than those SPS having a DBU core at STP, 8.0 – 9.2 wt%, due to its lower viscosity. Similarly **2-10a** has a CO₂ uptake of >9.0 wt% where this uptake is lowered to 7.1% with a more sterically encumbered alcohol **2-7b**.

Other SPS that incorporate DBU have been developed to address the volatility issues that are found in the dual-component systems. Park and co-workers synthesized dimeric alkanolamidines that feature two molecules of DBU tethered by a dihydroxy-substituted chain (Figure 2.5, **2-8**) for use as a solid sorbent of CO₂.¹⁴ Due to the low diffusion of CO₂ through the solid alkanolamidine, the solid showed poor CO₂ uptake. Park and co-workers speculated that by dispersing the alkanolamidines into porous silica at a loading of 35% to increase the surface area, the CO₂ uptake would also increase. Dai and co-workers developed a non-volatile CO₂ capture agent, by a 1:1 mixture of DBU and an alcohol-functionalized ionic liquid (IL) (Figure 2.5, **2-9**).¹⁵ Having the alcohol tethered to the non-volatile IL reacts with CO₂ and DBU to form the alkylcarbonate. Dai and co-workers heated the system up to 500 °C and observed that the mass loss was only CO₂. They were able to demonstrate its reactivity over three cycles where there was a loss in reactivity after each cycle. Table 2.1 lists some of the SPS with their loading capacities of CO₂ at 25 °C and 1 atm. Higher CO₂ loading is achieved under elevated pressure.

Table 2.1. CO₂-uptake by select SPS systems.^{3c}

Sorbent	CO ₂ Capacity (wt%) ^a	CO ₂ Binding Mode	Ref.
DBU/1-hexanol	15	Alkylcarbonate	1b
TMG/1-hexanol	17	Alkylcarbonate	1b
2-1	12	Carbamate	9
2-2	12	Carbamate	9
2-3b	10	Alkylcarbonate	13
2-5a	18	Alkylcarbonate	14
2-5b	5 ^b	Alkylcarbonate	3a
2-8	1	Alkylcarbonate	14
2-9	8	Alkylcarbonate	3a

^aChemically bound CO₂ only, observed capacity at 25 °C and 1 atm of CO₂. ^bAbsorption at 0.34 MPa

2.2.3 Alkanolamines for use as Zwitterionic Switchable Solvents

Industrially, a popular technique for CO₂ capture from flue gas streams is chemical absorption using primary or secondary alkanolamines such as monoethanolamine (MEA), diethanolamine (DEA), and *N*-methyldiethanolamine (MDEA).¹⁶ With the use of alkanolamines, that contain a secondary amine, CO₂ absorption can be achieved with low partial pressures by forming stable carbamate species. Unfortunately, the absorption process with the above amines normally includes the use of a solvent (in industry, the word ‘solvent’ is erroneously used to refer to the dissolved base rather than the liquid it is dissolved in), in most cases water, which can lead to a high regeneration temperature of 120 °C, corrosiveness, and solvent loss during solvent reclamation.^{17,18} For instance, when aqueous MEA is used as an absorbent, the regeneration of it from the corresponding carbamate accounts for 40 – 60% of the total operational cost.^{17,18} An alternative to MEA, DEA, and MDEA, is a hindered alkanolamine, such as 2-amino-2-methyl-1-propanol (AMP). AMP has been studied extensively because it reacts with CO₂ and water to produce a bicarbonate species that is thermally less stable than the corresponding carbamate species.¹⁶⁻¹⁸ There are features that are attractive about AMP in terms of regeneration and

corrosion, though the desorption temperature is above 100 °C, which is not favourable for industrial applications.

Non-aqueous CO₂-absorbents in industry rely on physical dissolution under pressure. Examples of non-amine trapping technologies include Selexol[®] (polyethylene glycols), Rectisol[®] (chilled methanol) and Purisol[®] (*N*-methylpyrrolidone) that operate under pressure to capture CO₂ and the regeneration of the material and release of CO₂ is by depressurization. While release of CO₂ and recovery of the material is facile through depressurization, the materials exhibit low weight capacities and do not operate well below a pressure of 2.1 MPa.

Heldebrant and co-workers investigated low molecular weight tertiary alkanolamines as CO₂ capture agents that operate through a pressure-swing.^{3a} The development of tertiary alkanolamines for CO₂ capture was to address the issues of low weight capacities and release of CO₂ at ambient conditions unlike other non-aqueous absorbents for CO₂ capture that exist in industry and perform poorly under ambient conditions.^{3a} The tertiary ethanolamines studied were DEA, *N,N'*-dimethylethanolamine (DMEA), *N,N'*-diisopropyl-ethanolamine (DIPEA) and 2-(dimethylamino)-2-methyl-1-propanol (2-DMAM-PrOH). Tertiary amines in the presence of alcohols show little to no interaction with CO₂. Tertiary ethanolamines do not readily react with CO₂ under ambient conditions,¹⁹ but do so under elevated pressures. For example, under elevated pressures (0.7 – 3.4 MPa), DMEA captures CO₂ via two modes simultaneously, zwitterionic alkylcarbonate DMEA-CO₂ and physical absorption. The regeneration of DMEA is achieved from simple depressurization. Related to solvent polarity effects, the trend for chemical absorption of CO₂ is DMEA (20 wt.%, 44 mol%) > DEA (16 wt.%, 43 mol%) > DIPEA (16 wt.%, 57 mol%).^{3a}

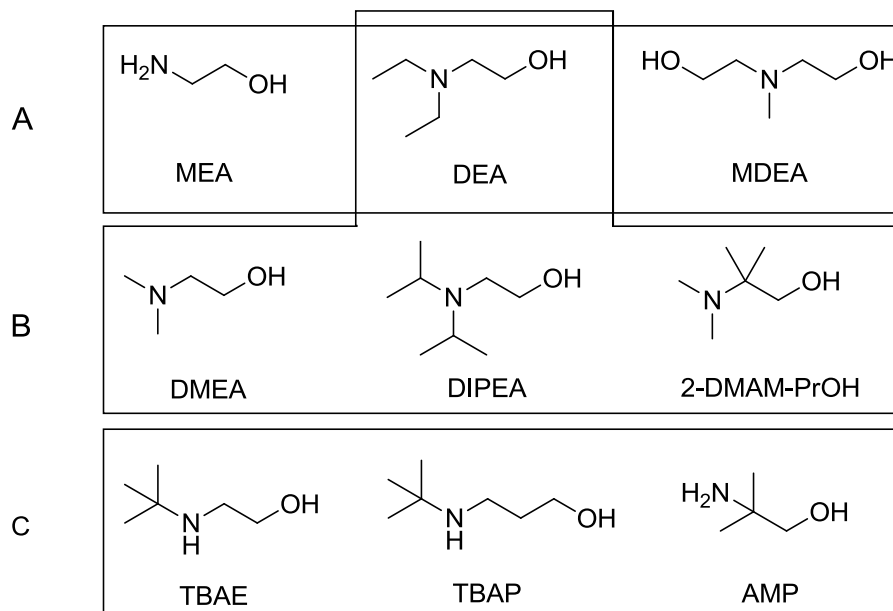
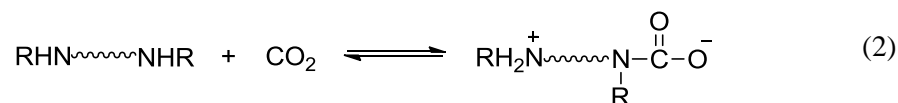
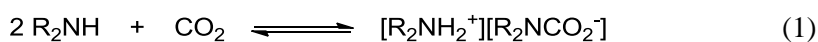


Figure 2.6. Alkanolamines for CO₂ capture: (A) industrial chemical absorbents, (B) pressure-swing physical sorbents, (C) sterically hindered chemical absorbents.

Following the idea of placing steric bulk around the amine, Park and co-workers investigated regenerable non-aqueous CO₂ absorption systems that feature a *tert*-butyl group at a secondary amine centre.²⁰ The hindered alkanolamines, 2-[(1,1-dimethylethyl)amino]-ethanol (TBAE) and 1-[(1,1-dimethylethyl)amino]-2-propanol (TBAP), react with CO₂ in a 1:1 molar ratio through the hydroxyl group, forming a zwitterionic alkylcarbonate species. The *tert*-butyl group attached to the amino group blocks the approach of CO₂ to the nitrogen atom, and forces the CO₂ to interact with the hydroxyl group. Through ATR-IR and ¹³C NMR spectroscopy, Park and co-workers were able to confirm the interaction of CO₂ with the hydroxyl group of the hindered alkanolamine. The interaction of the CO₂ with a hydroxyl group of an alkanolamine is unusual and has not been seen with other alkanolamines including MEA, DEA, and AMP.^{1a,21-23} They also found that regeneration of the hindered alkanolamines is easier when the reaction was performed in a diol, in their case ethane-1,2-diol, than in water.

2.2.4 Secondary Diamines for SPS and CO₂ Capture

Aside from secondary amines, we speculated that diamines could prove to be useful zwitterionic switchable solvents. Intramolecularly, one nitrogen atom can act as the CO₂ capture site producing a carbamate ion while the second nitrogen atom is protonated. Additionally, the diamine could have two roles, to act as a switchable polarity solvent and a potential CO₂ capturing agent (eq 2). Diamines as zwitterionic solvents might address issues of volatility, low CO₂ uptake, high heat capacity and a lower polarity swing that plagued previously reported systems. Addition of CO₂ to a liquid diamine producing a liquid zwitterion, would be appropriate for use as a switchable solvent.



2.3 Results and Discussion

2.3.1 Investigation of Secondary Diamines as Switchable Polarity Solvents

The secondary diamines that were examined all have different substituents around the nitrogen atoms and varying carbon chain lengths between them that might influence the reactivity with CO₂. The liquid diamines that were screened as possible liquid zwitterionic SPS are shown below (Figure 2.7). The candidates feature different substituents on the N-atoms as well as different tethers between the two nitrogen atoms.

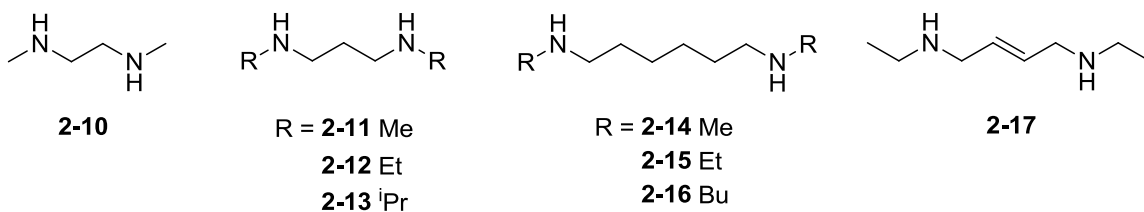
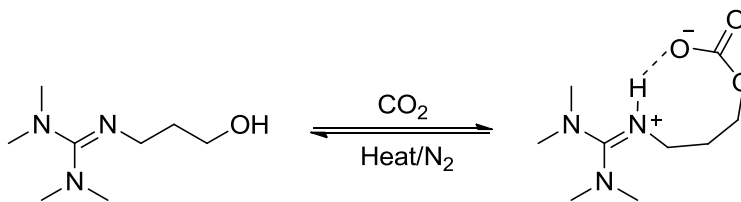


Figure 2.7. Diamine candidates for zwitterionic switchable polarity solvents.

N,N'-Diethyl-2-butene-1,4-diamine **2-17** is a diamine that has an alkene within the carbon chain tether, that adds rigidity to the structure. The rigidity would prevent the anionic carbamate group from interacting with the positively charged nitrogen centre. Heldebrant and co-workers found that a cyclic carbonate is formed by the addition of CO₂ to an alkanol-guanidine with a chain length of three carbons (Scheme 2.8) to give a thermodynamically stable 8-membered ring.¹³ The non-viscous liquid that formed was unable to release CO₂ upon heating to 100 °C.



Scheme 2.8. Formation of 8-membered ring with alkanol-guanidine and CO₂.¹³

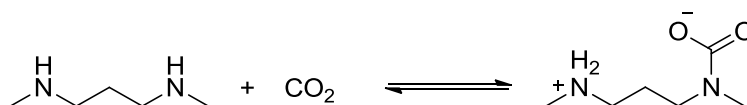
The crystal packing of the zwitterions may change according to the differences in chain length. For example, the carbon chain tether that features six carbons in comparison to two carbons might provide more flexibility and the resulting zwitterion upon the addition of CO₂ would be a liquid due to a longer carbon chain length.

The CO₂ was applied to the neat diamines open to air and under ambient conditions. Steps to maintain dry conditions were avoided in order to design a system that would lead to a more practical application and obviate the need for scrupulously dry conditions. It was observed

that upon bubbling CO₂ into the neat liquid diamines to form the zwitterions, they became more viscous and within seconds, the viscous solutions turned to solid carbamate salts. It is possible that under scrupulously dry conditions, the zwitterions that were formed would not have solidified, though for reasons that will be explained later, the presence of water does influence whether a zwitterionic solid is formed.

The zwitterions formed from diamines (**2-10** – **2-17**) were soluble in CDCl₃ and were characterized by ¹H and ¹³C NMR spectroscopy (for chemical shift assignment see Appendix B, Table B.1.). For all the secondary diamines, a minimal downfield shift is exhibited for all the peaks in the ¹H NMR spectra after the absorption of CO₂. There are two sets of peaks found in the ¹H and ¹³C NMR spectra which indicated a half-equivalent of CO₂ uptake and not a mixture of carbamate salt, acid and unreacted amine. In contrast to what is observed with secondary amines, spectroscopic and conductivity data show that a mixture of carbamate salt, carbamic acid, and unreacted amine is formed when CO₂ is added to secondary amine SPS.⁴ CO₂ uptake for compound **2-17** was not complete, in that the ¹³C NMR spectrum showed three signals that corresponded to alkene carbon atoms. The signals were located at 124.7, 129.6, and 133.2 ppm, where the peak at 129.6 ppm corresponds to starting diamine. In the ¹H NMR spectra of the diamines following the addition of CO₂, a broad peak, in the range of 9-10 ppm, is exhibited and corresponds to the protonated amine [N-H]⁺. IR spectroscopy was used to analyze all the carbamate salts formed from the secondary diamines. The IR spectrum of **2-11** did not exhibit a band at 835 cm⁻¹ consistent with the bicarbonate ion. Although, the IR spectra for all the carbamate salts did show a band at 1545 cm⁻¹, which is characteristic for the carbamate anion peak, [H₂NCO₂]⁻.

N,N'-Dimethyl-1,3-propanediamine **2-11** is representative of all other secondary diamines that we tested. Upon bubbling CO₂ into the diamine, a solid carbamate salt is formed rather than a non-viscous liquid, which would be ideal for a zwitterionic switchable solvent. The zwitterionic structure is shown below (Scheme 2.9). The ¹H NMR spectrum of **2-11b** exhibits minor changes in chemical shifts except for positions 5 and 6 (see Appendix B, Table B.1 **2-11 a** and **b**) where the peaks have shifted downfield by 0.9 and ~0.6 ppm respectively. The *N*-bound proton has shifted from 1.0 ppm to 10.6 ppm, which is indicative of the nitrogen converting from a neutral to a positively charged centre. In the ¹³C NMR spectrum there is a new peak that appears at 163.9 ppm that corresponds to the carbamate central carbon.



Scheme 2.9. Addition of CO₂ to **2-11** to form zwitterionic salt **2-11b**.

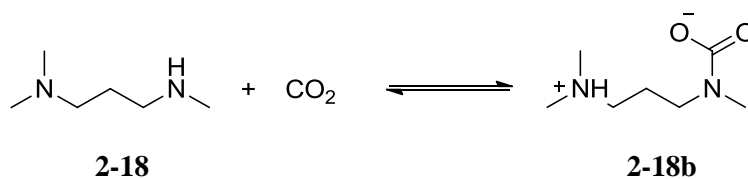
Crystals of the **2-11** CO₂ adduct were grown from a hexane solution of the complex *via* slow evaporation in a CO₂ atmosphere. X-ray crystallography confirmed the formation of a zwitterionic salt (Figure 2.8) where the carbon dioxide is directly bound to the nitrogen centre and the second nitrogen centre is protonated. The molecular structure illustrates that intramolecularly one of the nitrogen atoms has acted as a nucleophile and the other a proton donor. The molecular structure of **2-11** also illustrates that with wet conditions there is no formation of a bicarbonate salt which is readily formed with DBU in the presence of water.^{1d} The zwitterionic salt of **2-11** co-crystallized with one water molecule (Figure 2.8). The water molecule is an integral part of the hydrogen-bonding network in the structure, which suggests that if water were absent then the solid zwitterionic salt might not be as stable. However, treating thoroughly anhydrous **2-11** with CO₂ resulted in the formation of a solid.



Figure 2.8. Molecular structure and extended network of **2-11b** and CO₂. Displacement ellipsoids for non-H atoms are shown at 50% probability level.

2.3.2 A Diamine Containing one Secondary and one Tertiary Amine

The addition of CO₂ to the secondary diamines all gave solid zwitterionic salts, where a diamine that contained one tertiary and one secondary amine gave a liquid zwitterionic salt. CO₂ was bubbled into the neat liquid *N,N'*-trimethyl-1,3-propanediamine **2-18**; the viscosity of the liquid increased greatly, but there was no solidification that was observed. The zwitterionic liquid product **2-18b** is shown below (Scheme 2.10).



Scheme 2.10. Addition of CO₂ to **2-18** to form zwitterionic salt **2-18b**.

The ATR-IR spectrum of the viscous liquid showed the disappearance of the N-H band at 3298 cm⁻¹ and the appearance of a band at 1545 cm⁻¹ that corresponds to the carbamate anion.²⁴

There was no peak at 835 cm^{-1} that is indicative of a bicarbonate anion. The ^1H NMR spectrum of **2-18b** had minor changes where the chemical shifts of the carbon-bound protons move slightly downfield, with the exception of positions 5 and 7 (see numbering scheme in Appendix B, Table B.1 for **2-18** and **2-18b**) where the signals have shifted downfield by 0.6 and 0.4 ppm, respectively. A new peak appeared at 10.6 ppm that is consistent with a dialkylammonium cation. In the ^{13}C NMR spectrum, a new peak appears at 161.1 ppm that corresponds to the carbamate central carbon. High resolution ESI-mass spectrometry (positive mode) was measured for **2-18** and corresponded to the calculated $M + 1$ peak of 161.13 m/z . Of the nine diamines that were examined, **2-18** was the only one that afforded a reversible zwitterionic liquid at ambient temperature and pressure.

The uptake of CO_2 increased the mass of the liquid **2-18** by 28%. If **2-18** were to have complete uptake, then the mass of liquid **2-18** would theoretically increase by 38%. The lower than theoretical uptake of CO_2 was probably due to incomplete conversion of **2-18**, which could contribute to why the liquid did not solidify in the presence of CO_2 . Even though there was the possibility of incomplete conversion, the uptake of CO_2 by **2-18** was close to double that of other single-component SPS systems (Table 2.1) such as that of **2-5** and **2-3** that have a CO_2 uptake of 18 wt.%¹⁴ and 10 wt.%¹³ respectively. Additionally, it exhibited higher CO_2 uptake than the dual-component SPS; DBU/1-hexanol and TMG/1-hexanol have a CO_2 capacity of 15 wt.%^{2a} and 17 wt.%^{2a} respectively.

The polarity of the **2-18b** was measured using the solvatochromic probe Nile red, where the higher λ_{max} values (nm) indicate the higher polarity form. The λ_{max} value of neat **2-18** was measured before and after the addition of CO_2 . After the sample was sparged with CO_2 for 20 minutes, the wavelengths shifted from 523 nm to 534 nm. The polarity of **2-18b** was moderate and comparable to the polarity of THF (Figure 2.9). The amount of polarity change was comparable to that observed with simple secondary amines such as ethyl-*N*-butylamine.⁴ The

polarity change generated by treating **2-18** with CO₂ shows it has comparable polarity swing to the previously reported switchable ionic liquids. Conversion to the neutral amine, the lower polarity form, was achieved by bubbling argon through the viscous solution at 60 °C. The ¹H NMR spectrum after the removal CO₂ confirmed complete conversion back to the starting diamine.

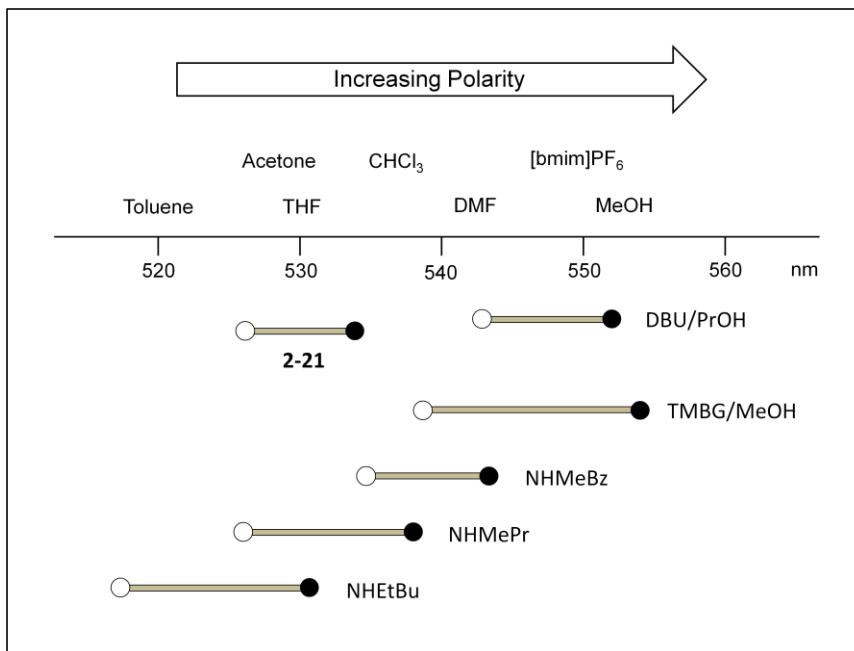


Figure 2.9. A comparison of the polarity ranges of several SPS (white circles indicate the low-polarity form, black circles indicate the high polarity form). The scale is the λ_{\max} for Nile red solvatochromic dye dissolved in the solvent. Select traditional solvents are indicated above the scale for comparison ([bmim]PF₆ = 1-butyl-3-methylimidazolium hexafluorophosphate).⁴ Polarity change of **2-18** illustrated.

2.4 Conclusion and Future Considerations

Various diamines were tested for their use as single-component liquid zwitterionic SPS and as CO₂ adsorbents to address issues of volatility, heat capacity, polarity, and uptake of CO₂. The secondary diamines that were screened featured different substituents and tether lengths between the two nitrogen atoms. Reactivity was not affected by differing substitution, tether

length and rigidity of the secondary diamines. The bubbling of CO₂ into the liquid diamines produced solid zwitterionic salts, which were not feasible as liquid SPS. The molecular structure of **2-11b** was determined with X-ray crystallography and confirmed the zwitterionic structure. One water molecule co-crystallized with zwitterion indicating that the presence of water does not prevent the formation of the carbamate; in contrast the addition of CO₂ to wet DBU readily forms a bicarbonate salt. The H-bonding network was supported by the water molecules in the crystal structure of **2-11b** and therefore could facilitate the formation of a solid zwitterionic salt. However, even with thoroughly dried **2-11**, a solid zwitterionic salt was still formed after the introduction of CO₂.

Compound **2-18**, which contains a secondary nitrogen atom and a tertiary nitrogen atom, gave a liquid zwitterionic SPS after the introduction of CO₂. The polarity of **2-18** was similar to that of THF and has a comparable polarity range to that of simple secondary amines. Because the polarity change was not larger than that of switchable ionic liquids, there was no clear advantage to using switchable zwitterionic liquids as solvents, especially in industrial applications.

Compound **2-18** does not have a larger polarity change than switchable ionic liquids, though its CO₂ uptake ability was higher than several switchable ionic liquids. It has a gravimetric uptake of CO₂ of 28%, twice the amount of CO₂ uptake of most other SPS listed in Table 2.1. A conventional solvent that was not switchable was developed by Davis and co-workers that has an amine tethered imidazolium IL that also absorbed 7.4% CO₂ by weight as a carbamate, though it took three hours to reach saturation.²⁵ Saturation of **2-18** with CO₂ was achieved within minutes of bubbling and the release of CO₂ and regeneration of **2-18** was at 60 °C and bubbling of argon or nitrogen, much milder conditions than what was needed for several of the SPS that are described in previous sections.

Future considerations would be further screening of other diamines that contain a secondary and tertiary amines. A zwitterionic liquid formed with a diamine that had the above

characteristics. The release and capture of CO₂ varies between a secondary amine and a tertiary amine. The addition of CO₂ to a secondary amine forms a carbamic acid and with a second equivalent of amine, a carbamate salt. A tertiary amine forms the bicarbonate salt in the presence of water and CO₂. The interplay between a secondary amine and tertiary amine affording different reactivity with CO₂ can be further explored.

Future research for compound **2-18**, would be a full investigation of its utility as a CO₂ capture agent. The corrosiveness of **2-18** to metals should be evaluated, as should its performance as a capture agent in water. Large CO₂ uptake was afforded by neat **2-18**, whereas a conventional sorbent like MEA operates in an aqueous solution because of its corrosiveness to metals. Multiple cycles of CO₂ capture and release should be tested with **2-18** to determine its robustness. The CO₂ uptake should be measured when **2-18** is in contact with gas mixtures having CO₂ partial pressures significantly lower than 0.1 MPa and having other reactive components such as water, CS₂, sulfur oxides, and/or nitrogen oxides. In addition to screening other diamines, the structure of **2-18** could be the framework for the synthesis of larger analogous structures, leading to the design of a more robust molecule.

2.5 Experimental Methods

2.5.1 General Considerations

All secondary amines were used as received and purchased from Sigma-Aldrich and Acros Organics. High resolution mass spectra (HRMS) ESI for **2-18b** was obtained on a Qstar XL QqTOF from Applied Biosystems/MDS Sciex. The IR spectra for compounds, **2-11**, **2-11b**, **2-18**, and **2-18b** were obtained on a Varian Scimitar 1000 FTIR equipped with the Pike MIRacle™ ZnSe ATR accessory. ¹H and ¹³C NMR spectra for compounds **2-10** – **2-18** were obtained on a Bruker AVANCE-400 MHz NMR spectrometer where each sample was referenced to tetramethylsilane. The NMR spectra of the CO₂ treated amines were obtained by bubbling CO₂

into a septa capped NMR tube that had 0.1 mL amine in dry CDCl_3 . Data collection for the crystal of **2-11b** was acquired on a Bruker SMART APEX II X-ray diffractometer.

2.5.2 IR Spectroscopic Data for the Bases Before and After CO_2 Treatment

***N, N'* – Dimethyl-1,3-propanediamine (2-11).** (neat, cm^{-1}) **Before CO_2 treatment:** 3280 m (N-H stretch), 2929 m (C-H stretch), 2879 m (C-H stretch), 2841 m (C-H stretch), 2786 s (C-H stretch), 2694 w (C-H stretch), 1473 s (C-H bend), 1446 s (C-H bend), 1124 s (C-N stretch), 739 s. **After CO_2 treatment:** 3289 w (N-H stretch), 2928 m (C-H stretch), 2840 m (C-H stretch), 2787 m (C-H stretch), 2405 m (C-H stretch), 2361 m (C-H stretch), 1545 s ($[\text{H}_2\text{NCO}_2^-]$), 1471 s (C-H bend), 1372 s (C-H bend), 1255 s (C-N stretch), 1038 s, 807 s, 757s.

***N,N,N'* – Trimethyl-1,3-propanediamine (2-18).** (neat, cm^{-1}) **Before CO_2 treatment:** 3298 w (N-H stretch), 2940 s (C-H stretch), 2857 m (C-H stretch), 2814 s (C-H stretch), 2783 s (C-H stretch), 2764 s (C-H stretch), 1739 w (N-H bend), 1460 s (C-H bend), 1376 w (C-H bend), 1263 w (C-N stretch), 1150 m, 1122 m, 1041 s, 839 s, 743 s. **After CO_2 treatment:** 2941 m (C-H stretch), 2814 m (C-H stretch), 2762 m (C-H stretch), 2462 w (C-H stretch), 1683 w (CO stretch), 1624 w (N-H bend), 1545 w ($[\text{H}_2\text{NCO}_2^-]$), 1460 s (C-H bend), 1376 s (C-H bend), 1305 m (C-H bend), 1262 s (C-N stretch), 1040 s, 808 m.

2.5.3 Gravimetric Uptake of CO_2 by *N,N,N'*-Trimethyl-1,3-propanediamine (2-18b)

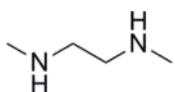
Compound **2-18** (0.30 mL, 2.05 mmol) was added to a flame-dried 1 dram vial and sealed with a rubber septa and massed. CO_2 was bubbled into the amine at room temperature and 1 bar to form the zwitterions. The mass was measured at 10 min intervals for 100 min although no further mass increase was observed after the first 10 min.

2.5.4 Polarity Measurement of *N,N,N'*-Trimethyl-1,3-propanediamine (2-18b)

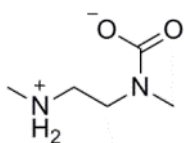
Approximately 3 mL of the amine was placed in a 1 cm quartz cuvette where a sufficient amount of Nile red was added on a needle tip to give an absorbance between that of 0.5 and 1.0. The cuvette was then bubbled with atmospheric CO₂ for a period of 20 min or until the viscosity of the amine changed. A UV-visible spectrum was measured again. The experiment was done in triplicate, where the average of all three is the reported measurement.

2.5.5 Spectroscopic Data for Diamines Without (Species a) and With (Species b) CO₂

N,N'-Dimethylethylenediamine (2-10)



Species a: ¹H NMR (400 MHz, CDCl₃) δ 2.69 (s, 4H), 2.44 (s, 4H), 1.17 (brs, 2H) ppm; ¹³C {¹H} NMR (400 MHz, CDCl₃) 51.5, 36.5 ppm.

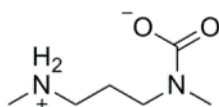


Species b: ¹H NMR (400 MHz, CDCl₃) δ 9.02 (brs, 2H), 3.23 (brs, 1H), 2.93 (brs, 1H), 2.50 (t, 2H, *J* = 8 Hz), 2.29 (s, 6H) ppm; ¹³C {¹H} NMR (400 MHz, CDCl₃) 161.9, 58.7, 44.9, 38.6 ppm.

N,N'-Dimethyl-1,3-propanediamine (2-11)

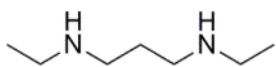


Species a: ¹H NMR (400 MHz, CDCl₃) δ 2.64 (m, 4H), 2.43 (s, 6H), 1.67 (p, 2H), 1.05 (brs, 2H) ppm; ¹³C {¹H} NMR (400 MHz CDCl₃) 50.5, 36.6, 30.1 ppm.

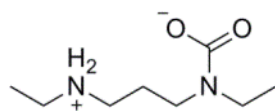


Species b: ¹H NMR (400 MHz, CDCl₃) δ 10.17 (brs, 2H), 3.40 (brs, 2H), 2.91 (brs, 2H), 2.86 (brs, 3H), 2.58 (brs, 3H), 1.88 (brs, 2H) ppm; ¹³C {¹H} NMR (400 MHz, CDCl₃) 163.8, 44.9, 44.4, 34.1, 31.7, 23.8 ppm.

N,N'-Diethyl-1,3-propanediamine (2-12)

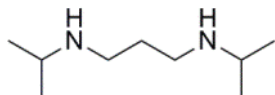


Species a: ^1H NMR (400 MHz, CDCl_3) δ 2.66 (q, 4H, $J = 6.96$), 2.65 (t, 4H, $J = 7.12$), 1.69 (p, 2H, $J = 7.04$), 1.19 (brs, 2H), 1.10 (t, 6H, $J = 7.12$) ppm; ^{13}C $\{^1\text{H}\}$ NMR (400 MHz, CDCl_3) 48.3, 44.1, 30.6, 15.2 ppm.

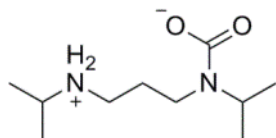


Species b: ^1H NMR (400 MHz, CDCl_3) δ 10.09 (brs, 2H), 3.41 (brs, 2H), 3.26 (brs, 2H), 2.91 (brs, 4H), 1.85 (m, 2H), 1.31 (brs, 3H), 1.11 (brs, 3H) ppm; ^{13}C $\{^1\text{H}\}$ NMR (400 MHz, CDCl_3) 163.6, 42.7, 42.1, 41.4, 41.0, 25.1, 13.9, 11.6 ppm.

N,N'-Di-*iso*-propyl-1,3-propanediamine (2-13)

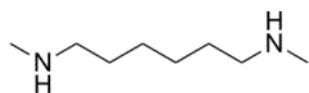


Species a: ^1H NMR (400 MHz, CDCl_3) δ 2.78 (m, 2H), 2.65 (m, 4H), 1.66 (m, 2H), 1.06 (m, 12H) ppm; ^{13}C $\{^1\text{H}\}$ NMR (400 MHz, CDCl_3) 48.7, 46.1, 31.1, 21.8 ppm.

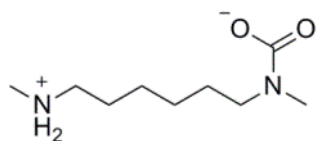


Species b: ^1H NMR (400 MHz, CDCl_3) δ 9.23 (brs, 1H), 4.48 (brs, 1H), 3.31 (brs, 2H), 3.16 (brs, 1H), 2.88 (brs, 3H), 1.78 (brs, 2H), 1.32 (brs, 6H), 1.08 (brs, 6H) ppm; ^{13}C $\{^1\text{H}\}$ NMR (400 MHz, CDCl_3) 163.5, 46.9, 48.1, 40.7, 37.9, 28.6, 21.8, 19.2 ppm.

N,N'-Dimethyl-1,6-hexanediamine (2-14)

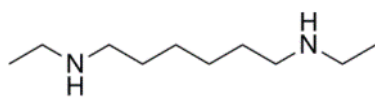


Species a: ^1H NMR (400 MHz, CDCl_3) δ 2.57 (q, 4H, $J = 7.5$ Hz), 2.43 (s, 6H), 1.50 (m, 4H), 1.35 (m, 4H), 1.21 (brs, 2H) ppm; ^{13}C $\{^1\text{H}\}$ NMR (400 MHz, CDCl_3) 52.0, 36.4, 29.8, 27.2 ppm.

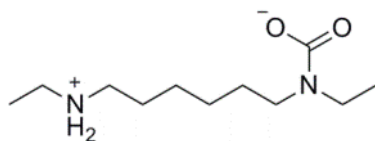


Species b: ^1H NMR (400 MHz, CDCl_3) δ 10.18 (brs, 1H), 3.23 (brs, 2H), 2.83 (brs, 4H), 2.54 (brs, 2H), 1.65 (brs, 2H), 1.51 (brs, 2H), 1.32 (brs, 4H) ppm; ^{13}C $\{^1\text{H}\}$ NMR (400 MHz, CDCl_3) 162.6, 48.4, 34.0, 32.9, 27.7, 26.1 ppm.

***N,N'*-Diethyl-1,6-hexanediamine (2-15)**

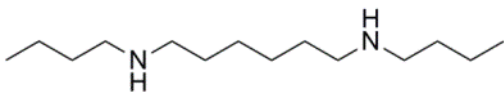


Species a: ^1H NMR (400 MHz, CDCl_3) δ 2.68 (m, 4H), 2.62 (m, 4H), 1.51 (m, 4H), 1.36 (m, 4H), 1.12 (m, 6H), 0.98 (brs, 2H) ppm; ^{13}C { ^1H } NMR (400 MHz, CDCl_3) 49.7, 44.0, 30.1, 27.2, 15.2 ppm.

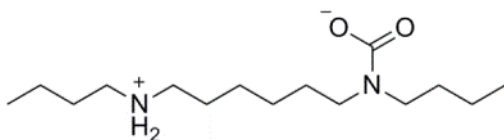


Species b: ^1H NMR (400 MHz, CDCl_3) δ 8.92 (brs, 1H), 3.21 (brs, 4H), 2.78 (brs, 2H), 2.71 (brs, 2H), 1.60 (brs, 2H), 1.51 (brs, 2H), 1.32 (brs, 4H), 1.21 (brs, 3H), 1.08 (brs, 3H) ppm; ^{13}C NMR (400 MHz, CDCl_3) 161.8, 47.5, 46.1, 42.6, 41.2, 28.8, 27.8, 26.8, 13.8, 13.1 ppm.

***N,N'*-Dibutyl-1,6-hexanediamine (2-16)**

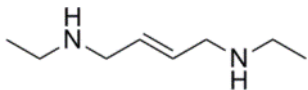


Species a: ^1H NMR (400 MHz, CDCl_3) δ 2.58 (m, 8H), 1.46 (m, 8H), 1.34 (m, 8H), 0.91 (m, 8H) ppm; ^{13}C { ^1H } NMR (400 MHz, CDCl_3) 50.1, 49.8, 32.4, 30.2, 27.4, 20.5, 13.9 ppm.

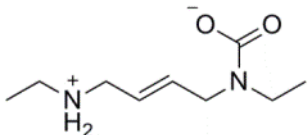


Species b: ^1H NMR (400 MHz, CDCl_3) δ 8.88 (brs, 2H), 3.18 (brs, 4H), 2.69 (brs, 4H), 1.58 (brs, 4H), 1.51 (brs, 4H), 1.31 (brs, 8H), 0.91 (t, 6H, $J = 7.3$ Hz) ppm; ^{13}C { ^1H } NMR (400 MHz, CDCl_3) 161.6, 48.2, 46.4, 30.3, 28.4, 26.9, 20.3, 13.9 ppm.

N,N'-Diethyl-2-butene-1,4-diamine (2-17)

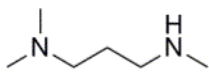


Species a: ^1H NMR (400 MHz, CDCl_3) δ 5.69 (m, 2H), 3.23 (m, 4H), 2.65 (q, 4H, $J = 7.04$ Hz), 1.11 (t, 6H, $J = 7.04$ Hz), 1.02 (brs, 2H) ppm; ^{13}C $\{^1\text{H}\}$ NMR (400 MHz, CDCl_3) 130.2, 51.3, 43.6, 15.3 ppm.

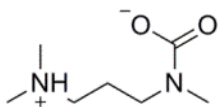


Species b: ^1H NMR (400 MHz, CDCl_3) δ 8.73 (brs, 2H), 5.72 (brs, 2H), 3.86 (brs, 2H), 3.36 (brs, 2H), 3.24 (brs, 2H), 2.76 (brs, 2H), 1.19 (brs, 2H), 1.07 (brs, 2H) ppm; ^{13}C $\{^1\text{H}\}$ NMR (400 MHz, CDCl_3) 161.4, 133.2, 129.6, 124.7, 49.3, 48.8, 47.6, 40.7, 13.5, 12.7 ppm.

N,N,N'-Trimethyl-1,3-propanediamine (2-18)



Species a: ^1H NMR (400 MHz, CDCl_3) δ 2.53 (t, 2H, $J = 7.1$ Hz), 2.35 (s, 3H), 2.23 (t, 2H, $J = 7.4$ Hz), 2.14 (s, 6H), 1.57 (p, 2H, $J = 7.1$ Hz), 1.13 (brs, 1H) ppm; ^{13}C $\{^1\text{H}\}$ NMR (400 MHz, CDCl_3) 57.9, 50.5, 45.4, 36.5, 27.9 ppm.



Species b: ^1H NMR (400 MHz, CDCl_3) δ 10.54 (brs, 1H), 3.07 (brs, 2H), 2.69 (brs, 3H), 2.30 (t, 2H, $J = 7.1$), 2.19 (brs, 6H), 1.69 (p, 2H, $J = 7.1$) ppm; ^{13}C $\{^1\text{H}\}$ NMR (400 MHz CDCl_3) 161.1, 56.7, 47.2, 44.8, 34.0, 25.1 ppm.

2.6 References

- 1) a) Jessop, P. G.; Heldebrant, D. J.; Xiaowang, L.; Eckert, C. A.; Liotta, C. L. *Nature*, **2005**, *436*, 1102. b) Phan, L.; Li, X.; Heldebrant, D. J.; Wang, R.; Chiu, D.; John, E.; Huttenhower, H.; Pollet, P.; Eckert, C. A.; Liotta, C. L.; Jessop, P. G. *Ind. Eng. Chem. Res.*, **2008**, *47*, 539 – 545. c) Heldebrant, D. J.; Jessop, P. G.; Thomas, C. A.; Eckert, C. A.; Liotta, C. L. *J. Org. Chem.* **2005**, *70*, 5335 – 5338.
- 2) a) Heldebrant, D. J.; Yonker, C. R.; Jessop, P. G.; Phan, L. *Energy Environ. Sci.* **2008**, *1*, 487-493. b) Jessop, P. G.; Heldebrant, D. J.; Li, X. W.; Lu, J.; Hallet, J. P.; Jones, R. S.; Pollet, P. Thomas, C. A.; Eckert, C. A.; Liotta, C. L. *Abstr. Pap. Am. Chem. Soc.* **2005**,

- 229, U971. c) Heldebrant, D. J., Yonker, C. R.; Jessop, P. G.; Phan, L. *Chem. Eur.J.* **2009**, *15*, 7619 – 7627.
- 3) a) Rainbolt, J. E.; Koech, P.K.; Yonker, C.R.; Zheng, F.; Main, D.; Weaver, M.L.; Linehan, J.C.; Heldbrant, D.J. *Energy Environ. Sci.*, **2011**, *4*, 480 – 484. b) Heldebrant, D.J.; Koech, P.K.; Rainbolt, J.E.; Zheng, F.; Smurthwaite, T.; Freeman, C.J.; Oss, M.; Leito, I. *Chem. Eng. J.* **2011**, *171*, 794 – 800. c) Jessop, P.G.; Mercer, S.M.; Heldebrant, D.J. *Energy Environ. Sci.* **2012**, *5*, 7240 – 7253.
- 4) Phan, L.; Andreatta, J. R.; Horvey, L. K.; Edie, C. F.; Luco, A.L.; Mirchandi, A.; Darensbourg, D. J.; Jessop, P.G. *J. Org. Chem.*, **2008**, *73*, 127 – 132. b) Jessop, P. G.; Phan, L.; Carrier, A.; Robinson, S.; Dürr, C. J.; Harjani, J. R. *Green Chem.* **2010**, *12*, 809 – 814.
- 5) a) Yamada, T.; Lukac, P.J.; George, M.; Weiss, R.G. *Chem. Mater.* **2007**, *19*, 967 – 969. b) Yamada, T.; Lukac, P.J.; Yu, T.; George, M.; Weiss, R.G. *Chem. Mater.* **2007**, *19*, 4761 – 4768. c) Yu, T.; Yamada, T.; Gaviola, G.C.; Weiss, R.G. *Chem. Mater.* **2008**, *20*, 5337 – 5344.
- 6) Hunter, B.A.; Glenn, H.D., U.S. Patent 2,635,124, 1953.
- 7) a) Jensen, A.; Christensen, R.; Faurholt, C. *Acta Chem. Scand.* **1952**, *6*, 1086 – 1089. b) Jensen, A.; Jensen, M.B.; Faurholt, C. *Acta Chem. Scand.* **1952**, *6*, 1073 – 1085.
- 8) Schroth, W.; Schädler, H.-D.; Andersch, J.Z. *Chem.* **1989**, *29*, 129 – 135.
- 9) a) Hart, R.; Pollet, P.; Hahne, D. J.; John, E.; Llopis-Mestre, J. V.; Blasucci, V.; Huttenhower, H.; Leitner, W.; Eckert, C. A.; Liotta, C. L. *Tetrahedron* **2010**, *66*, 1082 – 1090. b) Blasucci, V.; Hart, R.; Mestre, V. L.; Hahne, D. J.; Burlager, M.; Huttenhower, H.; Thio, B. J. R.; Pollet, P.; Liotta, C. L.; Eckert, C. A. *Fuel* **2010**, *89*, 1315 – 1319.
- 10) a) Blasucci, V.; Hart, R.; Pollet, P.; Liotta, C. L.; Eckert, C. A. *Fluid Phase Equilib.* **2010**, *294*, 1 – 6. b) Blasucci, V.; Dilek, C.; Huttenhower, H.; John, E.; Llopis-Mestre, V.; Pollet, P.; Eckert, C.A.; Liotta, C.L. *Chem. Commun.* **2009**, 116 – 118.
- 11) Phan, L.; Brown, H.; Peterson, T.; White, J.; Hodgson, A.; Jessop, P.G. *Green Chem.* **2009**, *11*, 53 – 59.
- 12) Samorì, C.; Torri, C.; Samorì, G.; Fabbri, D.; Galetti, P.; Guerrini, F.; Pistocchi, R.; Tagliavini, E. *Bioresour. Technol.* **2010**, *101*, 3274 – 3279.
- 13) Heldebrant, D.J.; Koech, P.K.; Ang, M.T.C.; Liang, C.; Rainbolt, J.E.; Yonker, C.R.; Jessop, P.G. *Green Chem.* **2010**, *12*, 713 – 721.
- 14) Kim, M.; Park, J.-W. *Chem. Commun.* **2010**, *46*, 2507 – 2509.

- 15) a) Wang, C.; Mahurin, S.M.; Luo, H.; Baker, G.A.; Li, H.; Dai, S. *Green Chem.* **2010**, *12*, 870 – 874. b) Wang, C.; Luo, H.; Jiang, D.-E.; Li, H.; Dai, S. *Angew. Chem. Int. Ed.* **2010**, *49*, 5978 – 5981.
- 16) Lee, D. H.; Choi, W. J.; Moon, S. J.; Ha, S. H.; Kim, I. G.; Oh, K. J. *Korean J. Chem. Eng.* **2008**, *25*, 279 – 284.
- 17) Sartori, G.; Savage, D. W. *Ind. Eng. Chem. Fundam.*, **1983**, *22*, 239 – 249.
- 18) Xu, S.; Wang, Y. W.; Otto F. D.; Mather, A. E. *Chem. Eng. Sci.* **1996**, *51*, 841 – 850.
- 19) a) Versteeg, G.F.; van Swaaij, W.P.M. *Chem. Eng. Sci.* **1988**, *43*, 587 – 591. b) Bosch, H.; Versteeg, G.F.; van Swaaij, *Chem. Eng. Sci.*, **1989**, *44*, 2723 – 2734.
- 20) Im, J.; Hong, S.Y.; Cheon, Y.; Lee, J.; Lee, J.S.; Kim, H.S.; Cheong, M.; Park, H. *Energy Environ. Sci.* **2011**, *4*, 4284 – 4289.
- 21) Xie, H.-B.; Zhou, Y.; Zhang, Y.; Johnson, J.K. *J. Phys. Chem. A* **2010**, *114*, 11844 – 11852.
- 22) Vaidya, P.D.; Kenig, E.Y. *Chem. Eng. Technol.* **2007**, *30*, 1467 – 1474.
- 23) Le Tourneux, D.; Iliuta, I.; Iliuta, M.C.; Fradette, S.; Larachi, F. *Fluid Phase Equilib.* **2008**, *268*, 121 – 129.
- 24) Hisatsune, C. *Can. J. Chem.* **1984**, *62*, 945 – 948.
- 25) Bates, E. D.; Mayton, R. D.; Ntai, I.; Davis, J. H. *J. Am. Chem. Soc.* **2002**, *124*, 926 – 927.

Chapter 3

Unexpected Reactivity of CS₂ with N-Containing Compounds

3.1 Introduction

Carbon dioxide and carbon disulfide (CS₂) are chemically-similar waste products in flue gas streams.¹ While CS₂ is a liquid in its stable form, in flue gas it can be found as a vapour due to its low partial pressure. Synthetically, CS₂ is an important reagent in industry. It is used as an important component for the synthesis of rayon and cellophane and in the synthesis of metham sodium, a soil fumigant which is commonly used in the production of viscose.²

The creation of new carbon-carbon bonds is a central theme in organic chemistry. The activation of CS₂ and CO₂ and their incorporation into complex molecules is an attractive method for creating C-C bonds due to the abundance of these C1 sources. Because CS₂ is valence isoelectronic to CO₂, but substantially more electrophilic, CS₂ can be used to model the reactivity of CO₂. CO₂ and CS₂ activation has been achieved using transition metals,³⁻⁸ where the strong nucleophilic character of the metal complex can activate the C=O and C=S bonds. In our research group, we have employed nitrogen-containing organic bases such as 1,8-diazabicyclo[5.4.0]undec-7-ene (DBU) to activate CO₂ or CS₂.⁹

As described in the previous chapter, it was demonstrated that CO₂ binding organic liquids (CO₂BOLs) – mixtures of an alcohol and base such as an amidine or guanidine – could reversibly capture and release CO₂. Alkylcarbonic acids that result from attack of the alcohol on CO₂ could be reversibly trapped as liquid alkylcarbonate salts in the presence of amidines and guanidines (Figure 3.1).⁹⁻¹² Lewis acid gases that are valence isoelectronic to CO₂, such as COS and CS₂, exhibit similar reactivity to that of CO₂ with mixtures of amidines and alcohols. Both COS and CS₂ have a central electrophilic carbon and exhibit the same reactivity patterns as CO₂

in the presence of DBU and alcohol mixtures, resulting in the formation of analogous structures, COSBOL and CS₂BOL (Figure 3.1).¹²

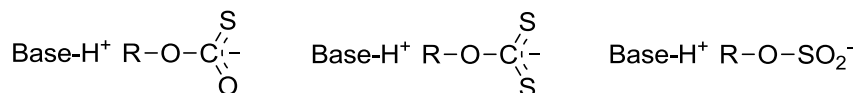
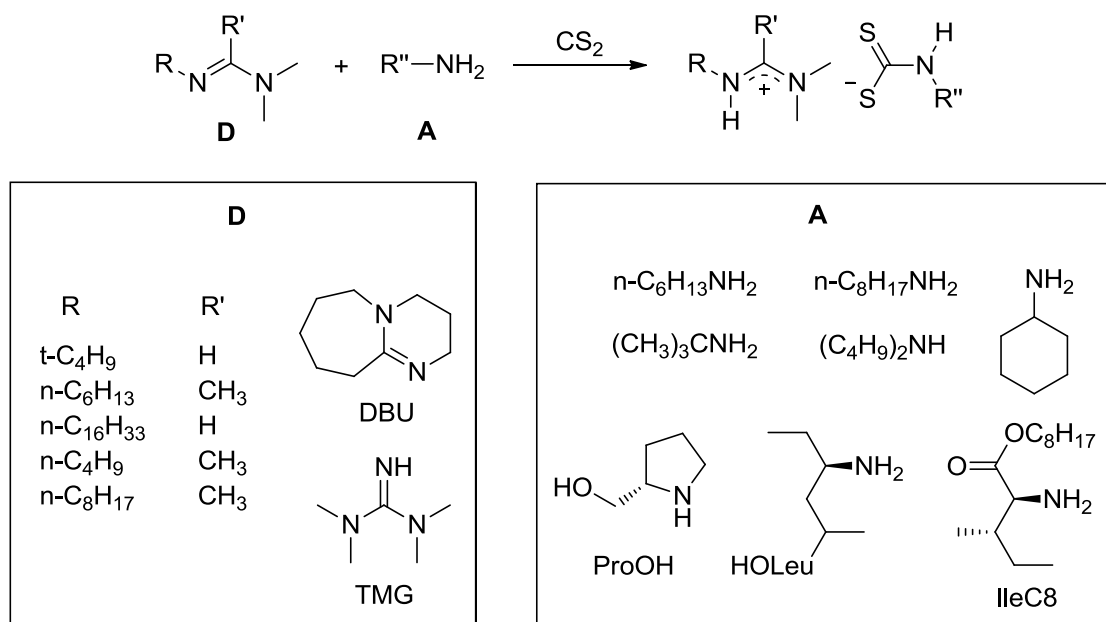


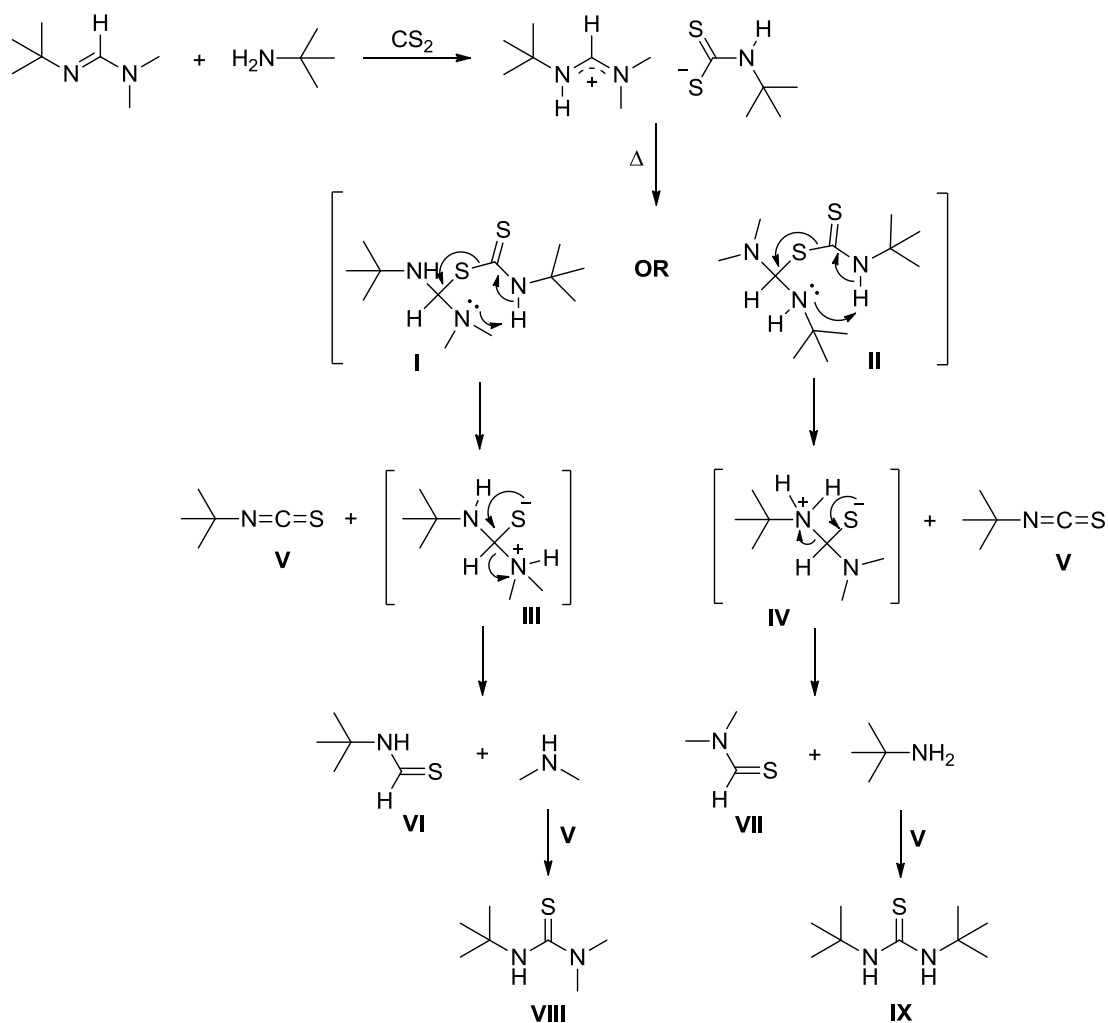
Figure 3.1. Starting from left: COSBOL salt, CS₂BOL salt, and SO₂BOL salt.¹²

Weiss and co-workers demonstrated that equimolar mixtures of amidine (**D**), an amine (**A**), and CS₂, can be transformed into room temperature ionic liquids (ILs), amidinium dithiocarbamates (Scheme 3.1).¹³ The amidinium dithiocarbamates are more thermally stable than their amidinium carbamate analogues, where CO₂ is added to amidine/amine mixtures, even in air. With temperatures above 50 °C and under an atmosphere of CO₂, amidinium carbamates decompose and lose a molecule of CO₂. The amidinium dithiocarbamates do not lose a molecule of CS₂ even with temperatures above 80 °C. The majority of the combinations found in Scheme 3.1 of amidine and amine remained a liquid at room temperature after the addition of CS₂. The combinations with the longest-chained linear amidine (carbon chain of 16) and amine did not produce a liquid at room temperature. Weiss and co-workers described the formation of the room temperature liquids with short-chained linear amidines, amines, and CS₂ because there is less ordering required for the smaller molecules in comparison to the long-chain linear amidines.¹³



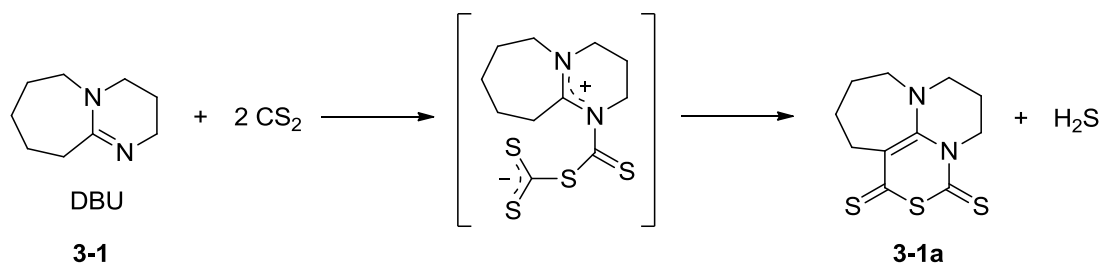
Scheme 3.1. Preparation of amidinium dithiocarbamates.¹³

The thermolysis of the amidinium dithiocarbamates leads to the formation of products including thioureas and thioformamides (Scheme 3.2). To gain insight into the mechanism of thermolysis, Weiss and co-workers isolated and identified the thermolysis products from the room temperature ionic liquid combination of a *t*-butyl amidine and *t*-butyl amine. They proposed that a covalent bond is first formed with the sulfur of the dithiocarbamate and the amidinium carbon atom followed by the addition of a proton to one of the nitrogen atoms of the amidine. The C-S bond of the CS₂ molecule results in the formation of an isothiocyanate (**V**) and a zwitterionic species (**III** or **IV**), that cleaves into a thioformamide (**VI** and **VII**) and an amine. The amines can then react with **V**, generating *N*-*tert*-butyl-*N'*,*N'*-dimethylthiourea (**VIII**) or *N,N'*-di-*tert*-butylthiourea (**IX**).¹³ Weiss and co-workers found that the pathways were consistent with the presence of dimethylamine and *t*-butylamine that were captured as their hydrochloride salts.^{13b}



Scheme 3.2. Proposed mechanism for the thermolysis of an amidinium dithiocarbamate.¹³

It has been demonstrated that the combination of DBU and an alcohol can capture CS_2 , forming a CS_2BOL (Figure 3.1),¹⁴ where the formation of a CS_2BOL does not form when DBU and CS_2 are reacted together at room temperature without an alcohol. At moderate temperatures, DBU does not react with CO_2 ,¹⁴ to form a stable detectable product, as described in the Introduction Chapter, the formation of a zwitterionic DBU- CO_2 adduct has been used to describe the observed reactivity with DBU and CO_2 . Upon reaction with two equivalents of CS_2 at room temperature the organosulfur compound **3-1a**, a trithioanhydride, is formed (Scheme 3.3).¹⁵



Scheme 3.3. Proposed mechanism for the reaction of DBU and CS₂¹⁵

Crystals of this compound were obtained in our lab by slow evaporation of hexanes over chloroform (Figure 3.2). The crystal structure had been previously reported by Vlasse and co-workers in an *Acta Cryst.* paper in 1986.¹⁵ Vlasse and co-workers prepared **3-1a** by refluxing a solution of DBU in CS₂ for 6 h and then removing the CS₂ by distillation, leaving behind an orange viscous material from which **3-1a** was precipitated. They also found that the DBU hydrogen sulfide salt was formed. The ring closing of the trithioanhydride occurs at the methylene that is *alpha* to the sp² carbon of the amidine. One would anticipate that having a *beta*-methylene is necessary for an amidine to react in this manner. Vlasse and co-workers proposed a mechanism, in which DBU reacts with two equivalents of CS₂, to first form a zwitterionic species with CS₂ from which cyclization occurs to yield trithioanhydride **3-1a** (Scheme 3.3). To date, there has not been any other study concerning the capture of CS₂ solely by DBU.

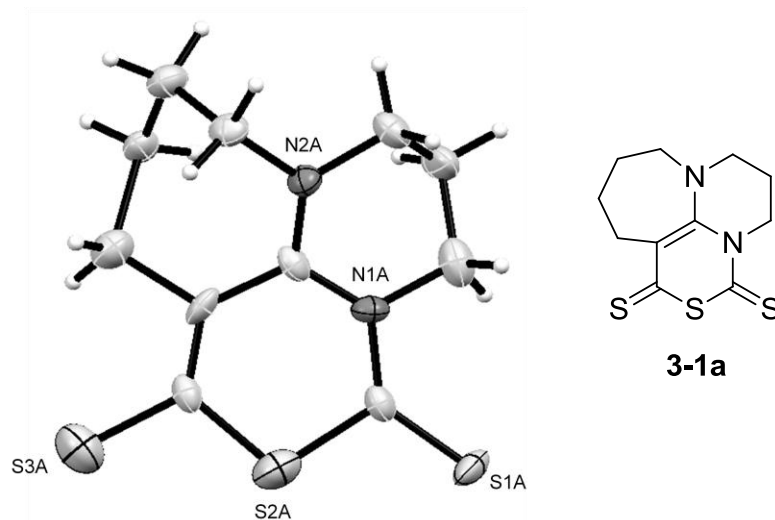
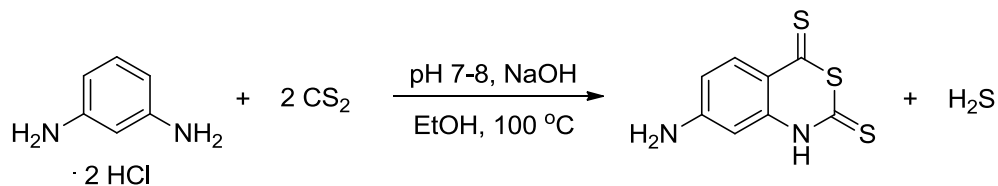
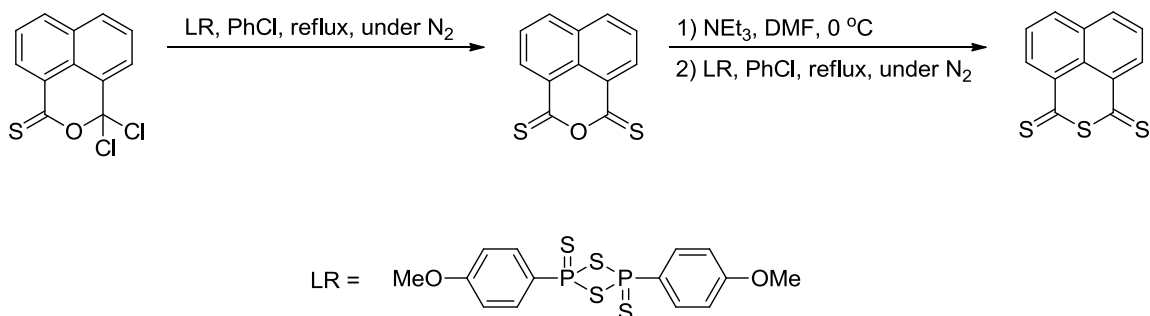


Figure 3.2. One of the two independent **3-1a** molecular structures isolated in the Jessop lab with ellipsoids drawn at 50 % probability level.

Structures that feature a cyclic trithioanhydride ring like that in **3-1a** are known, but to our knowledge, there are a limited number of reports where CS_2 alone is used for the thionation. A recent example is the hydrothermal reaction of 1,3-diaminobenzene and CS_2 ¹⁶ where the reaction mixture is first adjusted to a pH of 7-8 using sodium hydroxide in an autoclave and then heated for 96 h at 100 °C (Scheme 3.4). The first cyclic trithioanhydride that was synthesized was reported shortly before the crystal structure of **3-1a** was published, where an acid chloride derived from 1,8-naphthylidene anhydride was thionated using Lawesson's reagent in refluxing chlorobenzene (Scheme 3.5).¹⁷ The chloride derivative of 1,8-naphthalic anhydride is treated with Lawesson's reagent to give a dithioanhydride followed by the isomerization of the dithioanhydride with a catalytic amount of triethylamine in cold DMF. A second treatment with Lawesson's reagent in refluxing conditions affords the cyclic trithioanhydride with a naphthyl scaffold.



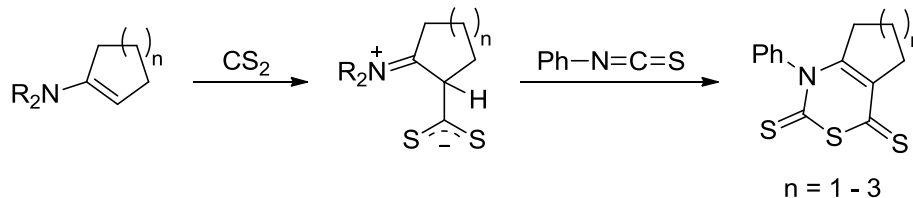
Scheme 3.4. Hydrothermal reaction forming a cyclic trithioanhydride from diaminobenzene and CS₂.¹⁶



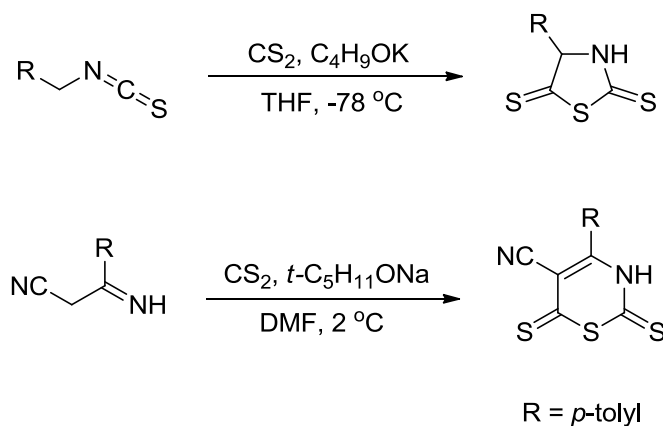
Scheme 3.5. Formation of the first reported cyclic trithioanhydride where thionation is done on a chloride derivative of 1,8-naphthalic anhydride using Lawesson's reagent (LR) in refluxing conditions.¹⁷

A general method to make the cyclic trithioanhydride is by using isothiocyanates in the presence of carbon disulfide and nucleophilic nitrogen compounds. An early example is by Gompper and co-workers, with the addition of CS₂ to tertiary amines followed by the addition of phenyl-isothiocyanate to form the cyclic trithioanhydride ring (Scheme 3.6).¹⁸ Muraoka and co-workers synthesized a number of structures that featured a cyclic trithioanhydride, except the addition of CS₂ was normally added as a second reagent.¹⁹ 4-Arylthiazolidene-2,5-dithiones were synthesized by treating alkyl benzyl isothiocyanates with CS₂ in the presence of potassium *t*-butoxide at -78 °C (Scheme 3.7, top).^{19b} 1,3-Thiazine-2,6-dithiones were synthesized by treating β-imino nitriles with two equivalents of CS₂ and *t*-pentyl oxide in DMF at low temperature

(Scheme 3.7, bottom).^{19c} Seemingly, the synthesis of **3-1a** is the only example where the use of CS₂ affords the cyclic trithioanhydride without additional reagents.

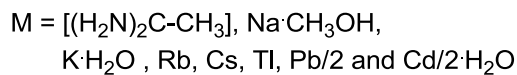
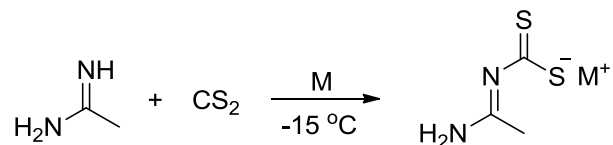


Scheme 3.6. Formation of a cyclic trithioanhydride ring with CS₂ and phenylisothiocyanate.^{18a}



Scheme 3.7. Synthesis of cyclic trithioanhydrides, 4-arylthiazolidene-2,5-dithiones (top)^{19b} and 1,3-thiazine-2,6-dithiones (bottom).^{19c}

Acetamidine, an acyclic amidine, does not form a cyclic trithioanhydride upon the reaction with CS₂. Gattow and co-workers studied the reaction of acetamidine and CS₂.²⁰ The addition of CS₂ to acetamidine gave a dithiocarbamate and an equivalent of acetamidinium salt. They were also able to isolate the dithiocarbamate with other counterions aside from the protonated acetamidine (Scheme 3.8).



Scheme 3.8. Reaction of acetamidine and CS₂ forming dithiocarbamates.²⁰

The molecular structure of the dithiocarbamate formed with acetamidine was determined with X-ray crystallography. The cation is associated with one anion through the hydrogen-bond bridges S···H-N and N···H-N, resulting in an eight-membered ring (Figure 3.3). While the nitrogen atoms of acetamidine bear hydrogens, deprotonation at either the amine or the methyl does not occur where a cyclic trithioanhydride can form. The addition of CS₂ is exclusively at the imino nitrogen atom. Decomposition of the structure occurs in solution at 20 °C.

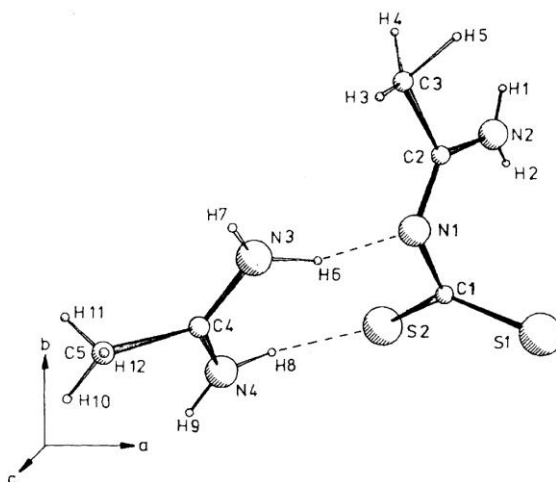
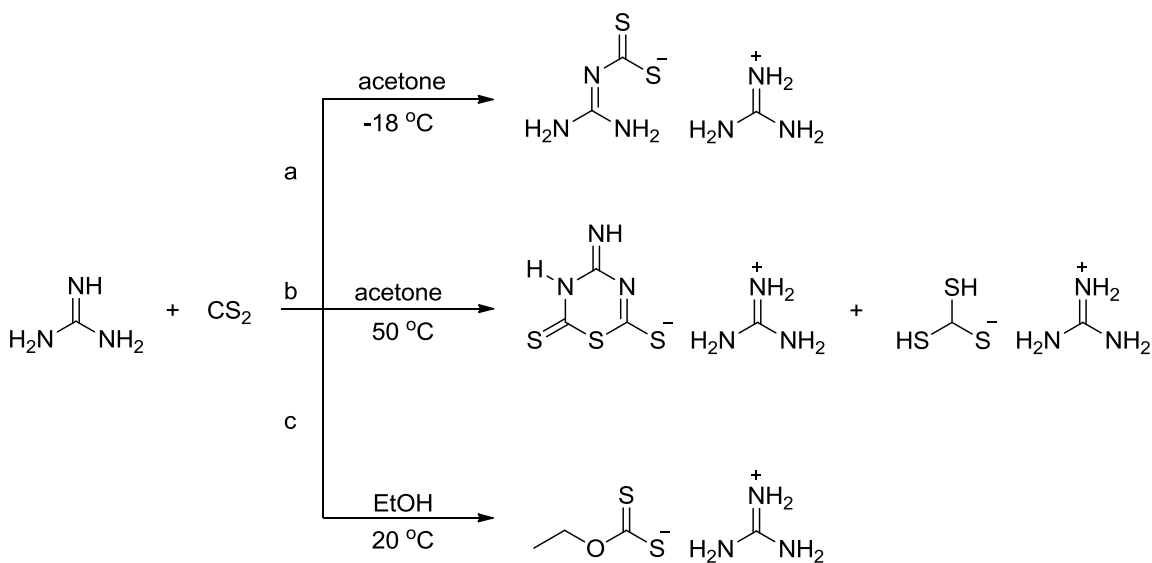


Figure 3.3. Molecular structure of acetamidine thiocarbamate and protonated acetamidine.^{20c}

Gattow and co-workers also investigated the reaction of CS₂ with guanidine, which is similar to acetamidine in that its three nitrogen atoms bear hydrogens.²¹ Interestingly, the reaction

with CS₂ produces different products depending on the temperature and solvent.^{21a} In cold aqueous acetone, the reaction of guanidine and CS₂ led to the formation of guanidinium guanidinodithioformate (Scheme 3.9, path a). When the reaction is heated, the reaction gave guanidinium trithiocarbonate and the guanidinium salt of 4-imino-2,6-dithio-1,3,5-thiadiazine (Scheme 3.9, path b) (a cyclic trithioanhydride). In contrast, in an ethanolic solution, guanidine reacts with CS₂ to form guanidinium ethyl xanthate (Scheme 3.9, path c) as observed in the CS₂BOLs (Figure 3.1).¹⁴



Scheme 3.9. Representation of the reaction of guanidine and CS₂ at three different conditions: path a) in acetone at -18 °C, path b) in acetone at 50 °C, and path c) in ethanol at 20 °C.^{21a}

Different guanidinodithioformates can be prepared with other counterions besides the guanidinium salt.^{21b} Formation of the guanidinodithioformic acid can be formed from the guanidinium guanidinodithioformate in aqueous solution with concentrated hydrochloric acid at 0 °C.^{21c} Gattow and co-workers were able to obtain crystals of the guanidinodithioformic acid that shows delocalization about the double bonds of the bound CS₂ and is stabilized by the hydrogen bonding between N-H...S.^{21d}

Herein, we report the reactivity of amidines and related compounds with CS₂, showing that the reaction outcome depends highly on the structure of the amidine base, yielding different products depending on whether the amidine and/or guanidine base is cyclic or acyclic. The characterization and synthesis of the products are reported including the first full characterization of the original cyclic trithioanhydride formed with DBU and CS₂.

3.2 Results and Discussion

3.2.1 Reaction of CS₂ and Cyclic Amidines

The cyclic amidines, DBU **3-1**, 1,5-diazabicyclo(4.3.0)non-5-ene **3-2** (DBN), and bis(1-methyl-4,5-dihydroimidazol-2-yl)methane **3-3**, were reacted with CS₂ and are shown in Figure 3.4. In general, each cyclic amidine was dissolved in an excess amount of CS₂ (2 to 3 equivalents) and stirred at room temperature overnight under an argon atmosphere. Unreacted CS₂ was removed under reduced pressure to leave an orange viscous material.

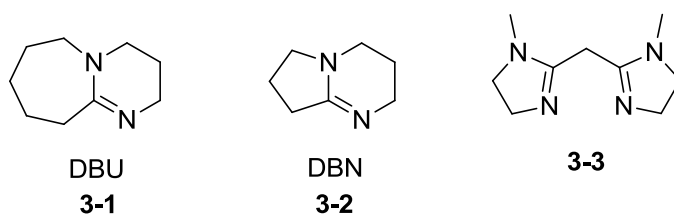
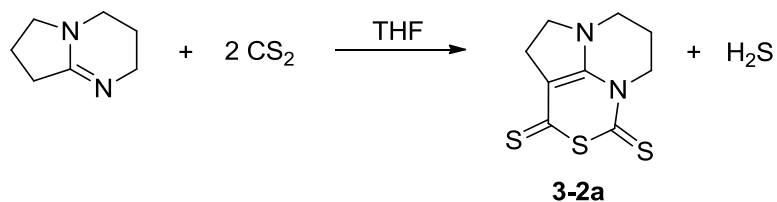


Figure 3.4. Cyclic amidines.

DBN is similar in structure to DBU except that it has a five membered instead of a seven membered ring. Upon reaction of three equivalents of CS₂ at room temperature with DBN in a small amount of THF, an immediate colour change occurred from clear and colourless to bright red (Scheme 3.10). After the reaction mixture was stirred overnight, a dark orange viscous material formed. A yellow solid was easily precipitated from the viscous orange layer by addition of dichloromethane and ethyl acetate. The ¹H NMR spectrum of the yellow precipitate differed

from DBN but the number of signals and their multiplicities did correspond to the expected chemical environments of a trithioanhydride product analogous to **3-1a**. Needle-like crystals of the yellow precipitate were grown by slow evaporation of chloroform over hexanes. X-ray crystallography confirmed a cyclic trithioanhydride structure **3-2a** derived from DBN (Figure 3.5).



Scheme 3.10. Preparation of cyclic trithioanhydrides **3-2a**.

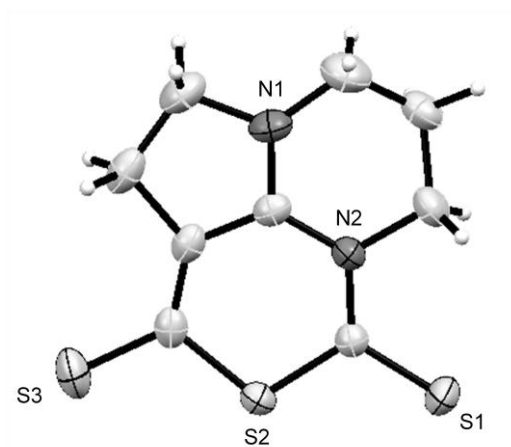
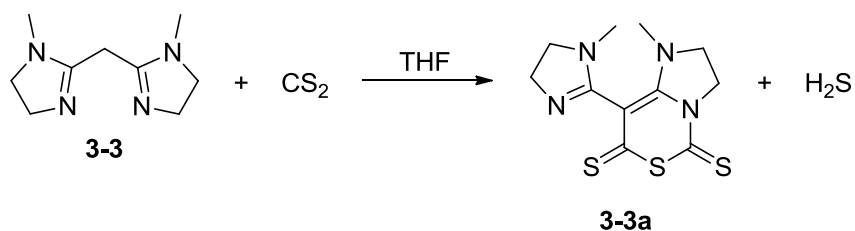


Figure 3.5. Molecular structure of **3-2a**. Displacement ellipsoids for non-H atoms are shown at the 50% probability level and H atoms are represented by circles of arbitrary size.

The bisamidine **3-3**, like DBU and DBN, features a methylene that is β to the basic nitrogen atoms. Upon reaction of two equivalents of CS_2 with **3-3** in THF, the clear mixture

immediately turned into a dark yellow solution (Scheme 3.11). After the reaction was stirred overnight an orange precipitate formed. Following column chromatography using alumina with 5% methanol in ethyl acetate, a yellow solid was isolated. Characterization of the plate-like crystals by X-ray crystallography confirmed the cyclic trithioanhydride structure **3-3a** derived from **3-3** (Figure 3.6). Within the unit cell, there is a major (~53%) and a minor conformer (~47%). In the major conformer (Figure 3.6, molecule A) the methyl groups point away from each other, and in the minor conformer (Figure 3.6, molecule B) the methyl groups face towards each other.



Scheme 3.11. Preparation of cyclic trithioanhydride **3-3a**.

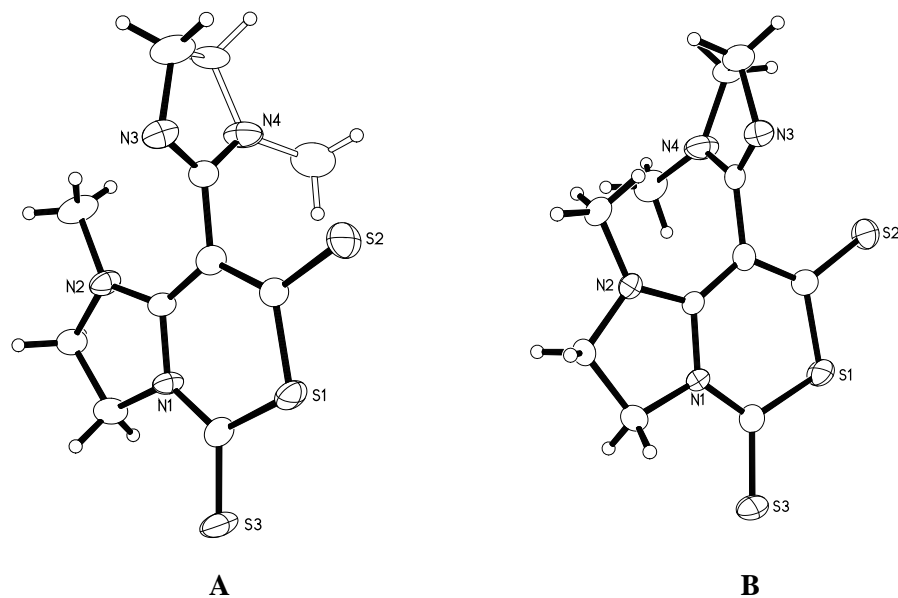


Figure 3.6. Molecular structure of **3-3a**: major conformer **A** (~53%) and minor conformer **B** (~47%). Displacement ellipsoids for non-H atoms are shown at the 50% probability level and H atoms are represented by circles of arbitrary size.

Upon the formation of a cyclic trithioanhydride, one equivalent of dihydrogen sulfide is evolved and as a result the amidinium hydrogen salt can be formed in conjunction. The amount and nature of the amidinium hydrogen salt varies between the different cyclic amidines. The corresponding hydrogen sulfide salt that forms from the synthesis of **3-1a** is described by Vlasse and co-workers as being a red oil,¹⁵ where the red oil was then treated with potassium hydroxide to remove the hydrogen sulfide. From the synthesis of **3-1a** in our lab, the corresponding hydrogen sulfide salt of DBU was observed in our lab and isolated as a red coloured oil. The corresponding hydrogen sulfide salt that results from the formation of **3-2a** is reddish brown oil, similar in nature to the one that is formed from the synthesis of **3-1a**. The reddish brown oil isolated from the synthesis of **3-2a** was dissolved in D₂O wherein the ¹H NMR a shift at 8.6 ppm is attributed to the H₂S. The hydrogen sulfide salt that results from the formation of **3-3a** is an orange solid. Crystals of the orange solid were grown by slow diffusion of hexanes over

chloroform, after which the molecular structure of the hydrogen sulfide salt was determined by X-ray crystallography (Figure 3.7).

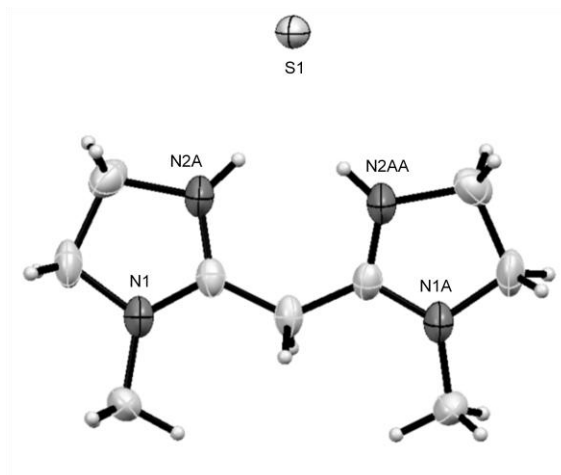


Figure 3.7. Molecular structure of hydrogen sulfide salt of **3-3**, isolated as a by-product from the synthesis of **3-3a**. Displacement ellipsoids for non-H atoms are shown at the 50% probability level and H atoms are represented by circles of arbitrary size.

3.2.2 Further Reactivity of Cyclic Amidine **3-3** with CS₂

The reaction of CS₂ with cyclic amidines (Figure 3.4) produces cyclic trithioanhydrides. Each cyclic trithioanhydride is formed about an imino nitrogen atom and a methylene that is *beta* to this imino nitrogen. Amidine **3-3** features two imidazoline rings and the cyclic trithioanhydride that forms with two equivalents of CS₂ is about the imino nitrogen atom of one ring and the bridging methylene. On two separate attempts to reproduce **3-3a**, two different compounds were isolated from each attempted reaction. One of the compounds showed formation of the cyclic trithioanhydride analogous to **3-3a** in the presence of hydrochloric acid, while the second compound remotely resembles that of the structure **3-3a**.

Synthesis of **3-3** first involves the formation of the bisamidine with a hydrochloric acid adduct, followed by the removal of this adduct with sodium hydride in the presence of a sparing amount of methanol. In an attempt to grow crystals of **3-3a** prepared from a sample of **3-3** that may have contained some residual HCl, a different molecular structure **3-3b** was determined from the reaction that is shown below (Figure 3.8). The molecular structure of **3-3b** is similar to that of **3-3a**, in that a cyclic trithioanhydride ring is formed but in the presence of hydrochloric acid and water. Interestingly, the formation of the cyclic trithioanhydride ring is favourable even in the presence of water, which is not the case for amidines in the presence of water and CO₂. Bicarbonate salt is formed with amidines in the presence of water and CO₂. The molecular structure of the bicarbonate salt of **3-3**, is prepared from reacting **3-3** with CO₂ and water in THF is shown below (Figure 3.9).

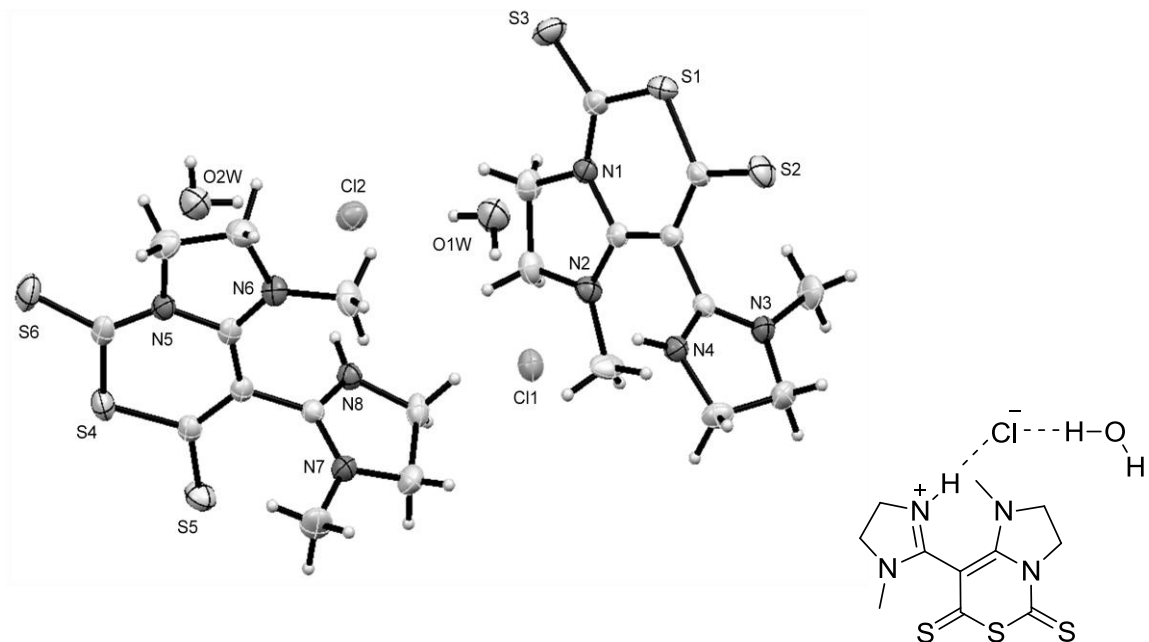


Figure 3.8. Molecular structure of **3-3b**. Displacement ellipsoids for non-H atoms are shown at the 50% probability level and H atoms are represented by circles of arbitrary size.

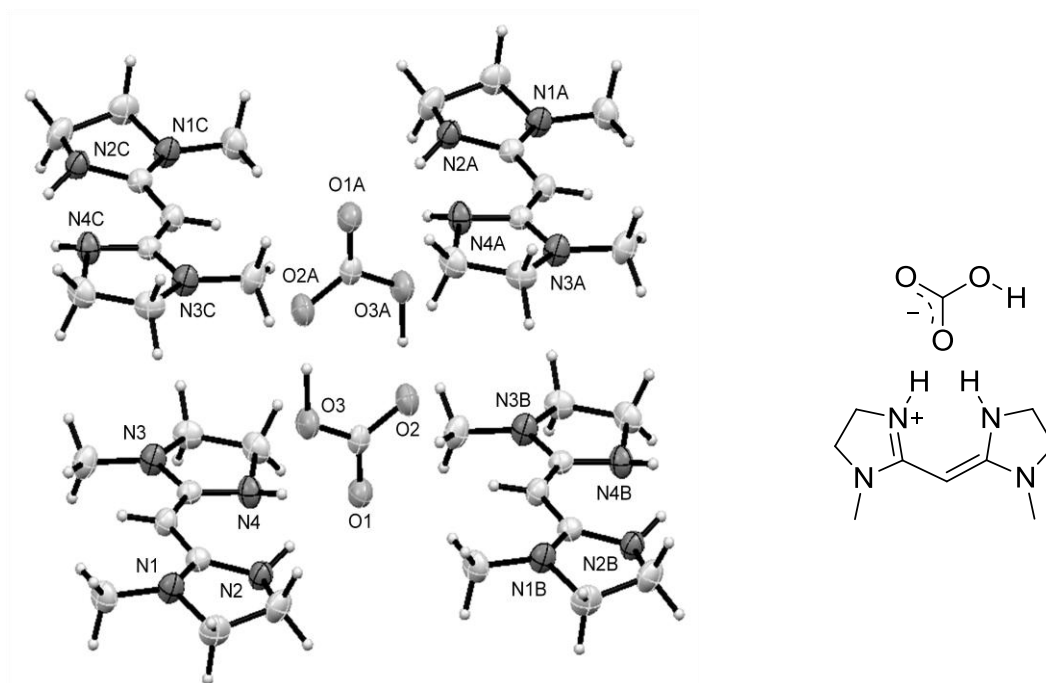


Figure 3.9. Molecular structure of bicarbonate salt formed with **3-3**. Displacement ellipsoids for non-H atoms are shown at the 50% probability level and H atoms are represented by circles of arbitrary size.

A reason for the presence of the hydrochloric acid in **3-3b** could be from the synthesis of **3-3** where the removal of the acid to give free bisamidine was not complete. Additionally, one would expect that protonation of a nitrogen atom on one of the rings would lower the probability of the cyclic trithioanhydride forming in that it occupies an imino nitrogen. The reaction of the hydrochloric acid salt of **3-3** with an excess amount of CS₂ did not show any observable change and the ¹H and ¹³C NMR spectra matched that of the starting material.

The reactivity of **3-3** and CS₂ is further shown by the isolation of a second structure in attempt to grow crystals of **3-3a** from a crude reaction mixture. Instead of yellow needle-like crystals that are attributed to **3-3a**, orange crystals that are parallelogram in shape precipitated out of solution. The molecular structure of the parallelogram-shaped crystals was determined by X-ray crystallography (Figure 3.10, **3-3c**). There are two heterocyclic six-membered rings that comprise **3-3c** and both are hydrogen bonding to a chloride ion. One of the six-membered rings is a pseudo cyclic trithioanhydride that is similar to that found in **3-3a** (Figure 3.10, molecule A of **3-3c**). The other second six-membered ring resembles a thiourea, where the thiocarbonyl is formed between two imino nitrogens of **3-3** (Figure 3.10, molecule B of **3-3c**). Like that of **3-3a**, the pseudo cyclic trithioanhydride of molecule A is formed about a methylene and an amino N-H that neighbours a thiocarbonyl, which is the only remaining fragment of the second imidazoline ring of the starting bisamidine **3-3**.

It is evident from the molecular structure that the two six-membered rings of **3-3c** are planar, where in molecule A the six-membered ring features a carbanion. The imidazoline in molecule A is perpendicular to the six-membered ring. The bond lengths of molecule A indicate that delocalization of either the positive or negative charges are confined to either the imidazoline or the six-membered ring respectively. The unit cell of **3-3c** (Figure 3.10) further illustrates that the two six-membered rings of each molecule in **3-3c** are planar. The formation of **3-3b** and **3-3c** could be dependent on the ratio comprising of **3-3** and its hydrochloride adduct form. The

formation of **3-3c** was not reproducible and could not be characterized. To the best of our knowledge, the structural motifs of the two six-membered rings have not been previously reported.

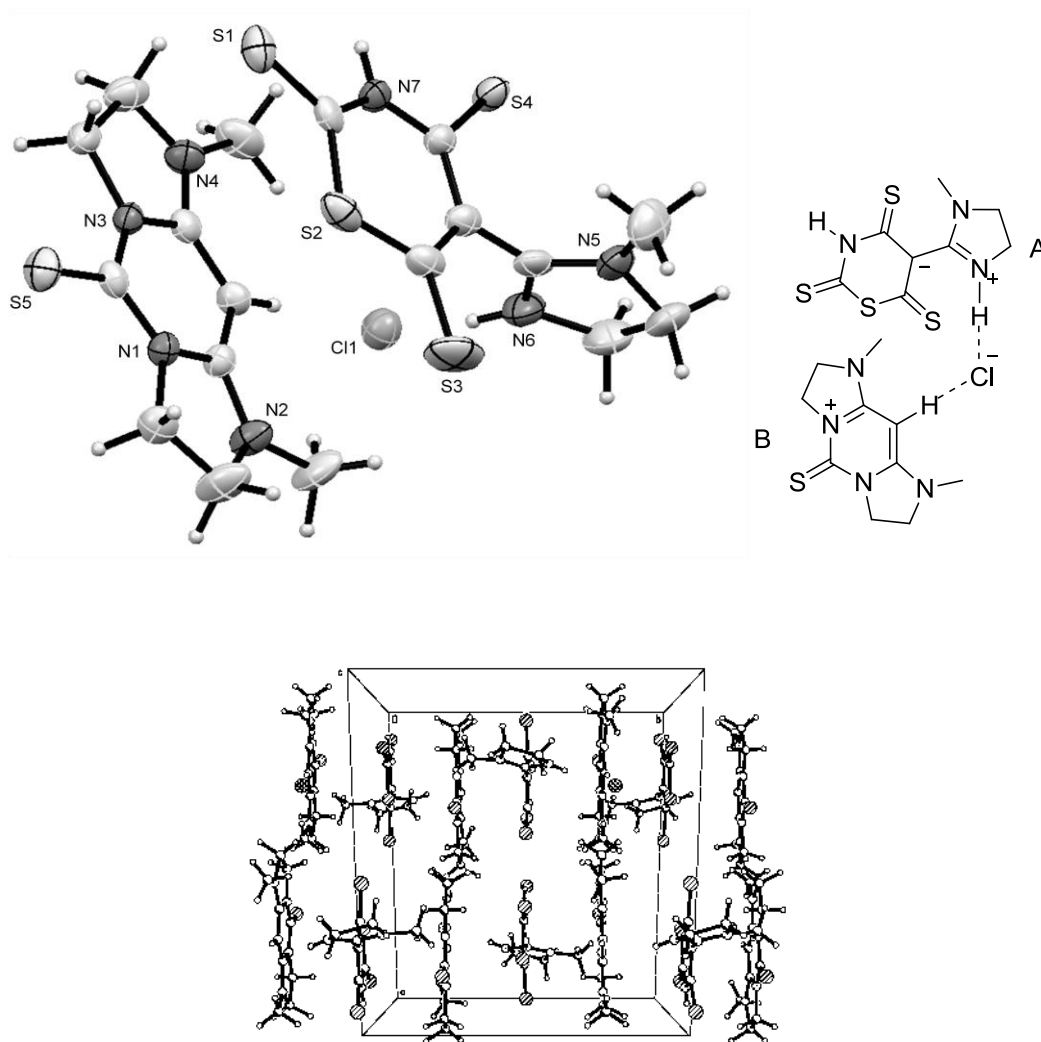


Figure 3.10. Molecular structure and unit cell packing of **3-3c**. Displacement ellipsoids for non-H atoms are shown at the 50% probability level and H atoms are represented by circles of arbitrary size.

3.2.3 Reaction of CS₂ with Cyclic Amidines Possessing an N-H Bond

Previously, cyclic amidines that were reacted with CS₂ featured an acidic methylene that was *beta* to the imino nitrogen centre and the two nitrogen atoms in the amidines were fully alkylated. With the exception of structure **3-3c**, reaction of CS₂ with the cyclic amidines featuring an imino nitrogen atom produced a cyclic trithioanhydride ring where all the atoms in the structure were neutral.

Cyclic amidines containing an N-H bond may exhibit different reactivity with CS₂. The cyclic amidine bearing an N-H site could act as a base and, in its protonated form, a proton donor. The N-H site is relatively more basic than an imino nitrogen site, so that it may capture CS₂ more readily than an acidic methylene that is present in the previous cyclic amidines. Having an N-H within a cyclic amidine might provide different reactivity with CS₂. A cyclic amidine that features a N-H site is 2-ethyl-2-imidazoline **3-4** (Figure 3.11).

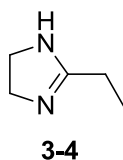


Figure 3.11. 2-Ethyl-2-imidazoline **3-4**

Upon the addition of CS₂ to **3-4** in THF at room temperature, a yellow precipitate forms that is insoluble in THF. The yellow powder from the reaction of CS₂ and **3-4** was separated from the solvent by filtration. After filtration, slow evaporation of the orange filtrate produced needle-like orange crystals that corresponded to a cyclic trithioanhydride structure **3-4a** (Figure 3.12). Seemingly, the formation of the cyclic trithioanhydride does not occur readily with **3-4**, in that orange compound **3-4a** was only a minority of the product; the majority of the material formed is an unknown yellow powder.

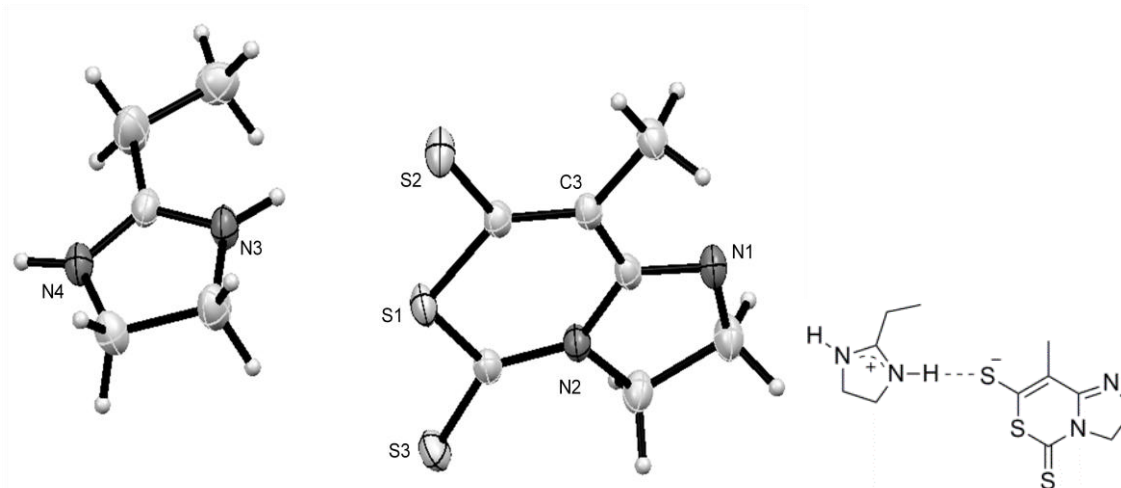
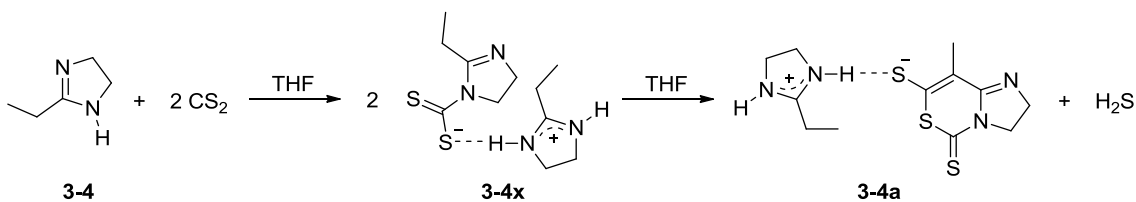


Figure 3.12. Molecular structure of **3-4a**. Displacement ellipsoids for non-H atoms are shown at the 50% probability level and H atoms are represented by circles of arbitrary size.

The yellow powder isolated from the reaction of **3-4** and CS_2 is not soluble in common organic solvents and the ^1H and ^{13}C NMR spectra of the yellow powder were obtained in deuterated dimethyl sulfoxide. The ^1H NMR spectrum of the yellow powder revealed two different sets of signals that correspond to protonated **3-4** and a second imidazoline species. The methylene signal for the protonated **3-4** is seen as a singlet at 3.61 ppm, indicative of a symmetric species. In contrast, the unknown imidazoline species has two triplets, 4.13 ppm and 3.34 ppm, that correspond to the two ring methylenes indicative of a C_s symmetry. The ^1H NMR spectrum of the yellow powder is consistent with structure **3-4x** but not with structure **3-4a** (Scheme 3.12), because the methyl signals appear as triplets, while for **3-4a**, a singlet would be expected. The ^{13}C NMR spectrum shows two sets of peaks that correspond to protonated **3-4** and the unknown imidazoline, with the addition of a quarternary signal at 215.3 ppm that could correspond to a CS_2 -adduct. It does not correspond to free CS_2 which has a signal at 192.58 ppm in ^{13}C NMR spectrum. The ^1H and ^{13}C NMR spectra could correspond to the formation of the dithiocarbamate salt of **4** (Scheme 3.12, **3-4x**), where decomposition of the salt would lead to the formation of **3-**

4a. Similarly, Sawa and co-workers reacted carbon disulfide with **3-4** to form 2-ethyl-2-imidazoline-1-carbodithioic acid,²² but the compound was characterized only by its melting point (95-8 °C).



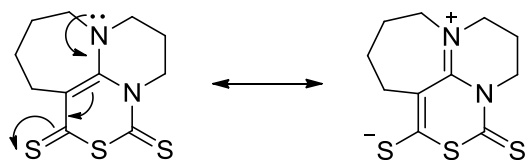
Scheme 3.12. Synthesis of **3-4a**, with proposed yellow precipitate structure **3-4x**.

The molecular structure of **3-4a** revealed that a cyclic trithioanhydride formed with 2-ethyl-2-imidazoline, though by complete deprotonation of the methylene that is *beta* to the nitrogen site. The reaction with CS₂ generates a salt, formed by protonated **3-4** and the cyclic trithioanhydride with an anionic sulfur (Figure 3.12). It can be speculated that the N-H site of **3-4** captured CS₂, where a second equivalent of imidazoline acted as a base.

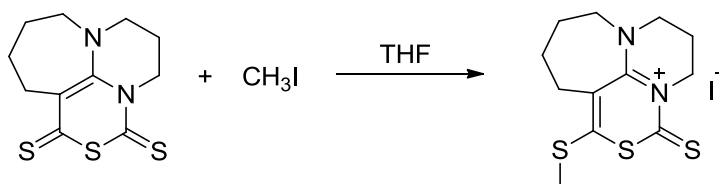
The ease with which the cyclic trithioanhydride is formed is dependent on which type of cyclic amidine is reacted with CS₂. The more hindered cyclic amidines such as that of DBU, DBN, and **3-3**, immediately formed stable cyclic trithioanhydrides with CS₂ and were isolated as orange solids. Upon the addition of CS₂ to cyclic amidine **3-4**, formation of the cyclic trithioanhydride is not favoured. Only a small amount of cyclic structure **3-4a** was isolated from the orange THF filtrate. According to ¹H and ¹³C NMR spectroscopy, the majority species, the yellow powder could be 2-ethyl-2-imidazoline-1-carbodithiocarbamate salt **3-4x**.

3.2.4 Methylation and Ring Opening of Cyclic Trithioanhydride **3-1a**

The cyclic trithioanhydride rings feature three sulfur atoms that could be susceptible to further reactivity and/or for usage in the formation of sulfur containing compounds. The cyclic trithioanhydrides formed from DBU and DBN are stable, and within the trithioanhydride ring, a nucleophilic sulfur is evident due to the resonance of the second amidinium nitrogen (Scheme 3.13). Reactivity at the more nucleophilic sulfur was observed when **3-1a** was reacted with one equivalent of iodomethane in THF at room temperature and allowed to stir overnight (Scheme 3.14). According to ^1H and ^{13}C NMR spectroscopy mono-methylation occurred exclusively at the most nucleophilic sulfur.



Scheme 3.13. Resonance of **3-1a** exhibiting the nucleophilic character of conjugated sulfur atom.



Scheme 3.14. Methylation of **3-1a** with iodomethane forming **3-1b**.

Crystals were grown by slow evaporation of chloroform over hexanes and X-ray crystallography confirmed methylation of **3-1a** at the more nucleophilic sulfur. The iodide is interacting with both the nitrogen centres of the DBU backbone (Figure 3.13). The molecular structure reveals that the bond length of N2-C1 is similar to that of N1-C1, which corresponds to positive charge about the two nitrogen atoms.

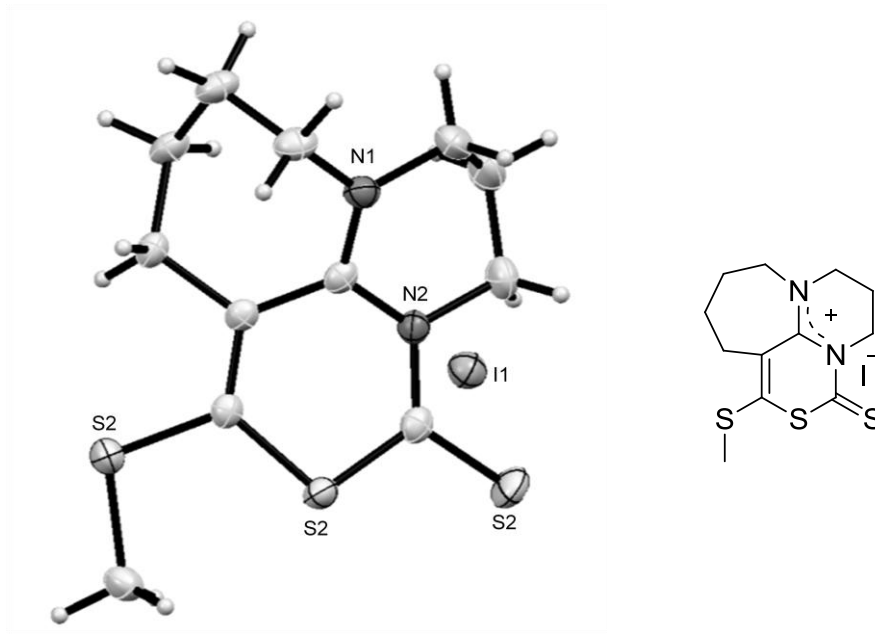
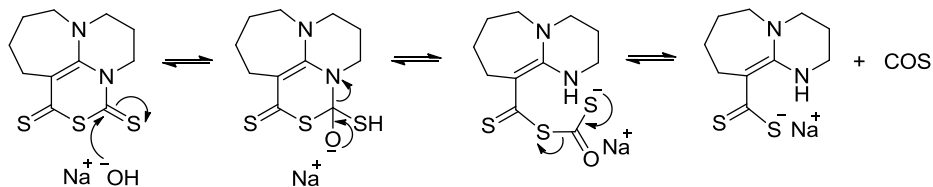


Figure 3.13. Molecular structure of **3-1b**. Displacement ellipsoids for non-H atoms are shown at the 50% probability level and H atoms are represented by circles of arbitrary size.

The ability to probe the cyclic trithioanhydride structure could lead to ring opening thus making the imino nitrogen and atoms within the structure accessible for further reactivity, as well as the synthesis of sulfur containing compounds. It was envisioned that by reacting the cyclic trithioanhydride with a strong nucleophile, such as sodium hydroxide, ring opening *via* the lone pair of the nitrogen atom in the DBU skeleton could be achieved (Scheme 3.15).



Scheme 3.15. Proposed mechanism of sodium hydroxide reacting with **3-1a** to a ring-opened structure.

When sodium hydroxide was reacted with **3-1a**, **3-1a** became soluble in water where originally it did not dissolve in water. One equivalent of sodium hydroxide was reacted with **3-1a** in water and the resulting solution was heated to 80 °C overnight. At first the orange solid **3-1a** was suspended in water, but within one hour the orange solid dissolved resulting in a clear light yellow solution. The following day, the clear yellow aqueous solution was extracted with dichloromethane. The organic layer was dried with magnesium sulfate and the organic solvent was removed under reduced pressure to give a light orange solid. The ¹H NMR spectrum of the isolated solid differed from that of **3-1a** (Figure 3.14, middle spectrum). The main difference between the ¹H NMR spectrum of **3-1a** and that of the orange solid is the chemical shift corresponding to the methylene that neighbours the imino nitrogen partaking in the cyclic trithioanhydride of **3-1a**. The chemical shift for the methylene in the ¹H NMR spectrum of **3-1a** is located at 3.1 ppm, where the corresponding signal for the orange solid is at 2.8 ppm. Crystals were not successfully grown from this product, though high-resolution mass spectrum of the unknown orange solid from the reaction of **3-1a** and sodium hydroxide gave a value of [M + Na]⁺ 251.0642 m/z that corresponds to the proposed ring-opened product (Scheme 3.15).

The proposed ring-opened product could have the potential to capture CO₂. The orange solid from the reaction of **3-1a** and sodium hydroxide, was dissolved in CD₂Cl₂ and placed into an NMR tube. To this solution, CO₂ was bubbled. The ¹H NMR spectrum of the CO₂-saturated solution was different from those of **3-1a** and the ¹H NMR spectrum of the proposed ring opened product (Figure 3.14, bottom spectrum). New chemical shifts appeared in the ¹H NMR spectrum of the CO₂ saturated solution that correspond to a new DBU based species. Attempts to isolate and fully characterize this species, were unsuccessful.

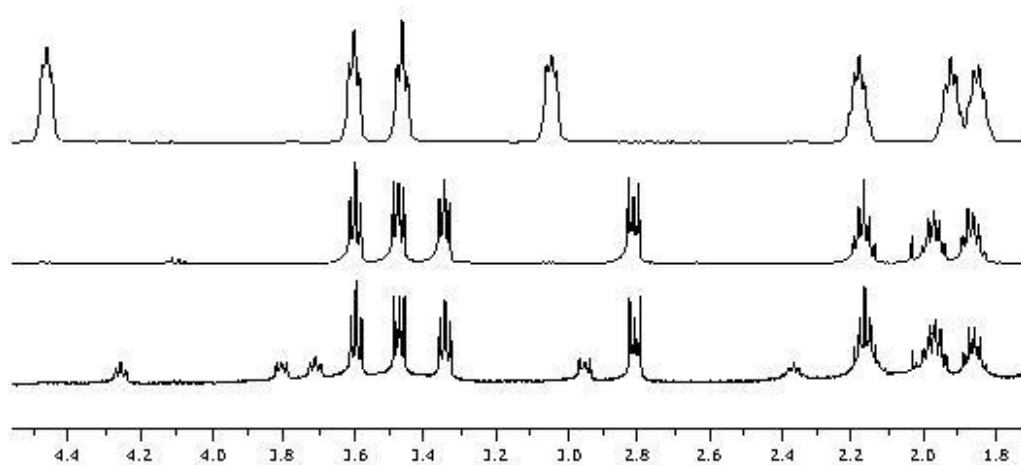
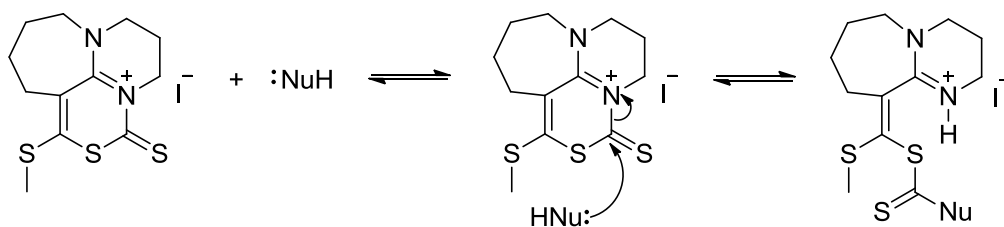


Figure 3.14. Stacked ^1H NMR spectra, 400 MHz, in CD_2Cl_2 at room temperature. Top spectrum: **3-1a**, middle spectrum: proposed ring-opened structure, and bottom spectrum: after bubbling CO_2 through solution of proposed ring-opened structure.

It can be envisioned that ring-opening can be achieved following a structural alteration of the trithioanhydride ring, thus providing the avenue for new reactivity. Following the methylation of **3-1a**, producing **3-1b**, the DBU skeleton features a positively charged nitrogen atom where the addition of electrons into this structure would possibly lead to ring-opening (Scheme 3.16). Reaction of **3-1b** with one equivalent of dimethylamine in THF led to the precipitation of a white solid after stirring overnight at room temperature.



Scheme 3.16. Proposed mechanism following the addition of a nucleophile to **3-1b**.

The ^1H NMR spectrum of the white precipitate exhibited two singlets at 3.57 ppm and 2.47 ppm. The singlet at 2.47 ppm corresponds to the methyl on the sulfur where this signal is shifted slightly upfield from its original position of 2.60 ppm as **3-1b**. The second singlet integrates to six protons, which infers the incorporation of the dimethylamino substituent into the structure. Unreacted dimethylamine should not be present in the system because it would otherwise be lost to evaporation, due to its high volatility.

Crystals were grown of the white powder by slow evaporation of dichloromethane over hexanes. The molecular structure that was determined from X-ray crystallography exhibited a ring-opened structure **3-1c** (Figure 3.15). The molecular structure of **3-1c** is the ring opened version of **3-1b**, though surprisingly, a chloride counterion is in place of the iodide counterion attributed to **3-1b**.

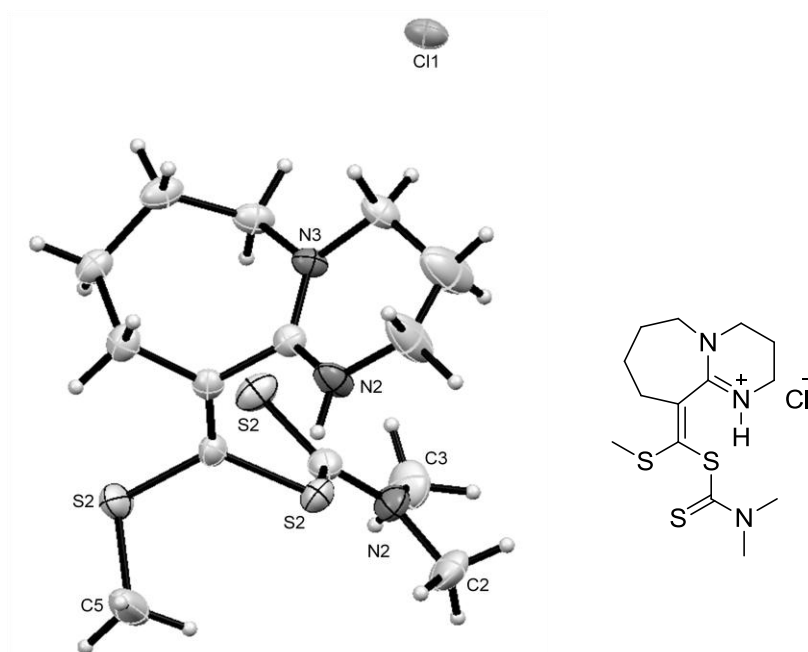
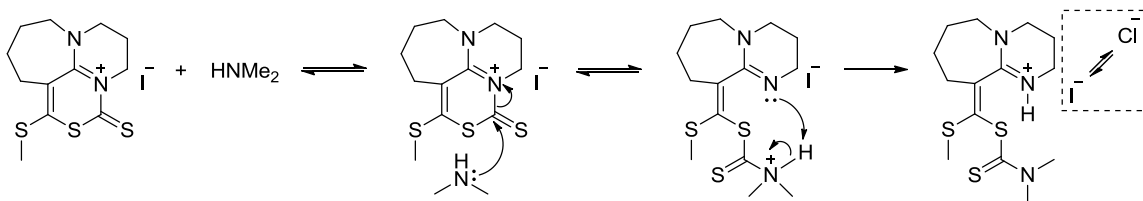


Figure 3.15. Molecular structure of **3-1c**. Displacement ellipsoids for non-H atoms are shown at the 50% probability level and H atoms are represented by circles of arbitrary size.

The positively charged nitrogen atom of **3-1b** renders it as an electrophile where the dimethylamine can attack to give the ring-opened structure. Protonation of the imino nitrogen can occur from the positively charged dimethylamine following attack at the neighbouring electrophilic thiocarbonyl or can also be from the small impurities of hydrochloric acid in the dichloromethane. Formation of **3-1c** could follow the mechanism shown below (Scheme 3.17).



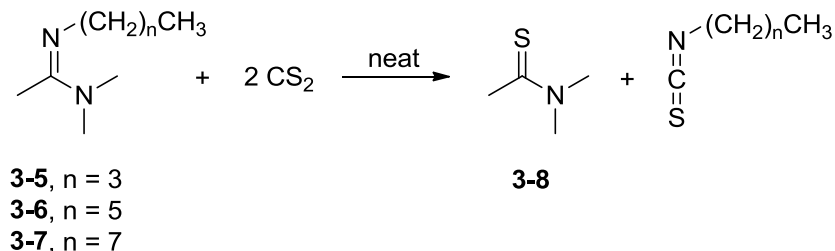
Scheme 3.17. Proposed mechanism for the formation of **3-1c**. Dashed box represents the proposed counterion exchange by crystal growth of **3-1c** by slow evaporation in dichloromethane.

The molecule showcases a structural motif that is related to dithiocarbamic acids and sulfur-containing alkaloids. Related dithiocarbamic acids that exhibit a dimethylamino group were studied as fungicides and for the synthesis of rubber.²³ Reported activities for sulfur-containing alkaloids involve cytotoxicity, antifungal, antiviral, and immunoresponsive activity.²⁴ This novel structural motif in **3-1c** about the DBU skeleton could potentially have bioactivity or can be used as a precursor for novel sulfur containing species. The interplay between the electrophilic site, the methylene *beta* to the imino nitrogen atom, and the imino nitrogen atom, that can act as an intramolecular base, could be exploited further to investigate new DBU-based structures in order enhance DBU's reactivity in organic transformations.

3.2.5 Reaction of CS₂ and Acyclic Amidines and an Acyclic Guanidine

It has been shown above that the reaction of cyclic amidines with CS₂ affords cyclic trithioanhydrides, where deprotonation and nucleophilic attack by CS₂ occur at an acidic site that is *beta* to the nitrogen centre. Acyclic amidines of the type shown below (Scheme 3.18) also have

sites *beta* to the nitrogen centre and that are vulnerable to deprotonation. Synthesis of such acyclic amidines follows the reaction between a primary amine and *N,N*-dimethylacetamide dimethyl acetal and upon the elimination of two equivalents of MeOH, a variety of acyclic amidines can be made in good yields.²⁵

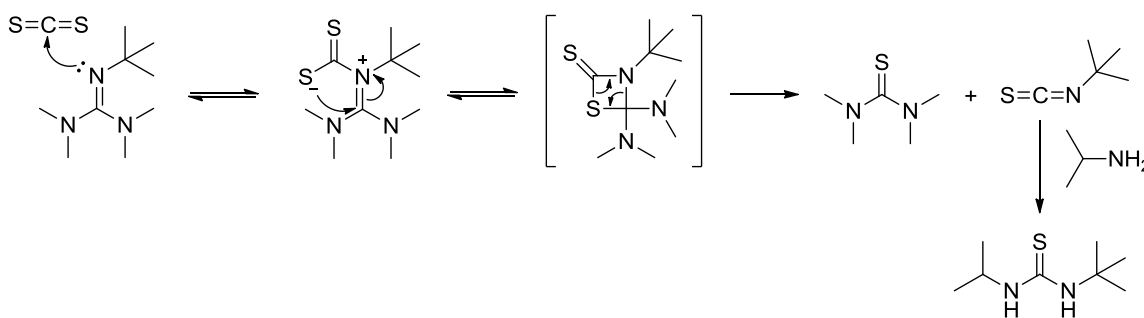


Scheme 3.18. Acyclic amidines **3-5** – **3-7** reacted with CS₂ forming *N,N*-dimethylthioacetamide **3-8** and alkylated isothiocyanates.

The addition of CS₂ to the acyclic amidines **3-5** – **3-7** does not lead to the formation of corresponding cyclic trithioanhydrides. The acyclic amidines dissolve in an excess amount of CS₂ (up to 3 eq) to give a deep red solution. After the solution was stirred overnight at room temperature, beige crystals precipitate out of solution leaving behind a deep red solution. While the acyclic amidines have sites *beta* to the nitrogen centre that are susceptible to deprotonation, the addition of CS₂ to the acyclic amidine forms *N,N*-dimethylthioacetamide **3-8** and isothiocyanates with the corresponding alkyl chains of **3-5** to **3-7**. The X-ray data obtained from the diffraction of **3-8** was highly disordered and a reasonable structure could not be solved. However both the ¹H and ¹³C NMR spectra of **3-8** and the isothiocyanates correspond to those reported in the literature.²⁶

Similar reactivity for guanidines was reported by Barton and co-workers where the addition of CS₂ to a pentaalkylated guanidine led to rapid formation of *N,N,N',N'*-tetramethylurea.²⁷ They proposed a mechanism where following the addition of CS₂ to the imino nitrogen of 2-*tert*-butyl-1,1,3,3-tetramethylguanidine, the nucleophilic sulfur of the appended CS₂

attacks the sp^2 hybridized carbon, creating a four membered cyclic transition state that rearranges to form the thiourea and *tert*-butyl isothiocyanate. Trapping the *tert*-butyl isothiocyanate was done by the addition of isopropylamine to the reaction mixture that produced *N-tert*-butyl-*N'*-isopropylthiourea (Scheme 3.19). The same reaction was done within our lab, without the addition of isopropylamine, and gave the *N,N,N',N'*-tetramethylurea as colourless crystals in near quantitative yield (Figure 3.16).



Scheme 3.19. Proposed mechanism for the formation of thiourea formed from pentaalkylated guanidine.²⁷

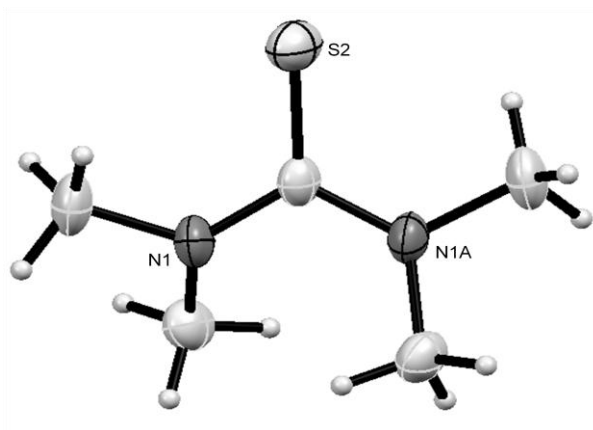


Figure 3.16. Molecular structure of *N,N,N',N'*-tetramethylthiourea. Displacement ellipsoids for non-H atoms are shown at the 50% probability level and H atoms are represented by circles of arbitrary size.

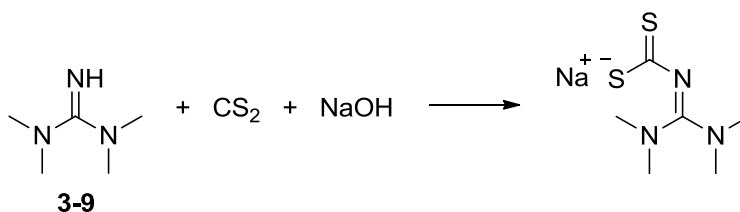
The synthesis of *N,N*-dimethylthioacetamide and the corresponding isothiocyanates by way of the reaction CS_2 to the acyclic amidines is atom economical, because there are no unwanted side products. The reaction occurs in near quantitative yield, where **3-8** precipitate was easily separated from the red supernatant by simply washing it with diethyl ether. The crude ^1H NMR spectrum of the red supernatant shows that the separated isothiocyanates are practically in their pure form. The X-ray data obtained from the diffraction of the crystals of **3-8** was highly disordered and a reasonable structure could not be solved. However, both the ^1H and ^{13}C NMR spectra of **3-8** and isothiocyanates correspond to those reported in the literature.²⁶ Generally, the synthesis of **3-8** is achieved by the thionation of the carbonyl of *N,N*-dimethylacetamide with a variety of thionating agents.^{26, 28-30} With other thionating agents, purification of the product uses solid phase extraction,²⁸ highly toxic side products are formed^{26, 28-30} and the use of solvents or base promoters are required.²⁹⁻³⁰ With the addition of CS_2 to the various acyclic amidines, the side products are *N,N'*-dimethylacetamide and the corresponding isothiocyanates, which could also be seen as useful reagents.

3.2.6 Reaction of CS_2 with Acyclic Guanidine that Features an Imino N-H Bond

Different reactivity is exhibited with CS_2 depending on whether an amidine is cyclic or acyclic. Bicyclic amidines where both nitrogen atoms are hindered give a cyclic trithioanhydride that forms between an imino nitrogen and a methylene that is *beta* to it. The reaction of CS_2 with ethyl imidazoline, a cyclic amidine that features an amino N-H, leads to the formation of cyclic trithioanhydride but with complete deprotonation about the *beta*-methylene producing a charged species and formation of a salt with protonated ethylimidazoline. Acyclic amidines that have no N-H bonds give a thioamide and corresponding isothiocyanate upon reaction with CS_2 . The same reactivity is found with a pentaalkylated guanidine, 2-*tert*-butyl-1,1,3,3-tetramethylguanidine, developed by Barton and co-workers.²⁷ The reactivity of CS_2 with an acyclic guanidine or

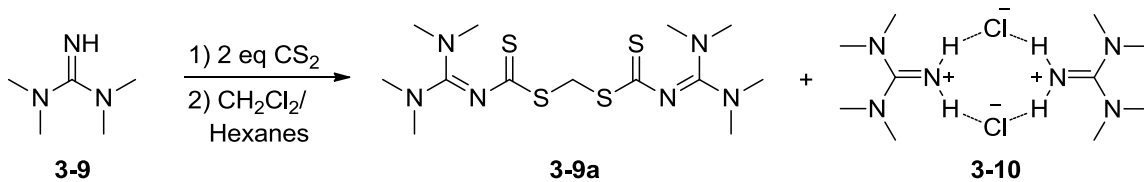
amidine that features an N-H at the imino nitrogen atom could potentially lead to a single CS₂ adduct, a thiocarbamic acid.

1,1,3,3-Tetramethylguanidine **3-9** is an acyclic guanidine that features an imino N-H (Scheme 3.20, **3-9**) and in the presence of CS₂ it has been used as a precursor for the synthesis of 5-dialkylamino-1,2,4-dithiazole-3-ones and 3-thiones for use as fungicides.³¹ The syntheses of such compounds first involve the formation of an alkali salt where **3-9** is reacted with CS₂ in the presence of a strong base such as sodium hydroxide (Scheme 3.20).



Scheme 3.20. Reaction of 1,1,3,3-tetramethylguanidine **3-9** and CS₂ in the presence of sodium hydroxide.³¹

In the Jessop Lab, the reaction of **3-9** and CS₂ produces an orange solid and when it is dissolved in a mixture of dichloromethane and hexanes gives a dimeric structure **3-9a**. The dimeric structure **3-9a** is formed having a methylene between two CS₂-adducts formed with the guanidine (Scheme 3.21). Similar to previous reports, a CS₂-**3-9** is formed before formation of the dimer. Dichloromethane is an electrophile where two CS₂-**3-9** adducts react with it through two anionic sulfurs. In the same reaction mixture the corresponding guanidinium salt forms with the chlorides that are lost from dichloromethane **3-10**. In the dichloromethane solution of **3-9a** and **3-10**, colourless needle-like crystals of **3-9a** and white opaque block shaped crystals of **3-10** grow alongside each other. The molecular structures of **3-9a** and **3-10** were confirmed by X-ray crystallography (Figure 3.17).



Scheme 3.21. Reaction of CS_2 and **3-9** in the presence of CH_2Cl_2 and hexanes to give **3-9a** and **3-10**.

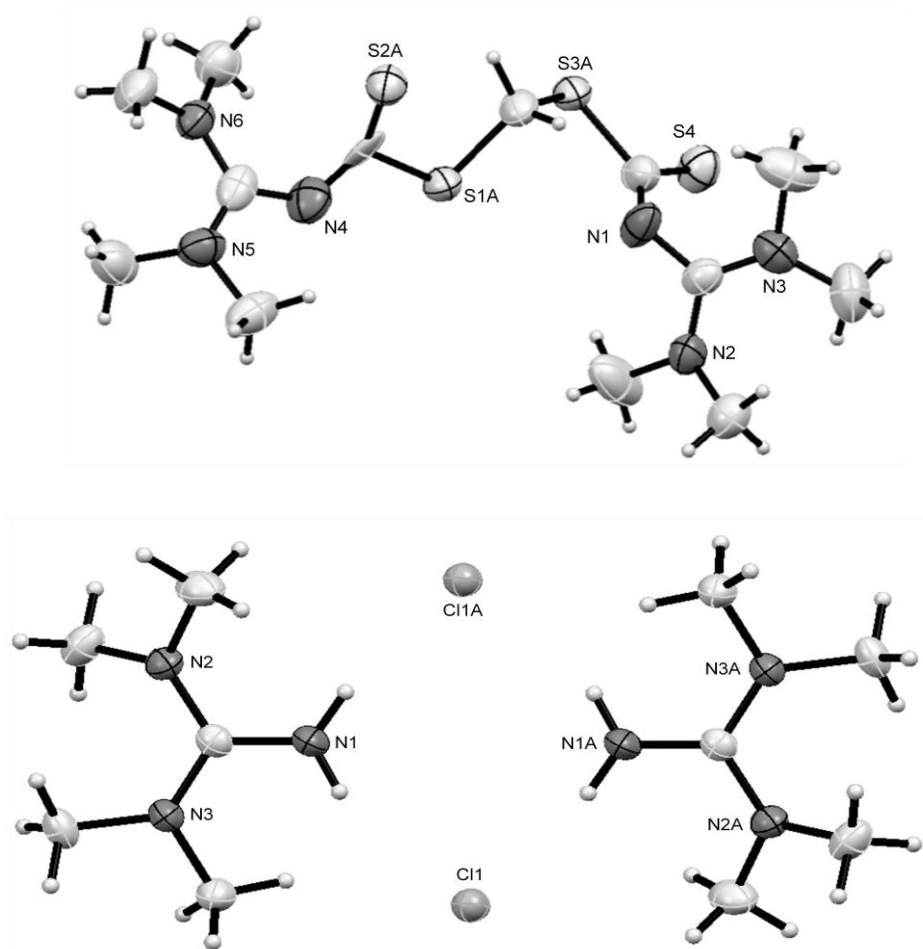
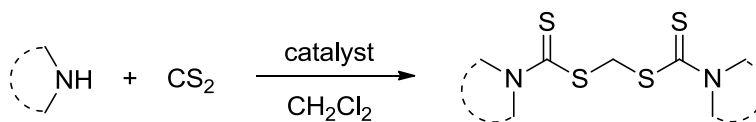


Figure 3.17. Molecular structures of **3-9a** and **3-10**. Displacement ellipsoids for non-H atoms are shown at the 50% probability level.

While the above reactivity has not been demonstrated with guanidines in the literature, similar reactivity can be found with the reaction of CS_2 and secondary amines with

dichloromethane forming dithiocarbamate compounds in alkali solution or with organic catalysts (Scheme 3.22).³² The preparation of such compounds are mainly reported in patents.^{33,34} Céspedes and co-workers looked at the reaction of thioanions formed by a variety of amines in the presence of CS₂ where the reaction poly(ethylene glycol) 1,500 was used as a phase transfer catalyst.³² Ranu and co-workers found that by using the ionic liquid 1-methyl-3-pentylimidazolium bromide ([pmIm]Br) at 0 °C, there was an acceleration in rate where the reaction occurs in minutes as opposed to the hours that it takes when PEG is used as a catalyst and at an operating temperature of 20 °C.³⁵ With the above conditions a variety of *N,N*-dialkyldithiocarbamates are prepared.



catalyst = PEG 1500 at 20 °C or [pmIm]Br at 0 °C

Scheme 3.22. Formation of *N,N*-Dialkyldithiocarbamates with secondary amines, CS₂, and dichloromethane.^{32, 35}

3.2.7 Reaction of CS₂ with Related N-Containing Compounds

It was proposed that compounds that contain heteroatoms in addition to nitrogen could react with CS₂ in a similar fashion to what is found with amidines that have an acidic site *beta* to the nitrogen centre forming a cyclic trithioanhydride. Five candidates were considered to react with CS₂ to form cyclic trithioanhydrides about the nitrogen and the methylene that is *beta* to it (Figure 3.18). The N-compounds (Figure 3.18, i-v) were reacted with an excess amount of CS₂. 3-Dimethylamino propiophenone (Figure 3.18, i) was first treated with an equivalent of triethylamine to remove the hydrochloride adduct, as it was purchased in its protonated form. There was no observable reactivity upon the addition of CS₂ to the above candidates with the

exceptions of 3-dimethylamino propiophenone (Figure 3.18, i) and 2-ethyl-2-oxazoline (Figure 3.18, v). With the other three candidates, the ^1H NMR spectra showed no change in chemical shifts from starting material and there was no observable change upon the addition of CS_2 .

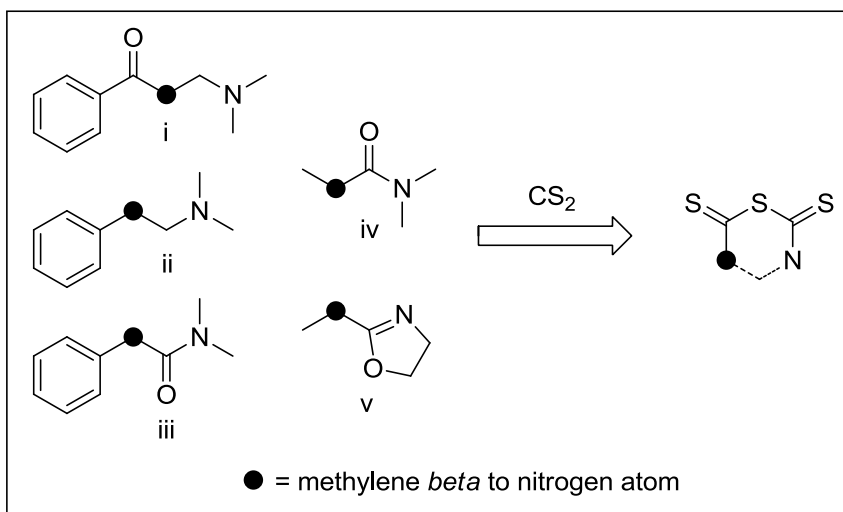
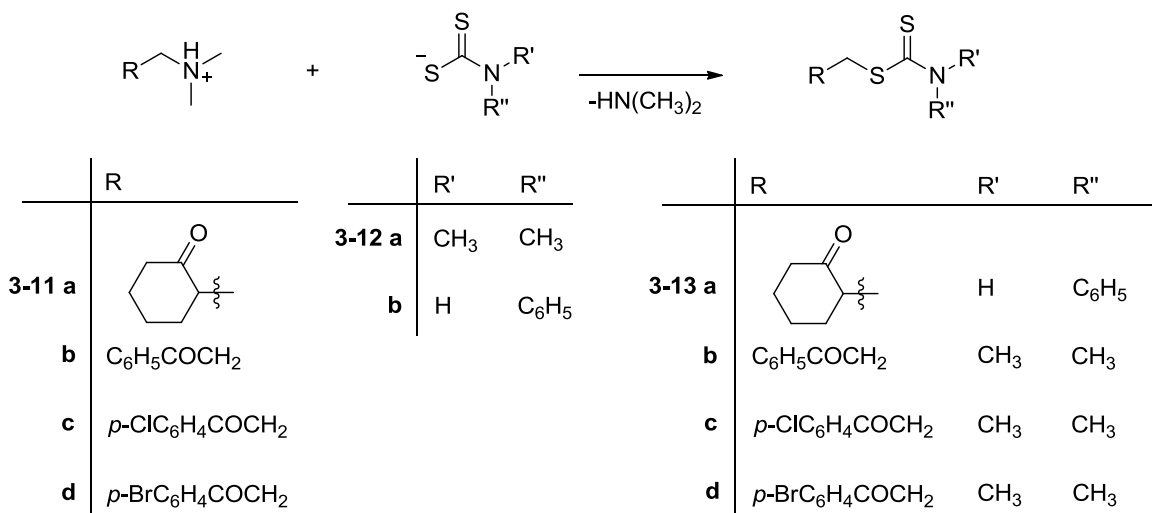


Figure 3.18. N-Containing compounds featuring a methylene *beta* to the nitrogen centre towards the formation of a cyclic trithioanhydride. 2-Ethyl-2-oxazoline (v) is also designated as **3-14**.

3-Dimethylamino propiophenone is a ketone Mannich base and its reactivity with CS_2 was previously reported. The reaction of CS_2 and these compounds do not produce a cyclic trithioanhydride. Matolcsy and co-workers demonstrated this reactivity with a variety of ketone Mannich bases (Scheme 3.23).³⁶ Reaction of these bases with dithiocarbamates, formed from the reaction of CS_2 and secondary amines, resulted in the elimination of the amine from the Mannich base and formation of *S*-(2-acylethyl) dithio-carbamates.



Scheme 3.23. Reaction of ketone Mannich bases with CS₂.³⁶

The reaction of CS₂ and 3-dimethylamino propiophenone hydrochloride was repeated in the Jessop lab and gave product **3-13b**, where the ¹H NMR spectrum matched that reported by Matolcsy and co-workers.³⁶ In the Jessop lab, crystals were grown by slow evaporation of chloroform over hexanes and the structure was determined through X-ray crystallography (Figure 3.19). The molecular structure shows insertion of the CS₂ moiety between the methylene and dimethylamino substituent.

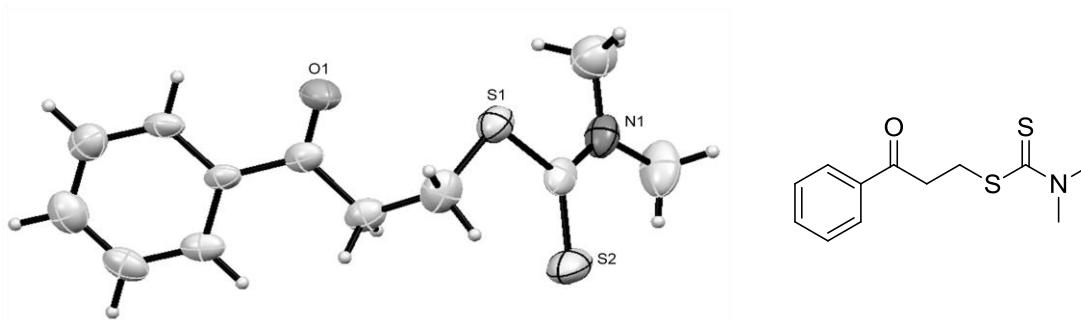
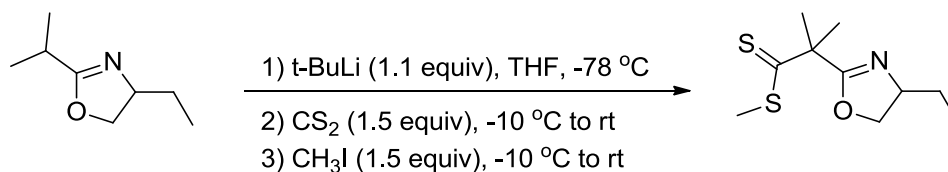


Figure 3.19. Molecular structure of **3-13b**. Displacement ellipsoids for non-H atoms are shown at the 50% probability level and H atoms are represented by circles of arbitrary size.

4-Ethyl-2-isopropyl-4,5-dihydrooxazole is similar in structure to 2-ethyl-2-oxazoline **3-14** (Figure 3.18, v) and its reactivity with CS_2 was previously reported.³⁷ Reaction of 4-ethyl-2-isopropyl-4,5-dihydrooxazole and CS_2 was for the synthesis of unsymmetrical bis(thiazolines) for use as ligands for Pd-catalyzed allylic substitution. The reaction first involved the treatment of 4-ethyl-2-isopropyl-4,5-dihydrooxazole with *t*-BuLi to afford deprotonation of the C-H of the isopropyl, then reaction of CS_2 and trapping the anion with methyl iodide (Scheme 3.24). Given the right conditions, the reaction of **3-14** with CS_2 could be similar to that of 4-ethyl-2-isopropyl-4,5-dihydrooxazole and CS_2 .



Scheme 3.24. Synthesis of dithiocarbamate methyl ester from 4-ethyl-2-isopropyl-4,5-dihydrooxazole.³⁷

Prior to knowing the reactivity of 2-*tert*-butyl-1,1,3,3-tetramethylguanidine or Barton's base with that of CS_2 ,²⁷ the guanidine was used in the reaction of 2-ethyl-2-oxazoline **3-14** (Figure 3.18-v) with CS_2 in attempt to deprotonate at the methylene of the ethyl group. From the

reaction the characteristic tetramethylthiourea formed from Barton's base as well as a pale yellow precipitate.

The ^1H and ^{13}C NMR spectra of the crude reaction solution showed methyl peaks consistent with tetramethylthiourea, **3-14**, and an unknown compound. The ^1H NMR spectrum did not indicate deprotonation at the methylene of the ethyl group of **3-14**, where aside from **3-14**, two new methylene signals are evident and exhibited as two separate quartets at 2.14, and 1.93 ppm. Correspondingly, there are two sets of signals for two other oxazoline backbones than **3-14**. Further downfield in the spectrum there are two broad singlets located at 5.96 and 9.12 ppm, which could be attributed to protonated **3-14** and possible formation of the hydrogen sulfide salt of **3-14** respectively. The third oxazoline species could be a dithiocarbamate; the ^{13}C NMR spectrum of the crude reaction mixture contains a quarternary carbon peak at 198.0 ppm that matches neither to the tetramethylurea or starting material. HRMS of the unknown yellow precipitate gives a molecular formula that corresponds to the zwitterionic adduct of **3-14**. Single crystals for X-ray crystallography of the unknown compound were not successfully grown in order to determine the molecular structure, though from spectroscopic data a mixture of products can be proposed (Figure 3.20).

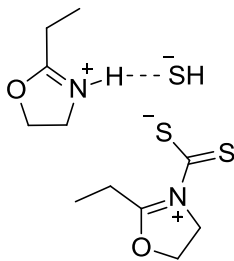


Figure 3.20. Proposed mixture of the unknown yellow precipitate from the reaction of **3-14** and CS_2 .

3.3 Conclusions and Future Considerations

Amidines can be used to activate CS₂ leading to the formation of new C-C bonds and useful products. Although a unifying theme of CS₂ activation with amidines and guanidines is nucleophilic attack of the nitrogen towards the electrophilic carbon centre, divergent reaction outcomes are observed depending on the amidine and guanidine structure. To our knowledge the reaction of DBU and CS₂ was the first example where an amidine can fixate CS₂ to form a cyclic trithioanhydride. This reactivity can be extended to other cyclic amidines, where the rigidity of the cyclic amidine determines whether a stable cyclic trithioanhydride is formed.

With regards to imidazolines, yellow precipitates were formed immediately after the addition of CS₂ which did not correspond to the formation of a cyclic trithioanhydride. Nonetheless, a cyclic trithioanhydride was formed with 2-ethyl-2-imidazoline after filtration of the yellow precipitate and concentration of the supernatant. Acyclic amidines provided completely different reactivity. Acetamides with varying alkyl chain lengths reacted with CS₂ to yield *N,N*-dimethylthioacetamide and alkyl-isothiocyanates in near quantitative yields. Thus, we have demonstrated that both cyclic and acyclic amidines are capable of activating CS₂ at ambient conditions, leading to the formation of a cyclic trithioanhydride or a thioamide and isothiocyanate depending on the amidine structure.

Reactivity of CS₂ can be extended to other nitrogen containing compounds. The molecular structure of the product formed from the reaction of CS₂ and 3-dimethylamino propiophenone further supported reports of CS₂ reactivity with a variety of ketone Mannich bases.³⁷ The reaction 2-ethyl-2-oxazoline and CS₂ in the presence of a guanidine gave possible formation of a dithiocarbamate salt. In contrast to the reaction of CS₂ with 4-ethyl-2-isopropyl-4,5-dihydrooxazole, that is similar in structure to 2-ethyl-2-oxazoline.

Future considerations would include the extension of the study to other nitrogen or other heteroatom containing compounds and investigation of their reactivity with CS₂. Whether the

structure of **3-3c** is reproducible should be further investigated since the novel structural motif found in **3-3c** could prove to be useful in the synthesis of sulfur containing compounds that could feature bioactivity. Ring-opening of the trithioanhydride ring was done with the use of a strong nucleophile or using the altered trithioanhydride structure and addition of a nucleophile. Ring-opening the trithioanhydride makes the sulfur atoms more accessible for further reactivity or for use as a sulfur transfer agent.

In addition, an important investigation would be the design and synthesis of such compounds where the addition and removal of CS₂ can be done reversibly. CS₂ is a component of waste streams, especially with regards to the production of viscose. It has been demonstrated¹² in the Jessop lab that the combination of an amidine and an alcohol affords the addition and removal of CS₂, albeit at a much higher temperature than what is needed for the addition and removal of CO₂. If there was a compound or mixture of compounds to afford the uptake and removal of CS₂ at temperatures comparable to that of the uptake and removal of CO₂, it could be useful for the sorption of CS₂ without the need for harsh conditions to sequester the compound.

3.4 Experimental Methods

3.4.1 General Considerations

All reactions were performed under an atmosphere of argon, unless otherwise indicated. All reagents with the exception of **3-3** were purchased from Sigma-Aldrich, Acros Organics, Alfa Aesar, and TCI America. Compound **3-3** was synthesized according to the literature protocol.³⁸ Reagents **3-4** and carbon disulfide (CS₂) were used as received and all other reagents were dried and purified according to literature protocols.³⁹ High resolution mass spectra (HRMS) ESI and EI for all compounds were obtained on a Qstar XL QqTOF from Applied Biosystems/MDS Sciex. Proton nuclear magnetic resonance (¹H NMR) and carbon-13 nuclear magnetic resonance (¹³C{¹H}NMR) spectra for all compounds were recorded with a Bruker AVANCE-400 MHz NMR spectrometer. Each sample is referenced to tetramethylsilane unless the NMR solvent used was D₂O, in which case the ¹H and ¹³C chemical shifts were referenced to residual solvent peaks where possible. Data collection for the crystal structures were done on a Bruker SMART APEX II X-ray diffractometer.

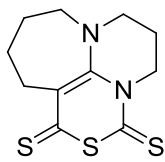
3.4.2 General Procedure for the Synthesis of Cyclic Trithioanhydrides

In a flame or oven-dried Schlenk-flask, carbon disulfide (0.4 mL, 6.6 mmol) was added dropwise at room temperature to a solution of DBU (0.5 mL, 3.3 mmol) in 2 mL of THF (dried over sodium ketyl). An immediate colour change was observed following the addition of carbon disulfide. The solution turned from clear and colourless to a deep red solution. The reaction was allowed to stir overnight at room temperature after which an amorphous orange solid precipitated out of solution. The organic solvents were removed under reduced pressure leaving behind an amorphous solid. After the amorphous solid stirred in dichloromethane (10 mL), an orange solid precipitated out of solution. The orange precipitate, **3-1a**, was collected by suction filtration leaving behind a reddish oily liquid where ¹H NMR spectroscopy confirmed it was a mixture of the hydrogen sulfide salt of DBU and DBU.

3.4.3 General Procedure for Growing the Crystals of the Cyclic Trithioanhydrides

The cyclic trithioanhydrides were collected as orange solids and are sparingly soluble in several organic solvents, though the solvents used to grow crystals of these compounds were chloroform and hexanes. A solution of approximately 20 mg of cyclic trithioanhydride was mixed with 2 mL of chloroform and then the mixture of soluble substrate and insoluble substrate were filtered through a small plug of celite in a short glass pipette into four 0.5 dram vials. The vials containing the cyclic trithioanhydride solution were then placed into four 4 dram vials containing approximately 2 mL of hexanes each. The 0.5 dram vials were capped loosely and were placed inside the larger vials, where the caps of the large vials are tightly shut. The crystals were grown by slow diffusion of hexanes into chloroform.

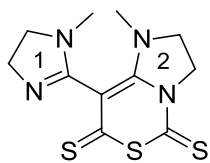
3.4.4 Spectroscopic Data for Cyclic Trithioanhydrides 3-1a, 3-2a, 3-3a, and H₂S salt of 3-3



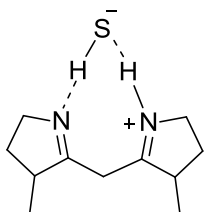
Compound 3-1a: EI-HRMS [M-I]⁺ calcd. for C₁₁H₁₄N₂S₃: 270.0319, found 270.0311; ¹H NMR (400 MHz, CDCl₃) δ 4.50 (m, 2H), 3.62 (t, 2H, *J* = 4 Hz), 3.49 (t, 2H, *J* = 4 Hz), 3.07 (m, 2H), 2.21 (p, 2H, *J* = 8 Hz), 1.93 (p, 2H, *J* = 4 Hz), 1.85 (p, 2H, *J* = 4 Hz) ppm; ¹³C{¹H} NMR (400 MHz, CDCl₃): 195.31, 193.29, 151.34, 118.63, 53.71, 49.55, 48.52, 29.62, 22.42, 21.66, 21.51 ppm. Isolated yield 85%.



Compound 3-2a: EI-HRMS [M-I]⁺ calcd for C₉H₁₀N₂S₃: 242.0006, found 241.9997 ¹H NMR (400 MHz, (CD₃)₂SO) δ 4.26 (m, 2H), 3.81 (m, 2H), 3.60 (m, 2H), 3.38 (m, 2H), 2.11 (p, 2H) ppm; ¹³C{¹H} NMR (400 MHz, CDCl₃) 197.2, 174.5, 151.6, 117.4, 53.5, 51.8, 45.5, 43.1, 26.1 ppm. Spectroscopically determined but not isolated.



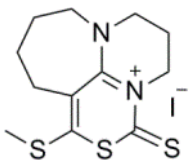
Compound 3-3a: EI-HRMS $[M-I]^+$ calcd for $C_4H_{11}N_4S_3$: 298.0381, found 298.0392; 1H NMR (400 MHz, $CDCl_3$) δ [Ring 1] 3.81 (t, 4H, $J = 9.2$ Hz), 3.50 (t, 4H, $J = 9.2$ Hz), 2.85 (s, 6H), [Ring 2] 4.51-4.34 (m, 2H), 4.09-3.92 (m, 2H), 3.87-3.76 (m, 1H), 3.75-3.67 (m, 2H), 3.33 (m, 1H); 3.23 (s, 3H), 2.89 (s, 3H) ppm; $^{13}C\{^1H\}$ NMR (400 MHz, $CDCl_3$) 197.2, 192.6, 190.0, 162.1, 150.0, 52.3, 50.6, 50.5, 47.8, 42.6, 45.8, 34.3, 33.1 ppm. Isolated yield 78%.



H₂S salt of 3-3: ESI-HRMS $[M-HS]^+$ calcd for $C_9H_{17}N_4$: 181.1453, found 181.1450; 1H NMR (400 MHz, CD_2Cl_2) δ 8.99 (brs, 2H), 3.65 (m, 4H), 3.52 (m, 4H), 2.87 (s, 6H) ppm; $^{13}C\{^1H\}$ NMR (400 MHz, CD_2Cl_2) 162.23, 55.96, 50.92, 42.42, 33.30 ppm. Isolated yield 17%.

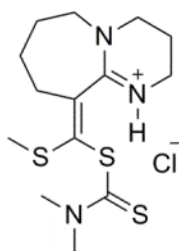
3.4.5 Procedure for the Synthesis of 3-1b and 3-1c

Synthesis of 3-1b: In a flame or oven-dried Schlenk flask, **3-1a** (0.2 g, 0.7 mmol) was suspended in 4 mL of dry THF. One equivalent of iodomethane was added carefully to the suspension. The orange suspension gradually dissolved into the THF and the resulting solution was left to stir overnight at room temperature. A yellow solid precipitated out of solution. The yellow precipitate was collected by suction filtration. The 1H NMR spectrum indicates that the yellow precipitate was a mixture of **3-1a** and **3-1b**. Compound **3-1b** was further purified by washing the precipitate with dichloromethane (10 mL) to remove **3-1a**.



Compound 3-1b: ESI-HRMS $[M-I]^+$ calcd for $C_{12}H_{17}N_2S_3$: 285.0553, found 285.0552; 1H NMR (400 MHz, CD_2Cl_2) δ 4.46 (t, 2H, $J = 8$ Hz), 4.07-3.92 (m, 2H), 2.89 (t, 2H, $J = 8$ Hz), 2.46-2.85 (m, 2H), 2.68 (s, 3H), 2.39 (p, 2H, $J = 4$ Hz), 2.09 (p, 2H, $J = 4$ Hz), 1.95 (p, 2H, $J = 4$ Hz) ppm; $^{13}C\{^1H\}$ NMR (600 MHz, $CDCl_3$) 185.16, 158.61, 156.11, 116.87, 57.37, 52.28, 49.90, 30.17, 22.57, 21.28, 20.22, 15.02 ppm. Isolated yield 54%.

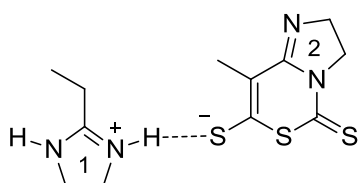
Synthesis of 3-1c: In a flame or oven-dried Schlenk-flask, **3-1b** (0.1 g, 0.24 mmol) was suspended in 2 mL of dry THF. Dimethylamine (0.24 mmol, 1.0 M in THF) is added dropwise to the mixture at room temperature. The resulting solution is left to stir overnight at room temperature. The following day, a white powder precipitates out of a light yellow solution. Under an argon atmosphere, the white precipitate is filtered off from the yellow solution. The white powder is **3-1c**, which was confirmed by 1H NMR spectroscopy. The THF is removed under reduced pressure to reveal a yellow precipitate, 1H NMR spectroscopy determined the yellow precipitate to be **3-1b**. Crystals of **3-1c** grown by slow evaporation of hexanes into a concentrated solution of **3-1c** dichloromethane.



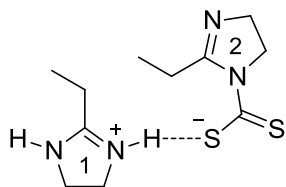
Compound 3-1c: ESI-HRMS $[M-Cl]^+$ calcd. for $C_{14}H_{24}N_3S_3$: 330.1132, found 330.1125; 1H NMR (400 MHz, $CDCl_3$) δ 9.37 (brs, 1H), 4.24 – 4.03 (m, 1H), 3.85 – 3.74 (m, 2H), 3.72 – 3.61 (m, 2H), 3.57 (s, 6H), 3.33 – 3.22 (m, 1H), 3.16 – 3.04 (m, 1H), 2.47 (s, 3H), 2.42 – 2.33 (m, 1H), 2.32 – 2.24 (m, 1H), 2.11 – 1.99 (m, 1H), 1.98 – 1.72 (m, 4H) ppm; $^{13}C\{^1H\}$ NMR (400 MHz, $CDCl_3$) 192.78, 161.10, 140.10, 138.51, 53.78, 48.02, 45.85, 43.51, 38.40, 31.89, 25.52, 25.47, 19.40, 16.72 ppm. Isolated yield 23%.

3.4.6 Synthesis of Compounds 3-4a and Proposed 3-4x

In a flame or oven-dried Schlenk-flask, carbon disulfide (0.36 mL, 6 mmol) was added dropwise at room temperature to a solution of 2-ethyl-2-imidazoline (0.2 g, 2 mmol) in 3 mL of THF (dried over sodium ketyl). The solution colour changed from a clear colourless to a yellow opaque solution. The solution was left to stir overnight at room temperature. A bright yellow solid precipitated out of solution. The yellow precipitate, designated as the proposed compound **3-4x**, was collected by suction filtration and washed with a minimal amount of THF (2 mL). The THF filtrate was collected and concentrated under reduced pressure. Crystals of **3-4a** were grown from the THF filtrate by slow evaporation.



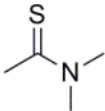
Compound 3-4a: EI-HRMS $[M-I]^+$ calcd for $C_{12}H_{18}N_4S_3$: 215.9850, found 215.9841; 1H NMR (400 MHz, $(CD_3)_2SO$) (Ratio 1 : 2 is 4:1) δ [Structure 1] 3.73 (s, 4H), 2.47 (q, 2H, $J = 7.6$ Hz), 1.13 (t, 3H, $J = 7.6$ Hz), [Structure 2] 4.08 (t, 2H, $J = 8.9$ Hz), 3.77 (t, 2H, $J = 8.9$ Hz), 2.00 (s, 3H) ppm. Isolated yield 16%.



Proposed Compound 3-4x: ESI-HRMS $[M+H]^+$ calcd for $C_9H_{11}N_2$: 99.0922, found 99.0825; 1H NMR (400 MHz, $(CD_3)_2SO$) (Ratio of 1 : 2 is 1 : 1) δ [Structure 1] 3.78 (s, 4H), 2.44 (q, 2H, $J = 7.6$ Hz), 1.11 (t, 3H, $J = 7.6$ Hz), [Structure 2] 4.21 (t, 2H, $J = 8.4$ Hz), 3.48 (t, 2H, $J = 8.4$ Hz), 3.14 (q, 2H, $J = 7.4$ Hz), 1.06 (t, 3H, $J = 7.4$ Hz) ppm; $^{13}C\{^1H\}$ NMR (400 MHz, $(CD_3)_2SO$) 215.3, 173.2, 166.8, 58.0, 49.1, 46.9, 45.0, 38.5, 29.5, 26.9, 20.3, 11.2, 9.8, 9.4 ppm. Isolated yield 75%.

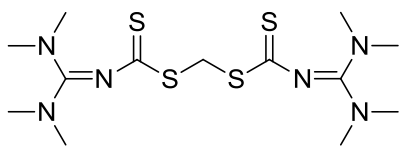
3.4.7 General Procedure for the Synthesis of 3-8

Acyclic amidines **3-5** to **3-7** were synthesized according to literature procedure²⁵ and purified by vacuum distillation. In a flame or oven-dried Schlenk-flask, an excess amount of carbon disulfide (~5 eq) was added to a stirring solution of acyclic amidine. The solution darkens in colour and was left to stir overnight. Beige crystals precipitated out of solution. To the solution mixture, a minimal amount of ether was added, which precipitated more beige crystals. The crystals were confirmed to be **3-8** by ¹H and ¹³C NMR spectroscopy; chemical shifts corresponded to the literature values.^{26a} The crystals were collected by suction filtration and washed with a minimal amount of ether and hexanes. The organic solvent and remaining carbon disulfide were removed under reduced pressure and a red oil was left behind. The red oil was confirmed to be isothiocyanate, that corresponded to reported literature chemical shifts.^{26b}

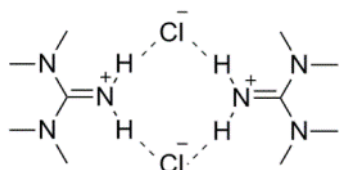
 **Compound 3-8:** Compound matches literature values.^{26b} EI-HRMS [M-I]⁺ calcd for C₄H₉NS: 103.0456, found 103.0451; ¹H NMR (400 MHz, CDCl₃) δ 3.50 (s, 3H), 3.31 (s, 3H), 2.66 (s, 3H) ppm; ¹³C{¹H} NMR (400 MHz, CDCl₃): 199.79, 44.36, 42.18, 32.74 ppm.

3.4.8 Synthesis of 3-9a and 3-10

In a flame or oven-dried Schlenk-flask, an excess amount of carbon disulfide (1.6 mL, 2.6 mmol) was used to dissolve *N,N,N',N'*-tetramethylguanidine **3-9** (0.1 mL, 0.8 mmol). The resulting solution was left to stir overnight where an orange viscous material formed. The residual amount of carbon disulfide was removed under reduced pressure leaving behind the orange viscous material. The orange viscous material was then placed into a 1 dram vial where dichloromethane (3 mL) was added to dissolve the material and left to sit overnight at room temperature. From the dichloromethane solution, **3-9a** and **3-10** co-crystallize. NMR data is a sample with both crystals.



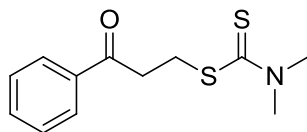
Compound 3-9a: TOF-HRMS $[M+H]^+$ calcd for $C_{13}H_{27}N_6S_4$: 395.1180, found 395.1187; 1H NMR (400 MHz, $CDCl_3$) δ 4.49 (s, 2H), 3.03 (s, 12H) ppm; $^{13}C\{^1H\}$ NMR (400 MHz, $CDCl_3$) 197.6, 169.2 ppm.



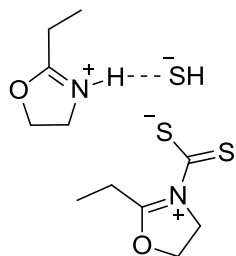
Compound 3-10: Compound matches literature value.⁴⁰ 1H NMR (400 MHz, $CDCl_3$) δ 8.58 (brs, 4H), 3.08 (s, 12H) ppm; $^{13}C\{^1H\}$ NMR (400 MHz, $CDCl_3$) 161.8, 40.3 ppm.

3.4.9 Synthesis of 3-13b and Spectroscopic Data of Proposed 3-14a

3-Dimethylamino propiophenone hydrochloride (0.10 g, 0.47 mmol) was placed in a flame or oven-dried Schlenk-flask and dissolved in 2 mL of dry THF. To this solution, one equivalent of dry triethylamine (0.07 mL, 0.4 mmol) was added at room temperature with stirring. After 10 min of stirring, two equivalents of carbon disulfide (0.60 mL, 0.94 mmol) were added dropwise to the solution. The solution colour changed from clear and colourless to clear and yellow. The resultant solution was left to stir overnight. The organic solvent and residual carbon disulfide were removed under reduced pressure leaving behind an off-white solid. 1H and ^{13}C NMR spectroscopy confirms the off white solid to be **3-13b**. Matolcsy and co-workers reported the 1H NMR spectrum of **3-13b** in $CDCl_3$ at 60 Hz.³⁶



Compound 3-13b: TOF-HRMS $[M-I]^+$ calcd for $C_{12}H_{15}NOS_2$: 253.0598, found 253.0595; 1H NMR (400 MHz, CD_3CN) δ 7.97 (d, 2H, $J = 7.4$), 7.62 (t, 1H, $J = 7.5$), 7.50 (t, 2H, $J = 7.5$), 3.60 (t, 2H, $J = 6.5$ Hz), 3.46 (t, 2H, $J = 6.5$ Hz) 2.24 (s, 6H) ppm; $^{13}C\{^1H\}$ NMR (400 MHz, CD_3CN) 205.3, 199.5, 197.3, 137.7, 134.3, 129.8, 128.9, 47.0, 45.7, 39.1, 32.4 ppm. Isolated yield%.



Proposed Mixture 3-14a: TOF-HRMS $[M-I]^+$ calcd for $C_6H_9NOS_2$: 175.0126, found 175.0126; 1H NMR (400 MHz, C_6D_6) δ 9.33 (brs, 1H), 7.04 (brs, 1H), 4.29 (t, 2H, $J = 5.3$ Hz), 3.96 (brs, 2H), 3.37 (m, 2H), 3.23 (m, 2H), 2.33 (q, 2H, $J = 7.6$ Hz), 2.15 (q, 2H, $J = 7.6$ Hz), 1.07 (m, 6H) ppm; $^{13}C\{^1H\}$ NMR (400 MHz, C_6D_6): 197.1, 173.9, 173.5, 60.8, 45.3, 38.4, 32.7, 28.4, 26.6, 8.9, 8.0 ppm.

3.5 References

- 1) Blake, N. J.; Streets, D. G.; Woo, J.-H.; Simpson, I. J.; Green, J.; Meinardi, S.; Kita, K.; Atlas, E.; Fuelberg, H. E.; Sachse, G.; Avery, M. A.; Vay, S. A.; Talbot, R. W.; Dibb, J. E.; Bandy, A. R.; Thornton, D. C.; Rowland, F. S.; Blake, D. R. *J. Geophys. Res.* **2004**, *109*, D15S05.
- 2) Lay, M. D. S.; Sauerhoff, M. W.; Saunders, D. R. in *Ullman's Encyclopedia of Industrial Chemistry*, Wiley-VCH, Weinheim, **2005**.
- 3) Butler, I. S.; Fenster, A. E. *J. Organomet. Chem.* **1974**, *66*, 161 – 194.
- 4) Chen, Y.; Peng, Y.; Chen, P.; Zhao, J.; Liu, L.; Li, Y.; Chen, S.; Qu, J. *Dalton Trans.*, **2010**, *39*, 3020 – 3025.
- 5) Lam, O. P.; Heinemann, F. W.; Meyer, K. *Angew. Chem. Int. Ed.*, **2011**, *50*, 5965 – 5968.
- 6) Haack, P.; Limberg, C.; Tietz, T.; Metzinger, R. *Chem. Commun.*, **2011**, *47*, 6374 – 6376.
- 7) Gibson, D. H. *Chem. Rev.*, **1996**, *96*, 2063 – 2095.
- 8) Yin, X.; Moss, J. R. *Coord. Chem. Rev.*, **1999**, *181*, 27 – 59.
- 9) Heldebrant, D. J.; Yonker, C. R.; Jessop, P. G.; Phan, L. *Energy Environ. Sci.* **2008**, *1*, 487 – 493.
- 10) Jessop, P. G.; Heldebrant, D. J.; Li, X. W.; Lu, J.; Hallet, J. P.; Jones, R. S.; Pollet, P.; Thomas, C. A.; Eckert, C. A.; Liotta, C. L. *Abstr. Pap. Am. Chem. Soc.* **2005**, *229*, U971.
- 11) Phan, L.; Chiu, D.; Heldebrant, D. J.; Huttenhower, H.; John, E.; Li, X. W.; Pollet, P.; Wang, R. Y.; Eckert, C. A.; Liotta, C. L.; Jessop, P. G. *Ind. Eng. Chem. Res.* **2008**, *47*, 539 – 545.
- 12) Heldebrant, D. J., Yonker, C. R.; Jessop, P. G.; Phan, L. *Chem. Eur. J.* **2009**, *15*, 7619 – 7627.

- 13) Yu, T.; Yamada, T.; Weiss, R. G. *Chem. Mater.* **2010**, *22*, 5492 – 5499.
- 14) Heldebrant, D.J.; Jessop, P.G.; Thomas, C.A.; Eckert, C.A.; Liotta, C.L. *J.Org.Chem.* **2005**, *70*, 5335 – 5338.
- 15) Vlasse, M.; Giandinoto, S.; Attarwala, S. T.; Okamoto, Y. *Acta Cryst.* **1986**, *C42*, 487 – 490.
- 16) Yu, Y.; Zhong, H.-P.; Yang, K.-B.; Huang, R.-B.; Zheng, L.-S. *Acta Cryst.*, **2005**, *E61*, o387 – o388.
- 17) Lakshmikantham, M. V.; Carroll, P.; Furst, G.; Levinson, M. I.; Cava, M. P. *J. Am. Chem. Soc.*, **1984**, *106*, 6084 – 6085.
- 18) a) Gompper, R.; Wetzels, B.; Elser, W. *Tetrahedron Lett.* **1968**, *9*, 5519 – 5522. b) Gompper, R.; Elser, B. *Angew. Chem. Int. Ed.* **1967**, *6*, 366 - 367.
- 19) a) Yamamoto, T.; Hirasawa, S.; Muraoka, M. *Bull. Chem. Soc. Jpn.* **1985**, *58*, 771 - 772. b) Yamamoto, T.; Itoh, M.; Saitoh, N. U.; Muraoka, M. *J. Chem. Soc. Perkin Trans. I.* **1990**, 2459 – 2463. c) Muraoka, M.; Yamamoto, T.; Yamaguchi, S.; Tonosaki, F. *J. Chem. Soc. Perkin Trans. I.* **1977**, 1273 – 1280. d) Yamamoto, T.; Muraoka, M. *J. Heterocycl. Chem.*, **1988**, *25*, 835 – 846. e) Leistner, S.; Wagner, G.; Giro, A. *Zeitschrift fuer Chemie* **1982**, *22*, 259 – 260. f) Walter, W. ; Fleck, T. ; Voß, J. ; Gerwin, M. *Justus Liebigs Annalen der Chemie* **1975**, 275 – 294.
- 20) a) Eul, W.; Gattow, G. *Z. anorg. allg. Chem.* **1986**, *537*, 189 – 197. b) Eul, W.; Gattow, G. *Z. anorg. allg. Chem.* **1986**, *538*, 151 – 158. c) Eul, W.; Kiel, G.; Gattow, G. *Z. anorg. allg. Chem.* **1986**, *542*, 182 – 192. d) Eul, W.; Gattow, G. *Z. anorg. allg. Chem.* **1986**, *543*, 81 – 88. e) Eul, W.; Kiel, G.; Gattow, G. *Z. anorg. allg. Chem.* **1987**, *544*, 149 – 158. f) Eul, W.; Gattow, G. *Z. anorg. allg. Chem.* **1987**, *545*, 125 – 133.
- 21) a) Gattow, V. G.; Eul, W. *Z. anorg. allg. Chem.* **1981**, *483*, 103 – 113. b) Gattow, V. G.; Eul, W. *Z. anorg. allg. Chem.* **1982**, *485*, 195 – 202. c) Gattow, V. G.; Eul, W. *Z. anorg. allg. Chem.* **1981**, *483*, 121 – 125. d) Gattow, V. G.; Kiel, G.; Eul, W. *Z. anorg. allg. Chem.* **1983**, *497*, 167 – 175.
- 22) Sawa, N.; Masahiro, H. *Nippon Kagaku Zasshi*, **1970**, *91(5)*, 466 – 469.
- 23) Wrobel, J.T.; Wojtasiewicz, K. In *The Alkaloids*: Brossi, A., Ed.; Academic: New York, 1992; pp. 249 – 297.
- 24) a) Matsuda, H.; Morikawa, T.; Oda, M.; Asao, Y.; Yoshikawa, M. *Bioorg. Med. Chem. Lett.* **2003**, *13*, 4445 – 4449. b) Wang, W.; Oda, T.; Fujita, A.; Mangindaan, R.E.P.; Nakazawa, T.; Ukai, K.; Kobayashi, H.; Namikoshi, M. *Tetrahedron*, **2007**, *63*, 409 – 412.

- 25) Harjani, J. R.; Liang, C.; Jessop, P. G. *J. Org. Chem.*, **2011**, *76*, 1683 – 1691.
- 26) a) Heyde, C.; Zug, I.; Hartmann, H. *Eur. J. Org. Chem.*, **2000**, 3273 – 3278. b) Nath, J.; Ghosh, H.; Yella, R.; Patel, B. K. *Eur. J. Org. Chem.* **2009**, 1849 – 1851. c) Yella, R.; Ghosh, H.; Murru, S.; Sahoo, S. K.; Patel, B. K. *Synth. Commun.* **2010**, *40*, 2083 – 2096. d) Li, D.; Shu, Y.; Li, P.; Zhang, W.; Ni, H.; Cao, Y. *Med. Chem. Res.* **2013**, *22*, 3119 – 3125.
- 27) Barton, D. H. R.; Elliott, J. D.; Géro, S. D. *J. Chem. Soc., Perkin Trans. I*, **1982**, 2085 – 2090.
- 28) Kaleta, Z.; Tárkányi, G.; Gömöry, Á.; Kálmán, F.; Nagy, T.; Soós, T. *Org. Lett.*, **2006**, *8*, 1093 – 1095.
- 29) a) Pipko, S. E.; Simurova, N. V.; Shvadchak, V. V.; Bezgubenko, L. V.; Luk'yanenko, S. N. *Russ. J. Gen. Chem.* **2006**, *76*, 1019 – 1021. b) Bezgubenko, L. V.; Pipko, S. E.; Sinitsa, A. D. *Russ. J. Gen. Chem.* **2008**, *78*, 1341 – 1344. c) Pathak, U.; Pandey, L. K.; Tank, R. *J. Org. Chem.*, **2008**, *73*(7), 2890 – 2893.
- 30) Ley, S. V.; Leach, A. G.; Storer, R. I. *J. Chem. Soc., Perkin Trans. I*, **2001**, *4*, 358 – 361.
- 31) Clapp, J. W.; Lies, T. A.; Lamb, G. U.S. Patent 3,520,897, 1970.
- 32) Céspedes, C.; Vega, J. *Phosphorus, Sulfur Silicon Relat. Elem.*, **1994**, *90*, 155 – 158.
- 33) Di Biase, S. A.; Bush, J. H. U.S. patent 5,015,368, 1991.
- 34) Roethling, T.; Guenther, E.; Haeupke, K.; Hoelzel, H.; Kochmann, W.; Luthardt, H.; Naumann, K.; Schwachula, G.; Thust, U. German (East) patent DD 204087, 1984.
- 35) Ranu, B. C.; Saha, A.; Banerjee, S. *Eur. J. Org. Chem.* **2008**, 519 – 523.
- 36) Matolcsy, G.; Bordás, B. *Chem. Ber.* **1973**, *106*, 1483 – 1486.
- 37) Betz, A.; Yu, L.; Reiher, M.; Gaumont, A.-C.; Jaffrès. P.-A.; Gulea, M. *J. Organomet. Chem.* **2008**, *693*, 2499 – 2508.
- 38) Aoki, M.; Kaneko, M.; Izumi, S.; Ukai, K.; Iwasawa, N. *Chem. Commun.* **2004**, 2568 – 2569.
- 39) Armarego, W. L. F.; Chai, C. L. L. *Purification of Laboratory Chemicals*, 5th ed.; Elsevier Science: Burlington, MA, 2003.
- 40) Chaudhry, S. C.; Kummer, D. *J. Organomet. Chem.* **1988**, *339*, 241 – 252.

Chapter 4

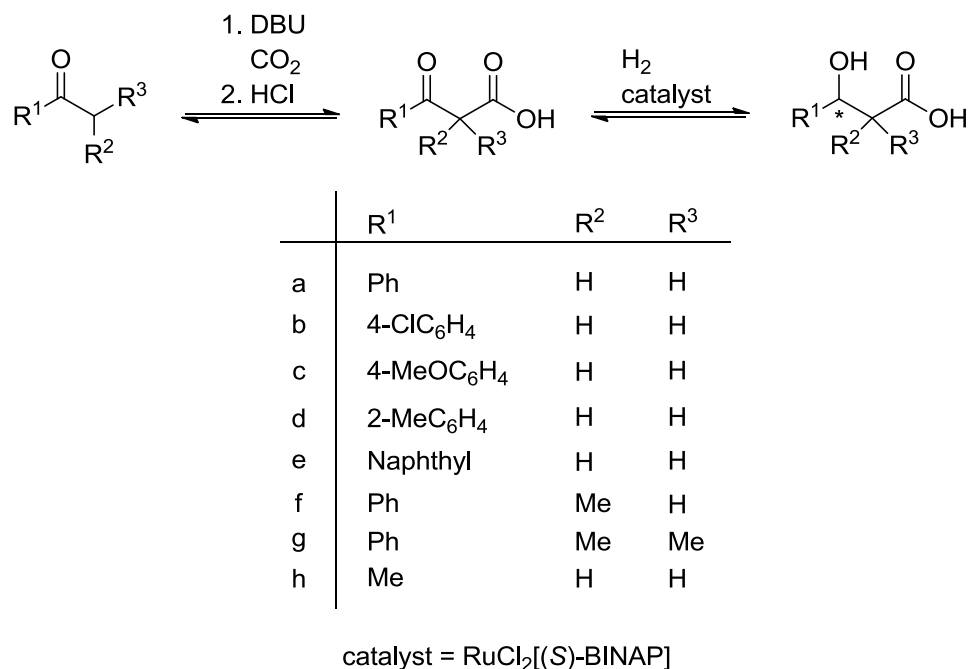
CO₂ as a Carbonyl Source for N-Containing Compounds

4.1 General Introduction

4.1.1 CO₂ Fixation for the Synthesis of β -Hydroxycarboxylic Acids

CO₂ is in the most oxidized state of carbon and the biggest challenge in establishing CO₂ in industry is overcoming its high stability to achieve CO₂ activation. One way to activate CO₂ is to recognize the electron deficiency of the carbonyl carbon and that CO₂ is readily attracted to both nucleophiles and electron donating groups. Previous research within the Jessop group has taken advantage of this unique reactivity to synthesize β -hydroxycarboxylic acids.¹ They have been shown to be useful building blocks for pharmaceuticals such as β -amino acids,² β -lactams,³ β -lactones,⁴ and pheromones.⁵ β -Hydroxycarboxylic acids also have precedence as precursors in anti-inflammatory drugs.⁶ Previously-developed stereoselective methods for the synthesis of β -hydroxycarboxylic acids are few and not ideal for industry as they require low temperatures and excess quantities of Grignard⁷ or sophisticated tin(II) reagents, which are highly sensitive and toxic.⁸

The use of CO₂ within the Jessop lab has also involved the interaction of DBU with CO₂. The synthesis of asymmetric β -hydroxycarboxylic acids affords the carboxylation of a ketone under 60 bar of CO₂ in combination with two equivalents of DBU without additional solvent, followed by catalytic asymmetric hydrogenation with RuCl₂[(*S*)-BINAP] (Scheme 4.1).¹ Despite the fact that DBU only has a pK_{aH(DMSO)} of 14, the substrates that were successfully carboxylated in the presence of CO₂ and DBU had CH bond acidities with pK_{a(DMSO)} values between 24-27. The way in which CO₂ and DBU were utilized for the synthesis of β -hydroxycarboxylic acids is relevant to both industrial and environmental needs.



Scheme 4.1. Carboxylation of ketones followed by asymmetric hydrogenation.¹

The performance of a nitrogen base for the deprotonation of organic substrates is related to CH-activation ability.⁹ DBU has proven to be an effective base for the carboxylation of activated CH groups that have much higher pK_a values than that of protonated DBU with a range of 24-27. While carboxylation can occur with a variety of ketones in the presence of DBU, there are ketones that have pK_a values higher than 27 where the carboxylation cannot occur in the presence of DBU (Figure 4.1). We studied amidines or guanidines that featured two nitrogen donors with the lone pairs of electrons pointing to the same site. Thus, its relative donor strength and overall basicity should be greater. Consequently, bases of this nature could be more efficient for the carboxylation of substrates that have pK_{a(DMSO)} values higher than 27.

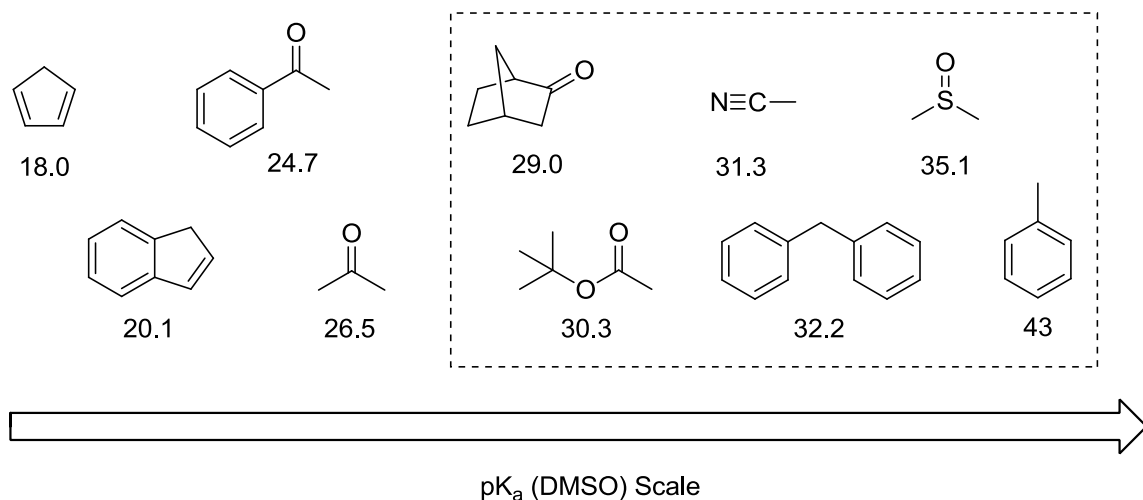


Figure 4.1. pK_a (DMSO) scale of select substrates: those in the dotted area are not carboxylated in the presence of DBU and CO₂.

Preliminary studies have shown that DBU **4-1** has a higher C-H activation ability than three investigated bases: 1,8-bis(tetramethylguanidino)-naphthalene (TMGN **4-2**) and bisamidines **4-3a** and **4-3b** (Figure 4.2). TMGN is derived from 1,8-bis(dimethylamino)naphthalene (DMAN), a highly basic compound commonly known as ‘Proton SpongeTM’.¹⁰ The reactivity of TMGN towards a proton is like that of DMAN, in that the captured proton is hydrogen bonded with two nitrogen atoms. In comparison to DMAN, TMGN also contains less sterically crowded proton-accepting sp²-nitrogen atoms. It was shown through time-resolved proton self-exchange reactions that it has a higher kinetic basicity than DMAN.¹⁰ In addition, TMGN has an experimental pK_{aH} value of 25.1 in MeCN which is seven orders of magnitude higher in basicity than DMAN.¹⁰ As for the bisamidines, the only reported pK_{aH} value is for the mono- and dicationic form of an analogous structure, bis(4,5-dihydroimidazol-2-yl)methane, that has hydrogens instead of methyl groups on the tertiary nitrogen centres. The authors based their measurement on pH-dependent UV spectra in a phosphate buffer that showed major changes around pH 8 and 11, exhibiting a strong absorption at 284 nm. This demonstrated

the presence of an enamine-imine tautomerization. The authors proposed that the mono- and dicationic forms must have $pK_{aH}(H_2O)$ values close to 11 and 8 respectively.¹¹

The candidates (Figure 4.2, **4-1** to **4-3**) below feature two donor sites for protonation and their relative pK_{aH} values should be larger than DBU, though none of the three candidates below were able to afford carboxylation of acetophenone at RT and 60 bar of CO_2 . Compound **4-3a** is not as good as DBU in C-H activation due to its tendency to tautomerize to a form where one of the nitrogen atoms is protonated, preventing C-H-activation of another molecule. It is apparent that there is something special about DBU that renders it superior for CO_2 fixation.

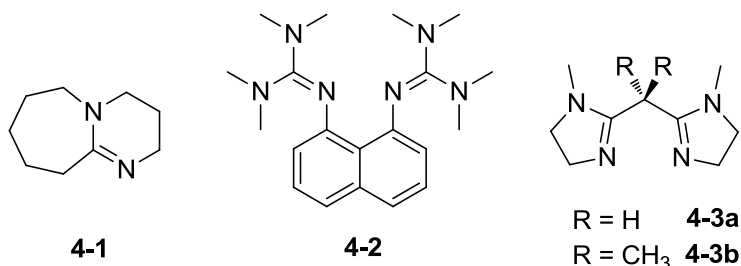


Figure 4.2. The structures of DBU (**4-1**), TMGN (**4-2**), bis(1-methyl-4,5-dihydroimidazol-2-yl)methane (**4-3a**), and 2,2'-bis(1-methyl-4,5-dihydroimidazol-2-yl)propane (**4-3b**).

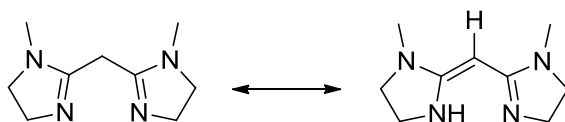


Figure 4.3. Tautomerization of **4-3a**.

The method for the synthesis of β -keto-carboxylic acids developed in the Jessop group could act as a stepping stone for the synthesis of other industrially relevant products. The extension of the above method can be achieved in three ways, with an emphasis on the partnership of DBU and CO_2 : 1) a determination whether the above process is feasible for the synthesis of α -amino acids starting from ketimines, 2) a determination of whether amidation of β -

benzoylacetic acid, which is made from the above method, can occur by the use of Lewis acid catalysts and 3) utilization of the Lewis acids for the synthesis of tetraalkylated ureas.

This chapter is divided according to the three preliminary investigations listed above. Each section will start with a general introduction for the conventional synthesis of each target compound with related examples: amino acids, amides, and ureas for research areas 1, 2, and 3, respectively. Following each general introduction will be the corresponding results and discussion section. From the above studies, concluding remarks and future work will be drawn at the end of the chapter relating each section to the other.

4.2 Towards the Synthesis of α -Amino Acids

4.2.1 Introduction to *N*-Alkylidenes and Their use in a Mannich-type Reaction

As a non-nucleophilic base, DBU has been used in other organic transformations. One example is in its use during Mannich-type reactions of α -aminoacetonitrile with 9-fluorenylidene and diphenylmethylene as the protecting and activating groups, respectively. Kobayashi and co-workers investigated the stereoselective Mannich-type reaction of *N*-fluorenylidene-protected α -aminoacetonitrile (**4-4**) using a base catalyst system (Table 4.1).¹² The advantage of this system is catalytic amounts of base can be used, while in previous reports for carbon-carbon bond forming reactions using *N*-alkylidene-protected α -aminoacetonitrile, in general a stoichiometric amount of a strong base was required and only a few previous examples were able to show the use of a catalytic amount of base.¹³ Kobayashi and co-workers demonstrated that 9-fluorenylidene is a good protecting and activating group for primary amine compounds, where in the presence of a weak base, such as metal phenoxide or guanidine, the *N*-fluorenylidene-protected glycine esters or α -amino-phosphonates reacted with imines to afford Mannich adducts in good yields and stereoselectivities.¹⁴ Kobayashi and co-workers investigated the Mannich-type reaction of **4-4** with diphenylphosphinylimine **4-5** using their previous reaction conditions.¹

Table 4.1. Stereoselective Mannich-type reactions of *N*-fluorenylidene-protected α -aminoacetonitrile (**4-4**)^a reported by Kobayashi's group.¹²

$\text{R}-\text{C}(\text{H})=\text{N}-\text{P}(\text{Ph})_2 + \text{Flu}-\text{C}(\text{H})=\text{N}-\text{C}(\text{H})-\text{CN} \xrightarrow[\text{Solvent}]{\text{Base catalyst, Additive}} \text{R}-\text{C}(\text{H})(\text{NH}-\text{P}(\text{Ph})_2)-\text{C}(\text{H})(\text{CN})-\text{NFlu}$

4-5 **4-4** Flu = 9-fluorenylidene **4-6**

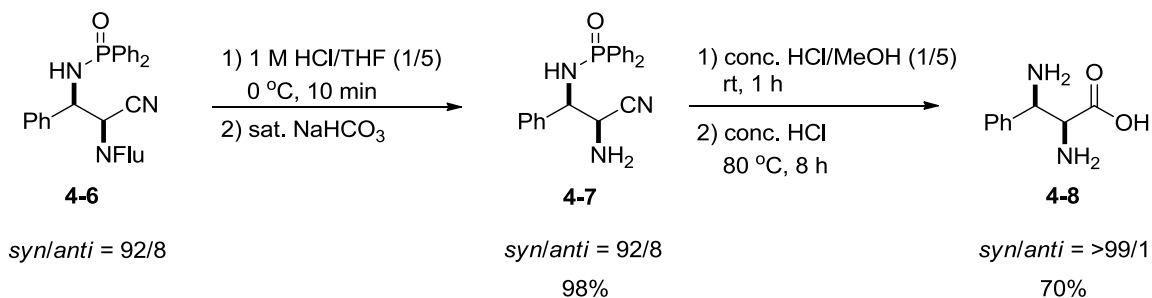
Entry	Base	Additive	Solvent	Yield ^b (%)	<i>syn/anti</i> ^b
1	KO ^t Bu	--	THF	68	60:40
2	KO ^t Bu	18-Crown-6	THF	91	64:36
3	Et ₃ N	--	THF	Trace	–
4	DBU	--	THF	90	63:37
5	TMG	--	THF	94	78:22
6	TMG	--	Et ₂ O	89	97:3

^a The reaction of **4-4** (0.24 mmol) with **4-5** (0.20 mmol) was performed in the presence of base (10 mol%) at 25 °C for 30 min in 0.05 M.

^b Yield and selectivity were determined by ¹H NMR spectroscopic analysis of the crude product using an internal standard.

A Kobayashi and co-workers¹² are listed in (Table 4.1) showed that potassium *tert*-butoxide (KO^tBu) and the organobases, DBU, 1,1,3,3-tetramethylguanidine (TMG), and triethylamine, could be used catalytically in the Mannich-type reaction. With KO^tBu, the presence of 18-crown-6 improved the yield, although the selectivity remained moderate (entry 2). The organobases, with the exception of triethylamine, were promising for the above reaction (entries 4-6). DBU and TMG were comparable bases for the reaction, although when TMG was used, greater product selectivity was achieved (entry 5). Using Et₂O as a solvent gave the highest diastereoselectivity (entry 6). In contrast, when *N*-diphenylmethylene-protected α -aminoacetonitrile was used instead of **4-4**, the reaction gave a yield of 12%.

The Mannich product **4-6** was subject to further reactivity. The two protecting groups, 9-fluorenylidene and the diphenylphosphinyl group, can be removed under different acidic conditions (Scheme 4.2). Removal of the 9-fluorenylidene is afforded under mild acidic conditions to give the mono-protected product **4-7**. The 1,2-diaminonitrile is obtained as the hydrochloride salt after a concentrated HCl/MeOH treatment, then further hydrolysis of the nitrile with concentrated HCl at 80 °C produces the 1,2-diaminocarboxylic acid **4-8** without loss of stereoselectivity.¹²

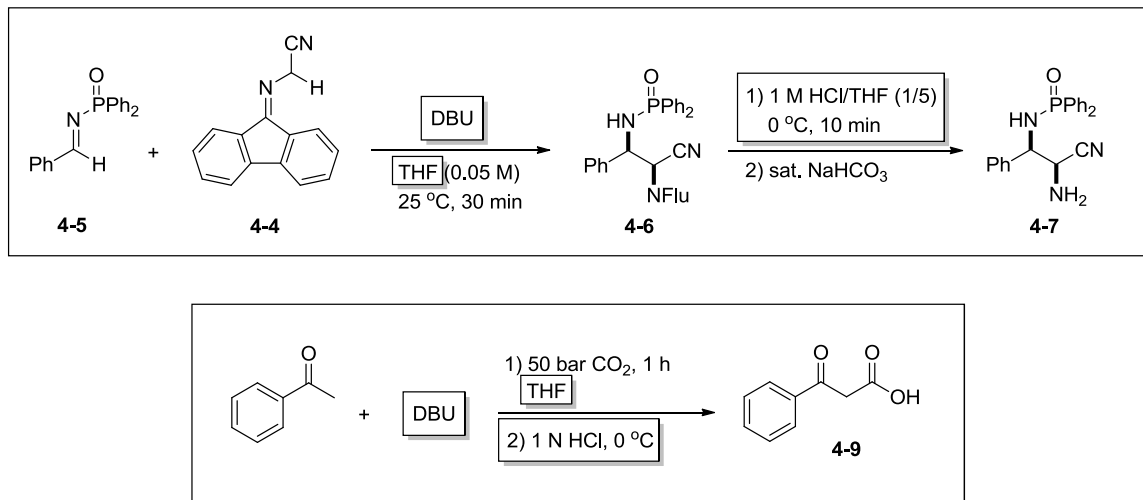


Scheme 4.2. Removal of amino protecting groups under acidic conditions followed by hydrolysis of the nitrile yielding the 1,2-diaminocarboxylic acid.

4.2.2 Correlating the Methods from the Jessop Lab and Kobayashi Lab

Correlations can be found between the Mannich-type reaction investigated by Kobayashi and co-workers,¹² and the synthesis of β -hydroxycarboxylic acids¹ investigated by the Jessop lab. As a representative example for the carboxylation of ketones, the carboxylation of acetophenone for the synthesis of benzoylacetic acid **4-9**, is shown alongside the Mannich-type reaction developed in the Kobayashi lab (Scheme 4.3). In both reactions, deprotonation of the substrate occurs by the addition of a base, such as DBU. For the carboxylation of acetophenone, the reaction can be done neat or in a small amount of THF. THF was the chosen solvent for the Mannich-type reactions conducted by Kobayashi and co-workers. Acidic work-up achieved

mono-deprotection to remove the 9-fluorenylidene group liberating the amine or protonation of the carboxylate to produce the benzoylacetic acid.



Scheme 4.3. Top reaction: Mannich-type reaction developed by Kobayashi and co-workers.¹² Bottom reaction: carboxylation of acetophenone with CO₂ developed by the Jessop Lab.¹

As previously noted, ketones that have $pK_{a(\text{DMSO})}$ values of 24-27 (Figure 4.1), values that are an order higher than that of the $pK_{a\text{H}}$ of DBU, can be deprotonated by the organobase and carboxylated under a pressure of CO₂. Structures analogous to *N*-fluorenylidene-protected α -aminoacetonitrile, having a benzyl group instead of a nitrile group, have pK_a 's within the range of the ketones that DBU is able to deprotonate and promote the carboxylation of (Figure 4.3). For the remainder of the thesis, *N*-alkylidene-protected α -amines will be referred to as 'ketimines.' Ketimine **4-10** having diphenylmethylene as a protecting group for benzylamine, features a higher $pK_{a(\text{DMSO})}$ of 24.3¹⁵ than the analogous structure **4-11** having a 9-fluorenylidene as a protecting group, ($pK_{a(\text{DMSO})}$ of 14.3).¹⁵ Ketimine **4-10** has a pK_a that is within range of the ketones that were successfully carboxylated by the combination of DBU and CO₂, while **4-11** can be deprotonated by DBU. The diphenylmethylene and 9-fluorenylidene groups are employed to protect the imine (Schiff base) and these protecting groups enhance the acidity of the α -hydrogen

through conjugated stabilization of the formed carbanion. In general, the corresponding α -hydrogen is less reactive due to the electron-donating ability of the neighbouring amine group. The imino-protecting groups can then be removed under weakly acidic conditions, as was illustrated by the Mannich-type reaction developed by Kobayashi and co-workers.¹²

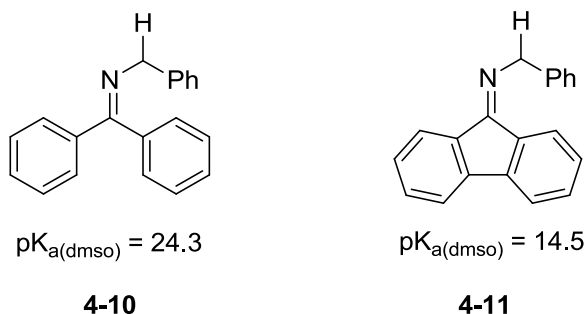
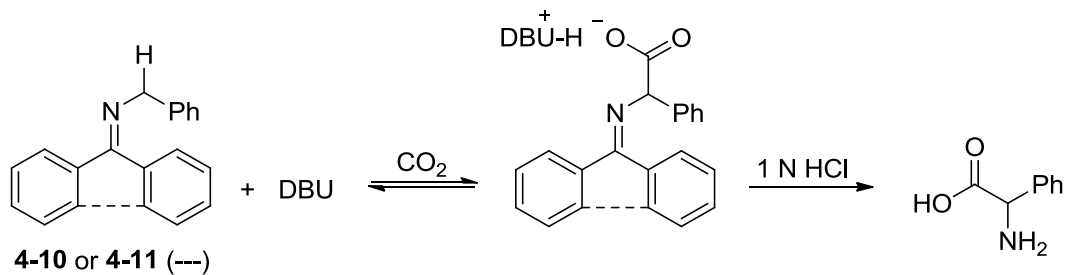


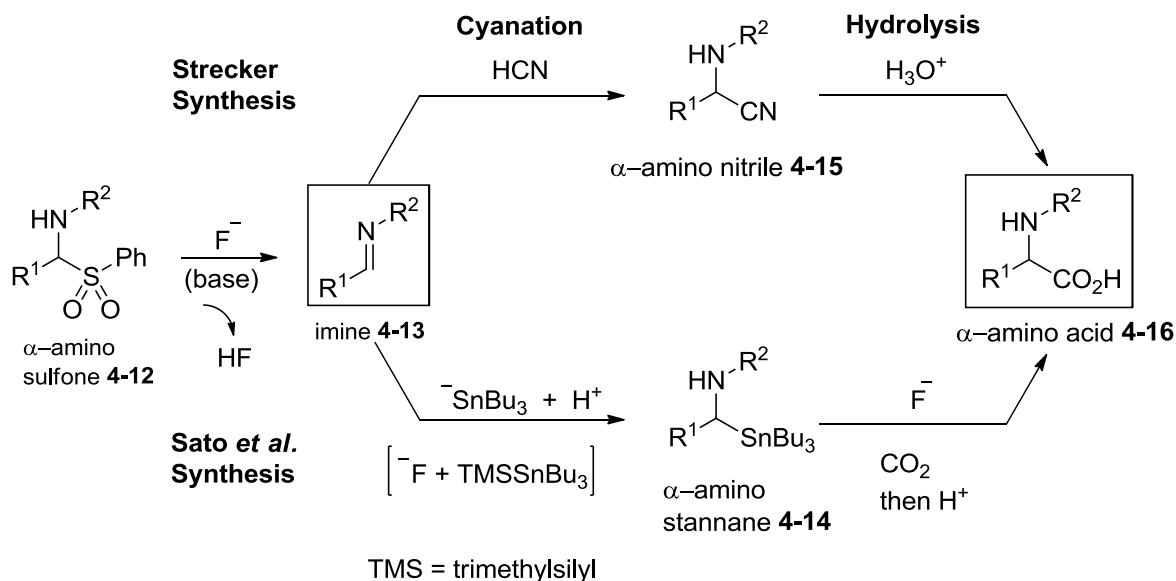
Figure 4.4. Ketimines with pK_{a} (DMSO) values: *N*-diphenylmethylene-protected α -aminotoluene **4-10** and *N*-fluorenylidene-protected α -aminotoluene **4-11**.

It was envisioned that the method for the carboxylation of ketones, developed in the Jessop lab, could be extended to the carboxylation of the above ketimines. Deprotonation of the ketimines **4-10** or **4-11** can be done with DBU, or another base, followed by the addition of CO_2 to afford carboxylation at the α -hydrogen. After formation of the carboxylate, an acidic work-up would remove the imino-protecting group and protonate the carboxylate to give a free amino acid (Scheme 4.4). In addition to having a benzyl group on the imino nitrogen, a variety of substituents could be installed on the imino nitrogen atom. The electron-donating or -withdrawing ability of the group on the imino nitrogen could affect the carbanion that is generated following deprotonation.



Scheme 4.4. Proposed synthesis using ketimines **4-10** and **4-11** in the presence of DBU and CO₂ for the synthesis of an amino acid.

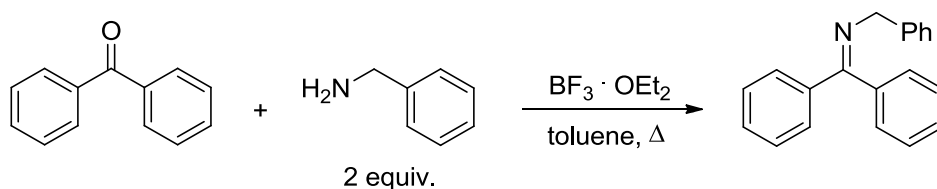
In 1850 Strecker used imine hydrocyanation with HCN followed by hydrolysis of the α -amino nitrile under acidic conditions to make α -amino acids.¹⁶ From this, the Strecker reaction became one of the most reliable methods for the synthesis of α -amino acids.¹⁷ The limitations of the Strecker reaction are the use of toxic hydrogen cyanide or an equivalent, and the hydrolysis of the α -amino nitrile with the use of strong acidic media at high temperatures. In recognition of the above drawbacks associated with the Strecker reaction, Sato and co-workers developed a one-pot synthesis of α -amino acids (Scheme 4.5) where they wanted to replace hydrogen cyanide as the carbon source with CO₂.¹⁸ The replacement of cyanide with CO₂ would lead to direct carboxylation of the imine, avoiding nitrile hydrolysis. They were able to achieve this by first base treating an α -amino sulfone **4-12**, to generate an imine **4-13** *in situ*. The generated imine **4-13** can then be converted into an α -amino stannane, **4-14**, by attack of the tributylstannyl anion in the presence of a fluoride source. The fluoride ion can further activate the α -amino stannane **4-15** by attacking the tin atom, which then induces carbanion-like reactivity at the sp³-hybridized carbon atom, which can then attack the electrophilic carbon of CO₂, to form the C-C bond and produce the α -amino acid **4-16**. To our knowledge, this is the only synthesis that incorporates CO₂ in the synthesis of α -amino acids from imines.¹⁸



Scheme 4.5. Synthetic strategies for the α -amino acids from α -amino sulfone.¹⁸

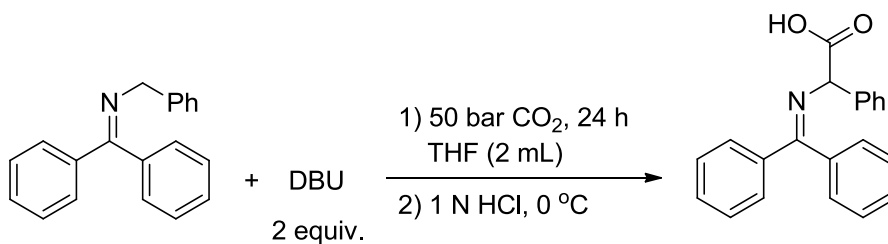
4.2.3 Results and Discussion: Preliminary Studies with Ketimine 4-10

As was previously mentioned, ketimines **4-10** and **4-11** have pK_a values within the range of the carboxylation afforded in the presence of DBU. A preliminary study was done with that of ketimine **4-10** that has a pK_a of 24.3, very close to that of acetophenone which has a pK_a of 24.7.¹⁵ Ketimine **4-10** was synthesized starting with benzophenone and a stoichiometric amount of trifluoroborate etherate and two equivalents of benzylamine under Dean-Stark conditions with toluene as the solvent (Scheme 4.6).

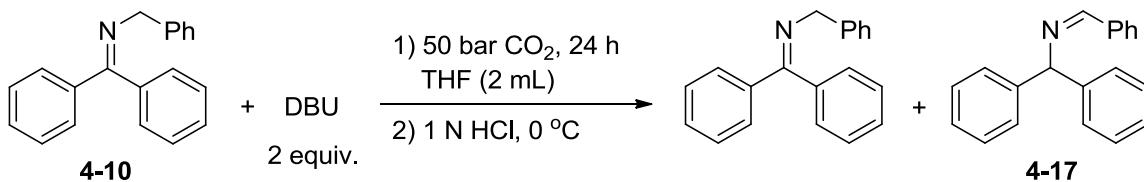


Scheme 4.6. Synthesis of **4-10** using benzophenone and benzylamine with trifluoroborate etherate under Dean-Stark conditions.

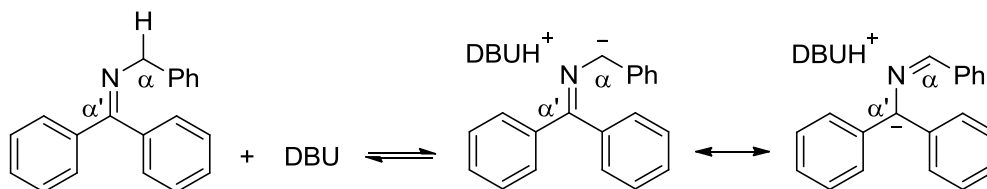
Ketimine **4-10** was subjected to the same reaction conditions developed in the Jessop Lab for the carboxylation of ketones using DBU (Scheme 4.7). However, upon the introduction of the DBU no colour change was observed, where formation of the anion was expected to result in the formation of a coloured solution. After analyzing the crude material by NMR spectroscopy (see SI) it is proposed that the compound formed was the isomerization product *N*-benzylidene-1,1-diphenylmethanamine **4-17** (Scheme 4.8). Aside from the starting material, the ¹H NMR spectrum contained two new singlets located at 5.6 and 8.4 ppm, which in combination with the signal at 160.4 ppm in the ¹³C NMR spectrum indicated **4-17**.¹⁹ In support of this claim, it is known in the literature that *N*-diphenylmethylenbenzylamine **4-10** can isomerize in the presence of a base^{19,20} or metal catalyst²¹ to **4-17**, in some cases under refluxing conditions.²⁰ Deprotonation of the methylene of **4-10** with DBU occurred, enabling **4-10** to undergo imine/enamine tautomerization; the double bond delocalized between the α - or α' -carbon atoms that neighbour the imino nitrogen (Scheme 4.9) and protonation can occur on the α - or α' -carbon atoms.



Scheme 4.7. Reaction conditions used towards the carboxylation of **4-10** using DBU for a base a pressure of CO₂.



Scheme 4.8. Attempted carboxylation of **4-10** with DBU and CO₂ which lead to the isolation of isomerized product **4-17**.



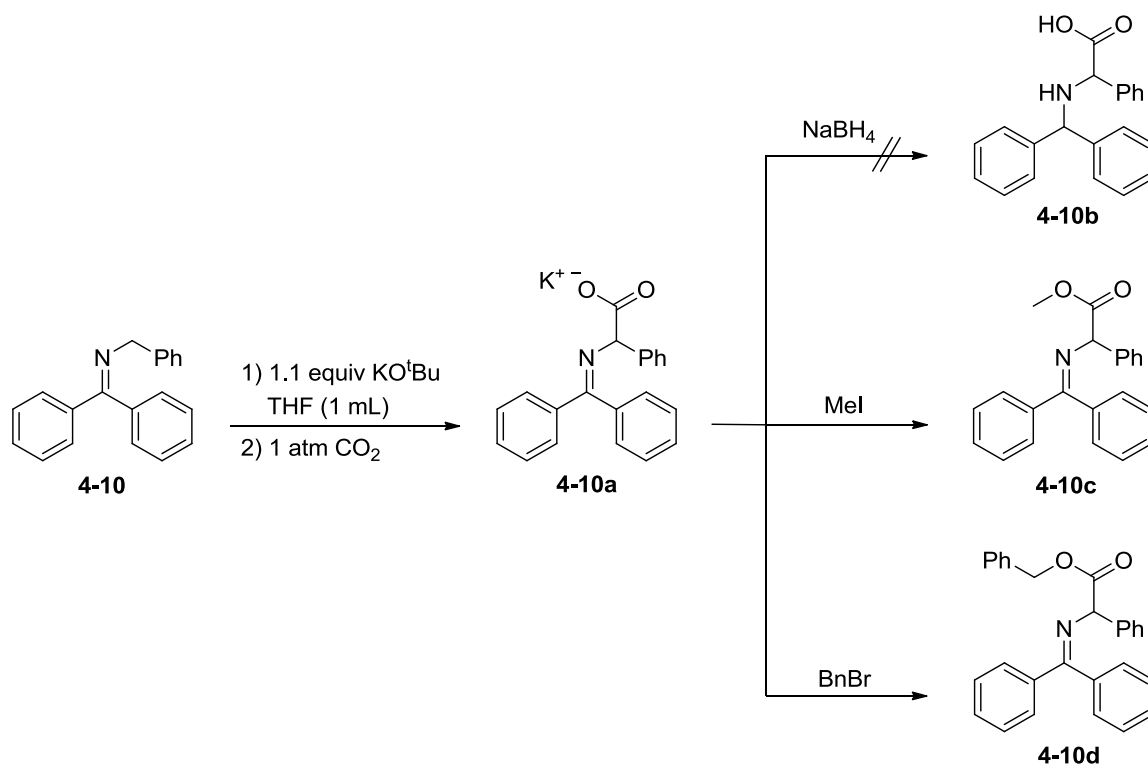
Scheme 4.9. Deprotonation of **4-10** with DBU to give imine/enamine tautomerization about α - and α' -carbon atoms.

Upon closer inspection of the ¹³C NMR spectrum of the crude reaction mixture from **4-10** with DBU and 50 bar of CO₂ (Scheme 4.8), there is a carbonyl peak that is at 196.6 ppm. While this shift is similar to that of the carbonyl peak for benzophenone, a byproduct following hydrolysis of **4-10**, only one other carbon signal corresponds to benzophenone in the ¹³C NMR spectrum of the crude reaction mixture. The ¹H NMR spectrum of the crude reaction mixture also shows a small peak at 10 ppm, which is within the ¹H NMR chemical shift range for a carboxylic acid signal. Perhaps due to the decomposition of this unknown product, the HRMS spectrum showed only starting material.

Unlike what was observed upon addition of DBU to deprotonate **4-10**, the addition of KO^tBu to deprotonate **4-10** in THF produced a colour change from clear yellow to a deep purple, indicative of the formed anion. There was no additional colour change after stirring the solution overnight at room temperature. When CO₂ was bubbled through the coloured solution at room temperature or at lower temperatures (-20 to 0 °C), the solution colour changed from deep purple

to a light yellow with a white precipitate. The ^1H NMR spectrum of the yellow oil that was isolated from the reaction mixture following work-up was that of the starting material **4-10** and **4-17** the isomerization product (Scheme 4.8). Even after the use of 50 bar of CO_2 , the resulting product was mixture of **4-10** and **4-17**.

Deprotonation of **4-10** did occur with various bases, producing a bright-coloured solution and similarly a colour change was observed following the addition of CO_2 to the solution that indicated carboxylation of **4-10** and/or protonation of tautomerized **4-10**, forming **4-17**. In attempts to isolate the carboxylated product of **4-10**, two methods were used: 1) addition of NaBH_4 to reduce the imine to form the analogous secondary imine of **4-10** and 2) addition of either iodomethane or benzyl bromide in attempt to alkylate any carboxylate formed during the reaction by the (Scheme 4.10). Ketimine **4-10** was first deprotonated using a slight excess of KO^tBu in a small amount of THF, CO_2 was bubbled into the solution until no further colour change was observed before addition of NaBH_4 , iodomethane, and/or benzyl bromide. The ^1H NMR spectra of the crude reaction mixtures from the above reactions did not indicate the formation of **4-10b** – **4-10d**, but the mass spectra taken from the alkylation crude product mixtures indicated the presence of **4-10c** and **4-10d**. The detection of **4-10c** and **4-10d** by mass spectrometry confirmed that the carboxylation of **4-10** did occur. Unfortunately, a method for isolating the carboxylation product was not found.



Scheme 4.10. Attempts to isolate carboxylated product of **4-10** by two methods: 1) reduction of imine by NaBH₄ and 2) addition of iodomethane or benzylbromide to esterify carboxylate.

The deprotonation of **4-10** did occur, though following the addition of CO₂ and analysis of the crude reaction mixtures with ¹H NMR spectroscopy, no carboxylate product was detected. The carboxylate that forms is not stable and was prone to decarboxylation. *N*-(Diphenylmethylene)-aminoacetonitrile **4-18** is a related ketimine to **4-10**, although it has an aminoacetonitrile group instead of a benzyl group. The aminoacetonitrile would influence the electronics of the formed anion, but the use of **4-18** did not lead to the formation of carboxylate product.

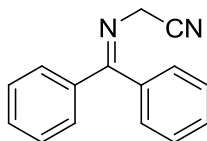
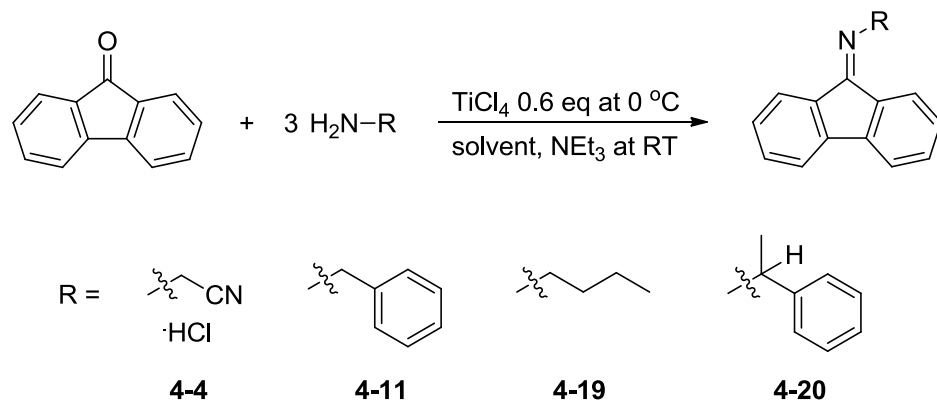


Figure 4.5. *N*-(diphenylmethylene)-aminoacetonitrile **4-18**.

The diphenylmethylene group might have an influence on the stability of the formed anion, in that it may not provide the right geometry. Changing the amine protecting group to a more rigid structure will change the geometry and thus influence the electronics of the formed anion. The 9-fluorenylidene is more rigid in structure than the diphenylmethylene and the rigidity may influence the formed anion following deprotonation. This possibility is explored in the next section.

4.2.4 Other Ketimine Candidates Towards the Synthesis of α -Amino Acids

Aside from **4-10**, other ketimines are of interest in that different groups substituted on the imino nitrogen would influence the sterics and electronics of the formed anion. The 9-fluorenylidene group was investigated as a protecting group for the amine (Scheme 4.11). Ketimine **4-11** features a lower pK_a of 14.5 than that of **4-10**, which gives more of an opportunity for DBU to deprotonate at the methylene. Three other ketimines, in addition to **4-11**, were considered to investigate the utility of the 9-fluorenylidene protecting group for the amine. The different electron-donating and withdrawing substituents on the imino nitrogen might also have an affect on the electronics of the formed anion. The ketimines that bear a 9-fluorenylidene group were synthesized using titanium tetrachloride at low temperature.

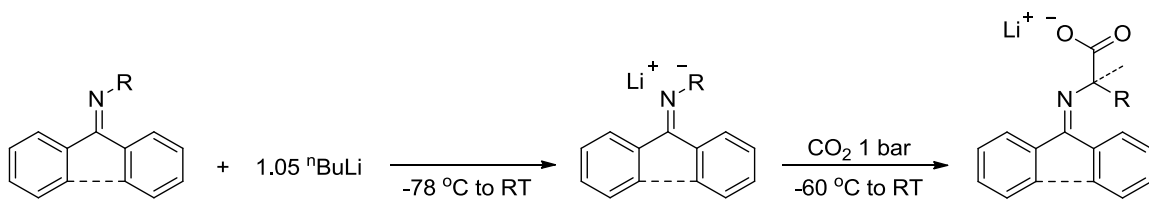


Scheme 4.11. Synthesis of ketimines that feature 9-fluorenylidene as an imino protecting group.

The investigated ketimines all have different substitution on the imino nitrogen, where the different groups would influence the electronics of the formed anion after deprotonation at the α -carbon. The *N*-fluorenylidene-protected α -aminoacetonitrile **4-4** is the same ketimine that gave promising results in the Mannich-type reaction developed by Kobayashi and co-workers.¹² The electron-withdrawing aminoacetonitrile group would stabilize the formed anion, perhaps allowing it to react with CO₂. The alkylated imino nitrogen of **4-19** would change the electronics of the formed anion, contrary to how the aminoacetonitrile group would influence the electronics of the anion. Both **4-11** and **4-20** would provide resonance stabilization of the anion that is formed, while **4-20** features a methyl group substituted about the α -carbon. The methyl group of **4-20** would prevent double deprotonation from occurring on the α -carbon, in addition act as a NMR spectroscopy handle to indicate reactivity about the neighbouring α -carbon.

In addition to using DBU and KO^tBu, lithium diisopropyl amide (LDA) and *n*-BuLi were also used to deprotonate the ketimines before attempting carboxylation at the methylene. The most reactive and strongest base was *n*-BuLi and different coloured solutions were observed for each ketimine after its addition. The ketimines were dissolved in a minimal amount of THF, cooled to -78 °C at which point *n*-BuLi was added. The CO₂ was added at -78 °C and the solution

was allowed to warm to room temperature (Scheme 4.12). Upon the addition of CO₂ a dramatic change in solution colour occurred. The coloured solutions of the formed anions from all the ketimines are noted in Table 2 below. Through NMR spectroscopic analysis of the reaction product mixtures, there was no indication of carboxylated product, and only starting material and various decomposition products were detected in each case. Interestingly, the isomerization product of **4-11** is formed following deprotonation of DBU under 50 bar of CO₂, like that of ketimine **4-10**.



Scheme 4.12. Deprotonation with *n*-BuLi and addition of CO₂.

Table 4.2. Solution colours of after addition of *n*-BuLi and addition of CO₂ for the investigated ketimines that have a diphenylmethylene (Ph₂C-) or 9-fluorenylidene (9-flu-) protecting-group (PG).

R =	Ph ₂ C-imines		9-flu-imines	
	After addition of <i>n</i> -BuLi	After addition of CO ₂	After addition of <i>n</i> -BuLi	After addition of CO ₂
			red	yellow
			red	brown orange
	red	yellow	fuchsia	green
	violet	yellow	purple	orange

The variation in protecting groups and substituents on the imino nitrogen atom did not afford any carboxylate product. Any such carboxylate formed from carbanions from the above ketimines were not stable. Destabilization is tentatively attributed to resonance along α - and α' -carbons (Scheme 4.9) and the basicity of the N-atom. With DFT calculations, Anders and co-workers investigated the reactivity of carbanions formed from an azomethine, 4-alkylidene-1,4-dihydropyridine system for their use as CO₂ transfer agents, in accordance to natural models like biotin.²² They attributed the CO₂ transfer ability of the azomethine to the resonance that occurs along the α -carbon. The results of Anders and co-workers relate to the observations in this study. The carbanion that is formed is not a strong nucleophile to capture CO₂, but may be useful as a CO₂ transfer agent.

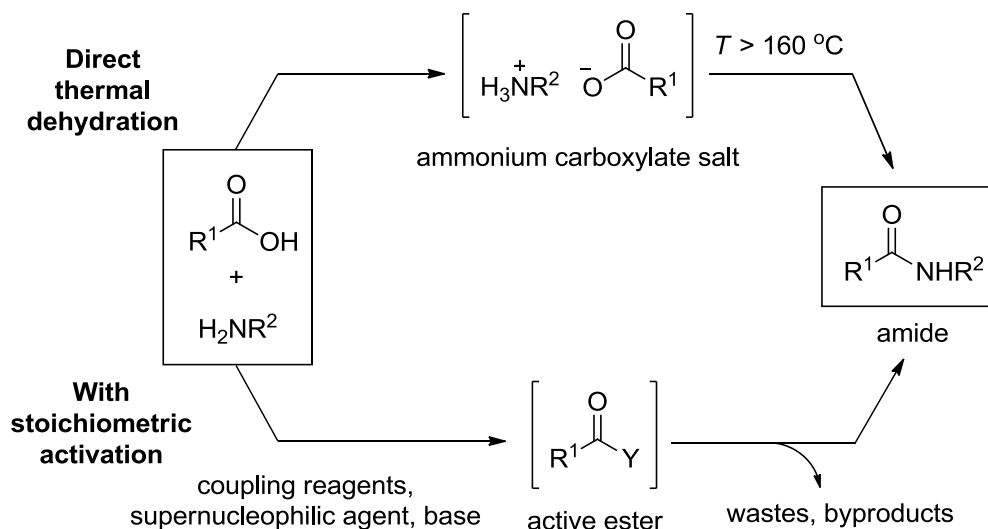
4.3 Preliminary Study of the Amidation of Benzoylacetic Acid

4.3.1 Synthesis of Amides and the use of Lewis Acid Catalysts for Amidation

The carboxylation of ketones in the presence of DBU and CO₂, followed by asymmetric hydrogenation, is an effective way to convert inexpensive ketones into optically active β -hydroxycarboxylic acids. As an extension to this method, it would be advantageous to further derivatize the β -hydroxycarboxylic acids towards more useful products, such as amides.

The amide bond is an important functionality in many natural products and the search for methods for its efficient formation is the subject of ongoing scientific study.^{23,24} The amide bond is thermodynamically stable, though a large activation energy is required to form it from a free carboxylic acid and amine. High temperatures, above 160 °C, are required to dehydrate the stable ammonium carboxylate salt that readily forms between a free carboxylic acid and amine, towards the formation of the amide bond (Scheme 4.13).²⁵ Alternatively, an unstable ester can first be formed and reacted with the amine, though this generally requires the use of toxic and or expensive reagents in stoichiometric quantities. Examples of these reagents are carbodiimides or

phosphonium or uranium salts which activate the ammonium carboxylate thus facilitating the dehydration step.²³ Although these are the most common methods of amide bond formation, there have been a few examples which are simple, greener and atom efficient.²⁶

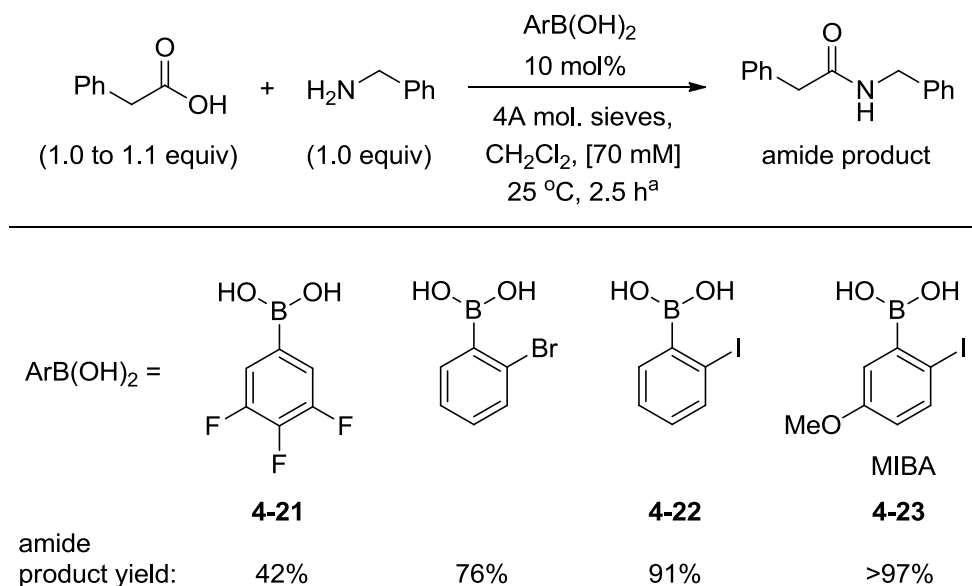


Scheme 4.13. Direct amide bond formation by reaction of a free carboxylic acids and amines.²⁶

The formation of an amide bond can be achieved by the use of aryl boronic acids. Yamamoto and co-workers described the use of electron-poor arylboronic acids as catalysts for direct amidations.^{27,28} Electron-poor arylboronic acids were found to be optimal, with the most efficient being the 3,4,5-trifluorophenylboronic acid, **4-21**, which still required refluxing the solvent at temperatures over 110 °C for several hours. Whiting and co-workers employed arylboronic acids such as (di-*iso*-propyl-aminomethyl)phenylboronic acid,^{29,30} and even boric acid alone in the amidation of carboxylic acids, again at temperatures of °C.³¹⁻³⁴ Thus, both the groups of Yamamoto and Whiting developed conditions for the synthesis of amides, although at elevated temperatures.

Hall and co-workers developed a method for amidation of free carboxylic acids using a catalytic amount of *ortho*-substituted aryl boronic acids under mild reaction conditions and room

temperature (Scheme 4.14).²⁶ The reaction also required the addition of 4 Å molecular sieves to scavenge the water, which is the byproduct of the reaction. Hall and co-workers found that electron-donating substituents are preferable, in particular an alkoxy substituent positioned *para* to an iodide. The optimal catalyst was found to be 5-methoxy-2-iodophenylboronic acid (MIBA, **4-23**). The boronic acid catalyst is recyclable and promotes the formation of amides from aliphatic carboxylic acids and amines. The structure of MIBA supports the theoretical study as there is a need for an electronically enriched *ortho*-iodo substituent where the iodide acts as a hydrogen-bond acceptor in the orthoaminal transition state.³⁵



^aReaction time is 1.5 h when ArB(OH)₂ is MIBA.

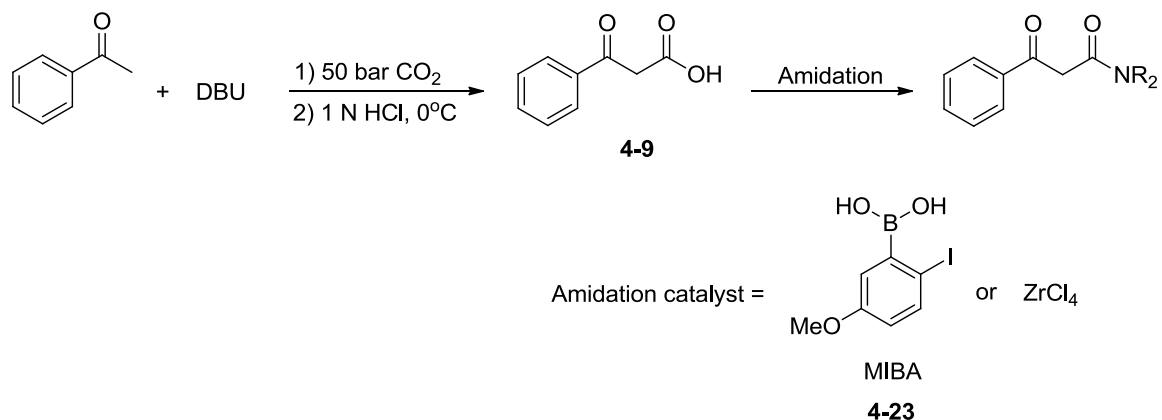
Scheme 4.14. Direct amidation of phenylacetic acid with benzylamine with various arylboronic acids with isolated amide product yields.

4.3.2 Results and Discussion: Attempted Amidation of Benzoylactic Acid

The synthesis of β -hydroxycarboxylic acids was carboxylation of a ketone requires 60 bar of CO₂ in combination with two equivalents of DBU without additional solvent followed by catalytic hydrogenation.¹ The first step of the method involves the formation and isolation of the β -ketocarboxylic acids (Scheme 4.1). For example, the synthesis of benzoylactic acid, a β -ketocarboxylic acid, uses acetophenone as the starting ketone; the acid was isolated in good yields with two equivalents of DBU and 60 bar of CO₂. The next step was problematic because the isolated β -ketocarboxylic acids are unstable, with respect to rapid decarboxylation in solution, the asymmetric hydrogenation must be faster than the decarboxylation. Discovery of more reactions that would derivatize the β -ketocarboxylic acids, aside from asymmetric hydrogenation, would expand the utility of the above method to other useful products.

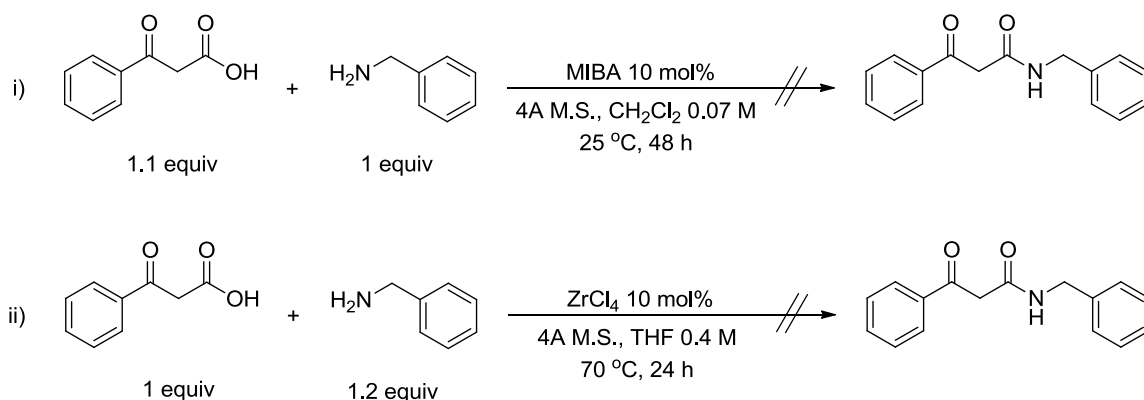
Amidation of the β -ketocarboxylic acids would generate stable β -ketoamides. The amide bond is a valuable functional group from a synthetic and industrial point of view.²⁶ β -Ketoamides have been proven to be versatile building blocks for the synthesis of heterocycles, some examples are pyrroles,³⁶ indoles,³⁷ and tetrahydroquinolines.³⁸

Using MIBA or another Lewis acid catalyst for the amidation of β -ketocarboxylic acids would be appealing since it would be a direct catalytic formation of primary amides. It has also been reported by Adolfsson and co-workers that ZrCl₄ is a catalyst for the amidation of a variety of carboxylic acids.³⁹ As previously discussed (Section 4.3.1), the formation of the amide bond has a high activation energy and requires the use of stoichiometric toxic reagents, or high temperatures or catalysts to overcome it. In ambient to near ambient conditions, formation of amide bonds can be achieved using MIBA **4-23**²⁶ and/or ZrCl₄³⁹ with carboxylic acids and various amines. In this initial study for the amidation of β -ketocarboxylic acids, benzoylactic acid was used. It can be synthesized in relatively good yields and is slower to decarboxylate than other β -ketocarboxylic acids from the previous study¹ (Scheme 4.15).



Scheme 4.15. Formation and proposed amidation of benzoylacetic acid with amidation catalysts MIBA and ZrCl_4 .

The same reaction conditions for MIBA and ZrCl_4 as amidation catalysts were used to afford the amidation of benzoylacetic acid. The reagents that were used in the initial studies for the amidation of benzoylacetic acid were those associated with the successful results that were reported for MIBA and ZrCl_4 . In the amidation reaction of phenylacetic acid, benzylamine gave the best isolated yields of 98%²⁶ (at RT) and 99%³⁹ (at 70 °C) where MIBA and ZrCl_4 were used as amidation catalysts respectively. Dichloromethane and THF were the ideal solvents for amidation reactions associated with MIBA and ZrCl_4 respectively. As a result, benzylamine and the two above solvents were used in the initial studies for the amidation of benzoylacetic acid (Scheme 4.16).



Scheme 4.16. Attempted amidation of benzoylacetic acid with ideal reaction conditions reported for MIBA and ZrCl_4 as amidation catalysts.

When the ideal conditions for amidation reactions, specific to MIBA or ZrCl_4 , were applied to benzoylacetic acid, no amide product was isolated. NMR spectroscopy showed a residual amount of benzylamine, acetophenone, carbamic acid, and what appeared to be benzoylacetic acid with some signals shifted. The signals in the ^1H NMR spectrum that correspond to the keto/enol tautomerization of benzoylacetic acid shifted from 5.7 ppm and 4.1 ppm to 5.3 and 4.8 ppm after the addition of MIBA and/or ZrCl_4 .

It was possible that the catalyst caused the change in signals of benzoylacetic acid. As a test, an NMR study was done with benzoylacetic acid and MIBA. When a stoichiometric amount of benzoylacetic acid was mixed with MIBA, the ^{11}B NMR spectrum of MIBA changed and the boron signal shifted from 28.8 ppm to 5.3 ppm. A ^{11}B NMR chemical shift around 5 ppm was within the shift range of 4-coordinate boron species. It is possible that the boron atom of MIBA could be interacting with the two carbonyl groups, thus ruining its catalytic reactivity. Similarly, the zirconium of ZrCl_4 could be interacting with the two carbonyl groups of benzoylacetic acid.

While the amidation catalysts, MIBA and ZrCl_4 have been proven to afford the amidation of various carboxylic acids, it was not successful for the amidation of the β -ketocarboxylic acid, benzoylacetic acid. A majority of the carboxylic acids that were investigated by Hall and co-

workers²⁶ as well as Adolfsson and co-workers³⁹ featured a methylene group neighbouring the carbonyl group and no coordinating group close in proximity. Seemingly, the presence of a second carbonyl group is deactivating to the amidation catalyst. In the case of benzoylactic acid, the carbonyl group is *beta* to the carboxylic acid where the Lewis acid catalysts would have the ability to interact with the two carbonyl groups that are proximal to each other. If this did occur the catalytic activity of the Lewis acid catalysts was reduced.

To the best of our knowledge, there are no reported examples of boron interacting with a keto acid like benzoylactic acid. However, in one account Marcantonatos investigated the *in situ* chelation of boric acid species with a related structure.⁴⁰ Calculations were done on the solution dynamics with continuous radiation to investigate the spin-orbit coupling of benzoylacetone. This was the only account that related to what was observed in our preliminary investigation of using MIBA for the amidation of benzoylactic acid. It is apparent that the boron does not distinguish the carboxylic acid group from the two neighbouring carbonyl groups. A way to make the carboxylic acid preferable to either Lewis catalyst is by protection of the secondary carbonyl group.

Benzoylactic acid undergoes keto/enol tautomerization that influences its ability to decarboxylate. It was demonstrated that the rate of decarboxylation of benzoylactic acid varied among different solvents.¹ Solvents other than THF and CH₂Cl₂ might afford amidation of benzoylactic acid, by slowing decarboxylation and providing more of an opportunity for amidation of benzoylactic acid.

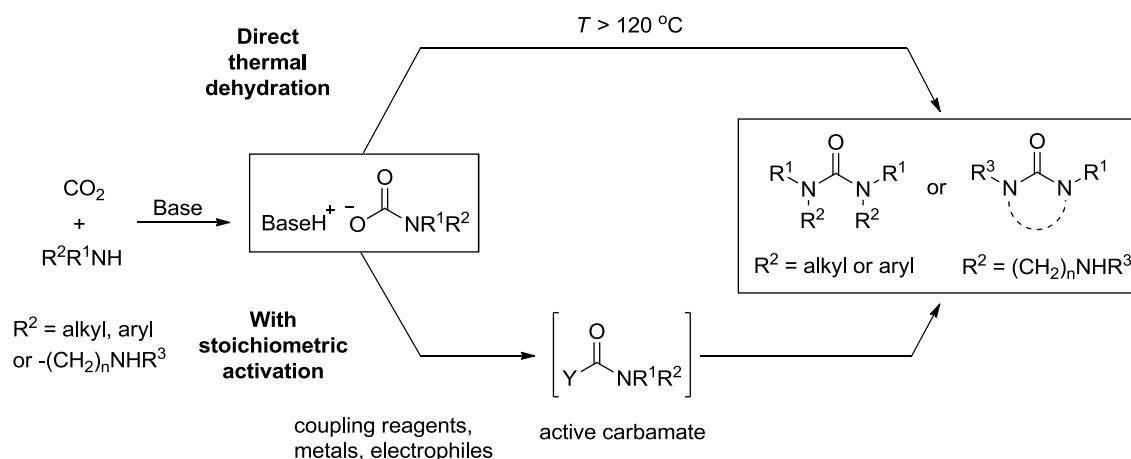
Isolation of the boron species that is formed with benzoylactic acid, with or without the presence of amine, would confirm the structure. While there has been no other account than the one above by Marcantonatos, related to benzoylactic acid, there might be reactivity with the combination of amine, CO₂ and the Lewis acid catalysts. An ASAP article by Wang and co-workers reports a CO₂ adduct from the reaction of CO₂ and amine/bis(2,4,6-

tris(trifluoromethyl)phenyl)boron pairs or FLPs.⁴¹ Investigation of the formed carbamate in the presence of MIBA might provide further insight into the reactivity of the Lewis acid catalysts.

4.4 Lewis Acid Catalysts for the Formation of Ureas

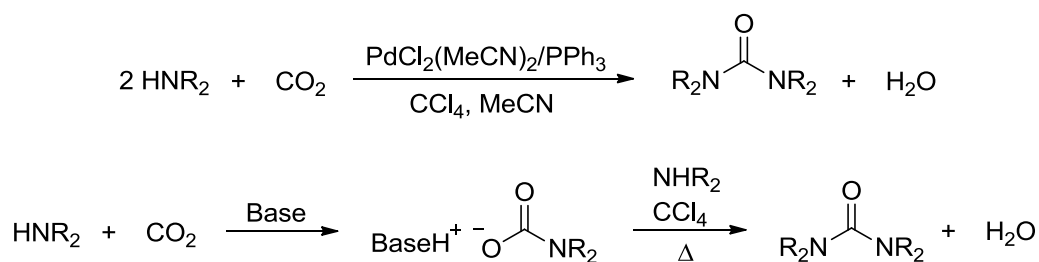
4.4.1 Synthesis of Ureas and the Search to Overcome the High Energy Barrier

The synthesis of tetraalkylated ureas with an amine and CO₂ is similar to the amidation of a carboxylic acid, in that a large amount of energy is required for the dehydration of the carbamate salt. Dialkylureas can be formed from CO₂ and primary amines with a variety of methods.⁴²⁻⁴⁵ However, the same conditions are not transferrable to using secondary amines and CO₂ to form tetraalkylureas, since there is the need to overcome the large energy barrier required for the dehydration of the carbamate salt (Scheme 4.17). The dehydration step can be achieved with the use of a catalyst at elevated temperatures (120 – 250 °C),^{46,47} few reports describe the use of CO₂ at ambient conditions.⁴⁸⁻⁵¹



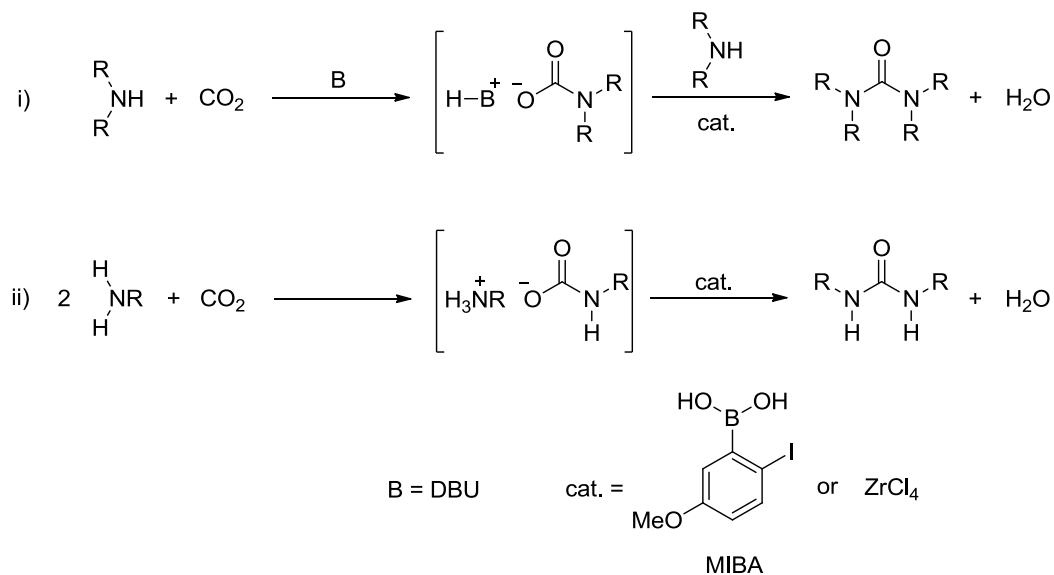
Scheme 4.17. Summary for the synthesis of tetraalkylated ureas (cyclic or acyclic) from either direct thermal dehydration or with stoichiometric activation.

It was previously reported that tetraalkylureas could be synthesized from CO₂ at moderate temperatures (below that of 100 °C) using large concentrations of PdCl₂(MeCN)₂ catalyst and a stoichiometric amount of triphenylphosphine in CCl₄/MeCN solvent system (Scheme 4.18).⁵² The above method was investigated in the Jessop lab to evaluate the use of sub-stoichiometric amounts of triphenylphosphine;⁴⁸ it was found that the Pd-catalyst had no effect on the urea synthesis and the CCl₄ solvent was required as a reagent. The reaction can be done at 60 °C in CCl₄ and can be weakly promoted by either DMAN or triphenylphosphine. A two-step method works best where the dialkylammonium dialkylcarbamate is produced *in situ* and then reacted with CCl₄ and free dialkylamine as opposed to a single-step procedure (Scheme 4.18).



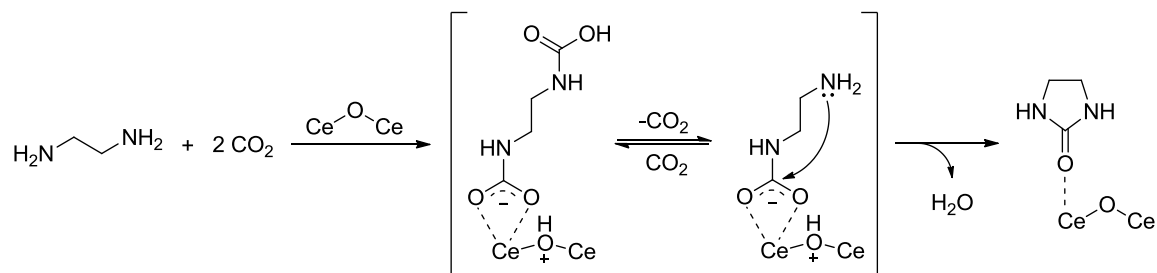
Scheme 4.18. Above: synthesis of tetraalkylated ureas using a Pd-catalyst and stoichiometric amount of triphenylphosphine.⁵² Below: two-step method developed in the Jessop lab for the synthesis of tetraalkylated ureas using CO₂ and CCl₄.⁴⁸

While MIBA or ZrCl₄ are promising amidation catalysts in the presence of carboxylic acids and secondary amines, whether their reactivity can be extended to the synthesis of tetraalkylureas has yet to be investigated. An ammonium carbamate salt has a similar structure to an ammonium carboxylate salt, a similarity that could allow MIBA and/or ZrCl₄ to catalyze the dehydrative amidation of the carbamate salt, giving a urea, in a similar manner as it does with a carboxylate to give an amide. With a carbamate salt in the presence of either of the Lewis acid catalysts, one can envision the formation of tetraalkylureas (Scheme 4.19).



Scheme 4.19. Proposed synthesis of ureas by initial formation of carbamates using i) secondary amines and equivalent of base (B = DBU) and ii) primary amines, where MIBA or ZrCl_4 would catalyze the reaction.

The formation of cyclic ureas starting from diamines was not unprecedented. It was previously reported that the formation of cyclic ureas derived from diamines would require the use of carbon monoxide, a toxic reagent.⁵³ Tomishige and co-workers demonstrated the formation of cyclic ureas from diamines using a heterogeneous catalyst cerium oxide (CeO_2).⁵⁴ The majority of the diamines that were reported were primary diamines or a diamine that featured a primary amine on one end with a secondary amine on the other. With 5 bar of CO_2 and a temperature of 160 °C, isolated yields of cyclic urea in 2-propanol were 97% to 99%. Using ethylenediamine as a representative diamine, Tomishige and co-workers investigated the effect of pressure, temperature, and the recyclability of the CeO_2 on the reaction system. They attributed the rate-determining step to be the nucleophilic attack of an amino group on a CeO -bound carbamate species (Scheme 4.20). Tomishige and co-workers also noted that some alkyl groups at the N-atom decreases the reactivity, which was attributed to the steric hindrance of the *N*-alkyl chains and/or basicity of the amines.



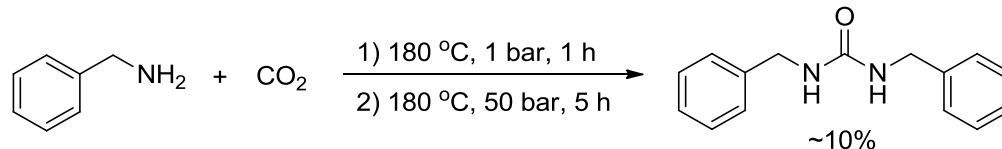
Scheme 4.20. Excerpt from proposed reaction mechanism of cyclic urea from CO₂ and ethylenediamine by CeO₂ reported by Tomishige and co-workers.⁵⁴

4.4.2 Results and Discussion: Investigation of Amidation Catalysts for Urea Synthesis

The preliminary investigation of urea formation in the presence of MIBA or ZrCl₄ first involved screening primary and secondary amines for the formation of dialkylureas. Carbamate salts can be formed from secondary amines with an equivalent of base, such as DBU or amine, or from two equivalents of primary amine.

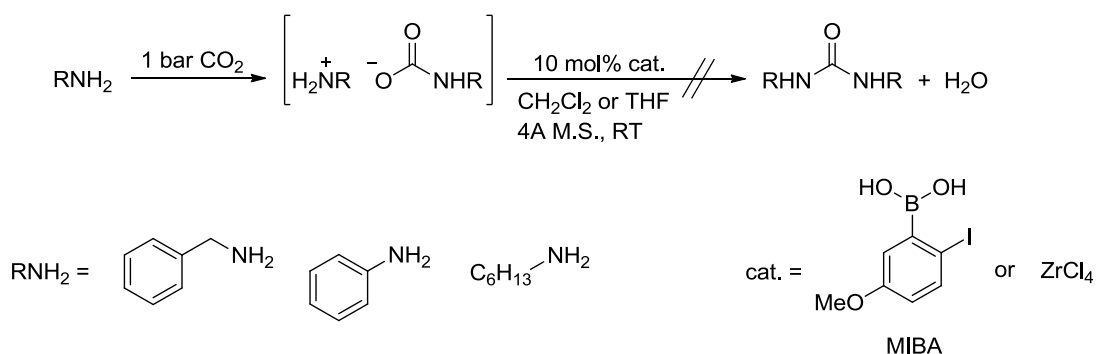
It has been previously reported that dialkylureas can be formed from amines and CO₂ with high temperatures and high pressures.^{44,45} According to Nakai and co-workers, they received >99% isolated yield of the dialkylurea with two equivalents of amine using 50 bar of CO₂ at 180 °C for 5 h.⁴⁵ As a preliminary investigation, this reported procedure was repeated in the Jessop lab with benzylamine and CO₂ (Scheme 4.21). Following a 5 h reaction time, the amount of dibenzylurea isolated was approximately 10% according to ¹H NMR spectroscopy. Under a higher pressure of CO₂, Zhao and co-workers could form benzylurea in an isolated yield of 30% after a reaction time of 4 h⁴⁴ where a comparable yield of dibenzylurea was achieved in the Jessop Lab when the reaction time was 12 h. According to the ¹H NMR spectrum of the crude reaction mixture after a 12 h reaction time, the yield of dibenzylurea was roughly 23%. Han and co-

workers used similar temperatures and pressures, though in the presence of an ionic liquid and N-methylpyrrolidone to achieve 46% isolated yield of dibenzylurea.⁴³



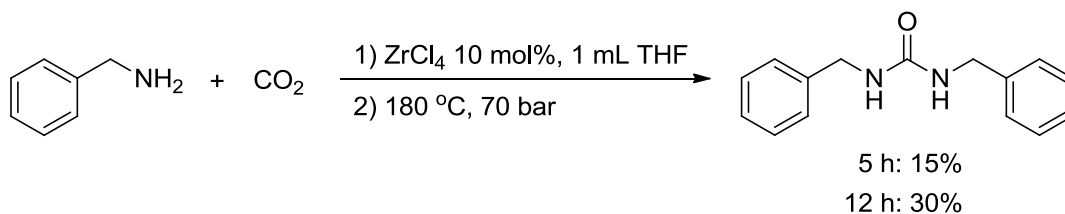
Scheme 4.21. Formation of dibenzylurea starting from benzylamine and CO₂ under 180 °C and 50 bar of CO₂ in absence of solvent. Yield of dibenzylurea calculated from ¹H NMR spectra.

The feasibility of MIBA or ZrCl₄ as catalysts for the synthesis of ureas was first investigated using primary amines and CO₂ towards the formation of symmetric dialkylureas under ambient conditions. The reaction conditions outlined for the amidation of carboxylic acids were used. Before adding the catalyst to the reaction, the carbamate was first formed through the addition of CO₂ into the solution of amine and solvent. It was found that with either catalyst, under ambient or near ambient conditions for MIBA or ZrCl₄ respectively, no dialkylated urea was formed (Scheme 4.22). Only the carbamate salt was detected by NMR spectroscopy.



Scheme 4.22. Attempts to prepare dialkylureas by initial formation of carbamate salts from amines and 1 bar of CO₂ followed by addition of 10 mol% MIBA or ZrCl₄. Piperidine was also tried without success.

It was thought that the application of higher temperatures and pressures might elicit the formation of dialkylureas in the presence of a Lewis acid catalyst. Benzylamine was first stirred with ZrCl_4 , with a small amount of THF (1 mL) used in order to dissolve the catalyst. Molecular sieves were added to the reaction mixture and then the vessel was heated to 180 °C and pressurized to 70 bar of CO_2 (Scheme 4.23). From the ^1H NMR spectra of the crude product mixture after 5 h and 12 h of reaction time, dibenzylurea was present in approximately 15% and 30% yield, respectively.



Scheme 4.23. Formation of dibenzylurea using high temperature and pressure in the presence of ZrCl_4 as a catalyst. Yield of dibenzylurea is approximated from ^1H NMR spectra.

Seemingly, there is not an appreciable difference in the amount of dibenzylurea that was produced under high temperature and pressure without or with the presence of catalyst. Under a high temperature and pressure in the presence of ZrCl_4 , there was an increase in the amount of dibenzylurea when the reaction time was increased to 12 h from 5 h. An observation that was common among all the attempts to synthesize ureas was the formation of carbamate salt and observed in the crude reaction mixture after removal of the solvent. The stability and amount of carbamate in the reaction mixture would influence the formation of urea. In the original reaction conditions for either MIBA or ZrCl_4 as amidation catalysts, the carboxylic acid was used in slight excess (1.1 to 1.2 equivalents) to the amine. In particular with MIBA as a catalyst, it was first stirred with the carboxylic acid and molecular sieves before addition of the amine. Perhaps using

a stoichiometric or excess amount of Lewis acid catalyst would afford the amidation of β -ketocarboxylic acids.

4.4.3 Investigation of Amidation Catalysts for the Synthesis of Tetralkylureas using a Diamine

In the Jessop lab, as described in Chapter 2, it was determined that the addition of CO_2 to secondary diamines produces a zwitterionic species even in the presence of water. The molecular structure of *N,N'*-dimethyl-1,3-propanediamine and CO_2 was determined by X-ray crystallography, with the zwitterionic species hydrogen bonded to a molecule of water (Figure 4.5). In addition to the solid state structure, the ^1H and ^{13}C NMR chemical shifts reflected the asymmetry of the diamine. The asymmetry in the diamine was generated by the capture of a CO_2 molecule by one nitrogen atom and the other nitrogen is protonated. This asymmetry was more evident in the ^1H NMR spectrum that exhibited two sets of chemical peaks.

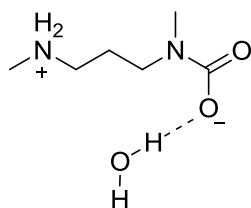
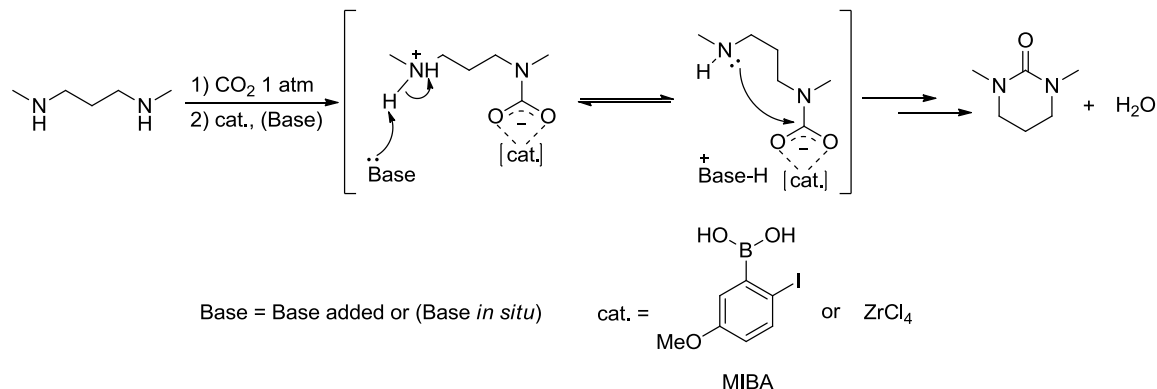


Figure 4.6. Drawing of zwitterionic *N,N'*-dimethyl-1,3-propanediamine CO_2 -adduct.

It is evident that in solution and in the solid state, the CO_2 -adduct formed with secondary diamines featured one equivalent of CO_2 . What is appealing about the zwitterionic structure is that the carbamate nitrogen site of the diamine could act as a coordinating site. With the carbamate attached to a pendant nitrogen atom, one can envision that amidation would cause ring

closure, leading to the synthesis of cyclic tetraalkylated urea (Scheme 4.24). This ring formation could be facilitated through the addition of a Lewis acid catalyst, such as MIBA or ZrCl_4 .

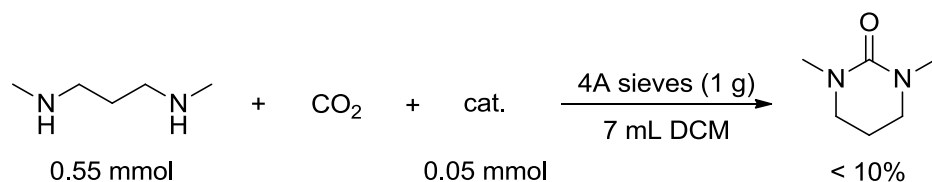


Scheme 4.24. Proposed synthesis and mechanism using N,N' -dimethyl-1,3-propanediamine for the synthesis of cyclic urea in the presence of a Lewis acid catalyst. A base can either be added or it can be *in situ* (Base).

The reactivity of CO_2 with N,N' -dimethyl-1,3-propanediamine was conclusive in solution and the solid state. Thus, it was chosen for the preliminary investigation towards the synthesis of cyclic ureas in the presence of Lewis acid catalysts. The zwitterionic species can be formed with atmospheric pressure of CO_2 , hence before the addition of solvent, CO_2 was bubbled into the diamine to form the zwitterion. Dichloromethane was chosen as the solvent for the preliminary experiments since it was reported to give the highest reactivity with MIBA²⁶ and was a relatively good solvent for ZrCl_4 .³⁹ After the addition of solvent, molecular sieves and the catalyst were added to the reaction mixture. The reaction was either conducted under a pressure of CO_2 or with CO_2 bubbled into the final reaction mixture for a period of 10 min. Table 4.3 lists the reaction conditions that were applied for the synthesis of cyclic urea starting from N,N' -dimethyl-1,3-propanediamine. What can be seen from Table 4.3 is that CO_2 pressure did not have an appreciable difference in the amount of cyclic urea produced and according to ^1H NMR

spectroscopy less than 10% of cyclic urea was detected. Further, the addition of DBU to the reaction mixture did not change the amount of cyclic urea that was produced (Table 4.3, entry 3).

Table 4.3. Attempts at the formation of cyclic urea starting from *N,N'*-dimethyl-1,3-propanediamine. All reaction conditions yielded trace amounts (<10%) of cyclic urea.



Entry	P (bar)	cat./Base	T (°C)
1	1	--	–
2	1	MIBA	–
3	1	MIBA/DBU	–
4	35	--	–
5	35	MIBA	100 °C
6	50	ZrCl ₄	80 °C

While the amount of cyclic urea formed from *N,N'*-dimethyl-1,3-propanediamine was small (<10%) with various reaction conditions, the method to form cyclic ureas from secondary diamines and CO₂, in the presence of a Lewis acid catalyst is promising. The synthesis of cyclic ureas by Tomishige and co-workers⁵⁴ was concurrent with this preliminary investigation. They did an extensive study to elucidate the optimal CO₂ pressure, solvent, concentration of catalyst, temperature and reaction time to afford high yields of cyclic urea. Similar studies can be applied using MIBA and ZrCl₄ as catalyst in order to find the optimal reaction conditions. In particular,

the amidation reactions with MIBA required that the catalyst stir with the carboxylic acid first. Perhaps changing the sequence in which reagents are added might affect the product outcome.

Comparisons can be made between the work of Tomishige and our preliminary investigation with *N,N'*-dimethyl-1,3-propanediamine. It can be noted that in the work of Tomishige and co-workers CO₂ pressure did not appreciably affect the reaction, a similar observation in our own preliminary study. *N,N'*-Dimethylethylenediamine was the only secondary diamine that Tomishige and co-workers reported in the paper with an isolated yield of 78%. Our preliminary investigation with *N,N'*-dimethyl-1,3-propanediamine gave the same amount of cyclic urea regardless of whether it was at room temperature or 100 °C. Tomishige and co-workers had their reactions operating above temperatures of 100 °C.

4.5 Conclusions and Future Considerations

4.5.1 Investigation of Ketimines towards the Synthesis of α -Amino Acids

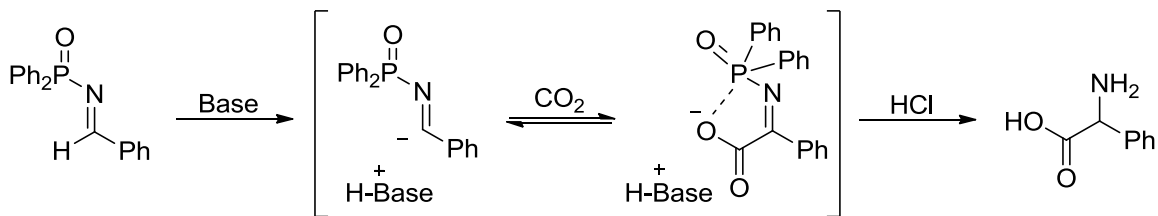
A variety of ketimines were studied in order to determine whether carboxylation can be afforded in the presence of DBU and eventually lead to the synthesis of α -amino acids. This method was envisioned following the previous report in the Jessop Lab involving deprotonation of ketones with pK_a's an order of magnitude higher than DBU. The ketimines that were studied featured either a diphenylmethylene or a 9-fluorenylidene protecting group about the amine. The substituents on the imino nitrogen of the ketimine were different according to sterics and electronics in order to influence the formed anion. A variety of bases were also used to deprotonate the various ketimines and produced different coloured anions; however, in all cases no product was observed. While a dramatic colour change was observed upon the addition of CO₂, the retrieval of starting material could be attributed to decomposition of the carboxylate.

To increase the likelihood of isolating a carboxylated product, after deprotonation and possible carboxylation of ketimine **4-10**, two methods were tested. The first method was an

attempt to reduce the imine following carboxylation with NaBH₄, which was not successful. The next method involved the addition of alkyl halides to promote esterification at the formed carboxylate. Although esterified product was detected by HRMS, insufficient quantities were generated to be visualized by NMR spectroscopy.

Interestingly, **4-10** showed different reactivity among the ketimines that were studied. Deprotonation of **4-10** with DBU and exposure to 60 bar CO₂ produced a small amount of an unknown species with a chemical shift in the ¹³C NMR spectrum of 198 ppm. However the small quantity produced and instability of **4-10** made no further exploration of this signal practical.

Due to the instability of the carboxylate that is formed with the above ketimines and CO₂, a future consideration would be to screen different protecting groups for the amine that would stabilize the anion upon deprotonation. One example that could stabilize the anion is diphenylphosphinylimine that was involved in the investigation of Kobayashi and co-workers for their Mannich-type reaction.¹² There are two factors that would make the diphenylphosphinylimine (DPP imine) an advantageous imine to investigate for carboxylation in the presence of DBU. One is that the DPP group can be removed under acidic conditions, much like the diphenylmethylene or 9-fluorenylidene group. The second factor is that the fully hybridized phosphorus atom of DPP is oxophilic, where the formed carboxylate on the α-carbon could be stabilized by this phosphorus atom (Scheme 4.25). For example, Stephan and co-workers demonstrated the capture of CO₂ with the use of an amidophosphorane that featured a phosphorus (V) centre in conjunction with a nearby amine group.⁵⁵



Scheme 4.25. Proposed synthesis of an α -amino acid with diphenylphosphinylamine and CO_2 .

4.5.2 Investigation of Lewis Acid Catalysts for Amidation of Benzoylactic Acid

MIBA and ZrCl_4 are useful catalysts for the amidation of a variety of carboxylic acids, though no amide product was formed with benzoylactic acid, a β -ketoacid, and benzylamine in the presence of either catalyst. A variety of β -ketocarboxylic acids were synthesized with the use of DBU and CO_2 . These β -ketocarboxylic acids were susceptible to decarboxylation. Further derivatization of the carboxylic acid group of the β -ketoacids would lead to even more valuable products.

Presence of a second carbonyl group *beta* to the carboxylic acid proved to be detrimental to the activity of both MIBA and ZrCl_4 , most likely through chelation, as suggested by analysis of the ^{11}B NMR spectra. The addition of benzylamine to benzoylactic acid enforced decarboxylation. As a future experiment, perhaps using an excess amount of Lewis acid catalyst would afford the amidation of β -ketocarboxylic acids.

4.5.3 Investigation of Lewis Acid Catalysts for Synthesis of Ureas

It was found that under ambient pressure of CO₂ and catalyst, dialkylureas were not formed from a variety of primary amines and one secondary amine, piperidine. Only 10% of dibenzylurea did form from benzylamine in the absence of catalyst and solvent at a temperature of 180 °C and CO₂ pressure of 50 bar, contrary to what was reported previously with the same reaction conditions.⁴⁵ Adding 10 mol% ZrCl₄ to the above reaction conditions improved the amount of dibenzylurea produced, though not appreciably. The main byproduct of the reactions above was the stable carbamate salt of benzylamine and CO₂, where the amount of free amine to act as an *in situ* base to CO₂ was not controlled.

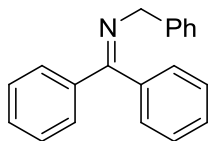
To address the need for free amine in solution to act as a base to capture an equivalent of CO₂, *N,N'*-dimethyl-1,3-propanediamine was considered since it was determined that it could capture an equivalent of CO₂ in solution and in the solid state. It was found that the cyclic urea was formed in low yield, independent of pressure of CO₂ with both MIBA and ZrCl₄ as the catalyst. Future work for the formation of cyclic ureas in the presence of either MIBA or ZrCl₄ would include the screening of other diamines, such as *N,N'*-dimethylethylenediamine, with the cyclic urea being a stable 5-membered ring, as well as other CO₂ pressures and temperatures.

4.6 Experimental Methods

4.6.1 General Considerations

All reactions and manipulations were carried out under an atmosphere of argon using standard Schlenk techniques unless otherwise stated. All reagents were purchased from Sigma-Aldrich, Acros Organics, and Alfa Aesar. Ketimine **4-18** was purchased from Sigma-Aldrich and used as received. High resolution mass spectra (HRMS) ESI and EI for all compounds were obtained on a Qstar XL QqTOF from Applied Biosystems/MDS Sciex. Proton nuclear magnetic resonance (^1H NMR) and ^{13}C nuclear magnetic resonance ($^{13}\text{C}\{^1\text{H}\}$ NMR) spectra for all compounds were recorded with a Bruker AVANCE-400 MHz NMR spectrometer where each sample was referenced to residual solvent peaks where possible. Data collection for the crystal structures were done on a Bruker SMART APEX II X-ray diffractometer.

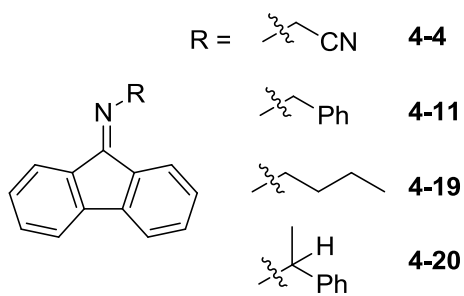
4.6.2 Synthesis of Ketimines



Synthesis of Compound 4-10: Benzophenone (0.5 g, 2.7 mmol) was added to a flame- or oven-dried two neck 100 mL flask that was fitted with a Dean-Stark apparatus and condenser. To this, 30 mL of dry toluene was added, of which 20 mL was used to dissolve benzophenone and 10 mL was used to fill the Dean-Stark apparatus. At room temperature, one equivalent of $\text{BF}_3\cdot\text{OEt}_2$ (0.34 mL, 2.7 mmol) was added dropwise to the solution. The solution colour changed from clear and colourless to a yellow opaque. After the mixture was stirred for 10 min at room temperature, benzylamine (0.45 mL, 4.1 mmol) was added dropwise over a period of 10 min. The resultant solution colour changes from yellow to colourless and a small amount of white precipitate forms. The solution was refluxed overnight at 150 °C, during which time the white precipitate goes into solution. After refluxing overnight the reaction was cooled and the solution was concentrated under reduced pressure leaving behind approximately 10% of the toluene. Water (20 mL) was added to concentrated

toluene layer to remove any remaining boron salt. The aqueous layer is extracted with a 50:50 mixture of ether:hexanes (3 x 20 mL). The organic fractions were collected and dried with MgSO₄. The organic solvents were removed under reduced pressure revealing compound **4-10** as a white solid. NMR data matched that of literature.⁵⁶ Isolated yield 84%. ¹H NMR (400 MHz, CDCl₃) δ 7.73 – 7.65 (m, 2H), 7.52 – 7.43 (m, 5H), 7.42 – 7.28 (m, 5H), 7.28 – 7.15 (m, 2H), 4.61 (s, 2H) ppm.

General Procedure for the Synthesis of Ketimines that have the 9-Fluorenylidene Group



The procedure to synthesize the 9-fluorenylidene containing ketimines was adapted from reported literature.⁵⁷ In a flame- or oven-dried Schlenk 100 mL flask, fluorenone (1.0 g, 5.5 mmol) was dissolved in 20 mL of dry dichloromethane producing a clear yellow coloured solution. To the solution of fluorenone at room temperature, 3.74 equivalents of the corresponding amine were added (NOTE: for **4-4**, aminoacetonitrile HCl was used as the amine, which requires the addition of an equal amount of dry NEt₃ to the amine solution. Hydrogen cyanide was a possible by-product, therefore the synthesis and handling of **4-4** must be done with extreme care). The resultant mixture was then immersed in an ice-bath. To the cooled solution, 0.6 equivalents of TiCl₄ (1.0 M in DCM) was added dropwise over a period of 15 min. The solution colour changed from a clear yellow to a dark orange with white precipitate. Following the addition of TiCl₄, the reaction was left to stir for an additional 20 minutes at 5 °C. The solution was warmed to room temperature and then left to stir for a maximum of 4 h. The solution was then filtered through a pad of Celite[®]. The solids that formed from the reaction were rinsed with dichloromethane (2 x 10 mL). The filtrate and washings were collected and combined and then the organic solvent was removed under reduced pressure. Water (20 mL) was added to the

concentrated residue. The aqueous layer was then extracted with 50:50 mixture of ether:hexanes (3 x 20 mL). The organic layer was collected, treated with Na₂CO₃ and dried with MgSO₄. After removal of the MgSO₄ by filtration, the organic solvents are removed under reduced pressure to isolate the ketimine. The chemical shifts for the ketimines matched those in the literature literature for compounds **4-4**,¹² **4-11**,^{14b} and **4-19**.^{14b} For compound **4-20** its chemical shifts were comparable to those of an analogous compound 2,7-dibromo-9-(phenylethylimino)fluorenone,⁵⁸ where the methine chemical shift would be in the same position.

Compound 4-4: ¹H NMR (400 MHz, CDCl₃) δ 7.87 – 7.75 (m, 1H), 7.73 – 7.61 (m, 2H), 7.60 – 7.39 (m, 3H), 7.38 – 7.21 (m, 2H), 5.02 (s, 2H) ppm. Isolated as a yellow solid in 74% yield.

Compound 4-11: ¹H NMR (400 MHz, CDCl₃) δ 7.99 – 7.90 (m, 2H), 7.72 (d, 1H, *J* = 7.5 Hz), 7.66 – 7.56 (m, 3H), 7.53 – 7.41 (m, 4H), 7.40 – 7.30 (m, 3H) ppm. Isolated as a yellow solid in 82% yield.

Compound 4-19: ¹H NMR (300 MHz, CDCl₃) δ 7.90 (d, 1H, *J* = 10.2 Hz), 7.85 (d, 1H, *J* = 9.8 Hz), 7.69 (d, 1H, *J* = 9.8 Hz), 7.60 (d, 1H, *J* = 9.8 Hz), 4.18 (t, 2H, *J* = 7.2 Hz), 1.96 (p, 2H, *J* = 7.2 Hz), 1.63 (p, 2H, *J* = 7.4 Hz), 1.06 (t, 3H, *J* = 7.4 Hz) ppm. Isolated as an orange oil in 85 % yield.

Compound 4-20: ¹H NMR (300 MHz, CDCl₃) δ 8.01 – 7.91 (m, 2H), 7.74 – 7.66 (m, 2H), 7.65 – 7.57 (m, 2H), 7.56 – 7.23 (m, 8H), 5.81 (q, 1H, *J* = 6.6 Hz), 1.76 (d, 3H, *J* = 6.6 Hz) ppm. Isolated as a yellow oil in 76% yield.

4.6.3 General Procedures for the Carboxylation of Ketimines using Various Bases and CO₂ Under a 50 bar Pressure of CO₂ with DBU or KO^tBu as a Base: In a glove-box under an atmosphere of nitrogen, a solution of ketimine (50 mg) in 1 mL of dry THF was placed in a 31 mL Parr vessel fitted with a glass sleeve. With stirring, two equivalents of DBU or 1.05

equivalents of KO^tBu were added to the solution and left to stir for 10 min at room temperature. The Parr vessel was then purged three times with CO₂ and pressurized to 50 bar. The reaction mixture was left to stir for 24 h at room temperature. ¹H NMR spectra in CDCl₃ were taken for the crude reaction mixtures. Work-up was done in accordance to the literature for the synthesis of β-ketocarboxylic acids.¹

Under an Ambient Pressure of CO₂ with KO^tBu as a Base: In a glove-box under an inert atmosphere of nitrogen, a solution of ketimine (50 mg) in 1 mL of dry THF was placed in a flame- or oven-dried Schlenk flask. With stirring, 1.05 equivalents of KO^tBu were added to the solution and left to stir for 10 min at room temperature, producing a bright coloured solution. The flask was then connected to a Schlenk line that was under an atmosphere of argon where the reaction mixture was stirred overnight at room temperature. CO₂ was bubbled into the solution until there was no further colour change observed and the reaction was left to stir at room temperature for 1 h under an atmosphere of CO₂. The reaction solution was then filtered through a plug of Celite[®] and ¹H NMR spectra were taken of the crude reaction mixtures.

Deprotonation with LDA or *n*-BuLi Followed by Carboxylation Under an Ambient Pressure of CO₂:

Generation of LDA *in situ*: *n*-BuLi (nominally 1.5 M in hexanes and purchased from Sigma-Aldrich) was titrated with *N*-benzylbenzamide to determine the actual concentration.⁵⁹ To a solution of di-isopropylamine (0.07 mL, 0.50 mmol) in THF (0.90 mL) at 0 °C was added *n*-BuLi (1.38 M in hexanes, 0.36 mL, 0.50 mmol) dropwise over 10 min with the internal temperature maintained below 5 °C. Stirring was continued at 0 °C for 10 min.

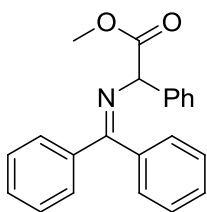
The LDA thus prepared was added dropwise through a cannula to a solution of **4-4** (0.13 g, 0.48 mmol) in THF (2 mL) and, if desired, an additive (0.5 mmol of 18-crown-6 or TMEDA)

was also added at $-78\text{ }^{\circ}\text{C}$ over 10 min with the internal temperature maintained below $-70\text{ }^{\circ}\text{C}$. The reaction mixture was allowed to warm to room temperature and stirred overnight. CO_2 was bubbled into the solution until there was no further colour change observed. The reaction solution was then filtered through a plug of Celite[®] and ^1H NMR spectra were taken of the crude reaction mixtures. Experiments with the other ketimines were performed similarly.

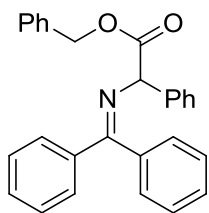
Under an Ambient Pressure of CO_2 with $n\text{-BuLi}$: The procedure was analogous to the method above where LDA was used as a base to deprotonate the ketimine.

From the NMR spectra of the crude reaction mixtures, the isomerization products formed from compounds **4-10** and **4-11** matched reported chemical shifts.^{60,61}

Alkylation of Formed Carboxylates: Alkylation of the unconfirmed carboxylate of **4-10b** was done when KO^tBu , LDA, or $n\text{-BuLi}$ were used as bases for deprotonation under an ambient pressure of CO_2 . Either iodomethane (1 equiv) or benzylbromide (2 equiv) were added at $-20\text{ }^{\circ}\text{C}$ to the reaction mixture following the addition of CO_2 .



Compound 4-10c: EI-HRMS $[\text{M-I}]^+$ calcd for $\text{C}_{22}\text{H}_{19}\text{NO}_2$: 329.1416, found 329.1409.



Compound 4-10d: ESI-HRMS $[\text{M+H}]^+$ calcd for $\text{C}_{28}\text{H}_{24}\text{NO}_2$: 406.1807, found 406.1800.

4.6.4 Attempted Amidation of Benzoylactic Acid

Procedure used with MIBA as an Amidation Catalyst: The procedure used towards the amidation of benzoylactic acid using MIBA as a catalyst was adapted from literature.²⁶ MIBA was synthesized according to the literature procedure.^{26c} Benzoylactic acid was synthesized according literature.¹

In a flame- or oven-dried Schlenk flask 10 mL, benzoylactic acid (0.030 g, 0.18 mmol, 1.1 equiv), MIBA (5 mg, 0.02 mmol, 10 mol%), and activated 4Å molecular sieves (0.30 g) were added. Dichloromethane (2 mL) was added and the mixture was stirred for 10 min at room temperature. To the mixture, benzylamine (0.018 mL, 0.016 mmol, 1 equiv) was added. A ¹H NMR spectrum of the crude reaction mixture was taken.

Procedure used with ZrCl₄ as an Amidation Catalyst: The procedure used towards the amidation of benzoylactic acid using ZrCl₄ as a catalyst was adapted from literature.³⁹

Benzoylactic acid (0.03 g, 0.18 mmol, 1 equiv), benzylamine (0.30 mL, 0.22 mmol, 1.2 equiv), ZrCl₄ (6 mg, 0.018 mmol, 10 mol%), activated 4Å molecular sieves (0.150 g), in THF (0.4 M) were placed in a sealed tube under a nitrogen atmosphere. The resultant mixture was stirred overnight at 70 °C. After the reaction was heated overnight, the resultant solution was filtered through a plug of silica using EtOAc/NEt₃ (200:1) as an eluent. A ¹H NMR spectrum in CDCl₃ of the crude reaction mixture, with formation of the doublet at 4.48 ppm attributed to the methylene α to the nitrogen atom of the product, *N*-benzyl-3-oxo-3-phenyl-propionamide.⁶²

4.6.5 Formation of Dialkylureas Using the Amidation Catalysts MIBA and ZrCl₄

Under an Ambient Pressure of CO₂: In a flame- or oven-dried Schlenk flask 25 mL, dry benzylamine (0.050 mL, 0.46 mmol, 1 equiv), catalyst (0.046 mmol, 10 mol%), and activated 4Å molecular sieves (0.25 g) were added. The mixture was either neat or in dry solvent (1 mL, CH₂Cl₂ for MIBA or THF for ZrCl₄) and was stirred for 10 min at room temperature. CO₂ was

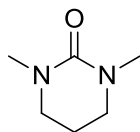
bubbled into the mixture for 10 min and the reaction was left to stir at room temperature or at 50 °C for 5 – 12 h. The organic solvents were removed under reduced pressure and ¹H NMR spectra were taken of the crude reaction mixtures in CDCl₃ where the presence of the methylene peak of dibenzylurea at 4.41 ppm was monitored.⁶³ Experiments with other primary amines and with piperidine were performed similarly.

Under a Pressure of CO₂: The procedure was analogous to the one above, though the reaction was placed into a 31 mL Parr vessel and then purged three times with CO₂ and pressurized to either 50 or 70 bar. For reactions that were done at 70, 100, and 180 °C, the vessel was heated before pressurization with CO₂. Experiments with other primary amines and with piperidine were performed similarly.

4.6.6 Formation of Cyclic Urea with *N,N'*-Dimethyl-1,3-propanediamine Using MIBA or ZrCl₄

Under an a Ambient Pressure of CO₂: In a flame- or oven-dried Schlenk flask 25 mL, dry *N,N'*-dimethylpropanediamine (0.60 mL, 4.9 mmol), catalyst (0.49 mmol, 10 mol%), and activated 4Å molecular sieves (1 g) were added. The mixture was either neat or in dry solvent (2 mL, CH₂Cl₂ for MIBA or THF for ZrCl₄) was added and the mixture was stirred for 10 min at room temperature. CO₂ was bubbled into the mixture for 10 min and the reaction was left to stir at room temperature or at 50 °C for 24 h. ¹H NMR spectra were taken of the crude reaction mixtures in CDCl₃ to confirm product formation.^{53d}

Under an Elevated Pressure of CO₂: The procedure was analogous to the one above, though the reaction was placed into a 31 mL Parr vessel and then purged three times with CO₂ and pressurized to either 35 or 50 bar. For reactions that were done at 80 and 100 °C, the vessel was heated before pressurization with CO₂. ¹H NMR spectra were taken of the crude reaction mixtures in CDCl₃ to confirm product formation. The ¹H NMR chemical shifts matched those in literature.^{53d}



1,3-Dimethyl-3,4,5,6-tetrahydropyrimidin-2(1H)-one: EI-HRMS [M-I]⁺ calcd for C₆H₁₂N₂O: 128.0950, found 128.0950.

4.7 References

- 1) Flowers, B. J.; Gautreau-Service, R.; Jessop, P. G. *Adv. Synth. Catal.*, **2008**, 350(180), 2947 – 2958.
- 2) Thaisrivongs, S.; Schostarez, H.J.; Pals, D.T.; Turner, J. *Med. Chem.* **1987**, 30, 1837 – 1842.
- 3) Schostarez, H.J. *J. Org. Chem.* **1988**, 53, 3628 – 3631.
- 4) Capozzi, G.; Roelens, S.; Talami, S. *J. Org. Chem.* **1993**, 58, 7932 – 7936.
- 5) Oertle, K.; Beyeler, H.; Duthaler, R.O.; Lottenbach, W.; Riediker, M.; Steiner, E. *Helv. Chim. Acta* **1990**, 73, 353.
- 6) Abdel-Rahman, H. M.; Hussein, M. A.; *Arch. Pharm.* **2006**, 339, 378 – 387.
- 7) Sisido, K.; Kumazawa, K.; Nozaki, H. *J. Am. Chem. Soc.* **1960**, 82, 125 – 129.
- 8) Abdel-Rahman, H. M.; Hussein, M. A.; *Arch. Pharm.* **2006**, 339, 378 – 387.
- 9) Pérez, E. R.; Santos, R. H. A.; Gambardella, M. T. P.; de Macedo, L. G. M.; Rodrigues-Filho, U. P.; Launay, J.-C.; Franco, D. W. *J. Org. Chem.*, **2004**, 69, 8005 - 8011.
- 10) Raab, V.; Kipke, J.; Gschwind, R.M.; Sundermeyer, J. *Chem. Eur. J.* **2002**, 8(7), 1682.
- 11) Akalay, D.; Drner, G.; Bats, J. W.; Bolte, M.; Gbel, M. W. *J. Org. Chem.* **2007**, 72(15), 5618.
- 12) Kobayashi, S.; Chen, Y.-J.; Matsumoto, M.; Yamashita, Y. *Tetrahedron*, **2012**, 68, 7558 – 7563.
- 13) a) Kobayashi, S.; Matsubara, R. *Chem.-Eur. J.* **2009**, 15, 10694 - 10700. b) Marrec, O.; Christophe, C.; Billard, T.; Langlois, B.; Vors, J.-P.; Pazenok, S.; *Adv. Synth. Catal.* **2010**, 352, 2825 – 2830. c) Robles-Machin, R.; Alonso, I.; Adrio, J.; Carretero, J. C. *Chem.-Eur. J.* **2010**, 16, 5286 – 5291.
- 14) a) Kobayashi, S.; Yazaki, R.; Seki, K.; Yamashita, Y. *Angew. Chem. Int. Ed.* **2008**, 47, 5613 - 5615. b) Chen, Y.-J.; Seki, K.; Yamashita, Y.; Kobayashi, S. *J. Am. Chem. Soc.* **2010**, 132, 3244 – 3245.
- 15) Taft, R. W.; Bordwell, F. G. *Acc.Chem. Res.* **1988**, 21, 463 – 469.
- 16) Strecker, A. *Justus Liebigs Ann. Chem.* **1850**, 75, 27-45.

- 17) Zeund, S. J.; Coughlin, M. P.; Lalonde, M. P.; Jacobsen, E. N. *Nature*, **2009**, *461*, 968 – 971.
- 18) Sato, Y.; Sugawara, M.; Chen, J.; Mita, T. *Angew. Chem. Int. Ed.* **2011**, *50*, 1393 – 1396.
- 19) Cainelli, G.; Giacomini, D.; Trerè, A.; Boyd, P. P. *J. Org. Chem.* **1996**, *61*, 5134 – 5139.
- 20) Dryanska, V.; Popandova, K.; Ivanov, C. *Synth. Commun.* **1987**, *17*, 211 – 217.
- 21) Burger, E. C.; Tunge, J. A. *J. Am. Chem. Soc.* **2006**, *128*, 10002 – 10003.
- 22) Hampe, D.; Günther, W.; Görls, H.; Anders, E. *Eur. J. Org. Chem.* **2004**, 4357 – 4372.
- 23) Montalbetti, C. A. G. N.; Falque, V. *Tetrahedron* **2005**, *61*, 10827 – 10852.
- 24) Carey, J. S.; Laffan, D.; Thomson, C.; Williams, M. T. *Org. Biomol. Chem.* **2006**, *4*, 2337 – 2347.
- 25) Jursic, B. S.; Zdravkovski, Z. *Synth. Commun.* **1993**, *23*, 2761 – 2770.
- 26) a) Hall, D. G.; Marion, O.; Al-Zoubi, R. M. *Angew. Chem.* **2008**, *120*, 2918 – 2921. b) Gernigon, N.; Al-Zoubi, R. M.; Hall, D. G. *J. Org. Chem.* **2012**, *77*, 8386 – 8400. c) Al-Zoubi, R. M.; Hall, D. G. *Org. Lett.*, **2010**, *12*, 2480 – 2483.
- 27) Ishihara, K.; Ohara, S.; Yamamoto, H. *J. Org. Chem.* **1996**, *61*, 4196 – 4197.
- 28) Maki, T.; Ishihara, K.; Yamamoto, H. *Tetrahedron* **2007**, *63*, 8645 – 8657.
- 29) Arnold, K.; Batsanov, A. S.; Davies, B.; Whiting, A. *Green Chem.* **2008**, *10*, 124 – 134.
- 30) Arnold, K.; Davies, B.; Héroult, D.; Whiting, A. *Angew. Chem., Int. Ed.* **2008**, *47*, 2673 – 2676.
- 31) Tang, P.; Krause, H.; Furstner, A. *Org. Synth.* **2005**, *81*, 262–267.
- 32) Mylavarapu, R. K.; Kondaiah, G. C. M. K.; Kolla, N.; Veeramalla, R.; Koilkonda, P.; Bhattacharya, A.; Bandichhor, R. *Org. Process Dev.* **2007**, *11*, 1065–1068.
- 33) Levonis, S. M.; Bornaghi, L. F.; Houston, T. A. *Aust. J. Chem.* **2007**, *60*, 821–823.
- 34) Starkov, P.; Sheppard, T. D. *Org. Biomol. Chem.* **2011**, *9*, 1320–1323.
- 35) Marcelli, T. *Angew. Chem. Int. Ed.* **2010**, *49*, 6840 – 6843.
- 36) Trautwein, A. W.; Sussmuth, R. D.; Jung, G. *Bioorg. Med. Chem. Lett.* **1998**, *8*, 2381 – 2384.
- 37) Ketcha, D. M.; Wilson, L. J.; Portlock, D. E. *Tetrahedron Lett.* **2000**, *41*, 6253 – 6257.
- 38) Abou-Elenien, G. M.; El-Anadouli, B. E.; Baraka, R. M. *J. Chem. Soc., Perkin Trans. 2* **1991**, 1377 – 1380.
- 39) a) Lundberg, H.; Tinnis, F.; Adolfsson, H. *Chem. Eur. J.* **2012**, *18*, 3822 – 3826 b) Tinnis, F.; Lundberg, H.; Adolfsson, H. *Adv. Synth. Catal.* **2012**, *354*, 2531 – 2536.
- 40) a) Marcantonatos, M.; *Inorg. Chim. Acta* **1976**, *19*, 109 – 115. b) Marcantonatos, M.; *Inorg. Chim. Acta* **1977**, *21*, 65 – 74.

- 41) Lu, Z.; Wang, Y.; Liu, J.; Lin, Y.-J.; Li, Z. H.; Wang, H. *Organomet.* article ASAP, publication date: September 12, 2013. DOI: 10.1021/om4007246
- 42) Ion, A.; Parvulescu, V.; Jacobs, P.; De Vos, D. *Green Chem.* **2007**, *9*, 158.
- 43) Jiang, T.; Ma, X.; Zhou, Y.; Liang, S.; Zhang, J.; Han, B. *Green Chem.* **2008**, *10*, 465 – 469.
- 44) Wu, C.; Cheng, H.; Liu, R.; Wang, Q.; Hao, Y.; Yu, Y.; Zhao, F. *Green Chem.* **2010**, *12*, 1811 – 1816.
- 45) Kawanami, H.; Ogawa, K.; Hioki, J.; Nakai, M. Jpn. Kokai Tokkyo Koho, 2012111711, 14 Jun 2012.
- 46) Nomura, R.; Hasegawa, Y.; Ishimoto, M.; Toyosaki, T.; Matsuda, H. *J. Org. Chem.* **1992**, *57*, 7339 – 7342.
- 47) Farlow, M. W.; Adkins, H. *J. Am. Chem. Soc.* **1935**, *57*, 2222 – 2223.
- 48) Tai, C.-C.; Huck, M. J.; McKoon, E. P.; Woo, T.; Jessop, P. G. *J. Org. Chem.* **2002**, *67*, 9070 – 9072.
- 49) Paz, J.; Pérez-Balado, C.; Iglesias, B.; Muñoz, L. *J. Org. Chem.* **2010**, *75*, 3037 – 3046.
- 50) Anderson, J. C.; Bou Moreno, R. *Org. Biomol. Chem.* **2012**, *10*, 1334 – 1338.
- 51) Porwanski, S.; Menuel, S.; Marsura, X.; Marsura, A. *Tetrahedron Lett.* **2004**, *45*, 5027 – 5029.
- 52) Morimoto, Y.; Fujiwara, Y.; Taniguchi, H.; Hori, Y.; Nagano, Y. *Tetrahedron Lett.* **1986**, *27*, 1809 – 1810.
- 53) a) McCusker, J. E.; Grasso, C. A.; Main, A. D.; McElwee – White, L. *Org. Lett.* **1999**, *1*, 961 – 964. b) Qian, F.; McCusker, J. E.; Zhang, Y.; Main, A. D.; Chlebowski, M.; Kokka, M.; McElwee – White, L. *J. Org. Chem.* **2002**, *67*, 4086 – 4092. c) Mizuno, T.; Nakai, T.; Mihara, M. *Heteroatom Chem.* **2009**, *20*, 64 – 68. d) Mizuno, T.; Nakai, T.; Mihara, M. *Synthesis* **2010**, *24*, 4251 – 4255.
- 54) Tamura, M.; Noro, K.; Honda, M.; Nakagawa, Y.; Tomishige, K. *Green Chem.* **2013**, *15*, 1567 – 1577.
- 55) Hounjet, L. J.; Caputo, C. B.; Stephan, D. W. *Angew. Chem. Int. Ed.* **2012**, *51*, 4714 – 4717.
- 56) O'Donnell, M.J.; Bennett, W. D.; Bruder, W. A.; Jacobsen, W. N.; Knuth, K.; LeClef, B.; Polt, R. L.; Bordwell, F. G.; Mrozack, S. R.; Cripe, T. A. *J. Am. Chem. Soc.* **1988**, *110*, 8520 – 8525.
- 57) Weingarten, H.; Chupp, J. P.; White, W. A. *J. Org. Chem.* **1967**, *32*, 3246 – 3249.
- 58) Asai, K.; Konishi, G.-I.; Sumi, K.; Kawauchi, S. *Polym. Chem.* **2010**, *1*, 321 – 325.

- 59) Burchat, A. F.; Chong, J. M.; Nielson, N. *J. Organomet. Chem.* **1997**, *542*, 281 – 283.
- 60) Eisenberger, P.; Bailey, A.; Crudden, C. *J. Am. Chem. Soc.* **2012**, *134*, 17384 – 17387.
- 61) Zhang, Y.; Lu, Z.; Desai, A.; Wulff, W. D. *Org. Lett.* **2008**, *10*, 5429 – 5432.
- 62) Neo, A. G.; Delgado, J.; Polo, C.; Marcaccini, S.; Marcos, C. F. *Tetrahedron Lett.* **2005**, *46*, 23 – 26.
- 63) Liu, P.; Wang, Z; Hu, X. *Eur. J. Org. Chem.* **2012**, 1994 – 2000.

Chapter 5

Conclusions and Future Work

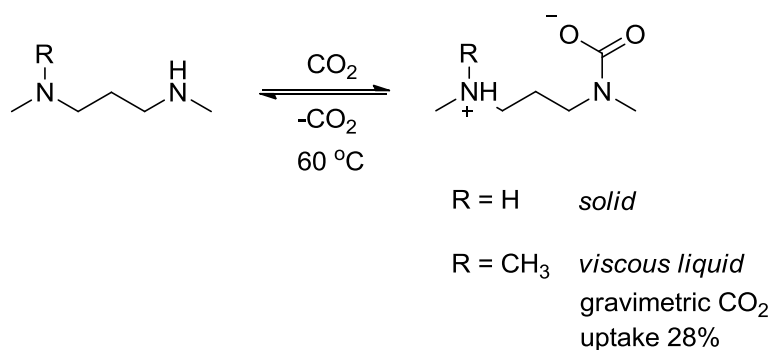
5.1 The Search for Zwitterionic SPS

Various diamines were tested as zwitterionic SPSs and CO₂ adsorbents, looking for improvements in terms of polarity swing and CO₂ uptake. These diamines differed from the amine and base/alcohol solvent systems investigated previously as the diamine forms a zwitterion upon the addition of CO₂ even in the presence of water. Previous base/alcohol systems would form the corresponding bicarbonate salt in the presence of water.

It was found that CO₂ reactivity was not affected by differing substitution, tether length and rigidity of the secondary diamines. The bubbling of CO₂ into the liquid diamines produced solid zwitterionic salts, which were therefore not viable as liquid SPS. The molecular structure of the carbamate formed from *N,N'*-dimethyl-1,3-propanediamine showed that a zwitterionic species is formed even in the presence of water. One nitrogen atom acts as the CO₂ capture site to produce a carbamate anionic centre and the second nitrogen atom is protonated. The presence of water did not prevent the formation of carbamate. With other N-compounds such as DBU, the formation of bicarbonate salt is readily formed in the presence of water. It was proposed that the hydrogen-bonding network afforded by the water molecules promoted the formation of a solid zwitterionic structure with the diamine, although even with completely dry conditions a solid zwitterionic salt still formed upon the addition of CO₂.

It was a diamine that contained one secondary nitrogen atom and one tertiary nitrogen atom that produced a liquid zwitterionic SPS after CO₂ uptake. The polarity of the zwitterionic SPS was similar to that of THF and the polarity swing was comparable to previous amine SPS. As a result, the moderate polarity range afforded by the liquid zwitterion is not an improvement from previously reported SPS systems.

The liquid zwitterionic species formed from the diamine may not be an improved SPS, though it was a very efficient CO₂ capture agent. The gravimetric uptake of CO₂ was 28%, nearly double the amount of other reported SPS CO₂ capturing agents. The capture of CO₂ was performed under an ambient pressure, in contrast to the alkanolamines discussed in Chapter 2 that required pressure (0.7 – 3.4 MPa, for DMEA) for CO₂ uptake. The temperature of 60 °C to regenerate the diamine was lower than what was required to release CO₂ from previous alkylcarbonate and carbamate salts.¹ It was postulated that combining a secondary and tertiary amine in the same molecule was what determines the ease of capture and release of CO₂.



Scheme 5.1. Formation of zwitterionic species with CO₂ with a secondary diamine (R = H) and a diamine containing both secondary and tertiary nitrogen centres (R = CH₃).

5.2 Unexpected Reactivity of CS₂ with N-Containing Compounds

CS₂ was valence isoelectronic to CO₂. In some cases, the reactivity of CS₂ with N-containing compounds mirrors that of CO₂, for example its addition to carbenes forming stable zwitterionic adducts,² its unusual reactivity was not the case with various amidines and guanidines has no parallel with known CO₂ chemistry.

The reaction of CS₂ with amidines and guanidines lead to the formation of new C-C and C-S bonds, and novel sulfur-containing compounds. For example, when CS₂ was reacted with a

hindered cyclic amidine, the cyclic trithioanhydride was formed. Looking at the structure of the hindered amidines in this study, the formation of the cyclic trithioanhydride was dependent on the acidic site that was *beta* to the nitrogen centre. The protons at the *beta* site are less labile than those found in TBD, but can be easily deprotonated. The formation of a zwitterionic DBU-CO₂ has been reported but not isolated or definitively visualized through single crystal X-ray crystallography. In DBU, the acidic site *beta* to the imino nitrogen could have an important role in regards to the reactivity of DBU with CO₂. As with TBD, perhaps DBU can act as a general base and H-bond donor.

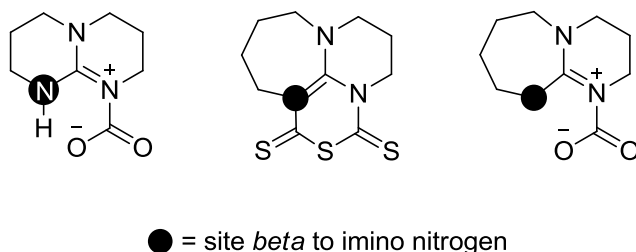


Figure 5.1. From left: TBD-CO₂ adduct, cyclic trithioanhydride of DBU, proposed DBU-CO₂ adduct.

In contrast, the cyclic trithioanhydride did not form when the amidine or guanidine had either an amino or imino N-H. 2-Ethyl-2-imidazoline was a cyclic amidine with an amino N-H and flexible ethyl chain. The major product from the reaction of the less hindered cyclic amidine with CS₂ was an unknown yellow solid that precipitated out of solution; the proposed structure was a thiocarbamate salt. A cyclic trithioanhydride was isolated from this reaction though as the minor product. Reaction of CS₂ with acyclic amidines lead to cleavage of a C=N bond forming a thioamide and isothiocyanate. When the imino nitrogen was not alkylated, like in a *N,N,N',N'*-tetraalkylated guanidine, a dimerized structure was formed from CS₂ and exposure to dichloromethane.

Unexpected reactivity with CS₂ and N-compounds was demonstrated, although parallel reactivity might be found with CO₂. Future work would include looking at the reactivity of CO₂ with the same N-containing compounds, at higher temperatures, to search for reactivity analogous to that of CS₂ at room temperature. CS₂ and CO₂ might also have parallel reactivity with organic compounds other than the N-containing ones within this research.

5.3 CO₂ as a Carbonyl Source for N-Containing Compounds

It is evident that DBU and CO₂ do interact in ways that make DBU a useful base for the fixation of CO₂ by organic transformations. The method for the synthesis of β-ketocarboxylic acids developed by our group used DBU to afford carboxylation of a ketone with CO₂.⁵ Three areas of investigation stemmed from the above method with special attention to the partnership between DBU and CO₂: 1) implementation of the above method for the carboxylation of ketimines towards the synthesis of α-amino acids, 2) amidation of benzoylacetate, a β-ketocarboxylic acid made from the above method, and 3) synthesis of tetraalkylureas.

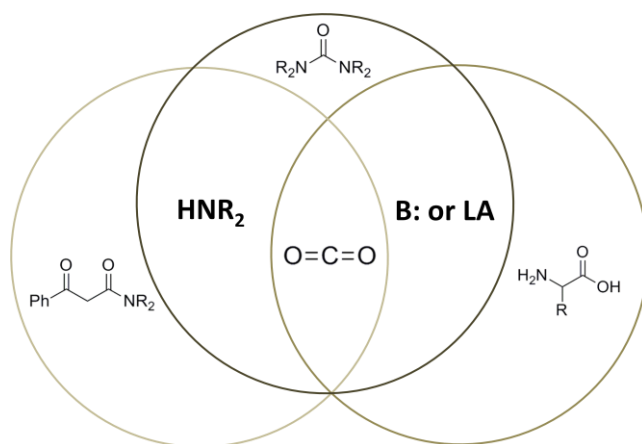


Figure 5.2. Illustration correlating CO₂ as a carbonyl source to the three areas of research: 1) synthesis of α-amino acids, 2) amidation of benzoylacetate, and 3) synthesis of ureas.

The ketimines studied were within the pK_a range of the ketones that were carboxylated with DBU and CO₂. The 9-fluorenylidene or diphenylmethylene imine protecting group can be

removed with acidic conditions, acidic conditions that can also protonate a formed carboxylate. Various ketimines were deprotonated with a number of bases that formed brightly-coloured solutions, indicative of carbanions being formed. However, following the addition of CO₂ and the reaction work up, ¹H NMR spectra for nearly all the crude reaction mixtures showed no formation of carboxylated product. It was postulated that the reason for the lack of product isolated was the low stability of the free acid formed due to the resonance along the α-carbons.

Interesting reactivity was observed from one ketimine, *N*-(diphenylmethylidene)-1-phenylmethylamine; after reaction with DBU and CO₂ (50 bar) there was evidence for the possible formation of carboxylate as well as isomerized product. The ¹H NMR spectrum of the crude reaction mixture showed a small peak at 10 ppm, within range of a carboxylic acid signal and in the ¹³C NMR spectrum, a peak at 196 ppm that could correspond to a carbonyl peak. Alkylation of the formed carboxylate was done by the addition of benzylbromide and iodomethane; where HRMS confirmed the formation of these esterified products. The isomerized product of *N*-(diphenylmethylidene)-1-phenylmethylamine was also detected in the ¹H and ¹³C NMR spectra which was interesting since the product was simply made with DBU and CO₂. Isomerization was also detected with, the other ketimine that had a benzyl-substituted imine, though protected with a 9-fluorenylidene group.

Amidation of benzoylactic acid did not occur in the presence of MIBA or ZrCl₄, two Lewis acid catalysts that were successfully used for the amidation of a variety of carboxylic acids. According to the ¹H NMR spectrum that was taken after the reaction of benzoylactic acid with either MIBA or ZrCl₄ and amine, there were no peaks that corresponded to the amide product. The methylene signals of benzoylactic acid shifted downfield, though this might be due to either the boron of MIBA or the zirconium of ZrCl₄ chelating to both carbonyl groups in benzoylactic acid. With the addition of amine, decarboxylation of benzoylactic acid occurred giving acetophenone.

Keto/enol tautomerization influences the decarboxylation of benzoylactic acid. The rate at which benzoylactic acid decarboxylates varies in different solvents.⁵ Solvents other than THF and CH₂Cl₂ might afford amidation of benzoylactic acid and slow decarboxylation.

Isolation of the boron species that is formed with benzoylactic acid, with or without the presence of amine, would give further insight into the reactivity of the Lewis acids as amidation catalysts. Investigation of the formed carbamate in the presence of MIBA might provide further insight into its catalytic reactivity. In addition, using an excess amount of Lewis acid catalyst might afford the amidation of β -ketocarboxylic acid and negate the possible interaction of either the boron or zirconium with the two carbonyl groups.

With the knowledge that MIBA and ZrCl₄ were efficient catalysts for amidation of carboxylic acids, the Lewis acid catalysts were investigated for the synthesis of tetraalkylureas, starting with a carbamate formed from an amine and CO₂. A preliminary investigation was done with the Lewis acid catalysts for the synthesis of dialkylureas. Only a small amount of dibenzylurea formed from benzylamine in the absence of catalyst and solvent with a temperature of 180 °C and CO₂ pressure of 50 bar, in contrast to what was reported with the same reaction conditions that stated an isolated yield of 99%.⁸ It was found that the addition of 10 mol% ZrCl₄ to the above reaction conditions improved the amount of dibenzylurea produced. Seemingly, the stable carbamate salt from benzylamine and CO₂ inhibited reactivity with the Lewis acid catalysts even with high temperatures and pressures of CO₂.

In relation to what was discussed in Chapter Two, a diamine produces a zwitterionic species with the addition of CO₂. *N,N'*-dimethyl-1,3-propanediamine captures one equivalent of CO₂ even in the presence of water. Having an intramolecular protonated amine, as opposed to an intermolecular protonated amine might change the reaction dynamics. *N,N'*-Dimethyl-1,3-propanediamine was used as a prospective diamine for the synthesis of cyclic urea, a tetraalkylurea. It was found that at ambient or above ambient pressures of CO₂ in the presence of

either MIBA or $ZrCl_4$, that the formation of cyclic urea was detected in the 1H NMR spectrum and in the HRMS spectrum. Concurrent research by Tomishige and co-workers showed cyclic ureas are formed from diamines and pressures of CO_2 ,⁹ while to the best of our knowledge, the formation of a tetraalkylated urea starting from *N,N'*-dimethyl-1,3-propanediamine at ambient conditions and in the presence of a Lewis acid catalyst has yet to be reported, especially with a moisture and air-stable catalyst such as MIBA.

An extensive study to elucidate the optimal CO_2 pressure, solvent, concentration of catalyst, temperature and reaction time might afford higher yields of cyclic urea. In particular, the amidation reactions with MIBA required that the catalyst stir with the carboxylic acid first. Perhaps changing the sequence in which reagents are added might affect the product outcome.

5.4 Closing Remarks

Conventionally, N-compounds are used to activate CO_2 . The methods described within this research sought avenues for new reactivity using such compounds. N-compounds that were studied exhibited unexpected reactivity with CO_2 and CS_2 , and when partnered with CO_2 in the presence of a boronic acid catalyst, a tetraalkylated urea was afforded. It was also evident that the design and development of other N-compounds was needed in order to effectively react with CO_2 .

The quest for efficient CO_2 activation manifests itself in all many areas of scientific research. Clues to achieve this goal can be found in areas that are outside the conventional methods used to capture and activate CO_2 . It has been further demonstrated that CO_2 activation can be achieved in a metal-free environment. This is especially important with regards to the impending shortage of precious metal reservoirs on Earth and the social issues that can develop from such a shortage. With perserverance, a keen sense of observation, and the ability to adapt, researchers will find innovative methods to combat the rising output of CO_2 .

5.5 References

- 1) a) Heldebrant, D. J.; Yonker, C. R.; Jessop, P. G.; Phan, L. *Energy Environ. Sci.* **2008**, *1*, 487 – 493. b) Jessop, P. G.; Heldebrant, D. J.; Li, X. W.; Lu, J.; Hallet, J. P.; Jones, R. S.; Pollet, P. Thomas, C. A.; Eckert, C. A.; Liotta, C. L. *Abstr. Pap. Am. Chem. Soc.* **2005**, 229, U971. c) Phan, L.; Chiu, D.; Heldebrant, D. J.; Huttenhower, H.; John, E.; Li, X. W.; Pollet, P.; Wang, R. Y.; Eckert, C. A.; Liotta, C. L.; Jessop, P. G. *Ind. Eng. Chem. Res.* **2008**, *47*, 539 – 545.
- 2) Delaude, L.; Demonceau, A.; Wouters, J. *Eur. J. Inorg. Chem.* **2009**, *13*, 1882 – 1891.
- 3) Keisewetter, M. K.; Scholten, M. D.; Kirn, N.; Weber, R. L.; Hedrick, J. L.; Waymouth, R. M. *J. Org. Chem.* **2009**, *74*, 9490 – 9496.
- 4) Sabot, C.; Kumar, K. A.; Antheaume, C.; Mioskowski, C. *J. Org. Chem.* **2007**, *72*, 5001 – 5004.
- 5) Flowers, B. J.; Gautreau-Service, R.; Jessop, P. G. *Adv. Synth. Catal.*, **2008**, *350*, 2947 – 2958.
- 6) Dryanska, V.; Popandova, K.; Ivanov, C. *Synth. Commun.* **1987**, *17*, 211 – 217.
- 7) Burger, E. C.; Tunge, J. A. *J. Am. Chem. Soc.* **2006**, *128*, 10002 – 10003.
- 8) Kawanami, H.; Ogawa, K.; Hioki, J.; Nakai, M. Jpn. Kokai Tokkyo Koho, 2012111711, 14 Jun 2012.
- 9) Tamura, m.; Noro, K.; Honda, M.; Nakagawa, Y.; Tomishige, K. *Green Chem.* **2013**, *15*, 1567 – 1577.

Appendix A

X-ray Crystallography Data

A.1. Zwitterionic Carbamate Salt 2-11b

Figure A.1. Molecular structure of 2-11b.

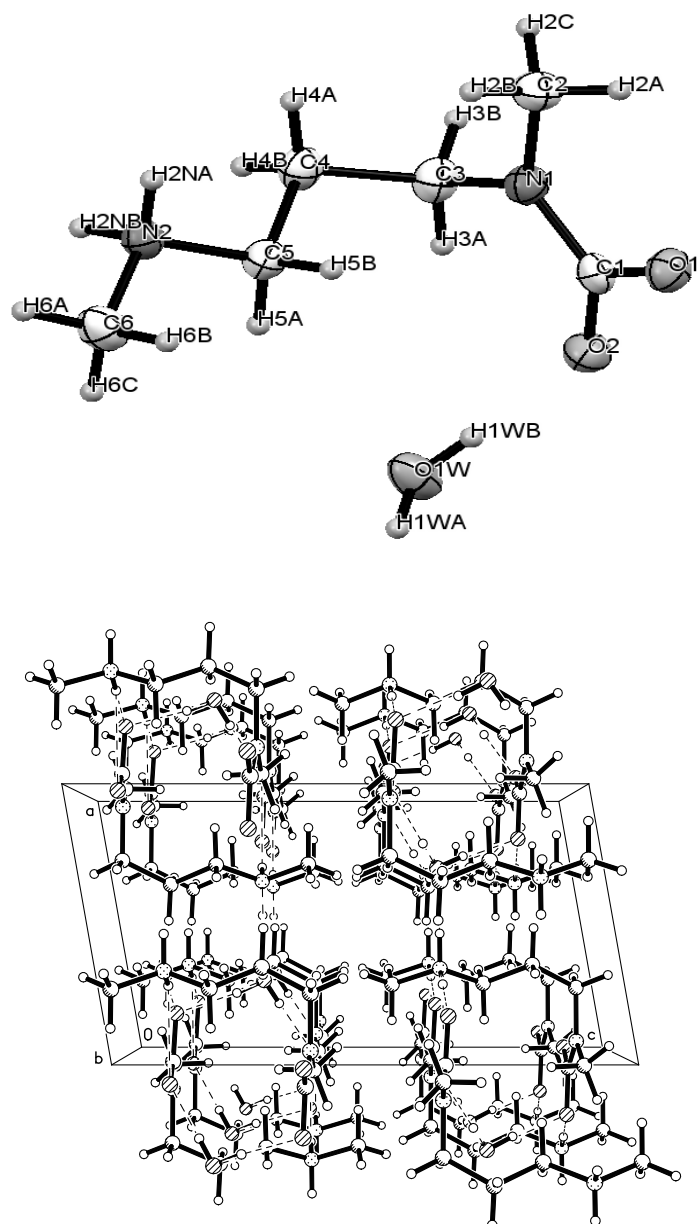


Table A.2. Crystal data and structure refinement for **2-11b**

Identification code	pj18	
Empirical formula	C ₆ H ₁₆ N ₂ O ₃	
Formula weight	164.21	
Temperature	180(2) K	
Wavelength	0.71073 Å	
Crystal system	Monoclinic	
Space group	P2(1)/c	
Unit cell dimensions	a = 7.7180(11) Å	α = 90°.
	b = 8.0326(11) Å	β = 100.043(2)°.
	c = 14.231(2) Å	γ = 90°.
Volume	868.8(2) Å ³	
Z	4	
Density (calculated)	1.255 Mg/m ³	
Absorption coefficient	0.099 mm ⁻¹	
F(000)	360	
Crystal size	0.20 x 0.10 x 0.06 mm ³	
Theta range for data collection	2.68 to 26.00°.	
Index ranges	-9 ≤ h ≤ 9, -9 ≤ k ≤ 9, -17 ≤ l ≤ 17	
Reflections collected	8347	
Independent reflections	1703 [R(int) = 0.0258]	
Completeness to theta = 26.00°	99.9 %	
Absorption correction	Multi-scan	
Max. and min. transmission	0.9941 and 0.9804	
Refinement method	Full-matrix least-squares on F ²	
Data / restraints / parameters	1703 / 0 / 118	
Goodness-of-fit on F ²	1.030	
Final R indices [I > 2σ(I)]	R1 = 0.0304, wR2 = 0.0791	
R indices (all data)	R1 = 0.0359, wR2 = 0.0829	
Largest diff. peak and hole	0.154 and -0.156 e.Å ⁻³	

Table A.3. Atomic coordinates ($\times 10^4$) and equivalent isotropic displacement parameters ($\text{\AA}^2 \times 10^3$) for **2-11b**. $U(\text{eq})$ is defined as one third of the trace of the orthogonalized U^{ij} tensor.

	x	y	z	$U(\text{eq})$
O(1)	8102(1)	-1334(1)	8533(1)	28(1)
O(2)	10446(1)	-3021(1)	8788(1)	30(1)
O(1W)	13002(1)	-4753(1)	8172(1)	35(1)
N(1)	10829(1)	-211(1)	8906(1)	26(1)
N(2)	13442(1)	650(1)	6538(1)	25(1)
C(1)	9772(1)	-1593(1)	8734(1)	23(1)
C(2)	10085(2)	1456(2)	8879(1)	31(1)
C(3)	12741(2)	-327(2)	9088(1)	29(1)
C(4)	13573(2)	481(2)	8294(1)	28(1)
C(5)	12896(2)	-319(1)	7332(1)	27(1)
C(6)	12865(2)	-142(2)	5593(1)	33(1)

Table A.4. Bond lengths [\AA] for **2-11b**

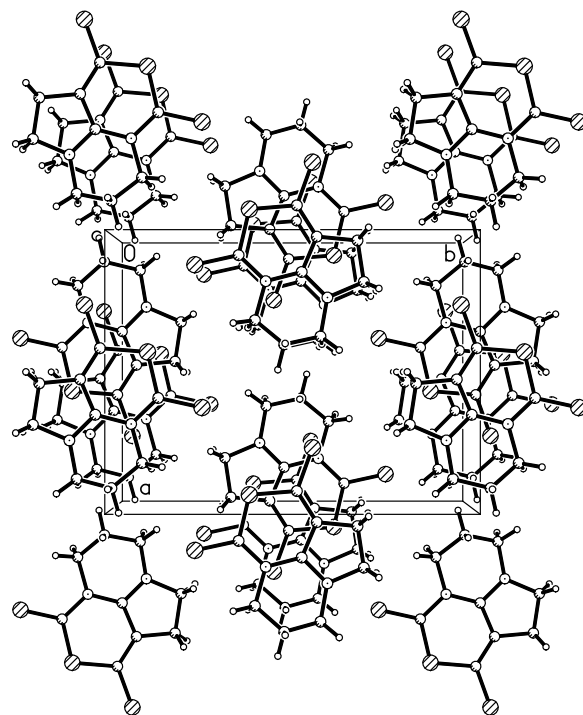
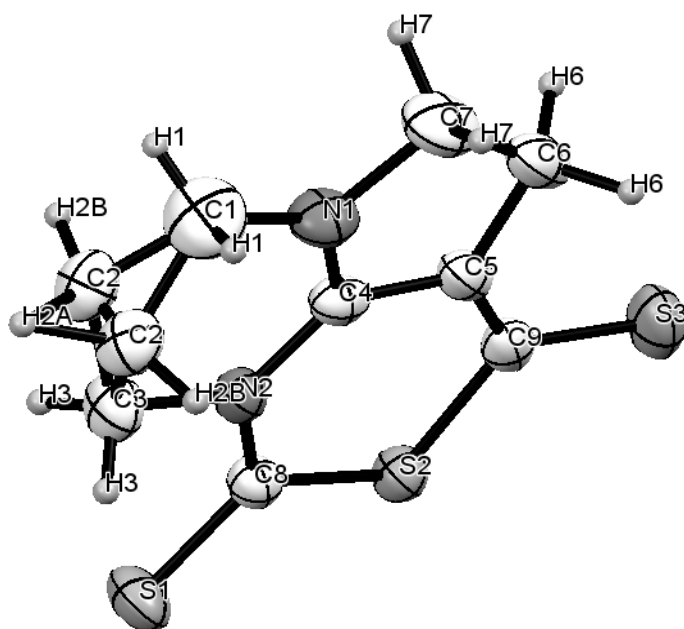
O(1)-C(1)	1.2877(13)	C(2)-H(2C)	0.9800
O(2)-C(1)	1.2565(14)	C(3)-C(4)	1.5369(16)
O(1W)-H(1WA)	0.873(17)	C(3)-H(3A)	0.9900
O(1W)-H(1WB)	0.871(19)	C(3)-H(3B)	0.9900
N(1)-C(1)	1.3738(15)	C(4)-C(5)	1.5199(16)
N(1)-C(2)	1.4551(15)	C(4)-H(4A)	0.9900
N(1)-C(3)	1.4563(15)	C(4)-H(4B)	0.9900
N(2)-C(6)	1.4844(15)	C(5)-H(5A)	0.9900
N(2)-C(5)	1.4926(14)	C(5)-H(5B)	0.9900
N(2)-H(2NA)	0.939(15)	C(6)-H(6A)	0.9800
N(2)-H(2NB)	0.941(15)	C(6)-H(6B)	0.9800
C(2)-H(2A)	0.9800	C(6)-H(6C)	0.9800
C(2)-H(2B)	0.9800		

Table A.5. Bond angles [°] for **2-11b**

H(1WA)-O(1W)-H(1WB)	108.0(15)	N(1)-C(3)-H(3B)	109.1
C(1)-N(1)-C(2)	121.30(9)	C(4)-C(3)-H(3B)	109.1
C(1)-N(1)-C(3)	122.14(9)	H(3A)-C(3)-H(3B)	107.8
C(2)-N(1)-C(3)	116.52(9)	C(5)-C(4)-C(3)	111.18(9)
C(6)-N(2)-C(5)	112.54(9)	C(5)-C(4)-H(4A)	109.4
C(6)-N(2)-H(2NA)	107.3(8)	C(3)-C(4)-H(4A)	109.4
C(5)-N(2)-H(2NA)	108.8(8)	C(5)-C(4)-H(4B)	109.4
C(6)-N(2)-H(2NB)	108.2(9)	C(3)-C(4)-H(4B)	109.4
C(5)-N(2)-H(2NB)	108.5(9)	H(4A)-C(4)-H(4B)	108.0
H(2NA)-N(2)-H(2NB)	111.5(12)	N(2)-C(5)-C(4)	111.33(9)
O(2)-C(1)-O(1)	123.30(10)	N(2)-C(5)-H(5A)	109.4
O(2)-C(1)-N(1)	119.99(10)	C(4)-C(5)-H(5A)	109.4
O(1)-C(1)-N(1)	116.70(10)	N(2)-C(5)-H(5B)	109.4
N(1)-C(2)-H(2A)	109.5	C(4)-C(5)-H(5B)	109.4
N(1)-C(2)-H(2B)	109.5	H(5A)-C(5)-H(5B)	108.0
H(2A)-C(2)-H(2B)	109.5	N(2)-C(6)-H(6A)	109.5
N(1)-C(2)-H(2C)	109.5	N(2)-C(6)-H(6B)	109.5
H(2A)-C(2)-H(2C)	109.5	H(6A)-C(6)-H(6B)	109.5
H(2B)-C(2)-H(2C)	109.5	N(2)-C(6)-H(6C)	109.5
N(1)-C(3)-C(4)	112.52(9)	H(6A)-C(6)-H(6C)	109.5
N(1)-C(3)-H(3A)	109.1	H(6B)-C(6)-H(6C)	109.5
C(4)-C(3)-H(3A)	109.1		

A.1.1 Compound 3-2a

Figure A.6. Molecular structure of 3-2a.



A.7. Crystal data and structure refinement for 3-2a

Identification code	pj23	
Empirical formula	C9 H10 N2 S3	
Formula weight	242.37	
Temperature	293(2) K	
Wavelength	0.71073 Å	
Crystal system	Orthorhombic	
Space group	Pnma	
Unit cell dimensions	a = 10.460(3) Å	$\alpha = 90^\circ$.
	b = 7.083(2) Å	$\beta = 90^\circ$.
	c = 13.866(5) Å	$\gamma = 90^\circ$.
Volume	1027.3(6) Å ³	
Z	4	
Density (calculated)	1.567 Mg/m ³	
Absorption coefficient	0.679 mm ⁻¹	
F(000)	504	
Crystal size	0.30 x 0.06 x 0.06 mm ³	
Theta range for data collection	2.44 to 25.98°.	
Index ranges	-12<=h<=12, -8<=k<=8, -15<=l<=17	
Reflections collected	7369	
Independent reflections	1096 [R(int) = 0.0323]	
Completeness to theta = 25.98°	100.0 %	
Absorption correction	Multi-scan	
Max. and min. transmission	0.9604 and 0.8221	
Refinement method	Full-matrix least-squares on F ²	
Data / restraints / parameters	1096 / 1 / 105	
Goodness-of-fit on F ²	1.054	
Final R indices [I>2sigma(I)]	R1 = 0.0315, wR2 = 0.0784	
R indices (all data)	R1 = 0.0392, wR2 = 0.0839	
Largest diff. peak and hole	0.358 and -0.281 e.Å ⁻³	

Table A.8. Atomic coordinates ($\times 10^4$) and equivalent isotropic displacement parameters ($\text{\AA}^2 \times 10^3$) for **3-2a**. $U(\text{eq})$ is defined as one third of the trace of the orthogonalized U^{ij} tensor.

	x	y	z	$U(\text{eq})$
S(1)	1243(1)	7500	7594(1)	45(1)
S(2)	-702(1)	7500	6149(1)	32(1)
S(3)	-2350(1)	7500	4474(1)	49(1)
N(1)	2389(2)	7500	4079(2)	41(1)
N(2)	1817(2)	7500	5715(2)	30(1)
C(1)	3753(4)	7500	4257(3)	65(1)
C(2)	4042(4)	6888(6)	5219(4)	43(1)
C(3)	3185(3)	7500	6000(3)	42(1)
C(4)	1498(3)	7500	4757(2)	31(1)
C(5)	261(3)	7500	4360(2)	32(1)
C(6)	396(3)	7500	3279(2)	43(1)
C(7)	1838(4)	7500	3111(3)	54(1)
C(8)	908(2)	7500	6430(2)	30(1)
C(9)	-836(3)	7500	4889(2)	32(1)

Table A.9. Bond lengths [\AA] for **3-2a**

S(1)-C(8)	1.652(3)	C(2)-C(2)#1	0.866(9)
S(2)-C(8)	1.728(3)	C(2)-C(3)	1.471(5)
S(2)-C(9)	1.753(3)	C(2)-H(2A)	1.08(3)
S(3)-C(9)	1.684(3)	C(2)-H(2B)	0.99(5)
N(1)-C(4)	1.324(3)	C(3)-C(2)#1	1.471(5)
N(1)-C(1)	1.447(5)	C(3)-H(3)	0.88(2)
N(1)-C(7)	1.462(4)	C(4)-C(5)	1.405(4)
N(2)-C(4)	1.369(4)	C(5)-C(9)	1.362(4)
N(2)-C(8)	1.373(3)	C(5)-C(6)	1.506(4)
N(2)-C(3)	1.485(3)	C(6)-C(7)	1.526(5)
C(1)-C(2)	1.434(6)	C(6)-H(6)	1.00(2)
C(1)-C(2)#1	1.434(6)	C(7)-H(7)	0.99(3)
C(1)-H(1)	0.880(13)		

Table A.10. Bond angles [°] for **3-2a**

C(8)-S(2)-C(9)	107.58(13)	C(2)#1-C(3)-C(2)	34.3(4)
C(4)-N(1)-C(1)	125.0(3)	C(2)#1-C(3)-N(2)	113.1(3)
C(4)-N(1)-C(7)	112.0(3)	C(2)-C(3)-N(2)	113.1(3)
C(1)-N(1)-C(7)	123.0(3)	C(2)#1-C(3)-H(3)	98.2(16)
C(4)-N(2)-C(8)	122.1(2)	C(2)-C(3)-H(3)	126.5(16)
C(4)-N(2)-C(3)	119.5(2)	N(2)-C(3)-H(3)	108.1(16)
C(8)-N(2)-C(3)	118.4(2)	N(1)-C(4)-N(2)	121.1(3)
C(2)-C(1)-C(2)#1	35.2(4)	N(1)-C(4)-C(5)	111.7(3)
C(2)-C(1)-N(1)	111.5(3)	N(2)-C(4)-C(5)	127.2(2)
C(2)#1-C(1)-N(1)	111.5(3)	C(9)-C(5)-C(4)	124.4(3)
C(2)-C(1)-H(1)	83(2)	C(9)-C(5)-C(6)	127.9(3)
C(2)-C(1)-H(1)	83(2)	C(4)-C(5)-C(6)	107.7(3)
C(2)#1-C(1)-H(1)	115(2)	C(5)-C(6)-C(7)	104.1(3)
N(1)-C(1)-H(1)	107.8(18)	C(5)-C(6)-H(6)	109.7(13)
C(2)#1-C(2)-C(1)	72.4(2)	C(7)-C(6)-H(6)	112.2(13)
C(2)#1-C(2)-C(3)	72.87(18)	N(1)-C(7)-C(6)	104.5(3)
C(1)-C(2)-C(3)	117.8(3)	N(1)-C(7)-H(7)	106.2(15)
C(2)#1-C(2)-H(2A)	66.4(9)	C(6)-C(7)-H(7)	114.0(15)
C(1)-C(2)-H(2A)	108.5(16)	N(2)-C(8)-S(1)	123.9(2)
C(3)-C(2)-H(2A)	102.4(17)	N(2)-C(8)-S(2)	120.8(2)
C(2)#1-C(2)-H(2B)	168(3)	S(1)-C(8)-S(2)	115.27(16)
C(1)-C(2)-H(2B)	99(3)	C(5)-C(9)-S(3)	127.5(2)
C(3)-C(2)-H(2B)	105(3)	C(5)-C(9)-S(2)	118.0(2)
H(2A)-C(2)-H(2B)	125(3)	S(3)-C(9)-S(2)	114.53(17)

A.1.2 Compound 3-1b

Figure A.11. Molecular structure of 3-1b.

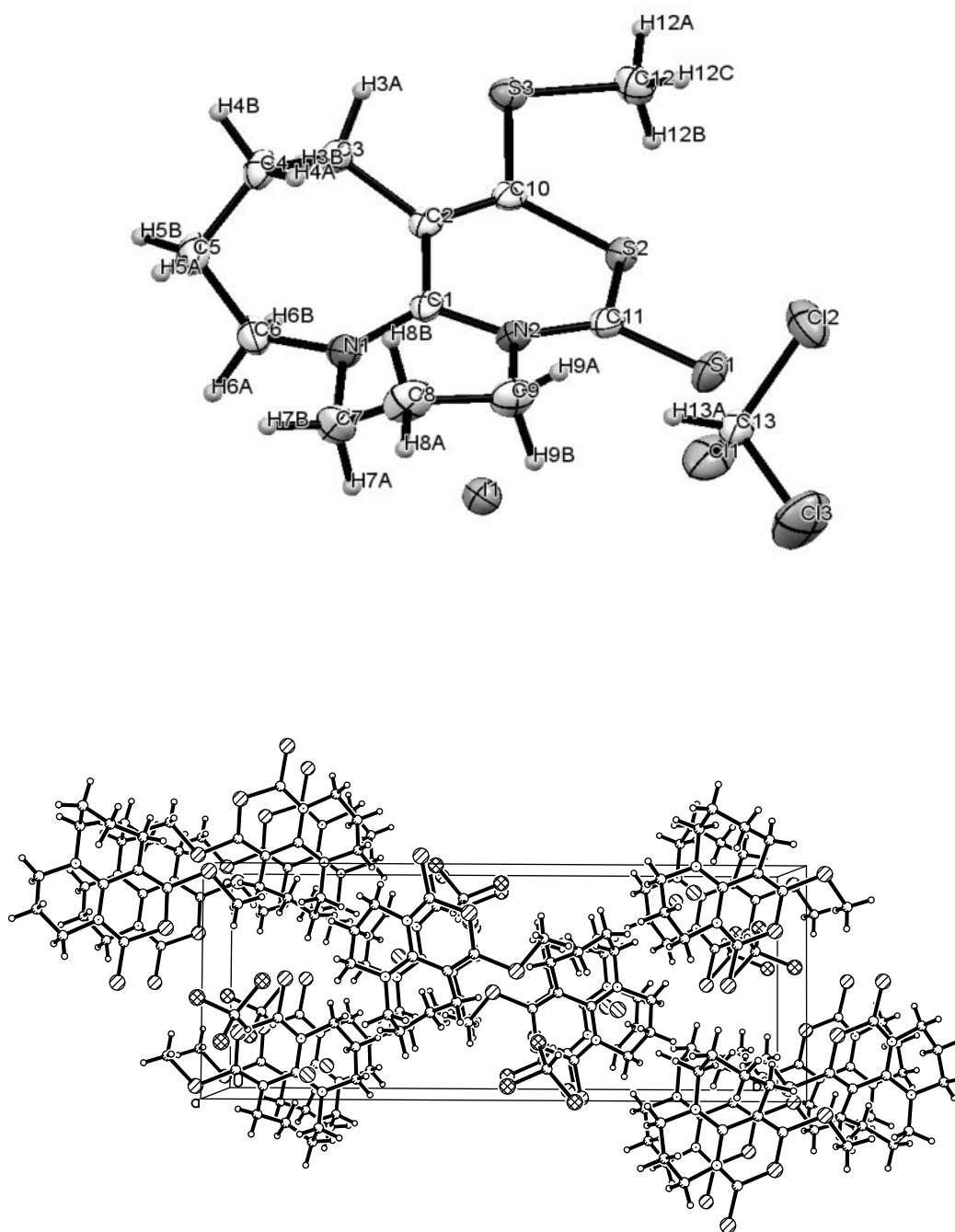


Table A.12. Crystal data and structure refinement for **3-1b**

Identification code	pj44	
Empirical formula	C13 H18 Cl3 I N2 S3	
Formula weight	531.72	
Temperature	180(2) K	
Wavelength	0.71073 Å	
Crystal system	Monoclinic	
Space group	P2(1)/n	
Unit cell dimensions	a = 8.7781(8) Å	$\alpha = 90^\circ$.
	b = 23.821(2) Å	$\beta = 92.406(2)^\circ$.
	c = 9.3214(9) Å	$\gamma = 90^\circ$.
Volume	1947.4(3) Å ³	
Z	4	
Density (calculated)	1.814 Mg/m ³	
Absorption coefficient	2.374 mm ⁻¹	
F(000)	1048	
Crystal size	0.30 x 0.30 x 0.10 mm ³	
Theta range for data collection	1.71 to 26.00°.	
Index ranges	-10<=h<=10, -29<=k<=29, -11<=l<=11	
Reflections collected	26107	
Independent reflections	3823 [R(int) = 0.0279]	
Completeness to theta = 26.00°	99.9 %	
Absorption correction	multi-scan	
Max. and min. transmission	0.7972 and 0.5361	
Refinement method	Full-matrix least-squares on F ²	
Data / restraints / parameters	3823 / 0 / 200	
Goodness-of-fit on F ²	1.245	
Final R indices [I>2sigma(I)]	R1 = 0.0311, wR2 = 0.0694	
R indices (all data)	R1 = 0.0321, wR2 = 0.0698	
Largest diff. peak and hole	0.933 and -0.764 e.Å ⁻³	

Table A.13. Atomic coordinates ($\times 10^4$) and equivalent isotropic displacement parameters ($\text{\AA}^2 \times 10^3$) for **3-1b**. $U(\text{eq})$ is defined as one third of the trace of the orthogonalized U^{ij} tensor.

	x	y	z	$U(\text{eq})$
I(1)	6604(1)	3186(1)	6106(1)	29(1)
S(1)	4002(1)	3666(1)	10105(1)	37(1)
S(2)	4153(1)	4438(1)	7794(1)	24(1)
S(3)	3046(1)	5195(1)	5448(1)	26(1)
N(1)	2374(3)	3081(1)	5192(3)	26(1)
N(2)	2737(3)	3434(1)	7507(3)	23(1)
C(1)	2552(4)	3520(1)	6035(3)	22(1)
C(2)	2457(4)	4084(1)	5450(3)	21(1)
C(3)	1420(4)	4221(2)	4145(4)	26(1)
C(4)	241(4)	3778(2)	3702(4)	29(1)
C(5)	943(4)	3289(2)	2920(4)	33(1)
C(6)	2475(4)	3134(2)	3628(4)	30(1)
C(7)	2141(5)	2510(2)	5738(5)	40(1)
C(8)	1323(5)	2550(2)	7121(5)	40(1)
C(9)	2273(5)	2895(2)	8184(4)	34(1)
C(10)	3166(4)	4515(1)	6156(3)	21(1)
C(11)	3517(4)	3798(1)	8408(4)	24(1)
C(12)	4057(5)	5619(2)	6779(4)	33(1)
C(13)	8297(4)	4302(2)	8603(4)	29(1)
Cl(1)	9862(1)	4434(1)	7547(1)	45(1)
Cl(2)	7622(1)	4938(1)	9298(1)	47(1)
Cl(3)	8829(2)	3841(1)	9999(2)	68(1)

Table A.14. Bond lengths [\AA] for **3-1b**

S(1)-C(11)	1.651(3)	C(5)-C(6)	1.519(5)
S(2)-C(11)	1.730(4)	C(5)-H(5A)	0.9900
S(2)-C(10)	1.734(3)	C(5)-H(5B)	0.9900
S(3)-C(10)	1.750(3)	C(6)-H(6A)	0.9900
S(3)-C(12)	1.804(4)	C(6)-H(6B)	0.9900
N(1)-C(1)	1.313(4)	C(7)-C(8)	1.506(6)
N(1)-C(6)	1.470(5)	C(7)-H(7A)	0.9900
N(1)-C(7)	1.471(5)	C(7)-H(7B)	0.9900
N(2)-C(11)	1.370(4)	C(8)-C(9)	1.510(6)
N(2)-C(1)	1.390(4)	C(8)-H(8A)	0.9900
N(2)-C(9)	1.495(4)	C(8)-H(8B)	0.9900
C(1)-C(2)	1.451(5)	C(9)-H(9A)	0.9900
C(2)-C(10)	1.358(5)	C(9)-H(9B)	0.9900
C(2)-C(3)	1.524(4)	C(12)-H(12A)	0.9800
C(3)-C(4)	1.523(5)	C(12)-H(12B)	0.9800
C(3)-H(3A)	0.9900	C(12)-H(12C)	0.9800
C(3)-H(3B)	0.9900	C(13)-Cl(3)	1.751(4)
C(4)-C(5)	1.520(5)	C(13)-Cl(1)	1.752(4)
C(4)-H(4A)	0.9900	C(13)-Cl(2)	1.760(4)
C(4)-H(4B)	0.9900	C(13)-H(13A)	1.0000

Table A.15. Bond angles [$^\circ$] for **3-1b**

C(11)-S(2)-C(10)	103.22(16)	H(6A)-C(6)-H(6B)	108.0
C(10)-S(3)-C(12)	103.80(17)	N(1)-C(7)-C(8)	108.3(3)
C(1)-N(1)-C(6)	121.0(3)	N(1)-C(7)-H(7A)	110.0
C(1)-N(1)-C(7)	123.0(3)	C(8)-C(7)-H(7A)	110.0
C(6)-N(1)-C(7)	115.9(3)	N(1)-C(7)-H(7B)	110.0
C(11)-N(2)-C(1)	123.1(3)	C(8)-C(7)-H(7B)	110.0
C(11)-N(2)-C(9)	115.0(3)	H(7A)-C(7)-H(7B)	108.4
C(1)-N(2)-C(9)	121.4(3)	C(7)-C(8)-C(9)	109.1(3)
N(1)-C(1)-N(2)	118.7(3)	C(7)-C(8)-H(8A)	109.9

N(1)-C(1)-C(2)	120.5(3)	C(9)-C(8)-H(8A)	109.9
N(2)-C(1)-C(2)	120.7(3)	C(7)-C(8)-H(8B)	109.9
C(10)-C(2)-C(1)	120.1(3)	C(9)-C(8)-H(8B)	109.9
C(10)-C(2)-C(3)	118.0(3)	H(8A)-C(8)-H(8B)	108.3
C(1)-C(2)-C(3)	121.5(3)	N(2)-C(9)-C(8)	110.0(3)
C(4)-C(3)-C(2)	116.4(3)	N(2)-C(9)-H(9A)	109.7
C(4)-C(3)-H(3A)	108.2	C(8)-C(9)-H(9A)	109.7
C(2)-C(3)-H(3A)	108.2	N(2)-C(9)-H(9B)	109.7
C(4)-C(3)-H(3B)	108.2	C(8)-C(9)-H(9B)	109.7
C(2)-C(3)-H(3B)	108.2	H(9A)-C(9)-H(9B)	108.2
H(3A)-C(3)-H(3B)	107.4	C(2)-C(10)-S(2)	123.3(3)
C(5)-C(4)-C(3)	112.2(3)	C(2)-C(10)-S(3)	119.9(3)
C(5)-C(4)-H(4A)	109.2	S(2)-C(10)-S(3)	116.77(19)
C(3)-C(4)-H(4A)	109.2	N(2)-C(11)-S(1)	124.7(3)
C(5)-C(4)-H(4B)	109.2	N(2)-C(11)-S(2)	121.0(3)
C(3)-C(4)-H(4B)	109.2	S(1)-C(11)-S(2)	114.3(2)
H(4A)-C(4)-H(4B)	107.9	S(3)-C(12)-H(12A)	109.5
C(6)-C(5)-C(4)	110.4(3)	S(3)-C(12)-H(12B)	109.5
C(6)-C(5)-H(5A)	109.6	H(12A)-C(12)-H(12B)	109.5
C(4)-C(5)-H(5A)	109.6	S(3)-C(12)-H(12C)	109.5
C(6)-C(5)-H(5B)	109.6	H(12A)-C(12)-H(12C)	109.5
C(4)-C(5)-H(5B)	109.6	H(12B)-C(12)-H(12C)	109.5
H(5A)-C(5)-H(5B)	108.1	Cl(3)-C(13)-Cl(1)	109.8(2)
N(1)-C(6)-C(5)	111.3(3)	Cl(3)-C(13)-Cl(2)	110.5(2)
N(1)-C(6)-H(6A)	109.4	Cl(1)-C(13)-Cl(2)	109.7(2)
C(5)-C(6)-H(6A)	109.4	Cl(3)-C(13)-H(13A)	108.9
N(1)-C(6)-H(6B)	109.4	Cl(1)-C(13)-H(13A)	108.9
C(5)-C(6)-H(6B)	109.4	Cl(2)-C(13)-H(13A)	108.9

A.1.3. Compound 3-1c

A.16. Molecular structure of 3-1c

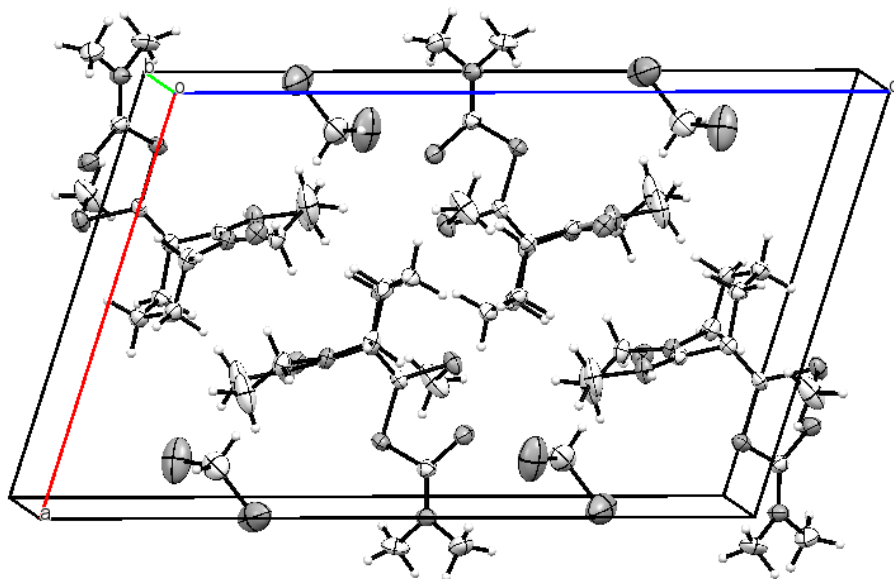
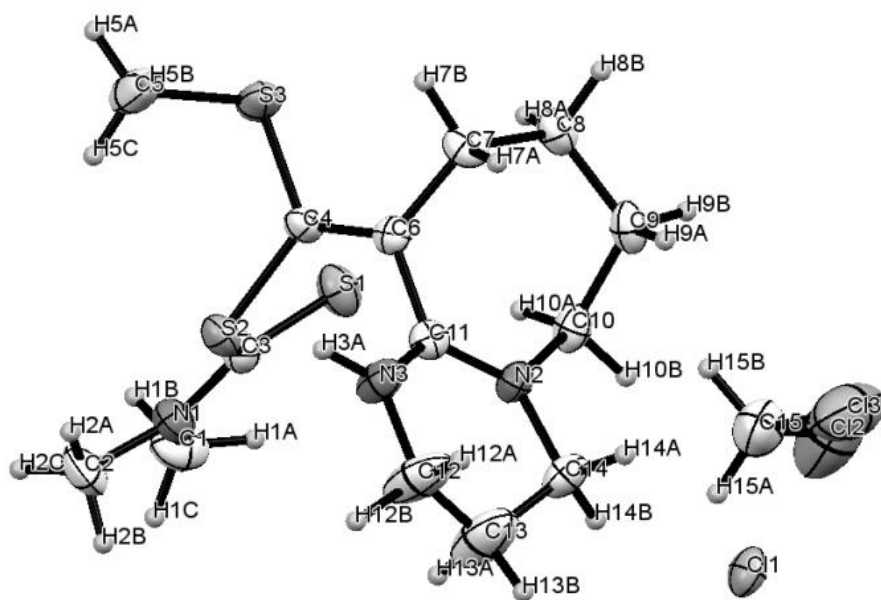


Table A.17. Crystal data and structure refinement for **3-1c**.

Identification code	pj80	
Empirical formula	C ₁₅ H ₂₆ Cl ₃ N ₃ S ₃	
Formula weight	450.92	
Temperature	180(2) K	
Wavelength	0.71073 Å	
Crystal system	Monoclinic	
Space group	P2(1)/c	
Unit cell dimensions	a = 12.2058(8) Å	α = 90°.
	b = 9.4889(6) Å	β = 107.4520(10)°.
	c = 19.5406(13) Å	γ = 90°.
Volume	2159.0(2) Å ³	
Z	4	
Density (calculated)	1.387 Mg/m ³	
Absorption coefficient	0.718 mm ⁻¹	
F(000)	944	
Crystal size	0.05 x 0.05 x 0.01 mm ³	
Theta range for data collection	1.75 to 26.00°.	
Index ranges	-15 ≤ h ≤ 15, -11 ≤ k ≤ 11, -24 ≤ l ≤ 24	
Reflections collected	21024	
Independent reflections	4226 [R(int) = 0.0480]	
Completeness to theta = 26.00°	99.9 %	
Absorption correction	multi-scan	
Max. and min. transmission	0.9929 and 0.9650	
Refinement method	Full-matrix least-squares on F ²	
Data / restraints / parameters	4226 / 0 / 221	
Goodness-of-fit on F ²	1.038	
Final R indices [I > 2σ(I)]	R1 = 0.0489, wR2 = 0.1093	
R indices (all data)	R1 = 0.0727, wR2 = 0.1236	
Largest diff. peak and hole	1.289 and -0.643 e.Å ⁻³	

Table A.18. Atomic coordinates ($\times 10^4$) and equivalent isotropic displacement parameters ($\text{\AA}^2 \times 10^3$) for **3-1c**. $U(\text{eq})$ is defined as one third of the trace of the orthogonalized U^{ij} tensor.

	x	y	z	$U(\text{eq})$
S(2)	1637(1)	8019(1)	407(1)	29(1)
S(3)	3442(1)	8875(1)	-292(1)	37(1)
S(1)	1906(1)	5719(1)	-605(1)	37(1)
Cl(3)	10263(1)	9190(2)	8302(1)	88(1)
Cl(1)	3347(1)	945(1)	1807(1)	34(1)
N(1)	-76(2)	6696(3)	-496(2)	34(1)
C(1)	-693(3)	5705(5)	-1050(2)	48(1)
C(3)	1068(3)	6747(4)	-285(2)	29(1)
C(4)	3100(3)	8051(3)	432(2)	25(1)
C(6)	3910(3)	7551(3)	1000(2)	23(1)
C(11)	3615(3)	6846(3)	1604(2)	24(1)
N(3)	3333(3)	7647(3)	2071(1)	34(1)
C(12)	3149(5)	7063(4)	2727(2)	59(1)
C(13)	2900(5)	5587(5)	2655(3)	71(2)
C(2)	-811(3)	7660(4)	-239(2)	47(1)
C(5)	2942(4)	10620(4)	-208(3)	63(1)
N(2)	3738(2)	5469(3)	1673(1)	25(1)
C(14)	3641(3)	4755(4)	2320(2)	32(1)
C(10)	4146(3)	4625(3)	1157(2)	30(1)
C(9)	5399(3)	4907(4)	1200(2)	33(1)
C(8)	5593(3)	6238(4)	818(2)	32(1)
C(7)	5186(3)	7585(4)	1105(2)	30(1)
C(15)	9062(4)	9195(5)	7533(2)	61(1)
Cl(2)	9005(2)	7638(2)	7037(1)	102(1)

Table A.19. Bond lengths [\AA] for **3-1c**

S(2)-C(4)	1.773(3)	C(2)-H(2A)	0.9800
S(2)-C(3)	1.791(3)	C(2)-H(2B)	0.9800
S(3)-C(4)	1.772(3)	C(2)-H(2C)	0.9800
S(3)-C(5)	1.790(4)	C(5)-H(5A)	0.9800
S(1)-C(3)	1.665(3)	C(5)-H(5B)	0.9800
Cl(3)-C(15)	1.756(5)	C(5)-H(5C)	0.9800
N(1)-C(3)	1.333(4)	N(2)-C(14)	1.472(4)
N(1)-C(1)	1.462(5)	N(2)-C(10)	1.484(4)
N(1)-C(2)	1.471(5)	C(14)-H(14A)	0.9900
C(1)-H(1A)	0.9800	C(14)-H(14B)	0.9900
C(1)-H(1B)	0.9800	C(10)-C(9)	1.530(5)
C(1)-H(1C)	0.9800	C(10)-H(10A)	0.9900
C(4)-C(6)	1.334(4)	C(10)-H(10B)	0.9900
C(6)-C(11)	1.491(4)	C(9)-C(8)	1.522(5)
C(6)-C(7)	1.509(4)	C(9)-H(9A)	0.9900
C(11)-N(3)	1.310(4)	C(9)-H(9B)	0.9900
C(11)-N(2)	1.318(4)	C(8)-C(7)	1.537(4)
N(3)-C(12)	1.473(4)	C(8)-H(8A)	0.9900
N(3)-H(3A)	0.8800	C(8)-H(8B)	0.9900
C(12)-C(13)	1.431(6)	C(7)-H(7A)	0.9900
C(12)-H(12A)	0.9900	C(7)-H(7B)	0.9900
C(12)-H(12B)	0.9900	C(15)-Cl(2)	1.756(5)
C(13)-C(14)	1.491(5)	C(15)-H(15A)	0.9900
C(13)-H(13A)	0.9900	C(15)-H(15B)	0.9900
C(13)-H(13B)	0.9900	C(2)-H(2A)	0.9800

Table A.20. Bond angles [°] for **3-1c**

C(4)-S(2)-C(3)	101.02(15)	S(3)-C(5)-H(5B)	109.5
C(4)-S(3)-C(5)	99.55(17)	H(5A)-C(5)-H(5B)	109.5
C(3)-N(1)-C(1)	120.7(3)	S(3)-C(5)-H(5C)	109.5
C(3)-N(1)-C(2)	124.2(3)	H(5A)-C(5)-H(5C)	109.5
C(1)-N(1)-C(2)	114.9(3)	H(5B)-C(5)-H(5C)	109.5
N(1)-C(1)-H(1A)	109.5	C(11)-N(2)-C(14)	120.5(3)
N(1)-C(1)-H(1B)	109.5	C(11)-N(2)-C(10)	121.2(3)
H(1A)-C(1)-H(1B)	109.5	C(14)-N(2)-C(10)	117.7(3)
N(1)-C(1)-H(1C)	109.5	N(2)-C(14)-C(13)	110.4(3)
H(1A)-C(1)-H(1C)	109.5	N(2)-C(14)-H(14A)	109.6
H(1B)-C(1)-H(1C)	109.5	C(13)-C(14)-H(14A)	109.6
N(1)-C(3)-S(1)	124.6(3)	N(2)-C(14)-H(14B)	109.6
N(1)-C(3)-S(2)	113.0(3)	C(13)-C(14)-H(14B)	109.6
S(1)-C(3)-S(2)	122.39(19)	H(14A)-C(14)-H(14B)	108.1
C(6)-C(4)-S(3)	122.0(2)	N(2)-C(10)-C(9)	113.7(3)
C(6)-C(4)-S(2)	120.4(2)	N(2)-C(10)-H(10A)	108.8
S(3)-C(4)-S(2)	117.55(18)	C(9)-C(10)-H(10A)	108.8
C(4)-C(6)-C(11)	121.6(3)	N(2)-C(10)-H(10B)	108.8
C(4)-C(6)-C(7)	125.6(3)	C(9)-C(10)-H(10B)	108.8
C(11)-C(6)-C(7)	112.7(3)	H(10A)-C(10)-H(10B)	107.7
N(3)-C(11)-N(2)	123.4(3)	C(8)-C(9)-C(10)	114.7(3)
N(3)-C(11)-C(6)	117.9(3)	C(8)-C(9)-H(9A)	108.6
N(2)-C(11)-C(6)	118.5(3)	C(10)-C(9)-H(9A)	108.6
C(11)-N(3)-C(12)	121.9(3)	C(8)-C(9)-H(9B)	108.6
C(11)-N(3)-H(3A)	119.1	C(10)-C(9)-H(9B)	108.6
C(12)-N(3)-H(3A)	119.1	H(9A)-C(9)-H(9B)	107.6
C(13)-C(12)-N(3)	111.5(3)	C(9)-C(8)-C(7)	113.3(3)
C(13)-C(12)-H(12A)	109.3	C(9)-C(8)-H(8A)	108.9
N(3)-C(12)-H(12A)	109.3	C(7)-C(8)-H(8A)	108.9
C(13)-C(12)-H(12B)	109.3	C(9)-C(8)-H(8B)	108.9
N(3)-C(12)-H(12B)	109.3	C(7)-C(8)-H(8B)	108.9
H(12A)-C(12)-H(12B)	108.0	H(8A)-C(8)-H(8B)	107.7

C(12)-C(13)-C(14)	115.0(4)	C(6)-C(7)-C(8)	111.5(3)
C(12)-C(13)-H(13A)	108.5	C(6)-C(7)-H(7A)	109.3
C(14)-C(13)-H(13A)	108.5	C(8)-C(7)-H(7A)	109.3
C(12)-C(13)-H(13B)	108.5	C(6)-C(7)-H(7B)	109.3
C(14)-C(13)-H(13B)	108.5	C(8)-C(7)-H(7B)	109.3
H(13A)-C(13)-H(13B)	107.5	H(7A)-C(7)-H(7B)	108.0
N(1)-C(2)-H(2A)	109.5	Cl(2)-C(15)-Cl(3)	110.8(3)
N(1)-C(2)-H(2B)	109.5	Cl(2)-C(15)-H(15A)	109.5
H(2A)-C(2)-H(2B)	109.5	Cl(3)-C(15)-H(15A)	109.5
N(1)-C(2)-H(2C)	109.5	Cl(2)-C(15)-H(15B)	109.5
H(2A)-C(2)-H(2C)	109.5	Cl(3)-C(15)-H(15B)	109.5
H(2B)-C(2)-H(2C)	109.5	H(15A)-C(15)-H(15B)	108.1
S(3)-C(5)-H(5A)	109.5		

A.1.4. Compound 3-3a

Figure A.21. Molecular structure of 3-3a

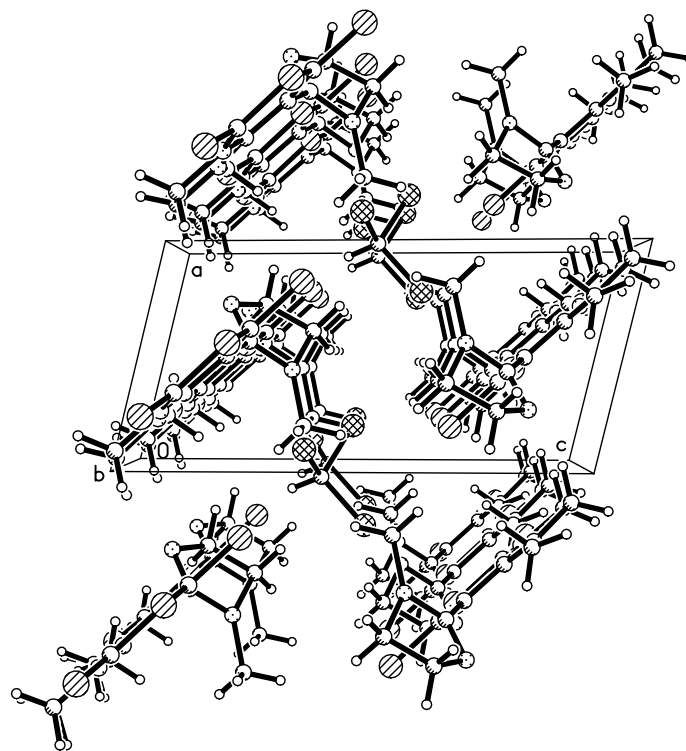
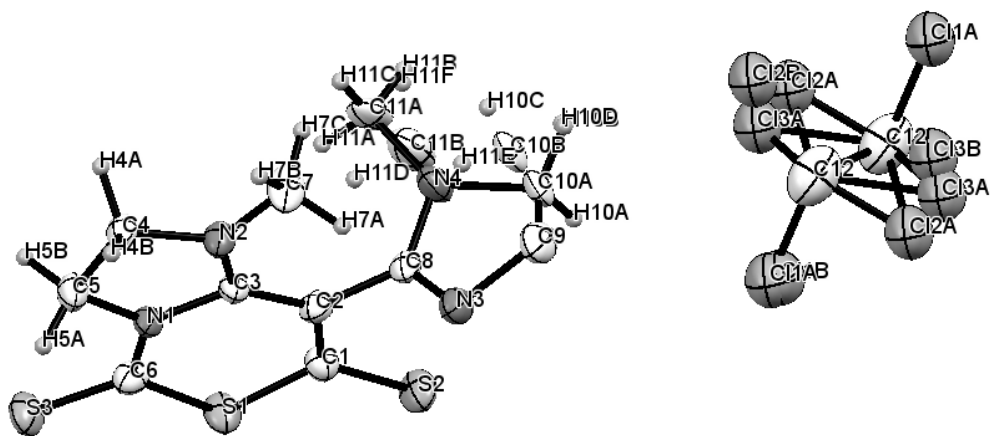


Table A.22. Crystal data and structure refinement for **3-3a**

Identification code	pj21	
Empirical formula	C11.50 H14.50 Cl1.50 N4 S3	
Formula weight	358.13	
Temperature	180(2) K	
Wavelength	0.71073 Å	
Crystal system	Triclinic	
Space group	P-1	
Unit cell dimensions	a = 6.3813(4) Å	$\alpha = 83.449(4)^\circ$.
	b = 9.6864(5) Å	$\beta = 75.967(4)^\circ$.
	c = 12.9889(8) Å	$\gamma = 86.619(4)^\circ$.
Volume	773.41(8) Å ³	
Z	2	
Density (calculated)	1.538 Mg/m ³	
Absorption coefficient	0.733 mm ⁻¹	
F(000)	370	
Crystal size	0.30 x 0.10 x 0.06 mm ³	
Theta range for data collection	2.53 to 26.00°.	
Index ranges	-7<=h<=7, -11<=k<=11, -16<=l<=15	
Reflections collected	5551	
Independent reflections	2973 [R(int) = 0.0358]	
Completeness to theta = 26.00°	98.2 %	
Absorption correction	multi-scan	
Max. and min. transmission	0.9574 and 0.8102	
Refinement method	Full-matrix least-squares on F ²	
Data / restraints / parameters	2973 / 16 / 219	
Goodness-of-fit on F ²	1.164	
Final R indices [I>2sigma(I)]	R1 = 0.0970, wR2 = 0.2471	
R indices (all data)	R1 = 0.1129, wR2 = 0.2550	
Largest diff. peak and hole	0.614 and -0.713 e.Å ⁻³	

Table A.23. Atomic coordinates ($\times 10^4$) and equivalent isotropic displacement parameters ($\text{\AA}^2 \times 10^3$) for **3-3a**. $U(\text{eq})$ is defined as one third of the trace of the orthogonalized U^{ij} tensor.

	x	y	z	$U(\text{eq})$
S(1)	5513(3)	9522(2)	2191(2)	33(1)
S(2)	7909(3)	7470(2)	3233(2)	37(1)
S(3)	2765(4)	11178(2)	1021(2)	37(1)
N(1)	2904(9)	8429(6)	1208(5)	24(1)
N(2)	2520(10)	6209(6)	1075(5)	28(1)
N(3)	7121(10)	4563(6)	1891(5)	31(1)
N(4)	4467(11)	4605(7)	3390(6)	37(2)
C(1)	6071(12)	7754(7)	2494(6)	27(2)
C(2)	5036(11)	6732(7)	2123(6)	26(2)
C(3)	3559(11)	7060(7)	1501(6)	22(1)
C(4)	997(12)	6923(7)	498(6)	27(2)
C(5)	1344(13)	8463(8)	537(7)	32(2)
C(6)	3616(12)	9628(7)	1438(6)	27(2)
C(7)	2604(14)	4692(8)	1164(8)	43(2)
C(8)	5608(11)	5258(7)	2444(6)	24(2)
C(9)	7141(14)	3163(8)	2528(8)	42(2)
C(10A)	6050(40)	3414(19)	3600(17)	40(5)
C(11A)	2190(30)	5018(19)	3883(14)	37(5)
C(10B)	5010(40)	3094(16)	3360(14)	37(5)
C(11B)	3390(40)	5320(20)	4324(16)	54(7)
C(12)	9820(40)	190(30)	4434(19)	64(6)
Cl(1A)	11070(30)	1790(17)	3970(20)	73(2)
Cl(2A)	7770(30)	363(17)	5560(15)	73(2)
Cl(3A)	11990(30)	-978(16)	4825(18)	73(2)
Cl(1B)	11170(20)	1684(13)	4071(19)	73(2)
Cl(2B)	7119(19)	411(12)	5159(12)	73(2)
Cl(3B)	11160(20)	-1168(11)	5047(12)	73(2)

Table A.24. Bond lengths [\AA] for **3-3a**

S(1)-C(6)	1.723(7)	C(11A)-H(11C)	0.9800
S(1)-C(1)	1.748(7)	C(10B)-H(10C)	0.9900
S(2)-C(1)	1.679(7)	C(10B)-H(10D)	0.9900
S(3)-C(6)	1.645(8)	C(11B)-H(11D)	0.9800
N(1)-C(6)	1.361(9)	C(11B)-H(11E)	0.9800
N(1)-C(3)	1.405(8)	C(11B)-H(11F)	0.9800
N(1)-C(5)	1.471(9)	C(12)-Cl(3B)#1	1.27(2)
N(2)-C(3)	1.331(8)	C(12)-Cl(3A)#1	1.54(3)
N(2)-C(7)	1.460(9)	C(12)-C(12)#1	1.54(5)
N(2)-C(4)	1.463(9)	C(12)-Cl(2A)#1	1.60(3)
N(3)-C(8)	1.264(9)	C(12)-Cl(1B)	1.69(3)
N(3)-C(9)	1.507(10)	C(12)-Cl(2A)	1.73(3)
N(4)-C(8)	1.372(10)	C(12)-Cl(3B)	1.74(3)
N(4)-C(11B)	1.47(2)	C(12)-Cl(1A)	1.76(3)
N(4)-C(10B)	1.487(16)	C(12)-Cl(2B)	1.77(3)
N(4)-C(11A)	1.490(19)	C(12)-Cl(3A)	1.86(3)
N(4)-C(10A)	1.532(18)	C(12)-Cl(2B)#1	2.17(3)
C(1)-C(2)	1.410(10)	Cl(1A)-Cl(2A)#1	2.24(2)
C(2)-C(3)	1.385(10)	Cl(1A)-Cl(3A)#1	2.30(3)
C(2)-C(8)	1.491(10)	Cl(2A)-Cl(3A)#1	0.731(18)
C(4)-C(5)	1.529(10)	Cl(2A)-C(12)#1	1.60(3)
C(4)-H(4A)	0.9900	Cl(2A)-Cl(1A)#1	2.24(2)
C(4)-H(4B)	0.9900	Cl(3A)-Cl(2A)#1	0.731(18)
C(5)-H(5A)	0.9900	Cl(3A)-C(12)#1	1.54(3)
C(5)-H(5B)	0.9900	Cl(3A)-Cl(1A)#1	2.30(3)
C(7)-H(7A)	0.9800	Cl(1B)-Cl(3B)#1	1.70(2)
C(7)-H(7B)	0.9800	Cl(1B)-Cl(2B)#1	2.473(17)
C(7)-H(7C)	0.9800	Cl(2B)-Cl(3B)#1	1.31(2)
C(9)-C(10A)	1.44(2)	Cl(2B)-C(12)#1	2.17(3)
C(9)-C(10B)	1.52(2)	Cl(2B)-Cl(1B)#1	2.473(17)
C(10A)-H(10A)	0.9900	Cl(3B)-C(12)#1	1.27(2)
C(10A)-H(10B)	0.9900	Cl(3B)-Cl(2B)#1	1.31(2)

C(11A)-H(11A)	0.9800	Cl(3B)-Cl(1B)#1	1.70(2)
C(11A)-H(11B)	0.9800		

Table A.25. Bond angles [°] for **3-3a**

C(6)-S(1)-C(1)	106.8(3)	N(2)-C(7)-H(7A)	109.5
C(6)-N(1)-C(3)	127.6(6)	N(2)-C(7)-H(7B)	109.5
C(6)-N(1)-C(5)	120.8(6)	H(7A)-C(7)-H(7B)	109.5
C(3)-N(1)-C(5)	111.6(5)	N(2)-C(7)-H(7C)	109.5
C(3)-N(2)-C(7)	129.1(6)	H(7A)-C(7)-H(7C)	109.5
C(3)-N(2)-C(4)	113.8(6)	H(7B)-C(7)-H(7C)	109.5
C(7)-N(2)-C(4)	117.0(6)	N(3)-C(8)-N(4)	117.3(7)
C(8)-N(3)-C(9)	105.0(7)	N(3)-C(8)-C(2)	123.4(7)
C(8)-N(4)-C(11B)	124.4(9)	N(4)-C(8)-C(2)	119.3(6)
C(8)-N(4)-C(10B)	106.6(8)	C(10A)-C(9)-N(3)	104.4(9)
C(11B)-N(4)-C(10B)	127.3(11)	C(10A)-C(9)-C(10B)	34.6(9)
C(8)-N(4)-C(11A)	122.3(9)	N(3)-C(9)-C(10B)	106.1(8)
C(11B)-N(4)-C(11A)	45.0(11)	C(9)-C(10A)-N(4)	101.1(13)
C(10B)-N(4)-C(11A)	117.5(11)	C(9)-C(10A)-H(10A)	111.6
C(8)-N(4)-C(10A)	101.3(9)	N(4)-C(10A)-H(10A)	111.6
C(11B)-N(4)-C(10A)	115.2(12)	C(9)-C(10A)-H(10B)	111.6
C(10B)-N(4)-C(10A)	33.9(9)	N(4)-C(10A)-H(10B)	111.6
C(11A)-N(4)-C(10A)	136.0(11)	H(10A)-C(10A)-H(10B)	109.4
C(2)-C(1)-S(2)	126.4(6)	N(4)-C(11A)-H(11A)	109.5
C(2)-C(1)-S(1)	120.8(6)	N(4)-C(11A)-H(11B)	109.5
S(2)-C(1)-S(1)	112.8(4)	N(4)-C(11A)-H(11C)	109.5
C(3)-C(2)-C(1)	122.6(7)	N(4)-C(10B)-C(9)	99.6(11)
C(3)-C(2)-C(8)	121.2(6)	N(4)-C(10B)-H(10C)	111.9
C(1)-C(2)-C(8)	116.2(6)	C(9)-C(10B)-H(10C)	111.9
N(2)-C(3)-C(2)	128.8(6)	N(4)-C(10B)-H(10D)	111.9
N(2)-C(3)-N(1)	107.7(6)	C(9)-C(10B)-H(10D)	111.9
C(2)-C(3)-N(1)	123.5(6)	H(10C)-C(10B)-H(10D)	109.6
N(2)-C(4)-C(5)	103.6(5)	N(4)-C(11B)-H(11D)	109.5
N(2)-C(4)-H(4A)	111.0	N(4)-C(11B)-H(11E)	109.5

C(5)-C(4)-H(4A)	111.0	H(11D)-C(11B)-H(11E)	109.5
N(2)-C(4)-H(4B)	111.0	N(4)-C(11B)-H(11F)	109.5
C(5)-C(4)-H(4B)	111.0	H(11D)-C(11B)-H(11F)	109.5
H(4A)-C(4)-H(4B)	109.0	H(11E)-C(11B)-H(11F)	109.5
N(1)-C(5)-C(4)	103.1(6)	Cl(3B)#1-C(12)-Cl(3A)#1	20.6(9)
N(1)-C(5)-H(5A)	111.1	Cl(3B)#1-C(12)-C(12)#1	75.9(18)
C(4)-C(5)-H(5A)	111.1	Cl(3A)#1-C(12)-C(12)#1	74.3(18)
N(1)-C(5)-H(5B)	111.1	Cl(3B)#1-C(12)-Cl(2A)#1	124.4(18)
C(4)-C(5)-H(5B)	111.1	Cl(3A)#1-C(12)-Cl(2A)#1	136.1(18)
C(6)-S(1)-C(1)	106.8(3)	C(12)#1-C(12)-Cl(2A)#1	66.9(17)
C(6)-N(1)-C(3)	127.6(6)	Cl(3B)#1-C(12)-Cl(1B)	68.5(15)
C(6)-N(1)-C(5)	120.8(6)	Cl(3A)#1-C(12)-Cl(1B)	88.7(16)
C(3)-N(1)-C(5)	111.6(5)	C(12)#1-C(12)-Cl(1B)	101(2)
C(3)-N(2)-C(7)	129.1(6)	Cl(2A)#1-C(12)-Cl(1B)	79.3(14)
C(3)-N(2)-C(4)	113.8(6)	Cl(3B)#1-C(12)-Cl(2A)	42.4(11)
C(7)-N(2)-C(4)	117.0(6)	Cl(3A)#1-C(12)-Cl(2A)	25.0(7)
C(8)-N(3)-C(9)	105.0(7)	C(12)#1-C(12)-Cl(2A)	58.1(16)
C(8)-N(4)-C(11B)	124.4(9)	Cl(2A)#1-C(12)-Cl(2A)	125.0(15)
C(8)-N(4)-C(10B)	106.6(8)	Cl(1B)-C(12)-Cl(2A)	109.7(16)
C(11B)-N(4)-C(10B)	127.3(11)	Cl(3B)#1-C(12)-Cl(3B)	121.0(16)
C(8)-N(4)-C(11A)	122.3(9)	Cl(3A)#1-C(12)-Cl(3B)	116.4(17)
C(11B)-N(4)-C(11A)	45.0(11)	C(12)#1-C(12)-Cl(3B)	45.1(14)
C(10B)-N(4)-C(11A)	117.5(11)	Cl(2A)#1-C(12)-Cl(3B)	40.6(9)
C(8)-N(4)-C(10A)	101.3(9)	Cl(1B)-C(12)-Cl(3B)	115.6(14)
C(11B)-N(4)-C(10A)	115.2(12)	Cl(2A)-C(12)-Cl(3B)	94.2(14)
C(10B)-N(4)-C(10A)	33.9(9)	Cl(3B)#1-C(12)-Cl(1A)	68.3(16)
C(11A)-N(4)-C(10A)	136.0(11)	Cl(3A)#1-C(12)-Cl(1A)	88.1(15)
C(2)-C(1)-S(2)	126.4(6)	C(12)#1-C(12)-Cl(1A)	106(2)
C(2)-C(1)-S(1)	120.8(6)	Cl(2A)#1-C(12)-Cl(1A)	83.5(13)
S(2)-C(1)-S(1)	112.8(4)	Cl(1B)-C(12)-Cl(1A)	5.5(16)
C(3)-C(2)-C(1)	122.6(7)	Cl(2A)-C(12)-Cl(1A)	110.3(15)
C(3)-C(2)-C(8)	121.2(6)	Cl(3B)-C(12)-Cl(1A)	120.7(16)
C(1)-C(2)-C(8)	116.2(6)	Cl(3B)#1-C(12)-Cl(2B)	47.8(11)
N(2)-C(3)-C(2)	128.8(6)	Cl(3A)#1-C(12)-Cl(2B)	27.6(9)

N(2)-C(3)-N(1)	107.7(6)	C(12)#1-C(12)-Cl(2B)	81.7(19)
C(2)-C(3)-N(1)	123.5(6)	Cl(2A)#1-C(12)-Cl(2B)	148.0(18)
N(2)-C(4)-C(5)	103.6(5)	Cl(1B)-C(12)-Cl(2B)	113.9(15)
N(2)-C(4)-H(4A)	111.0	Cl(2A)-C(12)-Cl(2B)	24.3(7)
C(5)-C(4)-H(4A)	111.0	Cl(3B)-C(12)-Cl(2B)	111.3(15)
N(2)-C(4)-H(4B)	111.0	Cl(1A)-C(12)-Cl(2B)	112.0(16)
C(5)-C(4)-H(4B)	111.0	Cl(3B)#1-C(12)-Cl(3A)	125.0(18)
H(4A)-C(4)-H(4B)	109.0	Cl(3A)#1-C(12)-Cl(3A)	127.1(15)
N(1)-C(5)-C(4)	103.1(6)	C(12)#1-C(12)-Cl(3A)	52.9(15)
N(1)-C(5)-H(5A)	111.1	Cl(2A)#1-C(12)-Cl(3A)	22.8(8)
C(4)-C(5)-H(5A)	111.1	Cl(1B)-C(12)-Cl(3A)	99.9(14)
N(1)-C(5)-H(5B)	111.1	Cl(2A)-C(12)-Cl(3A)	108.3(14)
C(4)-C(5)-H(5B)	111.1	Cl(3B)-C(12)-Cl(3A)	17.7(6)
H(5A)-C(5)-H(5B)	109.1	Cl(1A)-C(12)-Cl(3A)	104.6(14)
N(1)-C(6)-S(3)	123.0(6)	Cl(2B)-C(12)-Cl(3A)	127.9(16)
N(1)-C(6)-S(1)	118.7(5)	Cl(3B)#1-C(12)-Cl(2B)#1	112.0(15)
S(3)-C(6)-S(1)	118.4(4)	Cl(3A)#1-C(12)-Cl(2B)#1	122.0(15)

A.1.5. Hydrogen Sulfide Salt of 3-

Figure A.26. Molecular structure of hydrogen sulfide salt of 3-3

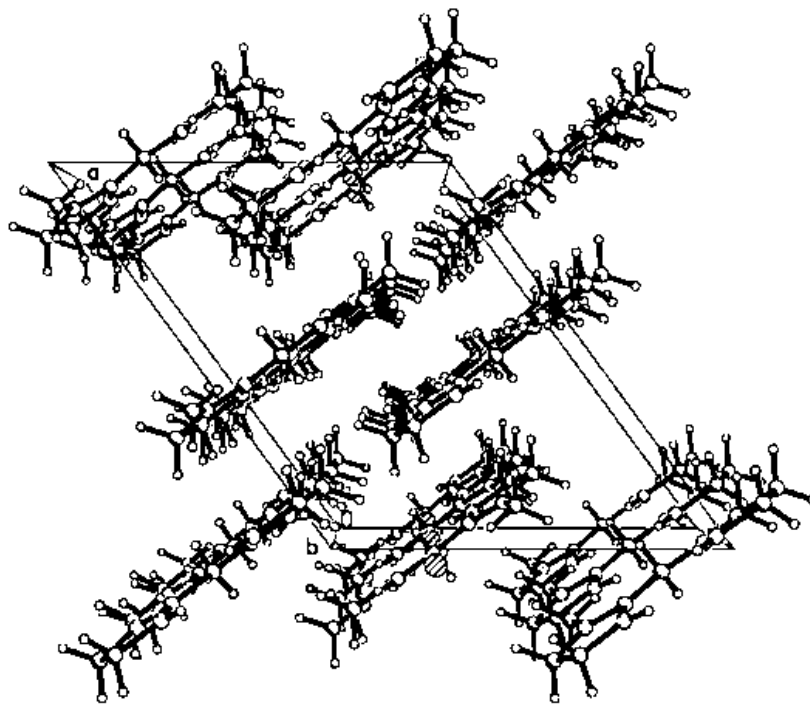
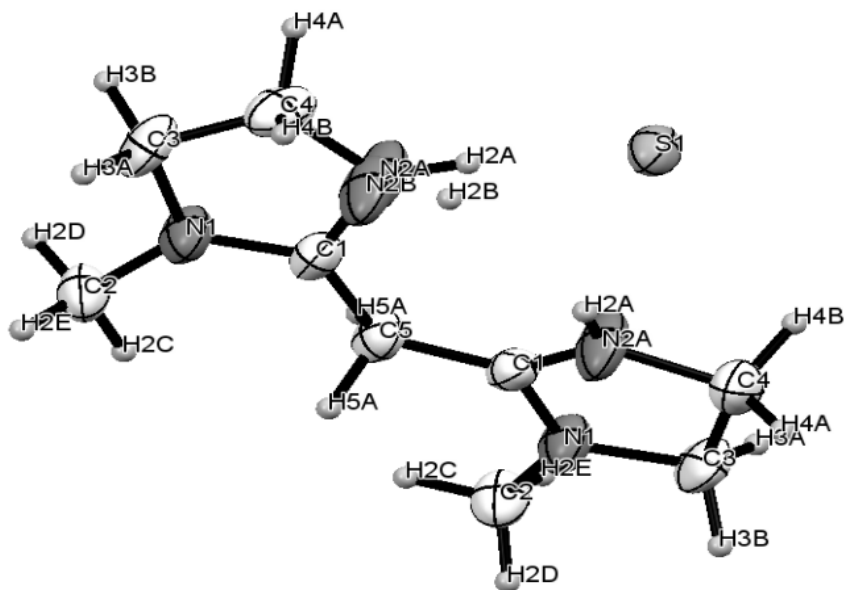


Table A.27. Crystal data and structure refinement for pj49

Identification code	pj49	
Empirical formula	C ₉ H ₁₈ N ₄ S	
Formula weight	214.33	
Temperature	180(2) K	
Wavelength	0.71073 Å	
Crystal system	Monoclinic	
Space group	C2/c	
Unit cell dimensions	a = 13.7218(6) Å	α = 90°.
	b = 8.6044(3) Å	β = 126.298(2)°.
	c = 11.5070(4) Å	γ = 90°.
Volume	1094.97(7) Å ³	
Z	4	
Density (calculated)	1.300 Mg/m ³	
Absorption coefficient	0.265 mm ⁻¹	
F(000)	464	
Crystal size	0.20 x 0.20 x 0.15 mm ³	
Theta range for data collection	3.00 to 26.00°.	
Index ranges	-16 ≤ h ≤ 16, -10 ≤ k ≤ 9, -14 ≤ l ≤ 14	
Reflections collected	5680	
Independent reflections	1069 [R(int) = 0.0176]	
Completeness to theta = 26.00°	99.6 %	
Absorption correction	Multi-scan	
Max. and min. transmission	0.9613 and 0.9489	
Refinement method	Full-matrix least-squares on F ²	
Data / restraints / parameters	1069 / 1 / 69	
Goodness-of-fit on F ²	1.278	
Final R indices [I > 2σ(I)]	R1 = 0.1073, wR2 = 0.2698	
R indices (all data)	R1 = 0.1080, wR2 = 0.2700	
Extinction coefficient	0.008(2)	
Largest diff. peak and hole	1.006 and -0.543 e.Å ⁻³	

Table A.28. Atomic coordinates ($\times 10^4$) and equivalent isotropic displacement parameters ($\text{\AA}^2 \times 10^3$) for pj49. $U(\text{eq})$ is defined as one third of the trace of the orthogonalized U^{ij} tensor.

	x	y	z	$U(\text{eq})$
N(1)	3705(5)	6717(7)	-107(5)	43(2)
N(2A)	3960(90)	4440(30)	900(110)	58(12)
N(2B)	4140(90)	4420(30)	770(110)	58(12)
C(1)	4297(5)	5953(8)	1137(6)	32(1)
C(2)	3720(7)	8367(7)	-329(7)	41(2)
C(3)	3025(6)	5742(9)	-1349(7)	49(2)
C(4)	3297(6)	4112(8)	-681(7)	46(2)
C(5)	5000	6654(11)	2500	35(2)
S(1)	5000	1242(3)	2500	37(1)

Table A.29. Bond lengths [\AA] for pj49

N(1)-C(1)	1.328(8)	C(2)-H(2D)	0.9800
N(1)-C(3)	1.427(9)	C(2)-H(2E)	0.9800
N(1)-C(2)	1.445(8)	C(3)-C(4)	1.536(10)
N(2A)-C(1)	1.358(18)	C(3)-H(3A)	0.9900
N(2A)-C(4)	1.50(10)	C(3)-H(3B)	0.9900
N(2A)-H(2A)	0.8800	C(4)-H(4A)	0.9900
N(2B)-C(1)	1.358(18)	C(4)-H(4B)	0.9900
N(2B)-C(4)	1.39(10)	C(5)-C(1)#1	1.401(7)
N(2B)-H(2B)	0.8800	C(5)-H(5A)	0.9900
C(1)-C(5)	1.401(7)	C(5)-H(5B)	0.9900
C(2)-H(2C)	0.9800		

Table A.29. Bond angles [°] for pj49

C(1)-N(1)-C(3)	114.1(6)	N(1)-C(3)-H(3A)	111.3
C(1)-N(1)-C(2)	127.8(6)	C(4)-C(3)-H(3A)	111.3
C(3)-N(1)-C(2)	118.0(5)	N(1)-C(3)-H(3B)	111.3
C(1)-N(2A)-C(4)	108(6)	C(4)-C(3)-H(3B)	111.3
C(1)-N(2A)-H(2A)	125.9	H(3A)-C(3)-H(3B)	109.2
C(4)-N(2A)-H(2A)	125.9	N(2B)-C(4)-N(2A)	14(6)
C(1)-N(2B)-C(4)	115(7)	N(2B)-C(4)-C(3)	102.0(19)
C(1)-N(2B)-H(2B)	122.4	N(2A)-C(4)-C(3)	103.3(17)
C(4)-N(2B)-H(2B)	122.4	N(2B)-C(4)-H(4A)	123.2
N(1)-C(1)-N(2B)	105(5)	N(2A)-C(4)-H(4A)	111.1
N(1)-C(1)-N(2A)	110(5)	C(3)-C(4)-H(4A)	111.1
N(2B)-C(1)-N(2A)	15(6)	N(2B)-C(4)-H(4B)	99.6
N(1)-C(1)-C(5)	124.8(7)	N(2A)-C(4)-H(4B)	111.1
N(2B)-C(1)-C(5)	130(5)	C(3)-C(4)-H(4B)	111.1
N(2A)-C(1)-C(5)	124(4)	H(4A)-C(4)-H(4B)	109.1
N(1)-C(2)-H(2C)	109.5	C(1)-C(5)-C(1)#1	129.1(9)
N(1)-C(2)-H(2D)	109.5	C(1)-C(5)-H(5A)	105.0
H(2C)-C(2)-H(2D)	109.5	C(1)#1-C(5)-H(5A)	105.0
N(1)-C(2)-H(2E)	109.5	C(1)-C(5)-H(5B)	105.0
H(2C)-C(2)-H(2E)	109.5	C(1)#1-C(5)-H(5B)	105.0
H(2D)-C(2)-H(2E)	109.5	H(5A)-C(5)-H(5B)	105.9
N(1)-C(3)-C(4)	102.4(5)	N(1)-C(3)-H(3A)	111.3

A.1.6. Compound 3-3b

Figure A.30. Molecular structure of 3-3b

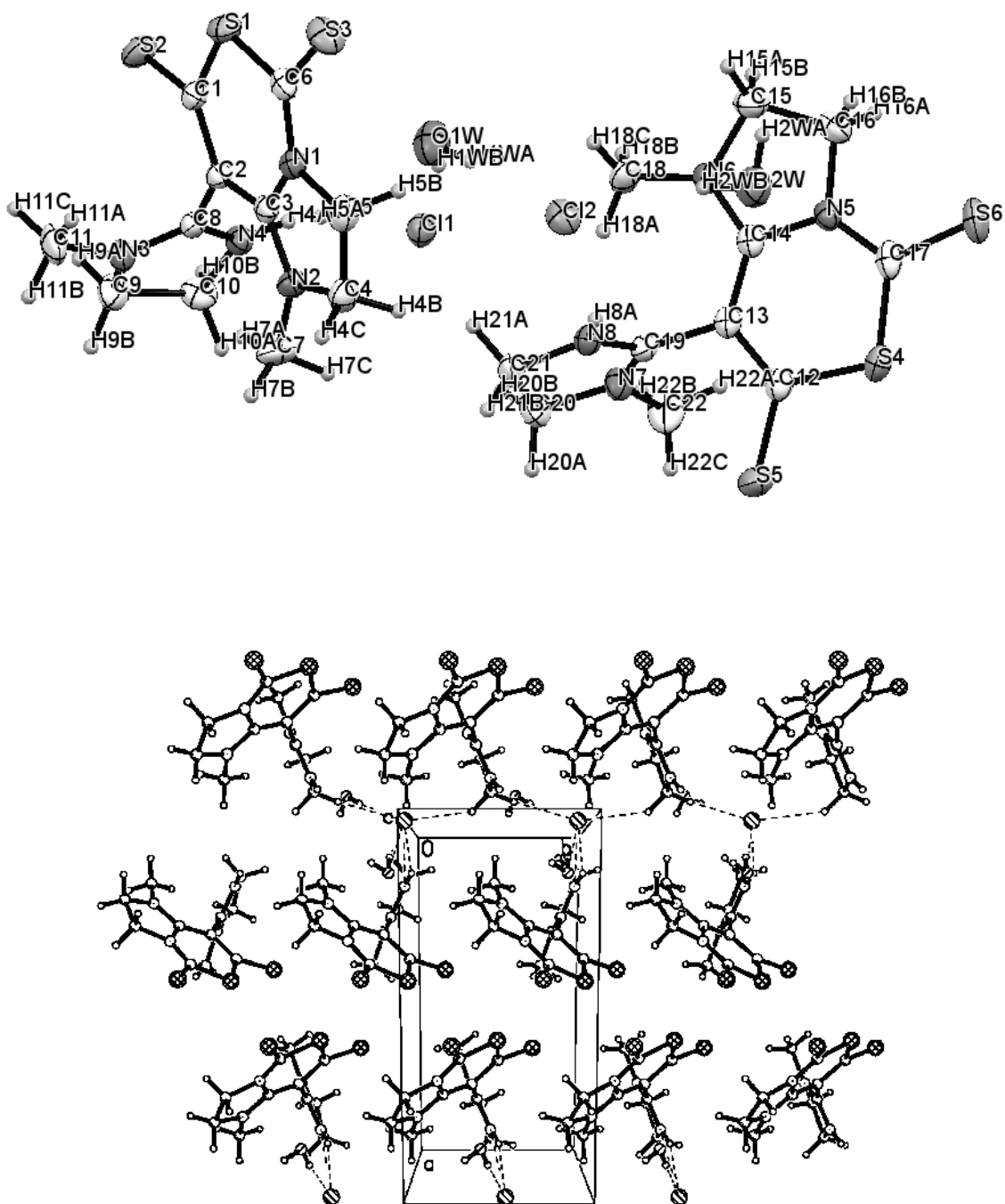


Table A.31. Crystal data and structure refinement for **3-3b**

Identification code	pj73c	
Empirical formula	C ₁₁ H ₁₇ Cl N ₄ O S ₃	
Formula weight	352.92	
Temperature	180(2) K	
Wavelength	0.71073 Å	
Crystal system	Monoclinic	
Space group	Pc	
Unit cell dimensions	a = 14.0021(2) Å	α = 90°.
	b = 6.5618(1) Å	β = 109.113(1)°.
	c = 18.1971(2) Å	γ = 90°.
Volume	1579.76(4) Å ³	
Z	4	
Density (calculated)	1.484 Mg/m ³	
Absorption coefficient	0.639 mm ⁻¹	
F(000)	736	
Crystal size	0.15 x 0.10 x 0.06 mm ³	
Theta range for data collection	2.37 to 26.00°.	
Index ranges	-17<=h<=17, -8<=k<=8, -22<=l<=22	
Reflections collected	9034	
Independent reflections	4671 [R(int) = 0.0181]	
Completeness to theta = 26.00°	99.6 %	
Absorption correction	Multi-scan	
Max. and min. transmission	0.9627 and 0.9103	
Refinement method	Full-matrix least-squares on F ²	
Data / restraints / parameters	4671 / 2 / 377	
Goodness-of-fit on F ²	1.023	
Final R indices [I>2σ(I)]	R1 = 0.0261, wR2 = 0.0691	
R indices (all data)	R1 = 0.0276, wR2 = 0.0704	
Absolute structure parameter	-0.02(5)	
Largest diff. peak and hole	0.329 and -0.288 e.Å ⁻³	

Table A.32. Atomic coordinates ($\times 10^4$) and equivalent isotropic displacement parameters ($\text{\AA}^2 \times 10^3$) for **3-3b**. $U(\text{eq})$ is defined as one third of the trace of the orthogonalized U^{ij} tensor.

	x	y	z	$U(\text{eq})$
Cl(1)	489(1)	5394(1)	6244(1)	31(1)
S(1)	-4023(1)	4919(1)	5867(1)	32(1)
S(2)	-3728(1)	6980(1)	4575(1)	37(1)
S(3)	-3946(1)	2416(1)	7195(1)	40(1)
N(1)	-2899(2)	1549(4)	6262(1)	24(1)
N(2)	-1809(2)	319(4)	5737(1)	26(1)
N(3)	-2604(2)	3270(4)	3838(1)	28(1)
N(4)	-1301(2)	4539(4)	4733(1)	25(1)
C(1)	-3410(2)	4972(4)	5167(1)	25(1)
C(2)	-2709(2)	3448(4)	5165(1)	22(1)
C(3)	-2456(2)	1812(4)	5685(1)	21(1)
C(4)	-1719(2)	-1072(5)	6383(2)	33(1)
C(5)	-2475(2)	-254(5)	6744(2)	31(1)
C(6)	-3552(2)	2803(4)	6447(1)	26(1)
C(7)	-1200(2)	-78(5)	5239(2)	36(1)
C(8)	-2202(2)	3733(4)	4573(1)	21(1)
C(9)	-1952(2)	3974(6)	3400(2)	36(1)
C(10)	-975(2)	4523(5)	4041(2)	32(1)
C(11)	-3624(2)	2527(6)	3449(2)	41(1)
Cl(2)	-239(1)	430(1)	8530(1)	35(1)
S(4)	4314(1)	118(1)	10449(1)	33(1)
S(5)	4020(1)	-1903(1)	9004(1)	37(1)
S(6)	4229(1)	2560(2)	11749(1)	41(1)
N(5)	3195(2)	3495(4)	10293(1)	25(1)
N(6)	2122(2)	4786(4)	9219(1)	27(1)
N(7)	2900(2)	1785(4)	7707(1)	30(1)
N(8)	1597(2)	519(3)	7955(1)	25(1)
C(12)	3709(2)	102(4)	9442(1)	26(1)
C(13)	3011(2)	1634(4)	9089(1)	23(1)
C(14)	2762(2)	3270(4)	9491(1)	23(1)

C(15)	2030(2)	6127(5)	9829(2)	36(1)
C(16)	2781(2)	5292(5)	10568(2)	34(1)
C(17)	3844(2)	2210(5)	10801(1)	28(1)
C(18)	1533(2)	5232(5)	8417(2)	36(1)
C(19)	2495(2)	1335(4)	8240(1)	22(1)
C(20)	2239(2)	1072(6)	6941(2)	39(1)
C(21)	1281(2)	432(5)	7101(1)	31(1)
C(22)	3918(2)	2509(6)	7826(2)	45(1)
O(1W)	-1056(2)	3987(5)	7156(2)	48(1)
O(2W)	1311(2)	1147(5)	10268(2)	47(1)

Table A.33. Bond lengths [\AA] for **3-3b**

S(1)-C(6)	1.738(3)	S(5)-C(12)	1.668(3)
S(1)-C(1)	1.754(3)	S(6)-C(17)	1.648(3)
S(2)-C(1)	1.668(3)	N(5)-C(17)	1.357(4)
S(3)-C(6)	1.648(3)	N(5)-C(14)	1.393(3)
N(1)-C(6)	1.351(3)	N(5)-C(16)	1.472(4)
N(1)-C(3)	1.395(3)	N(6)-C(14)	1.322(4)
N(1)-C(5)	1.477(4)	N(6)-C(18)	1.452(4)
N(2)-C(3)	1.317(3)	N(6)-C(15)	1.455(4)
N(2)-C(7)	1.456(4)	N(7)-C(19)	1.307(3)
N(2)-C(4)	1.461(3)	N(7)-C(22)	1.450(4)
N(3)-C(8)	1.306(3)	N(7)-C(20)	1.475(3)
N(3)-C(11)	1.454(4)	N(8)-C(19)	1.308(3)
N(3)-C(9)	1.470(3)	N(8)-C(21)	1.471(3)
N(4)-C(8)	1.310(3)	N(8)-H(8A)	0.8800
N(4)-C(10)	1.473(3)	C(12)-C(13)	1.403(4)
N(4)-H(4A)	0.8800	C(13)-C(14)	1.405(4)
C(1)-C(2)	1.401(4)	C(13)-C(19)	1.489(3)
C(2)-C(3)	1.398(4)	C(15)-C(16)	1.512(4)
C(2)-C(8)	1.484(3)	C(15)-H(15A)	0.9900
C(4)-C(5)	1.516(4)	C(15)-H(15B)	0.9900

C(4)-H(4B)	0.9900	C(16)-H(16A)	0.9900
C(4)-H(4C)	0.9900	C(16)-H(16B)	0.9900
C(5)-H(5A)	0.9900	C(18)-H(18A)	0.9800
C(5)-H(5B)	0.9900	C(18)-H(18B)	0.9800
C(7)-H(7A)	0.9800	C(18)-H(18C)	0.9800
C(7)-H(7B)	0.9800	C(20)-C(21)	1.522(4)
C(7)-H(7C)	0.9800	C(20)-H(20A)	0.9900
C(9)-C(10)	1.522(4)	C(20)-H(20B)	0.9900
C(9)-H(9A)	0.9900	C(21)-H(21A)	0.9900
C(9)-H(9B)	0.9900	C(21)-H(21B)	0.9900
C(10)-H(10A)	0.9900	C(22)-H(22A)	0.9800
C(10)-H(10B)	0.9900	C(22)-H(22B)	0.9800
C(11)-H(11A)	0.9800	C(22)-H(22C)	0.9800
C(11)-H(11B)	0.9800	O(1W)-H(1WA)	0.88(6)
C(11)-H(11C)	0.9800	O(1W)-H(1WB)	0.85(5)
S(4)-C(17)	1.733(3)	O(2W)-H(2WA)	0.86(5)
S(4)-C(12)	1.750(3)	O(2W)-H(2WB)	0.85(5)

Table A.34. Bond angles [°] for **3-3b**

C(6)-S(1)-C(1)	106.13(13)	C(17)-N(5)-C(14)	127.7(2)
C(6)-N(1)-C(3)	128.0(2)	C(17)-N(5)-C(16)	121.1(2)
C(6)-N(1)-C(5)	120.9(2)	C(14)-N(5)-C(16)	110.9(2)
C(3)-N(1)-C(5)	110.8(2)	C(14)-N(6)-C(18)	128.3(2)
C(3)-N(2)-C(7)	128.2(2)	C(14)-N(6)-C(15)	112.8(2)
C(3)-N(2)-C(4)	113.4(2)	C(18)-N(6)-C(15)	118.8(2)
C(7)-N(2)-C(4)	118.4(2)	C(19)-N(7)-C(22)	127.4(2)
C(8)-N(3)-C(11)	127.0(2)	C(19)-N(7)-C(20)	109.9(2)
C(8)-N(3)-C(9)	110.3(2)	C(22)-N(7)-C(20)	121.8(2)
C(11)-N(3)-C(9)	121.8(2)	C(19)-N(8)-C(21)	110.7(2)
C(8)-N(4)-C(10)	110.6(2)	C(19)-N(8)-H(8A)	124.7
C(8)-N(4)-H(4A)	124.7	C(21)-N(8)-H(8A)	124.7
C(10)-N(4)-H(4A)	124.7	C(13)-C(12)-S(5)	126.8(2)
C(2)-C(1)-S(2)	126.9(2)	C(13)-C(12)-S(4)	120.0(2)

C(2)-C(1)-S(1)	119.8(2)	S(5)-C(12)-S(4)	113.14(16)
S(2)-C(1)-S(1)	113.23(15)	C(12)-C(13)-C(14)	124.3(2)
C(3)-C(2)-C(1)	124.7(2)	C(12)-C(13)-C(19)	114.2(2)
C(3)-C(2)-C(8)	120.8(2)	C(14)-C(13)-C(19)	121.4(2)
C(1)-C(2)-C(8)	114.4(2)	N(6)-C(14)-N(5)	108.7(2)
N(2)-C(3)-N(1)	108.7(2)	N(6)-C(14)-C(13)	129.3(2)
N(2)-C(3)-C(2)	129.5(2)	N(5)-C(14)-C(13)	122.0(2)
N(1)-C(3)-C(2)	121.9(2)	N(6)-C(15)-C(16)	104.5(2)
N(2)-C(4)-C(5)	103.9(2)	N(6)-C(15)-H(15A)	110.9
N(2)-C(4)-H(4B)	111.0	C(16)-C(15)-H(15A)	110.9
C(5)-C(4)-H(4B)	111.0	N(6)-C(15)-H(15B)	110.9
N(2)-C(4)-H(4C)	111.0	C(16)-C(15)-H(15B)	110.9
C(5)-C(4)-H(4C)	111.0	H(15A)-C(15)-H(15B)	108.9
H(4B)-C(4)-H(4C)	109.0	N(5)-C(16)-C(15)	103.0(2)
N(1)-C(5)-C(4)	103.2(2)	N(5)-C(16)-H(16A)	111.2
N(1)-C(5)-H(5A)	111.1	C(15)-C(16)-H(16A)	111.2
C(4)-C(5)-H(5A)	111.1	N(5)-C(16)-H(16B)	111.2
N(1)-C(5)-H(5B)	111.1	C(15)-C(16)-H(16B)	111.2
C(4)-C(5)-H(5B)	111.1	H(16A)-C(16)-H(16B)	109.1
H(5A)-C(5)-H(5B)	109.1	N(5)-C(17)-S(6)	122.9(2)
N(1)-C(6)-S(3)	123.2(2)	N(5)-C(17)-S(4)	119.48(19)
N(1)-C(6)-S(1)	119.27(18)	S(6)-C(17)-S(4)	117.62(17)
S(3)-C(6)-S(1)	117.48(16)	N(6)-C(18)-H(18A)	109.5
N(2)-C(7)-H(7A)	109.5	N(6)-C(18)-H(18B)	109.5
N(2)-C(7)-H(7B)	109.5	H(18A)-C(18)-H(18B)	109.5
H(7A)-C(7)-H(7B)	109.5	N(6)-C(18)-H(18C)	109.5
N(2)-C(7)-H(7C)	109.5	H(18A)-C(18)-H(18C)	109.5
H(7A)-C(7)-H(7C)	109.5	H(18B)-C(18)-H(18C)	109.5
H(7B)-C(7)-H(7C)	109.5	N(7)-C(19)-N(8)	113.1(2)
N(3)-C(8)-N(4)	112.5(2)	N(7)-C(19)-C(13)	124.0(2)
N(3)-C(8)-C(2)	124.4(2)	N(8)-C(19)-C(13)	122.9(2)
N(4)-C(8)-C(2)	123.0(2)	N(7)-C(20)-C(21)	103.0(2)
N(3)-C(9)-C(10)	102.8(2)	N(7)-C(20)-H(20A)	111.2
N(3)-C(9)-H(9A)	111.2	C(21)-C(20)-H(20A)	111.2

C(10)-C(9)-H(9A)	111.2	N(7)-C(20)-H(20B)	111.2
N(3)-C(9)-H(9B)	111.2	C(21)-C(20)-H(20B)	111.2
C(10)-C(9)-H(9B)	111.2	H(20A)-C(20)-H(20B)	109.1
H(9A)-C(9)-H(9B)	109.1	N(8)-C(21)-C(20)	102.3(2)
N(4)-C(10)-C(9)	101.8(2)	N(8)-C(21)-H(21A)	111.3
N(4)-C(10)-H(10A)	111.4	C(20)-C(21)-H(21A)	111.3
C(9)-C(10)-H(10A)	111.4	N(8)-C(21)-H(21B)	111.3
N(4)-C(10)-H(10B)	111.4	C(20)-C(21)-H(21B)	111.3
C(9)-C(10)-H(10B)	111.4	H(21A)-C(21)-H(21B)	109.2
H(10A)-C(10)-H(10B)	109.3	N(7)-C(22)-H(22A)	109.5
N(3)-C(11)-H(11A)	109.5	N(7)-C(22)-H(22B)	109.5
N(3)-C(11)-H(11B)	109.5	H(22A)-C(22)-H(22B)	109.5
H(11A)-C(11)-H(11B)	109.5	N(7)-C(22)-H(22C)	109.5
N(3)-C(11)-H(11C)	109.5	H(22A)-C(22)-H(22C)	109.5
H(11A)-C(11)-H(11C)	109.5	H(22B)-C(22)-H(22C)	109.5
H(11B)-C(11)-H(11C)	109.5	H(1WA)-O(1W)-H(1WB)	107(4)
C(17)-S(4)-C(12)	106.22(13)	H(2WA)-O(2W)-H(2WB)	100(5)

A.1.7. Compound 3-3c

Figure A.35. Molecular structure of 3-3c

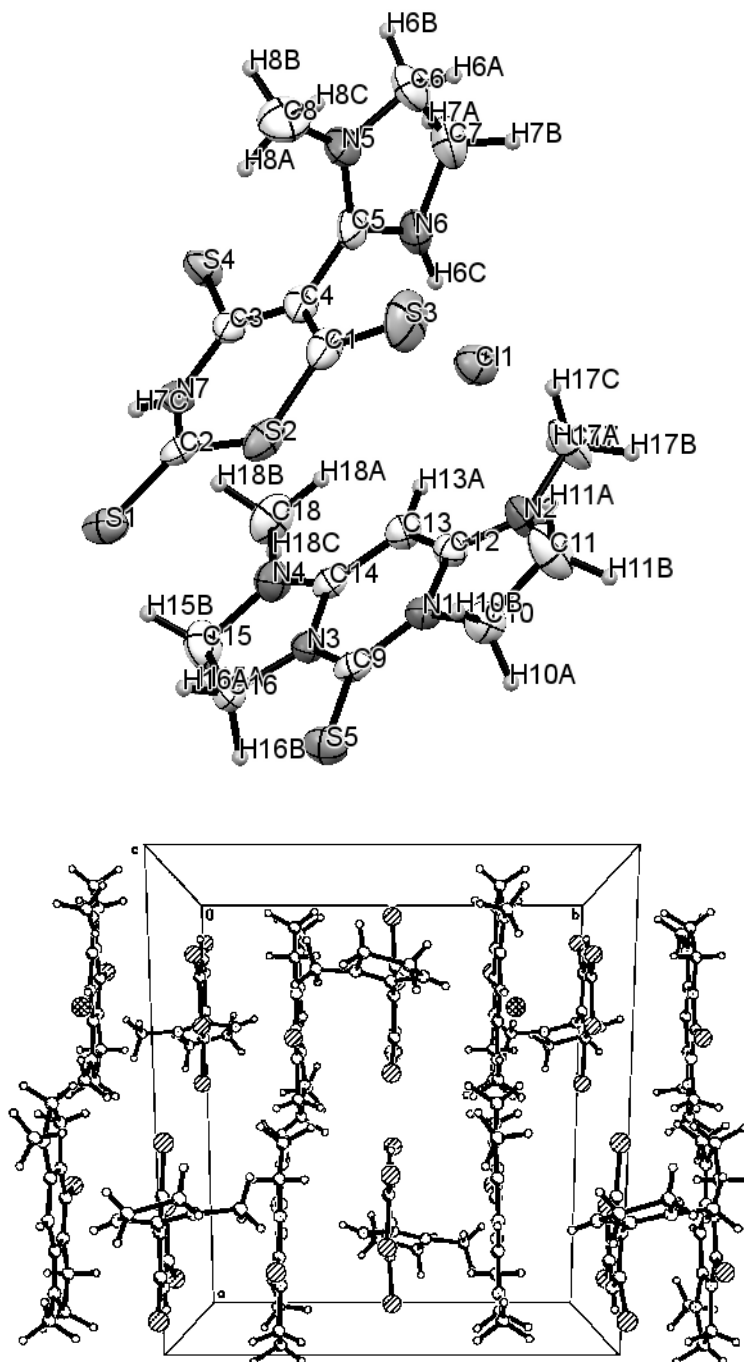


Table A.36. Crystal data and structure refinement for **3-3c**

Identification code	pj75a	
Empirical formula	C _{19.63} H _{25.63} Cl _{5.88} N ₇ S ₅	
Formula weight	728.16	
Temperature	180(2) K	
Wavelength	0.71073 Å	
Crystal system	Monoclinic	
Space group	P2(1)/n	
Unit cell dimensions	a = 15.6611(11) Å	α = 90°.
	b = 13.860(1) Å	β = 108.081(1)°.
	c = 16.5632(12) Å	γ = 90°.
Volume	3417.8(4) Å ³	
Z	4	
Density (calculated)	1.415 Mg/m ³	
Absorption coefficient	0.822 mm ⁻¹	
F(000)	1489	
Crystal size	0.30 x 0.30 x 0.15 mm ³	
Theta range for data collection	2.01 to 26.00°.	
Index ranges	-19<=h<=19, -17<=k<=17, -20<=l<=20	
Reflections collected	42220	
Independent reflections	6719 [R(int) = 0.0331]	
Completeness to theta = 26.00°	99.9 %	
Absorption correction	Multi-scan	
Max. and min. transmission	0.8866 and 0.7906	
Refinement method	Full-matrix least-squares on F ²	
Data / restraints / parameters	6719 / 0 / 250	
Goodness-of-fit on F ²	1.060	
Final R indices [I>2sigma(I)]	R1 = 0.0593, wR2 = 0.1709	
R indices (all data)	R1 = 0.0703, wR2 = 0.1786	
Largest diff. peak and hole	0.498 and -0.483 e.Å ⁻³	

Table A.37. Atomic coordinates ($\times 10^4$) and equivalent isotropic displacement parameters ($\text{\AA}^2 \times 10^3$) for **3-3c**. $U(\text{eq})$ is defined as one third of the trace of the orthogonalized U^{ij} tensor.

	x	y	z	$U(\text{eq})$
Cl(1)	7784(1)	7155(1)	11174(1)	44(1)
N(1)	6231(2)	7415(2)	7409(2)	29(1)
N(2)	5632(2)	7277(2)	8443(2)	39(1)
N(3)	7736(2)	7413(2)	7569(2)	28(1)
N(4)	8825(2)	7401(2)	8779(2)	38(1)
N(5)	7003(2)	10842(2)	10830(2)	45(1)
N(6)	7135(2)	9282(2)	10987(2)	49(1)
N(7)	8656(1)	9910(1)	9108(1)	30(1)
S(1)	8630(1)	9962(1)	7504(1)	43(1)
S(2)	7013(1)	9880(1)	8006(1)	41(1)
S(3)	5659(1)	9996(1)	8841(1)	66(1)
S(4)	9181(1)	10016(1)	10779(1)	37(1)
S(5)	6652(1)	7414(1)	5975(1)	41(1)
C(1)	6757(1)	9936(1)	8964(1)	38(1)
C(2)	8173(1)	9921(1)	8285(1)	31(1)
C(3)	8383(1)	9951(1)	9825(1)	30(1)
C(4)	7455(1)	9961(1)	9741(1)	33(1)
C(5)	7207(1)	10030(1)	10520(1)	39(1)
C(6)	6681(1)	10645(1)	11559(1)	57(1)
C(7)	6952(3)	9602(3)	11761(3)	63(1)
C(8)	6939(3)	11787(3)	10445(3)	63(1)
C(9)	6881(2)	7411(2)	7014(2)	29(1)
C(10)	5255(2)	7379(3)	6958(2)	39(1)
C(11)	4855(2)	7354(4)	7683(2)	58(1)
C(12)	6407(2)	7354(2)	8277(2)	29(1)
C(13)	7278(2)	7358(2)	8824(2)	30(1)
C(14)	7950(2)	7391(2)	8440(2)	29(1)
C(15)	9298(2)	7462(3)	8148(3)	45(1)
C(16)	8544(2)	7429(2)	7301(2)	36(1)
C(17)	5553(3)	7266(4)	9296(2)	55(1)

C(18)

9309(2)

7438(3)

9684(2)

49(1)

Table A.38. Bond lengths [\AA] for **3-3c**

N(1)-C(9)	1.369(4)	C(4)-C(5)	1.4618
N(1)-C(12)	1.379(4)	C(6)-C(7)	1.514(5)
N(1)-C(10)	1.480(4)	C(6)-H(6A)	0.9900
N(2)-C(12)	1.330(4)	C(6)-H(6B)	0.9900
N(2)-C(17)	1.456(4)	C(7)-H(7A)	0.9900
N(2)-C(11)	1.459(4)	C(7)-H(7B)	0.9900
N(3)-C(9)	1.368(4)	C(8)-H(8A)	0.9800
N(3)-C(14)	1.377(4)	C(8)-H(8B)	0.9800
N(3)-C(16)	1.466(4)	C(8)-H(8C)	0.9800
N(4)-C(14)	1.310(4)	C(10)-C(11)	1.517(5)
N(4)-C(18)	1.456(5)	C(10)-H(10A)	0.9900
N(4)-C(15)	1.459(5)	C(10)-H(10B)	0.9900
N(5)-C(5)	1.317(3)	C(11)-H(11A)	0.9900
N(5)-C(8)	1.446(5)	C(11)-H(11B)	0.9900
N(5)-C(6)	1.472(3)	C(12)-C(13)	1.384(4)
N(6)-C(5)	1.319(3)	C(13)-C(14)	1.389(4)
N(6)-C(7)	1.467(5)	C(13)-H(13A)	0.9500
N(6)-H(6C)	0.8800	C(15)-C(16)	1.528(5)
N(7)-C(2)	1.3386	C(15)-H(15A)	0.9900
N(7)-C(3)	1.3836	C(15)-H(15B)	0.9900
N(7)-H(7C)	0.8800	C(16)-H(16A)	0.9900
S(1)-C(2)	1.6632	C(16)-H(16B)	0.9900
S(2)-C(2)	1.7301	C(17)-H(17A)	0.9800
S(2)-C(1)	1.7548	C(17)-H(17B)	0.9800
S(3)-C(1)	1.6700	C(17)-H(17C)	0.9800
S(4)-C(3)	1.6848	C(18)-H(18A)	0.9800
S(5)-C(9)	1.645(3)	C(18)-H(18B)	0.9800
C(1)-C(4)	1.4067	C(18)-H(18C)	0.9800
C(3)-C(4)	1.4157		

Table A.39. Bond angles [°] for **3-3c**

C(9)-N(1)-C(12)	124.0(3)	N(5)-C(8)-H(8C)	109.5
C(9)-N(1)-C(10)	124.3(3)	H(8A)-C(8)-H(8C)	109.5
C(12)-N(1)-C(10)	111.4(3)	H(8B)-C(8)-H(8C)	109.5
C(12)-N(2)-C(17)	124.0(3)	N(3)-C(9)-N(1)	113.4(3)
C(12)-N(2)-C(11)	112.7(3)	N(3)-C(9)-S(5)	123.5(2)
C(17)-N(2)-C(11)	122.6(3)	N(1)-C(9)-S(5)	123.1(2)
C(9)-N(3)-C(14)	124.9(3)	N(1)-C(10)-C(11)	102.6(3)
C(9)-N(3)-C(16)	123.6(3)	N(1)-C(10)-H(10A)	111.3
C(14)-N(3)-C(16)	111.4(3)	C(11)-C(10)-H(10A)	111.3
C(14)-N(4)-C(18)	125.6(3)	N(1)-C(10)-H(10B)	111.3
C(14)-N(4)-C(15)	112.9(3)	C(11)-C(10)-H(10B)	111.3
C(18)-N(4)-C(15)	121.3(3)	H(10A)-C(10)-H(10B)	109.2
C(5)-N(5)-C(8)	126.5(3)	N(2)-C(11)-C(10)	104.2(3)
C(5)-N(5)-C(6)	110.3(2)	N(2)-C(11)-H(11A)	110.9
C(8)-N(5)-C(6)	122.3(3)	C(10)-C(11)-H(11A)	110.9
C(5)-N(6)-C(7)	110.5(3)	N(2)-C(11)-H(11B)	110.9
C(5)-N(6)-H(6C)	124.8	C(10)-C(11)-H(11B)	110.9
C(7)-N(6)-H(6C)	124.8	H(11A)-C(11)-H(11B)	108.9
C(2)-N(7)-C(3)	130.3	N(2)-C(12)-N(1)	108.7(3)
C(2)-N(7)-H(7C)	114.9	N(2)-C(12)-C(13)	129.9(3)
C(3)-N(7)-H(7C)	114.9	N(1)-C(12)-C(13)	121.3(3)
C(2)-S(2)-C(1)	105.8	C(12)-C(13)-C(14)	115.6(3)
C(4)-C(1)-S(3)	126.0	C(12)-C(13)-H(13A)	122.2
C(4)-C(1)-S(2)	119.9	C(14)-C(13)-H(13A)	122.2
S(3)-C(1)-S(2)	114.0	N(4)-C(14)-N(3)	109.3(3)
N(7)-C(2)-S(1)	123.3	N(4)-C(14)-C(13)	130.1(3)
N(7)-C(2)-S(2)	119.1	N(3)-C(14)-C(13)	120.5(3)
S(1)-C(2)-S(2)	117.6	N(4)-C(15)-C(16)	103.7(3)
N(7)-C(3)-C(4)	119.8	N(4)-C(15)-H(15A)	111.0
N(7)-C(3)-S(4)	118.1	C(16)-C(15)-H(15A)	111.0
C(4)-C(3)-S(4)	122.1	N(4)-C(15)-H(15B)	111.0
C(1)-C(4)-C(3)	124.9	C(16)-C(15)-H(15B)	111.0

C(1)-C(4)-C(5)	117.8	H(15A)-C(15)-H(15B)	109.0
C(3)-C(4)-C(5)	117.3	N(3)-C(16)-C(15)	102.5(3)
N(5)-C(5)-N(6)	111.6(2)	N(3)-C(16)-H(16A)	111.3
N(5)-C(5)-C(4)	124.22(14)	C(15)-C(16)-H(16A)	111.3
N(6)-C(5)-C(4)	124.12(14)	N(3)-C(16)-H(16B)	111.3
N(5)-C(6)-C(7)	102.41(19)	C(15)-C(16)-H(16B)	111.3
N(5)-C(6)-H(6A)	111.3	H(16A)-C(16)-H(16B)	109.2
C(7)-C(6)-H(6A)	111.3	N(2)-C(17)-H(17A)	109.5
N(5)-C(6)-H(6B)	111.3	N(2)-C(17)-H(17B)	109.5
C(7)-C(6)-H(6B)	111.3	H(17A)-C(17)-H(17B)	109.5
H(6A)-C(6)-H(6B)	109.2	N(2)-C(17)-H(17C)	109.5
N(6)-C(7)-C(6)	102.3(3)	H(17A)-C(17)-H(17C)	109.5
N(6)-C(7)-H(7A)	111.3	H(17B)-C(17)-H(17C)	109.5
C(6)-C(7)-H(7A)	111.3	N(4)-C(18)-H(18A)	109.5
N(6)-C(7)-H(7B)	111.3	N(4)-C(18)-H(18B)	109.5
C(6)-C(7)-H(7B)	111.3	H(18A)-C(18)-H(18B)	109.5
H(7A)-C(7)-H(7B)	109.2	N(4)-C(18)-H(18C)	109.5
N(5)-C(8)-H(8A)	109.5	H(18A)-C(18)-H(18C)	109.5
N(5)-C(8)-H(8B)	109.5	H(18B)-C(18)-H(18C)	109.5
H(8A)-C(8)-H(8B)	109.5		

A.1.8. Compound 3-4a

Figure A.40. Molecular structure of 3-4a

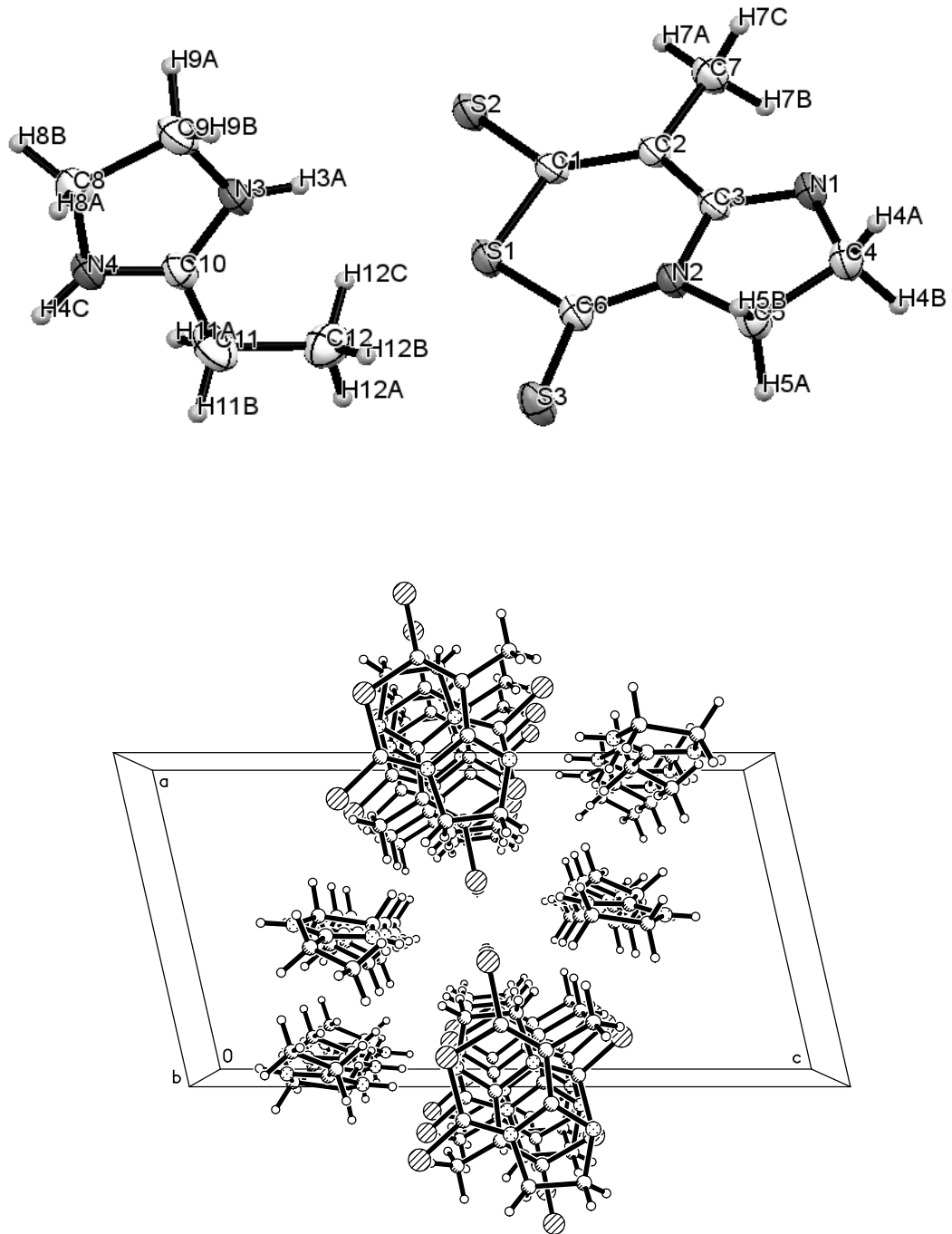


Table A.41. Crystal data and structure refinement for **3-4a**

Identification code	pj43	
Empirical formula	C ₁₂ H ₁₇ N ₄ S ₃	
Formula weight	313.48	
Temperature	180(2) K	
Wavelength	0.71073 Å	
Crystal system	Monoclinic	
Space group	P2(1)/n	
Unit cell dimensions	a = 9.9496(3) Å	α = 90°.
	b = 7.8669(3) Å	β = 102.783(2)°.
	c = 19.1610(5) Å	γ = 90°.
Volume	1462.61(8) Å ³	
Z	4	
Density (calculated)	1.424 Mg/m ³	
Absorption coefficient	0.499 mm ⁻¹	
F(000)	660	
Crystal size	0.30 x 0.20 x 0.08 mm ³	
Theta range for data collection	2.14 to 26.00°.	
Index ranges	-12 ≤ h ≤ 12, -9 ≤ k ≤ 9, -23 ≤ l ≤ 23	
Reflections collected	5509	
Independent reflections	2853 [R(int) = 0.0151]	
Completeness to theta = 26.00°	99.2 %	
Absorption correction	Multi-scan	
Max. and min. transmission	0.9612 and 0.8648	
Refinement method	Full-matrix least-squares on F ²	
Data / restraints / parameters	2853 / 0 / 172	
Goodness-of-fit on F ²	1.067	
Final R indices [I > 2σ(I)]	R1 = 0.0288, wR2 = 0.0720	
R indices (all data)	R1 = 0.0332, wR2 = 0.0754	
Largest diff. peak and hole	0.399 and -0.224 e.Å ⁻³	

Table A.42. Atomic coordinates ($\times 10^4$) and equivalent isotropic displacement parameters ($\text{\AA}^2 \times 10^3$) for **3-4a**. $U(\text{eq})$ is defined as one third of the trace of the orthogonalized U^{ij} tensor.

	x	y	z	U(eq)
S(1)	6218(1)	8051(1)	-920(1)	27(1)
S(2)	8863(1)	7226(1)	-45(1)	32(1)
S(3)	3346(1)	8653(1)	-1636(1)	32(1)
N(1)	4332(1)	6881(2)	872(1)	26(1)
N(2)	4127(1)	7698(2)	-277(1)	24(1)
N(3)	9530(2)	8421(2)	-1585(1)	28(1)
N(4)	9860(1)	8858(2)	-2661(1)	28(1)
C(1)	7135(2)	7369(2)	-67(1)	23(1)
C(2)	6466(2)	7026(2)	471(1)	22(1)
C(3)	5002(2)	7189(2)	379(1)	22(1)
C(4)	2853(2)	7147(2)	581(1)	31(1)
C(5)	2692(2)	7739(2)	-192(1)	30(1)
C(6)	4481(2)	8105(2)	-893(1)	24(1)
C(7)	7238(2)	6460(2)	1200(1)	29(1)
C(8)	10106(2)	10532(2)	-2331(1)	32(1)
C(9)	9873(2)	10226(2)	-1574(1)	35(1)
C(10)	9550(2)	7746(2)	-2213(1)	26(1)
C(11)	9262(2)	5927(3)	-2405(1)	43(1)
C(12)	8711(2)	4895(2)	-1869(1)	38(1)

Table A.43. Bond lengths [\AA] for **3-4a**

S(1)-C(6)	1.7402(16)	C(4)-H(4A)	0.9900
S(1)-C(1)	1.7699(16)	C(4)-H(4B)	0.9900
S(2)-C(1)	1.7141(16)	C(5)-H(5A)	0.9900
S(3)-C(6)	1.6661(16)	C(5)-H(5B)	0.9900
N(1)-C(3)	1.2940(19)	C(7)-H(7A)	0.9800
N(1)-C(4)	1.469(2)	C(7)-H(7B)	0.9800
N(2)-C(6)	1.3426(19)	C(7)-H(7C)	0.9800
N(2)-C(3)	1.420(2)	C(8)-C(9)	1.537(2)
N(2)-C(5)	1.474(2)	C(8)-H(8A)	0.9900
N(3)-C(10)	1.320(2)	C(8)-H(8B)	0.9900
N(3)-C(9)	1.459(2)	C(9)-H(9A)	0.9900
N(3)-H(3A)	0.8800	C(9)-H(9B)	0.9900
N(4)-C(10)	1.309(2)	C(10)-C(11)	1.489(3)
N(4)-C(8)	1.459(2)	C(11)-C(12)	1.505(3)
N(4)-H(4C)	0.8800	C(11)-H(11A)	0.9900
C(1)-C(2)	1.372(2)	C(11)-H(11B)	0.9900
C(2)-C(3)	1.434(2)	C(12)-H(12A)	0.9800
C(2)-C(7)	1.505(2)	C(12)-H(12B)	0.9800
C(4)-C(5)	1.526(2)	C(12)-H(12C)	0.9800

Table A.44. Bond angles [$^{\circ}$] for **3-4a**

C(6)-S(1)-C(1)	107.00(7)	S(3)-C(6)-S(1)	118.07(9)
C(3)-N(1)-C(4)	109.27(13)	C(2)-C(7)-H(7A)	109.5
C(6)-N(2)-C(3)	128.14(14)	C(2)-C(7)-H(7B)	109.5
C(6)-N(2)-C(5)	122.80(13)	H(7A)-C(7)-H(7B)	109.5
C(3)-N(2)-C(5)	109.06(12)	C(2)-C(7)-H(7C)	109.5
C(10)-N(3)-C(9)	110.72(14)	H(7A)-C(7)-H(7C)	109.5
C(10)-N(3)-H(3A)	124.6	H(7B)-C(7)-H(7C)	109.5
C(9)-N(3)-H(3A)	124.6	N(4)-C(8)-C(9)	102.78(14)
C(10)-N(4)-C(8)	111.13(13)	N(4)-C(8)-H(8A)	111.2
C(10)-N(4)-H(4C)	124.4	C(9)-C(8)-H(8A)	111.2

C(8)-N(4)-H(4C)	124.4	N(4)-C(8)-H(8B)	111.2
C(2)-C(1)-S(2)	128.27(13)	C(9)-C(8)-H(8B)	111.2
C(2)-C(1)-S(1)	121.12(12)	H(8A)-C(8)-H(8B)	109.1
S(2)-C(1)-S(1)	110.62(8)	N(3)-C(9)-C(8)	102.90(13)
C(1)-C(2)-C(3)	122.62(14)	N(3)-C(9)-H(9A)	111.2
C(1)-C(2)-C(7)	121.49(15)	C(8)-C(9)-H(9A)	111.2
C(3)-C(2)-C(7)	115.89(13)	N(3)-C(9)-H(9B)	111.2
N(1)-C(3)-N(2)	112.73(14)	C(8)-C(9)-H(9B)	111.2
N(1)-C(3)-C(2)	124.55(15)	H(9A)-C(9)-H(9B)	109.1
N(2)-C(3)-C(2)	122.72(13)	N(4)-C(10)-N(3)	112.47(15)
N(1)-C(4)-C(5)	107.10(13)	N(4)-C(10)-C(11)	122.67(15)
N(1)-C(4)-H(4A)	110.3	N(3)-C(10)-C(11)	124.86(15)
C(5)-C(4)-H(4A)	110.3	C(10)-C(11)-C(12)	115.42(15)
N(1)-C(4)-H(4B)	110.3	C(10)-C(11)-H(11A)	108.4
C(5)-C(4)-H(4B)	110.3	C(12)-C(11)-H(11A)	108.4
H(4A)-C(4)-H(4B)	108.5	C(10)-C(11)-H(11B)	108.4
N(2)-C(5)-C(4)	101.80(13)	C(12)-C(11)-H(11B)	108.4
N(2)-C(5)-H(5A)	111.4	H(11A)-C(11)-H(11B)	107.5
C(4)-C(5)-H(5A)	111.4	C(11)-C(12)-H(12A)	109.5
N(2)-C(5)-H(5B)	111.4	C(11)-C(12)-H(12B)	109.5
C(4)-C(5)-H(5B)	111.4	H(12A)-C(12)-H(12B)	109.5
H(5A)-C(5)-H(5B)	109.3	C(11)-C(12)-H(12C)	109.5
N(2)-C(6)-S(3)	123.55(12)	H(12A)-C(12)-H(12C)	109.5
N(2)-C(6)-S(1)	118.38(12)	H(12B)-C(12)-H(12C)	109.5

A.1.9. Tetramethylthiourea

Figure A.45. Molecular structure of tetramethylthiourea

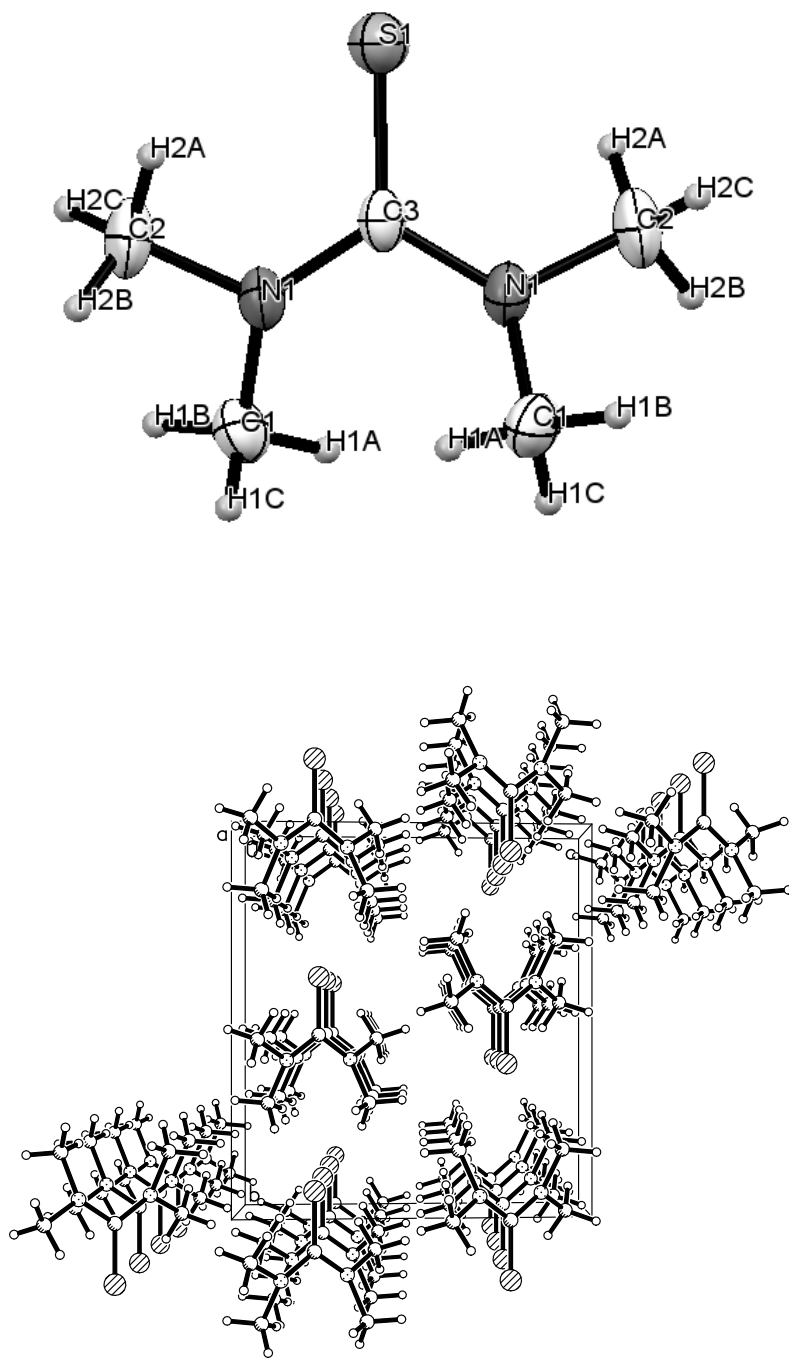


Table A.46. Crystal data and structure refinement for pj40

Identification code	pj40	
Empirical formula	C ₅ H ₁₂ N ₂ S	
Formula weight	132.23	
Temperature	180(2) K	
Wavelength	0.71073 Å	
Crystal system	Monoclinic	
Space group	C2/c	
Unit cell dimensions	a = 5.491(2) Å	α = 90°.
	b = 12.039(5) Å	β = 95.441(6)°.
	c = 10.986(5) Å	γ = 90°.
Volume	723.0(5) Å ³	
Z	4	
Density (calculated)	1.215 Mg/m ³	
Absorption coefficient	0.352 mm ⁻¹	
F(000)	288	
Crystal size	0.20 x 0.15 x 0.10 mm ³	
Theta range for data collection	3.38 to 25.50°.	
Index ranges	-6 ≤ h ≤ 6, -13 ≤ k ≤ 14, -13 ≤ l ≤ 11	
Reflections collected	1275	
Independent reflections	664 [R(int) = 0.0163]	
Completeness to theta = 25.50°	98.1 %	
Absorption correction	Multi-scan	
Max. and min. transmission	0.9657 and 0.9329	
Refinement method	Full-matrix least-squares on F ²	
Data / restraints / parameters	664 / 0 / 40	
Goodness-of-fit on F ²	1.090	
Final R indices [I > 2σ(I)]	R1 = 0.0359, wR2 = 0.0929	
R indices (all data)	R1 = 0.0420, wR2 = 0.0995	
Largest diff. peak and hole	0.362 and -0.159 e.Å ⁻³	

Table A.47. Atomic coordinates ($\times 10^4$) and equivalent isotropic displacement parameters ($\text{\AA}^2 \times 10^3$) for pj40. $U(\text{eq})$ is defined as one third of the trace of the orthogonalized U^{ij} tensor.

	x	y	z	$U(\text{eq})$
S(1)	0	-1052(1)	2500	41(1)
N(1)	1159(3)	947(1)	1686(1)	33(1)
C(1)	162(4)	1990(2)	1169(2)	39(1)
C(2)	3014(4)	447(2)	992(2)	42(1)
C(3)	0	346(2)	2500	29(1)

Table A.48. Bond lengths [\AA] for pj40

S(1)-C(3)	1.683(3)	C(1)-H(1C)	0.9800
N(1)-C(3)	1.355(2)	C(2)-H(2A)	0.9800
N(1)-C(2)	1.459(2)	C(2)-H(2B)	0.9800
N(1)-C(1)	1.463(2)	C(2)-H(2C)	0.9800
C(1)-H(1A)	0.9800	C(3)-N(1)#1	1.355(2)
C(1)-H(1B)	0.9800		

Table A.49. Bond angles [$^\circ$] for pj40

C(3)-N(1)-C(2)	121.29(17)	N(1)-C(2)-H(2A)	109.5
C(3)-N(1)-C(1)	122.21(15)	N(1)-C(2)-H(2B)	109.5
C(2)-N(1)-C(1)	113.89(15)	H(2A)-C(2)-H(2B)	109.5
N(1)-C(1)-H(1A)	109.5	N(1)-C(2)-H(2C)	109.5
N(1)-C(1)-H(1B)	109.5	H(2A)-C(2)-H(2C)	109.5
H(1A)-C(1)-H(1B)	109.5	H(2B)-C(2)-H(2C)	109.5
N(1)-C(1)-H(1C)	109.5	N(1)-C(3)-N(1)#1	115.4(2)
H(1A)-C(1)-H(1C)	109.5	N(1)-C(3)-S(1)	122.29(11)
H(1B)-C(1)-H(1C)	109.5	N(1)#1-C(3)-S(1)	122.29(11)

A.1.10 Compound 3-9a and 3-10

Figure A.50. Molecular structure of 3-9a

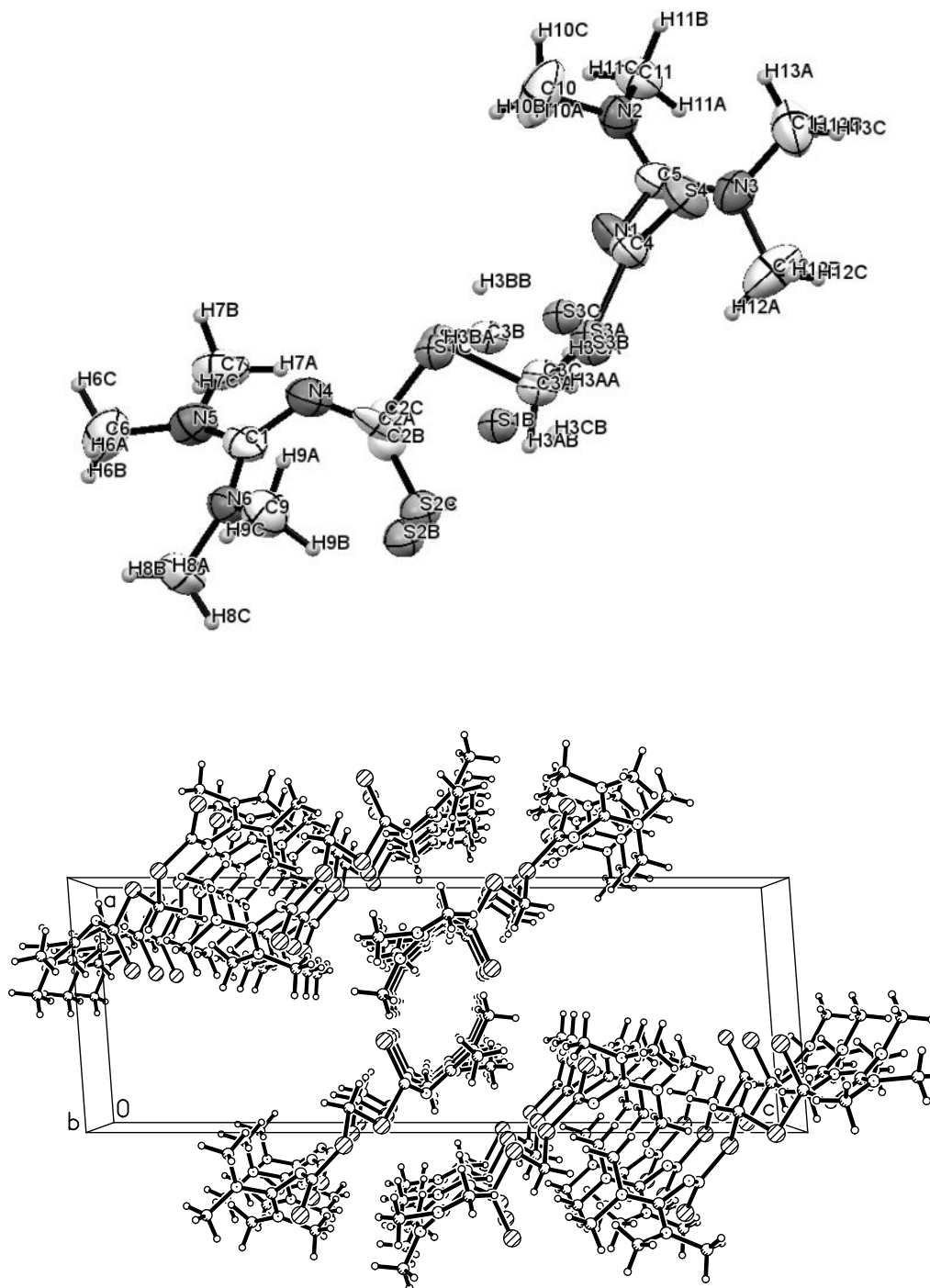


Table A.51. Crystal data and structure refinement for **3-9a**

Identification code	pj25	
Empirical formula	C13 H26 N6 S4	
Formula weight	394.64	
Temperature	180(2) K	
Wavelength	0.71073 Å	
Crystal system	Monoclinic	
Space group	P2(1)/c	
Unit cell dimensions	a = 9.4672(7) Å	$\alpha = 90^\circ$.
	b = 7.9457(5) Å	$\beta = 94.234(5)^\circ$.
	c = 26.707(2) Å	$\gamma = 90^\circ$.
Volume	2003.5(2) Å ³	
Z	4	
Density (calculated)	1.308 Mg/m ³	
Absorption coefficient	0.481 mm ⁻¹	
F(000)	840	
Crystal size	0.30 x 0.10 x 0.06 mm ³	
Theta range for data collection	3.06 to 26.00°.	
Index ranges	-11<=h<=11, -9<=k<=9, -32<=l<=21	
Reflections collected	8105	
Independent reflections	3889 [R(int) = 0.0669]	
Completeness to theta = 26.00°	98.8 %	
Absorption correction	Multi-scan	
Max. and min. transmission	0.9717 and 0.8690	
Refinement method	Full-matrix least-squares on F ²	
Data / restraints / parameters	3889 / 40 / 245	
Goodness-of-fit on F ²	1.049	
Final R indices [I>2sigma(I)]	R1 = 0.0780, wR2 = 0.1977	
R indices (all data)	R1 = 0.1331, wR2 = 0.2331	
Largest diff. peak and hole	0.732 and -0.392 e.Å ⁻³	

Table A.52. Atomic coordinates ($\times 10^4$) and equivalent isotropic displacement parameters ($\text{\AA}^2 \times 10^3$) for **3-9a**. $U(\text{eq})$ is defined as one third of the trace of the orthogonalized U^{ij} tensor.

	x	y	z	$U(\text{eq})$
N(1)	11309(5)	10128(6)	1976(2)	60(1)
N(2)	13045(5)	8404(6)	2356(2)	52(1)
N(3)	11809(5)	10231(6)	2837(2)	56(1)
N(4)	8393(5)	7095(8)	242(2)	63(1)
N(5)	7584(5)	4733(7)	-185(2)	60(1)
N(6)	6707(5)	7359(6)	-440(2)	50(1)
S(1A)	9562(4)	9024(5)	867(1)	48(1)
S(2A)	6365(17)	8470(30)	751(7)	50(2)
S(3A)	10151(4)	12406(8)	1351(2)	48(1)
S(1B)	8061(7)	9801(10)	1106(3)	48(1)
S(2B)	5708(9)	7807(12)	734(3)	50(2)
S(3B)	9916(11)	12330(20)	1379(6)	48(1)
S(1C)	9506(10)	9448(11)	747(3)	48(1)
S(2C)	6410(30)	8660(70)	710(17)	50(2)
S(3C)	10538(8)	12180(10)	1202(3)	48(1)
S(4)	12667(2)	13122(2)	1970(1)	59(1)
C(1)	7535(5)	6399(9)	-116(2)	54(2)
C(2A)	7994(13)	8228(15)	522(5)	44(4)
C(3A)	8840(17)	10600(20)	1264(7)	50(3)
C(2B)	7600(20)	8030(40)	617(13)	44(12)
C(3B)	9894(18)	10400(30)	968(9)	50(3)
C(2C)	8090(20)	7930(30)	632(8)	30(9)
C(3C)	9080(50)	10630(50)	1306(16)	50(3)
C(4)	11446(6)	11645(8)	1809(2)	54(2)
C(5)	12089(6)	9627(7)	2392(2)	46(1)
C(6)	7422(8)	3939(9)	-679(2)	76(2)
C(7)	8229(6)	3695(10)	219(2)	72(2)
C(8)	5392(6)	6743(10)	-692(2)	71(2)
C(9)	6933(7)	9153(9)	-486(2)	68(2)
C(10)	13609(10)	8060(10)	1873(3)	95(3)

C(11)	13357(6)	7129(8)	2744(2)	62(2)
C(12)	10521(8)	11260(10)	2891(3)	86(2)
C(13)	12863(8)	10335(10)	3260(2)	80(2)

Table A.53. Bond lengths [Å] for **3-9a**

N(1)-C(4)	1.294(7)	S(3C)-C(3C)	1.883(17)
N(1)-C(5)	1.349(6)	S(4)-C(4)	1.680(6)
N(2)-C(5)	1.336(7)	C(3A)-H(3AA)	0.9900
N(2)-C(10)	1.458(7)	C(3A)-H(3AB)	0.9900
N(2)-C(11)	1.463(7)	C(3B)-H(3BA)	0.9900
N(3)-C(5)	1.326(7)	C(3B)-H(3BB)	0.9900
N(3)-C(13)	1.453(8)	C(3C)-H(3CA)	0.9900
N(3)-C(12)	1.483(8)	C(3C)-H(3CB)	0.9900
N(4)-C(2A)	1.247(11)	C(6)-H(6A)	0.9800
N(4)-C(2C)	1.284(16)	C(6)-H(6B)	0.9800
N(4)-C(1)	1.328(7)	C(6)-H(6C)	0.9800
N(4)-C(2B)	1.495(15)	C(7)-H(7A)	0.9800
N(5)-C(1)	1.338(8)	C(7)-H(7B)	0.9800
N(5)-C(7)	1.456(7)	C(7)-H(7C)	0.9800
N(5)-C(6)	1.460(8)	C(8)-H(8A)	0.9800
N(6)-C(1)	1.358(7)	C(8)-H(8B)	0.9800
N(6)-C(9)	1.448(8)	C(8)-H(8C)	0.9800
N(6)-C(8)	1.455(7)	C(9)-H(9A)	0.9800
S(1A)-C(2A)	1.803(10)	C(9)-H(9B)	0.9800
S(1A)-C(3A)	1.811(11)	C(9)-H(9C)	0.9800
S(2A)-C(2A)	1.711(14)	C(10)-H(10A)	0.9800
S(3A)-C(4)	1.774(7)	C(10)-H(10B)	0.9800
S(3A)-C(3A)	1.897(10)	C(10)-H(10C)	0.9800
S(1B)-C(3B)	1.862(15)	C(11)-H(11A)	0.9800
S(1B)-C(2B)	1.950(15)	C(11)-H(11B)	0.9800
S(2B)-C(2B)	1.845(17)	C(11)-H(11C)	0.9800
S(3B)-C(4)	1.863(13)	C(12)-H(12A)	0.9800

S(3B)-C(3B)	1.885(16)	C(12)-H(12B)	0.9800
S(1C)-C(2C)	1.815(15)	C(12)-H(12C)	0.9800
S(1C)-C(3C)	1.836(16)	C(13)-H(13A)	0.9800
S(2C)-C(2C)	1.722(18)	C(13)-H(13B)	0.9800
S(3C)-C(4)	1.829(8)	C(13)-H(13C)	0.9800

Table A.54. Bond angles [°] for **3-9a**

C(4)-N(1)-C(5)	119.7(5)	N(1)-C(4)-S(3C)	117.9(5)
C(5)-N(2)-C(10)	119.6(5)	S(4)-C(4)-S(3C)	109.5(4)
C(5)-N(2)-C(11)	123.7(5)	S(3A)-C(4)-S(3C)	18.7(2)
C(10)-N(2)-C(11)	115.4(5)	N(1)-C(4)-S(3B)	113.0(7)
C(5)-N(3)-C(13)	123.0(5)	S(4)-C(4)-S(3B)	116.2(7)
C(5)-N(3)-C(12)	120.5(5)	S(3A)-C(4)-S(3B)	7.3(6)
C(13)-N(3)-C(12)	114.6(5)	S(3C)-C(4)-S(3B)	24.7(5)
C(2A)-N(4)-C(2C)	17.4(14)	N(3)-C(5)-N(2)	120.6(5)
C(2A)-N(4)-C(1)	122.4(7)	N(3)-C(5)-N(1)	119.8(5)
C(2C)-N(4)-C(1)	129.5(10)	N(2)-C(5)-N(1)	119.2(5)
C(2A)-N(4)-C(2B)	18.1(13)	N(5)-C(6)-H(6A)	109.5
C(2C)-N(4)-C(2B)	17.5(14)	N(5)-C(6)-H(6B)	109.5
C(1)-N(4)-C(2B)	112.1(10)	H(6A)-C(6)-H(6B)	109.5
C(1)-N(5)-C(7)	118.4(5)	N(5)-C(6)-H(6C)	109.5
C(1)-N(5)-C(6)	123.3(5)	H(6A)-C(6)-H(6C)	109.5
C(7)-N(5)-C(6)	115.8(6)	H(6B)-C(6)-H(6C)	109.5
C(1)-N(6)-C(9)	121.6(5)	N(5)-C(7)-H(7A)	109.5
C(1)-N(6)-C(8)	122.7(5)	N(5)-C(7)-H(7B)	109.5
C(9)-N(6)-C(8)	114.7(5)	H(7A)-C(7)-H(7B)	109.5
C(2A)-S(1A)-C(3A)	102.1(7)	N(5)-C(7)-H(7C)	109.5
C(4)-S(3A)-C(3A)	103.9(9)	H(7A)-C(7)-H(7C)	109.5
C(3B)-S(1B)-C(2B)	102.7(9)	H(7B)-C(7)-H(7C)	109.5
C(4)-S(3B)-C(3B)	95.5(10)	N(6)-C(8)-H(8A)	109.5
C(2C)-S(1C)-C(3C)	106.0(9)	N(6)-C(8)-H(8B)	109.5
C(4)-S(3C)-C(3C)	91.1(19)	H(8A)-C(8)-H(8B)	109.5
N(4)-C(1)-N(5)	119.0(6)	N(6)-C(8)-H(8C)	109.5

N(4)-C(1)-N(6)	121.2(6)	H(8A)-C(8)-H(8C)	109.5
N(5)-C(1)-N(6)	119.5(5)	H(8B)-C(8)-H(8C)	109.5
N(4)-C(2A)-S(2A)	128.1(12)	N(6)-C(9)-H(9A)	109.5
N(4)-C(2A)-S(1A)	106.6(9)	N(6)-C(9)-H(9B)	109.5
S(2A)-C(2A)-S(1A)	120.5(12)	H(9A)-C(9)-H(9B)	109.5
S(1A)-C(3A)-S(3A)	108.9(6)	N(6)-C(9)-H(9C)	109.5
S(1A)-C(3A)-H(3AA)	109.9	H(9A)-C(9)-H(9C)	109.5
S(3A)-C(3A)-H(3AA)	109.9	H(9B)-C(9)-H(9C)	109.5
S(1A)-C(3A)-H(3AB)	109.9	N(2)-C(10)-H(10A)	109.5
S(3A)-C(3A)-H(3AB)	109.9	N(2)-C(10)-H(10B)	109.5
H(3AA)-C(3A)-H(3AB)	108.3	H(10A)-C(10)-H(10B)	109.5
N(4)-C(2B)-S(2B)	127.6(11)	N(2)-C(10)-H(10C)	109.5
N(4)-C(2B)-S(1B)	135.0(12)	H(10A)-C(10)-H(10C)	109.5
S(2B)-C(2B)-S(1B)	97.4(7)	H(10B)-C(10)-H(10C)	109.5
S(1B)-C(3B)-S(3B)	93.6(10)	N(2)-C(11)-H(11A)	109.5
S(1B)-C(3B)-H(3BA)	113.0	N(2)-C(11)-H(11B)	109.5
S(3B)-C(3B)-H(3BA)	113.0	H(11A)-C(11)-H(11B)	109.5
S(1B)-C(3B)-H(3BB)	113.0	N(2)-C(11)-H(11C)	109.5
S(3B)-C(3B)-H(3BB)	113.0	H(11A)-C(11)-H(11C)	109.5
H(3BA)-C(3B)-H(3BB)	110.4	H(11B)-C(11)-H(11C)	109.5
N(4)-C(2C)-S(2C)	122(2)	N(3)-C(12)-H(12A)	109.5
N(4)-C(2C)-S(1C)	105.8(12)	N(3)-C(12)-H(12B)	109.5
S(2C)-C(2C)-S(1C)	116(2)	H(12A)-C(12)-H(12B)	109.5
S(1C)-C(3C)-S(3C)	90.4(9)	N(3)-C(12)-H(12C)	109.5
S(1C)-C(3C)-H(3CA)	113.6	H(12A)-C(12)-H(12C)	109.5
S(3C)-C(3C)-H(3CA)	113.6	H(12B)-C(12)-H(12C)	109.5
S(1C)-C(3C)-H(3CB)	113.6	N(3)-C(13)-H(13A)	109.5
S(3C)-C(3C)-H(3CB)	113.6	N(3)-C(13)-H(13B)	109.5
H(3CA)-C(3C)-H(3CB)	110.8	H(13A)-C(13)-H(13B)	109.5
N(1)-C(4)-S(4)	130.3(4)	N(3)-C(13)-H(13C)	109.5
N(1)-C(4)-S(3A)	118.2(5)	H(13A)-C(13)-H(13C)	109.5
S(4)-C(4)-S(3A)	111.4(4)	H(13B)-C(13)-H(13C)	109.5

Compound 3-10

Figure A.55. Molecular structure of 3-10

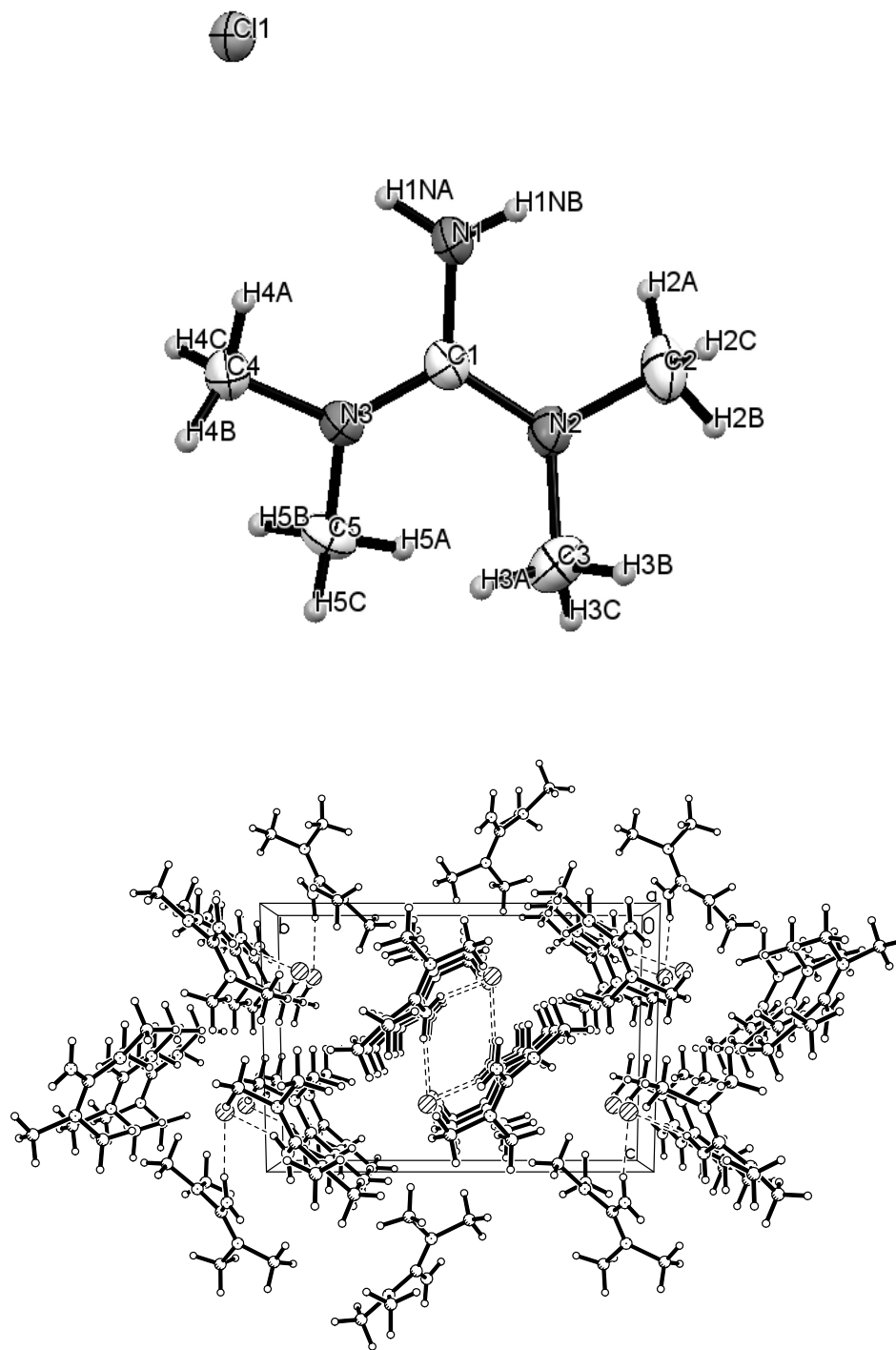


Table A.56. Crystal data and structure refinement for **3-10**

Identification code	pj25a	
Empirical formula	C ₅ H ₁₄ Cl N ₃	
Formula weight	151.64	
Temperature	180(2) K	
Wavelength	0.71073 Å	
Crystal system	Monoclinic	
Space group	P2(1)/n	
Unit cell dimensions	a = 6.9787(2) Å	α = 90°.
	b = 13.1814(4) Å	β = 104.780(3)°.
	c = 9.2918(4) Å	γ = 90°.
Volume	826.46(5) Å ³	
Z	4	
Density (calculated)	1.219 Mg/m ³	
Absorption coefficient	0.389 mm ⁻¹	
F(000)	328	
Crystal size	0.25 x 0.15 x 0.08 mm ³	
Theta range for data collection	3.09 to 25.99°.	
Index ranges	-8<=h<=8, -16<=k<=16, -8<=l<=11	
Reflections collected	5075	
Independent reflections	1620 [R(int) = 0.0387]	
Completeness to theta = 25.99°	99.6 %	
Absorption correction	Multi-scan	
Max. and min. transmission	0.9696 and 0.9091	
Refinement method	Full-matrix least-squares on F ²	
Data / restraints / parameters	1620 / 0 / 93	
Goodness-of-fit on F ²	1.085	
Final R indices [I>2sigma(I)]	R1 = 0.0379, wR2 = 0.0869	
R indices (all data)	R1 = 0.0528, wR2 = 0.0928	
Extinction coefficient	0.043(5)	
Largest diff. peak and hole	0.205 and -0.199 e.Å ⁻³	

Table A.57. Atomic coordinates ($\times 10^4$) and equivalent isotropic displacement parameters ($\text{\AA}^2 \times 10^3$) for **3-10**. $U(\text{eq})$ is defined as one third of the trace of the orthogonalized U^{ij} tensor.

	x	y	z	$U(\text{eq})$
N(1)	3102(3)	858(1)	1004(2)	33(1)
N(2)	206(2)	1782(1)	645(2)	29(1)
N(3)	1165(2)	725(1)	2691(2)	28(1)
C(1)	1495(3)	1107(1)	1446(2)	26(1)
C(2)	811(3)	2498(2)	-345(3)	43(1)
C(3)	-1930(3)	1699(2)	506(2)	38(1)
C(4)	2027(3)	-234(2)	3340(2)	36(1)
C(5)	45(3)	1258(2)	3586(2)	32(1)
Cl(1)	6553(1)	-824(1)	2384(1)	30(1)

Table A.58. Bond lengths [\AA] for **3-10**

N(1)-C(1)	1.330(3)	C(2)-H(2C)	0.9800
N(1)-H(1NA)	0.86(2)	C(3)-H(3A)	0.9800
N(1)-H(1NB)	0.88(2)	C(3)-H(3B)	0.9800
N(2)-C(1)	1.346(2)	C(3)-H(3C)	0.9800
N(2)-C(2)	1.455(3)	C(4)-H(4A)	0.9800
N(2)-C(3)	1.467(2)	C(4)-H(4B)	0.9800
N(3)-C(1)	1.335(2)	C(4)-H(4C)	0.9800
N(3)-C(5)	1.459(2)	C(5)-H(5A)	0.9800
N(3)-C(4)	1.462(2)	C(5)-H(5B)	0.9800
C(2)-H(2A)	0.9800	C(5)-H(5C)	0.9800
C(2)-H(2B)	0.9800	C(2)-H(2C)	0.9800

Table A.59. Bond angles [°] for **3-10**

C(1)-N(1)-H(1NA)	117.7(15)	N(2)-C(3)-H(3A)	109.5
C(1)-N(1)-H(1NB)	118.6(14)	N(2)-C(3)-H(3B)	109.5
H(1NA)-N(1)-H(1NB)	121(2)	H(3A)-C(3)-H(3B)	109.5
C(1)-N(2)-C(2)	121.16(17)	N(2)-C(3)-H(3C)	109.5
C(1)-N(2)-C(3)	121.34(16)	H(3A)-C(3)-H(3C)	109.5
C(2)-N(2)-C(3)	116.45(16)	H(3B)-C(3)-H(3C)	109.5
C(1)-N(3)-C(5)	123.23(16)	N(3)-C(4)-H(4A)	109.5
C(1)-N(3)-C(4)	122.67(16)	N(3)-C(4)-H(4B)	109.5
C(5)-N(3)-C(4)	113.94(16)	H(4A)-C(4)-H(4B)	109.5
N(1)-C(1)-N(3)	121.31(17)	N(3)-C(4)-H(4C)	109.5
N(1)-C(1)-N(2)	119.35(18)	H(4A)-C(4)-H(4C)	109.5
N(3)-C(1)-N(2)	119.30(17)	H(4B)-C(4)-H(4C)	109.5
N(2)-C(2)-H(2A)	109.5	N(3)-C(5)-H(5A)	109.5
N(2)-C(2)-H(2B)	109.5	N(3)-C(5)-H(5B)	109.5
H(2A)-C(2)-H(2B)	109.5	H(5A)-C(5)-H(5B)	109.5
N(2)-C(2)-H(2C)	109.5	N(3)-C(5)-H(5C)	109.5
H(2A)-C(2)-H(2C)	109.5	H(5A)-C(5)-H(5C)	109.5
H(2B)-C(2)-H(2C)	109.5	H(5B)-C(5)-H(5C)	109.5

A.1.11. Compound 3-13b

Figure A.60. Molecular structure of 3-13b

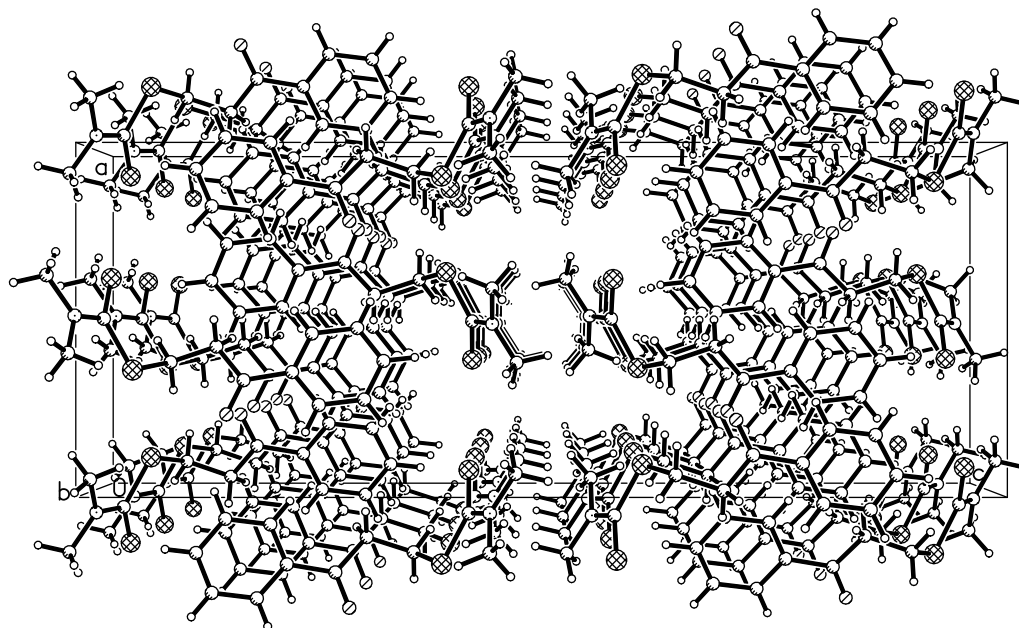
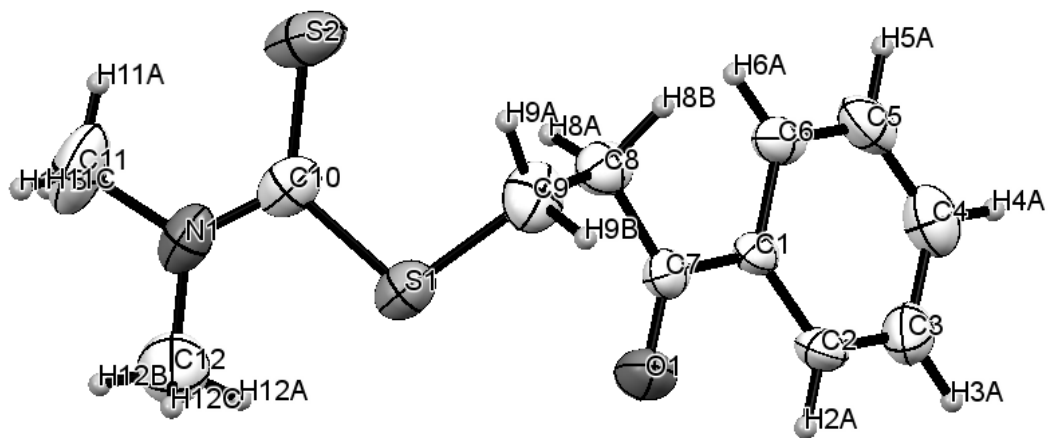


Table A.61. Crystal data and structure refinement for **3-13b**

Identification code	pj31	
Empirical formula	C ₁₂ H ₁₅ N O S ₂	
Formula weight	253.37	
Temperature	180(2) K	
Wavelength	0.71073 Å	
Crystal system	Orthorhombic	
Space group	Pbca	
Unit cell dimensions	a = 11.6301(6) Å	α = 90°.
	b = 7.1907(4) Å	β = 90°.
	c = 30.5211(14) Å	γ = 90°.
Volume	2552.4(2) Å ³	
Z	8	
Density (calculated)	1.319 Mg/m ³	
Absorption coefficient	0.396 mm ⁻¹	
F(000)	1072	
Crystal size	0.30 x 0.20 x 0.04 mm ³	
Theta range for data collection	3.40 to 25.99°.	
Index ranges	-11 ≤ h ≤ 14, -8 ≤ k ≤ 8, -32 ≤ l ≤ 37	
Reflections collected	9511	
Independent reflections	2494 [R(int) = 0.1406]	
Completeness to theta = 25.99°	99.5 %	
Absorption correction	Multi-scan	
Max. and min. transmission	0.9843 and 0.8904	
Refinement method	Full-matrix least-squares on F ²	
Data / restraints / parameters	2494 / 0 / 147	
Goodness-of-fit on F ²	1.000	
Final R indices [I > 2σ(I)]	R1 = 0.0628, wR2 = 0.0936	
R indices (all data)	R1 = 0.1648, wR2 = 0.1217	
Largest diff. peak and hole	0.230 and -0.197 e.Å ⁻³	

Table A.62. Atomic coordinates ($\times 10^4$) and equivalent isotropic displacement parameters ($\text{\AA}^2 \times 10^3$) for **3-13b**. $U(\text{eq})$ is defined as one third of the trace of the orthogonalized U^{ij} tensor.

	x	y	z	$U(\text{eq})$
N(1)	-105(3)	6667(5)	500(1)	51(1)
O(1)	2441(2)	4406(4)	1895(1)	55(1)
S(1)	1291(1)	4731(1)	983(1)	48(1)
S(2)	-1083(1)	3464(2)	723(1)	69(1)
C(1)	1359(3)	3718(4)	2526(1)	33(1)
C(2)	2199(3)	4398(5)	2805(2)	40(1)
C(3)	2059(4)	4353(5)	3251(2)	53(1)
C(4)	1068(4)	3620(5)	3430(2)	55(1)
C(5)	214(4)	2969(5)	3159(2)	50(1)
C(6)	356(3)	3020(5)	2708(2)	39(1)
C(7)	1568(3)	3719(5)	2046(2)	38(1)
C(8)	700(3)	2835(5)	1749(2)	44(1)
C(9)	1108(4)	2588(5)	1282(2)	54(1)
C(10)	-33(3)	5037(6)	714(1)	43(1)
C(11)	-1130(4)	7184(7)	251(2)	77(2)
C(12)	823(4)	8038(6)	494(2)	72(2)

Table A.63. Bond lengths [\AA] for **3-13b**

N(1)-C(10)	1.344(5)	C(5)-C(6)	1.387(6)
N(1)-C(11)	1.461(5)	C(5)-H(5A)	0.9500
N(1)-C(12)	1.462(5)	C(6)-H(6A)	0.9500
O(1)-C(7)	1.219(4)	C(7)-C(8)	1.498(5)
S(1)-C(10)	1.759(4)	C(8)-C(9)	1.511(5)
S(1)-C(9)	1.805(4)	C(8)-H(8A)	0.9900
S(2)-C(10)	1.665(4)	C(8)-H(8B)	0.9900
C(1)-C(6)	1.385(5)	C(9)-H(9A)	0.9900
C(1)-C(2)	1.385(5)	C(9)-H(9B)	0.9900
C(1)-C(7)	1.488(6)	C(11)-H(11A)	0.9800
C(2)-C(3)	1.371(6)	C(11)-H(11B)	0.9800
C(2)-H(2A)	0.9500	C(11)-H(11C)	0.9800
C(3)-C(4)	1.380(6)	C(12)-H(12A)	0.9800
C(3)-H(3A)	0.9500	C(12)-H(12B)	0.9800
C(4)-C(5)	1.376(5)	C(12)-H(12C)	0.9800
C(4)-H(4A)	0.9500	C(5)-C(6)	1.387(6)

Table A.64. Bond angles [$^\circ$] for **3-13b**

C(10)-N(1)-C(11)	121.6(4)	C(7)-C(8)-H(8A)	108.7
C(10)-N(1)-C(12)	123.2(3)	C(9)-C(8)-H(8A)	108.7
C(11)-N(1)-C(12)	115.1(4)	C(7)-C(8)-H(8B)	108.7
C(10)-S(1)-C(9)	103.9(2)	C(9)-C(8)-H(8B)	108.7
C(6)-C(1)-C(2)	118.4(4)	H(8A)-C(8)-H(8B)	107.6
C(6)-C(1)-C(7)	122.2(4)	C(8)-C(9)-S(1)	114.5(3)
C(2)-C(1)-C(7)	119.4(4)	C(8)-C(9)-H(9A)	108.6
C(3)-C(2)-C(1)	121.2(4)	S(1)-C(9)-H(9A)	108.6
C(3)-C(2)-H(2A)	119.4	C(8)-C(9)-H(9B)	108.6
C(1)-C(2)-H(2A)	119.4	S(1)-C(9)-H(9B)	108.6
C(2)-C(3)-C(4)	120.1(4)	H(9A)-C(9)-H(9B)	107.6
C(2)-C(3)-H(3A)	120.0	N(1)-C(10)-S(2)	123.7(3)

C(4)-C(3)-H(3A)	120.0	N(1)-C(10)-S(1)	113.0(3)
C(5)-C(4)-C(3)	119.6(4)	S(2)-C(10)-S(1)	123.3(3)
C(5)-C(4)-H(4A)	120.2	N(1)-C(11)-H(11A)	109.5
C(3)-C(4)-H(4A)	120.2	N(1)-C(11)-H(11B)	109.5
C(4)-C(5)-C(6)	120.1(4)	H(11A)-C(11)-H(11B)	109.5
C(4)-C(5)-H(5A)	119.9	N(1)-C(11)-H(11C)	109.5
C(6)-C(5)-H(5A)	119.9	H(11A)-C(11)-H(11C)	109.5
C(1)-C(6)-C(5)	120.5(4)	H(11B)-C(11)-H(11C)	109.5
C(1)-C(6)-H(6A)	119.7	N(1)-C(12)-H(12A)	109.5
C(5)-C(6)-H(6A)	119.7	N(1)-C(12)-H(12B)	109.5
O(1)-C(7)-C(1)	120.6(4)	H(12A)-C(12)-H(12B)	109.5
O(1)-C(7)-C(8)	120.4(4)	N(1)-C(12)-H(12C)	109.5
C(1)-C(7)-C(8)	119.1(4)	H(12A)-C(12)-H(12C)	109.5
C(7)-C(8)-C(9)	114.1(3)	H(12B)-C(12)-H(12C)	109.5

A.1.12. Bicarbonate salt of 3-3

Figure A.65. Molecular structure of bicarbonate salt of 3-3

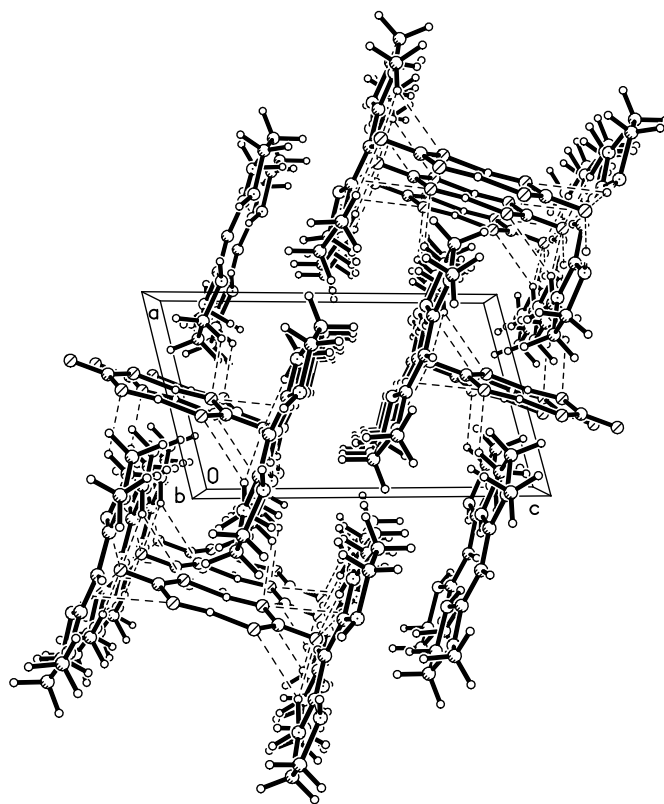
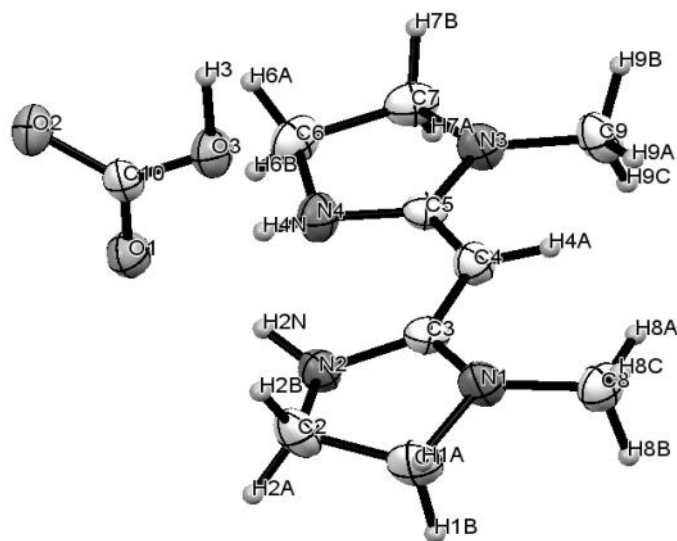


Table A.66. Crystal data and structure refinement for pj29a_5

Identification code	pj29a_5	
Empirical formula	C10 H18 N4 O3	
Formula weight	242.28	
Temperature	180(2) K	
Wavelength	0.71073 Å	
Crystal system	Triclinic	
Space group	P-1	
Unit cell dimensions	a = 6.8191(2) Å	$\alpha = 100.9590(10)^\circ$.
	b = 7.9360(2) Å	$\beta = 102.0960(10)^\circ$.
	c = 11.5882(3) Å	$\gamma = 99.6820(10)^\circ$.
Volume	587.70(3) Å ³	
Z	2	
Density (calculated)	1.369 Mg/m ³	
Absorption coefficient	0.103 mm ⁻¹	
F(000)	260	
Crystal size	0.30 x 0.30 x 0.20 mm ³	
Theta range for data collection	2.68 to 26.00°.	
Index ranges	-8<=h<=8, -9<=k<=9, 0<=l<=14	
Reflections collected	4632	
Independent reflections	4632 [R(int) = 0.0000]	
Completeness to theta = 26.00°	100.0 %	
Absorption correction	TWINABS	
Max. and min. transmission	0.9797 and 0.9698	
Refinement method	Full-matrix least-squares on F ²	
Data / restraints / parameters	4632 / 0 / 166	
Goodness-of-fit on F ²	1.084	
Final R indices [I>2sigma(I)]	R1 = 0.0519, wR2 = 0.1388	
R indices (all data)	R1 = 0.0560, wR2 = 0.1428	
Largest diff. peak and hole	0.371 and -0.332 e.Å ⁻³	

Table A.67. Atomic coordinates ($\times 10^4$) and equivalent isotropic displacement parameters ($\text{\AA}^2 \times 10^3$) for pj29a_5. $U(\text{eq})$ is defined as one third of the trace of the orthogonalized U^{ij} tensor.

	x	y	z	$U(\text{eq})$
N(1)	6632(2)	5958(2)	3905(1)	35(1)
N(2)	5101(2)	8179(2)	3784(1)	33(1)
N(3)	-347(2)	4242(2)	1465(1)	35(1)
N(4)	705(2)	7096(2)	2200(1)	34(1)
C(1)	8087(2)	7450(2)	4755(1)	41(1)
C(2)	7250(2)	8998(2)	4397(1)	39(1)
C(3)	4879(2)	6402(2)	3405(1)	27(1)
C(4)	3156(2)	5202(2)	2659(1)	30(1)
C(5)	1262(2)	5521(2)	2129(1)	26(1)
C(6)	-1315(2)	6902(2)	1384(1)	39(1)
C(7)	-2158(2)	4914(2)	1040(1)	36(1)
C(8)	6891(2)	4201(2)	3967(1)	38(1)
C(9)	-542(2)	2384(2)	1411(1)	37(1)
C(10)	4032(2)	10276(2)	1488(1)	28(1)
O(1)	3362(2)	10409(1)	2423(1)	35(1)
O(2)	3971(2)	11449(1)	854(1)	36(1)
O(3)	4793(2)	8919(1)	1138(1)	38(1)

Table A.68. Bond lengths [Å] for pj29a_5

N(1)-C(3)	1.3486(17)	N(4)-C(6)	1.4640(17)
N(1)-C(8)	1.4479(17)	C(1)-C(2)	1.529(2)
N(1)-C(1)	1.4517(17)	C(3)-C(4)	1.3851(18)
N(2)-C(3)	1.3671(17)	C(4)-C(5)	1.3956(18)
N(2)-C(2)	1.4637(18)	C(6)-C(7)	1.530(2)
N(3)-C(5)	1.3416(17)	C(10)-O(1)	1.2554(16)
N(3)-C(9)	1.4458(17)	C(10)-O(2)	1.2912(16)
N(3)-C(7)	1.4559(16)	C(10)-O(3)	1.3056(15)
N(4)-C(5)	1.3595(17)	N(4)-C(6)	1.4640(17)

Table A.69. Bond angles [°] for pj29a_5

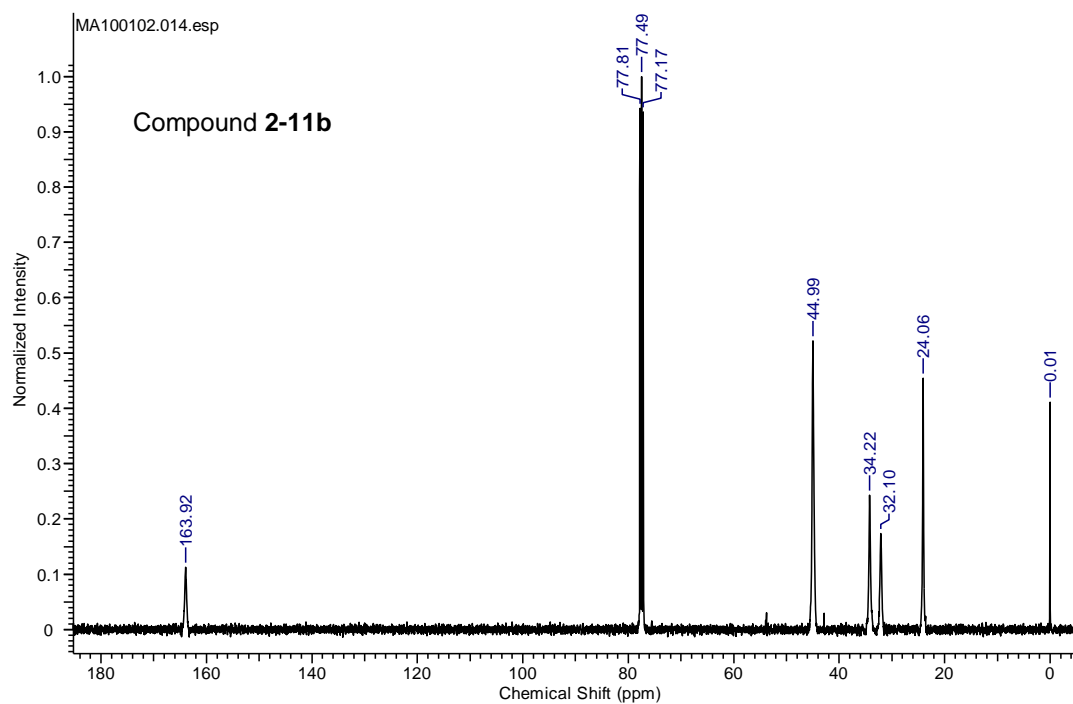
C(3)-N(1)-C(8)	126.22(11)	N(1)-C(3)-C(4)	123.89(12)
C(3)-N(1)-C(1)	111.85(11)	N(2)-C(3)-C(4)	127.43(12)
C(8)-N(1)-C(1)	118.85(11)	C(3)-C(4)-C(5)	128.21(12)
C(3)-N(2)-C(2)	109.99(11)	N(3)-C(5)-N(4)	109.01(11)
C(5)-N(3)-C(9)	125.74(11)	N(3)-C(5)-C(4)	123.30(12)
C(5)-N(3)-C(7)	112.58(11)	N(4)-C(5)-C(4)	127.68(12)
C(9)-N(3)-C(7)	119.81(11)	N(4)-C(6)-C(7)	103.07(11)
C(5)-N(4)-C(6)	110.84(11)	N(3)-C(7)-C(6)	102.49(11)
N(1)-C(1)-C(2)	101.86(11)	O(1)-C(10)-O(2)	121.42(11)
N(2)-C(2)-C(1)	102.26(11)	O(1)-C(10)-O(3)	119.53(11)
N(1)-C(3)-N(2)	108.66(11)	O(2)-C(10)-O(3)	119.05(11)

Appendix B

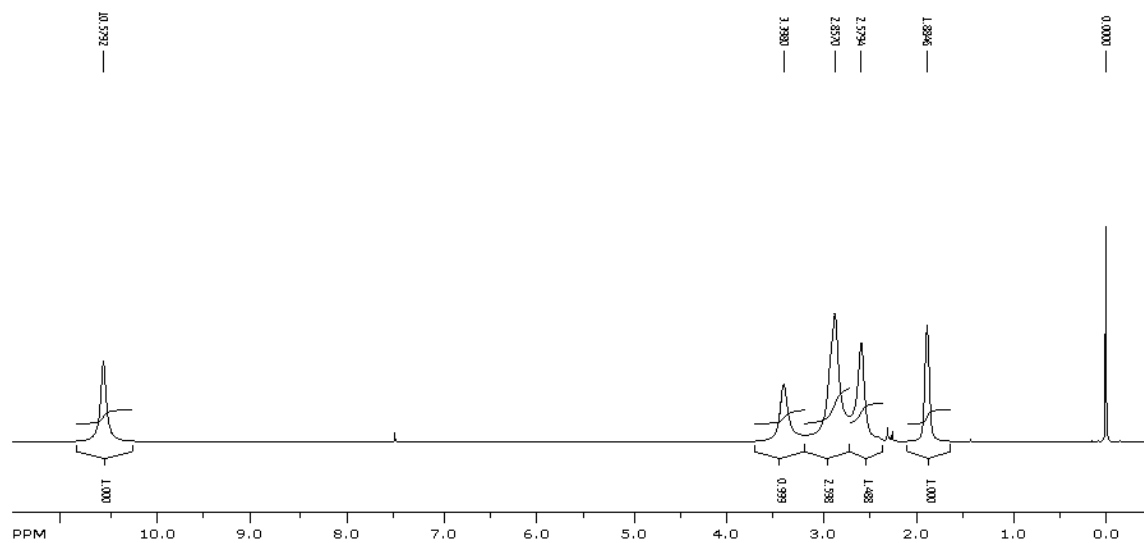
NMR Spectra of Compounds

B.1. NMR Data for Zwitterionic Carbamate Salts of 2-11 and 2-18

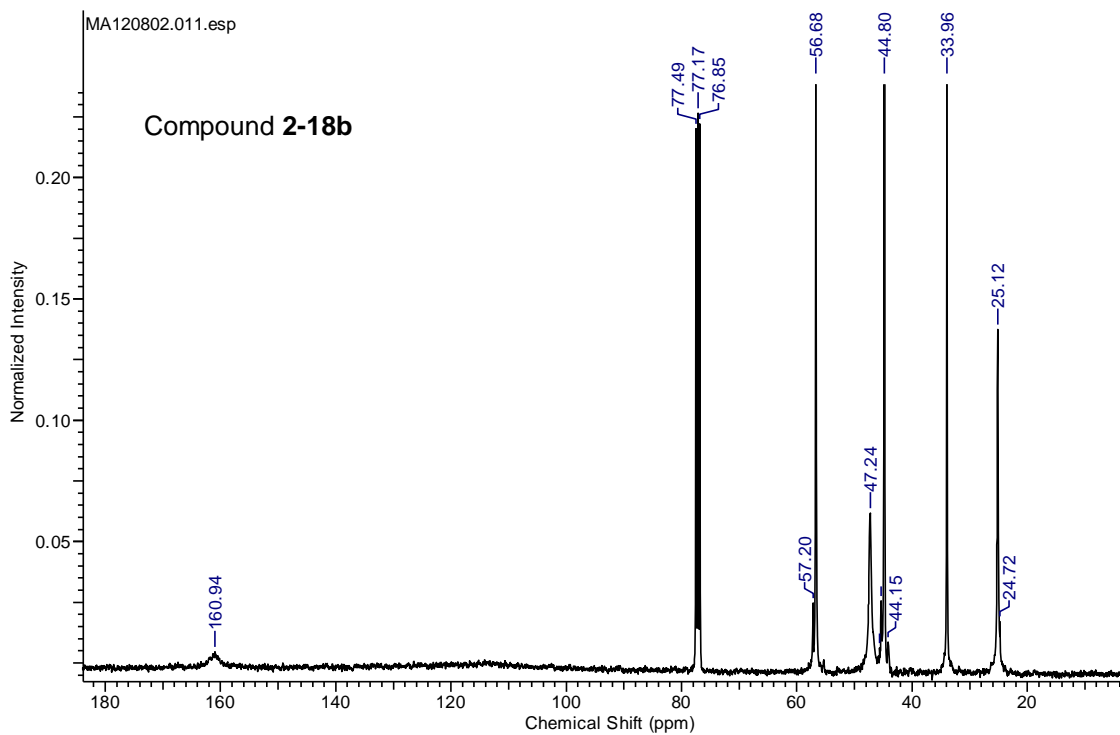
^{13}C $\{^1\text{H}\}$ NMR spectrum of compound **2-11b** (400 MHz, CDCl_3)



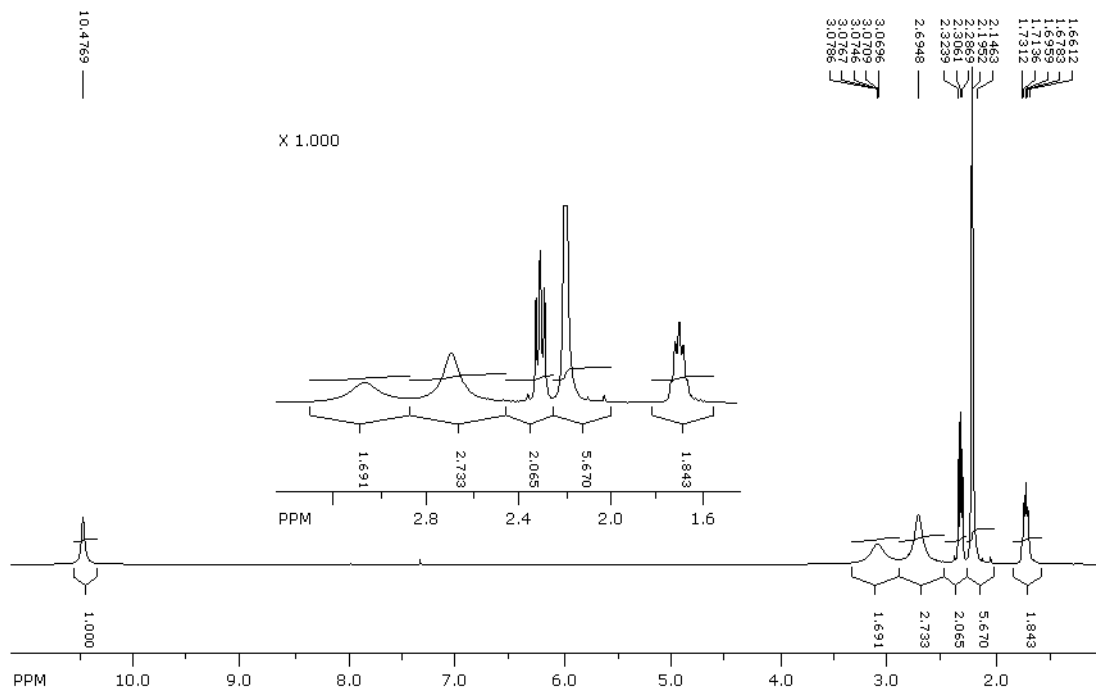
^1H NMR spectrum of compound **2-11b** (400 MHz, CDCl_3)



^{13}C $\{^1\text{H}\}$ NMR spectrum of compound **2-18b** (400 MHz, CDCl_3)



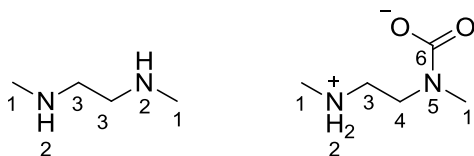
^1H NMR spectrum of compound **2-18b** (400 MHz, CDCl_3)



B.1.1. NMR Chemical Shift Assignments for Compounds 2-10 to 2-18

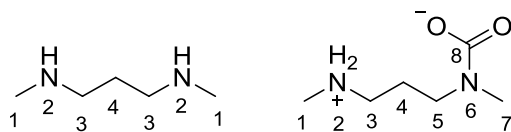
Table B.1. ^1H and ^{13}C NMR chemical shifts of secondary diamines in CDCl_3 without (species **a**) and with CO_2 (species **b**: unless otherwise noted, the signals are broad singlets). Assignments of chemical shifts were done using two-dimensional NMR spectroscopy.

2-10 *N, N'*-Dimethylethylenediamine



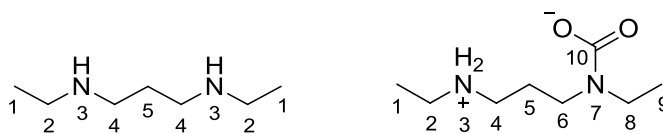
^1H	1	2	3	4	5	7
a	2.44 (s)	1.17 (br)	2.69 (s)	--	--	--
b	2.29	9.02	2.50 (t)	3.23, 2.93	--	--
^{13}C	1	2	3	4	5	7
a	36.5	--	51.5	--	--	--
b	44.9	--	58.7	38.6	--	161.9

2-11 *N, N'*-Dimethyl-1,3-propanediamine



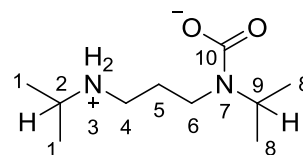
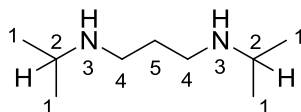
¹ H	1	2	3	4	5	6	7	8
a	2.43 (s)	1.05 (br)	2.64 (m)	1.67 (p)	--	--	--	--
b	2.86	10.17	3.40	1.88	2.91	--	2.58	--
¹³ C	1	2	3	4	5	6	7	8
a	36.6	--	50.5	30.1	--	--	--	--
b	34.1	--	44.9	23.8	44.4	--	31.7	163.8

2-12 *N, N'*-Diethyl-1,3-propanediamine



¹ H	1	2, 4	3	5	6, 8	7	9	10
a	1.10 (t)	2.66 (q), 2.65 (t)	1.19 (br)	1.69 (p)	--	--	--	--
b	1.31	2.91	10.09	1.85	3.41, 3.26	--	1.11	--
¹³ C	1	2, 4	3	5	6, 8	7	9	10
a	15.2	48.3, 44.1	--	30.6	--	--	--	--
b	11.6	42.7, 41.0	10.1	25.1	42.1, 41.4	--	13.9	163.6

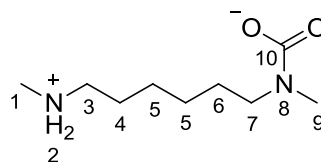
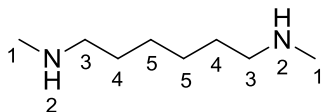
2-13 *N, N'*-Di-*iso*-propyl-1,3-propanediamine



¹ H	1, 8	2	3	4, 6	5	7	9	10
a	1.06 (m), --	2.78 (m)	--	2.65 (m), --	1.66 (m)	--	--	--
b	1.32, 1.08	3.16	9.2	2.88, 3.31	1.78	--	4.48	--

¹³ C	1, 8	2	3	4, 6	5	7	9	10
a	22.9, --	48.7	--	46.1, --	31.1	--	--	--
b	21.8, 19.2	48.1	--	37.9, 40.7	28.6	--	46.9	163.5

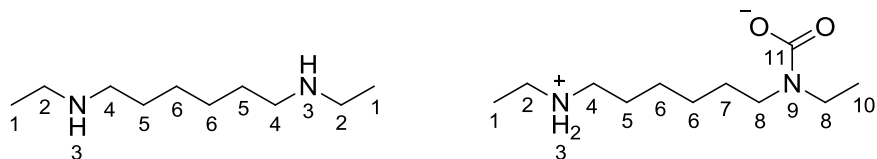
2-14 *N, N'*-Dimethyl-1,6-hexanediamine



¹ H	1,9	2	3, 7	4, 6	5	8	10
a	2.43 (s), --	1.21	2.57 (q), --	1.50 (m), --	1.35(m)	--	--
b	2.83, 2.54	10.18	3.23, 2.83	1.65, 1.51	1.32	--	--

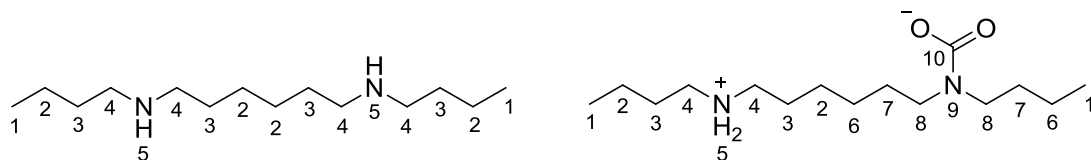
¹³ C	1,9	2	3, 7	4, 6	5	8	10
a	36.4	--	52.0, --	29.8, --	27.2	--	--
b	34.0, 32.9	--	48.4	27.7	26.1	--	162.6

2-15 *N, N'*-Diethyl-1,6-hexanediamine



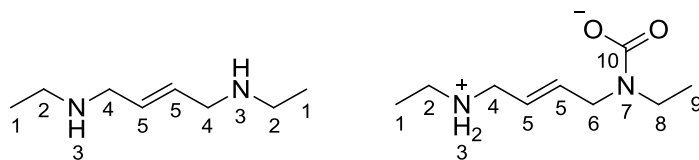
¹ H	1	2, 4	3	5	6	7	8	9	10	11
a	1.1(m)	2.68, 2.62	1.0(br)	1.51(m)	1.36(m)	--	--	--	--	--
b	1.21	2.79, 2.71	8.92	1.60	1.32	1.51	3.21	--	1.08	--
¹³ C	1	2,4	3	5	6	7	8	9	10	11
a	15.2	44.0, 49.7	--	30.1	27.2	--	--	--	--	--
b	13.1	42.6, 47.5	--	28.8	26.8	27.8	41.2, 46.1	--	13.8	161.8

2-16 *N, N'*-Dibutyl-1,6-hexanediamine



¹ H	1	2	3	4	5	6	7	8	9	10
a	0.91 (t)	1.34 (m)	1.46 (m)	2.58 (t)	0.91 (ov)	--	--	--	--	--
b	0.91 (t)	1.31	1.58	2.69	8.88	1.51	3.18	--	--	--
¹³ C	1	2	3	4	5	6	7	8	9	10
a	13.9	27.4, 20.5	30.2, 32.4	49.8, 50.1	--	--	--	--	--	--
b	13.9	20.3	30.3	48.2	--	26.9	28.4	46.4	--	161.6

2-17 *N,N'*-Diethyl-2-butene-1,4-diamine



¹ H	1	2	3	4	5	6	7	8	9	10
a	1.11 (t)	2.65 (q)	1.02 (br)	3.23 (m)	5.69 (m)	--	--	--	--	--
b	1.19	2.76	8.73	3.86	5.72	3.36	--	3.24	1.07	--

¹³ C	1	2	3	4	5	6	7	8	9	10
a	15.3	43.6	--	51.3	130.2	--	--	--	--	--
b	13.5	40.7	--	47.6	124.7, 129.6, 133.2	48.8, 49.3	--	41.4, 42.1	12.7	161.4

2-18 *N, N, N'*-Trimethyl-1,3-propanediamine

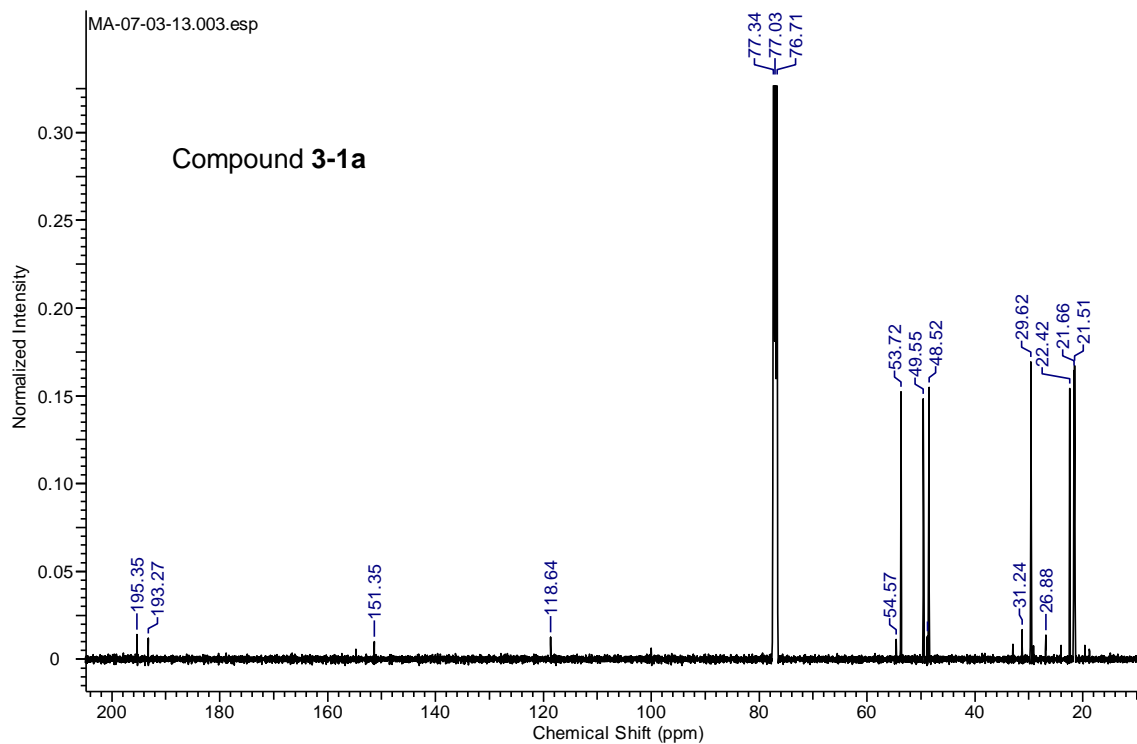


¹ H	1	2	3	4	5	6	7	8
a	2.14 (s)	--	2.23 (t)	1.57 (p)	2.53 (t)	1.13 (br)	2.35 (s)	--
b	2.19	10.54	2.30 (t)	1.69 (p)	3.07	--	2.69	--

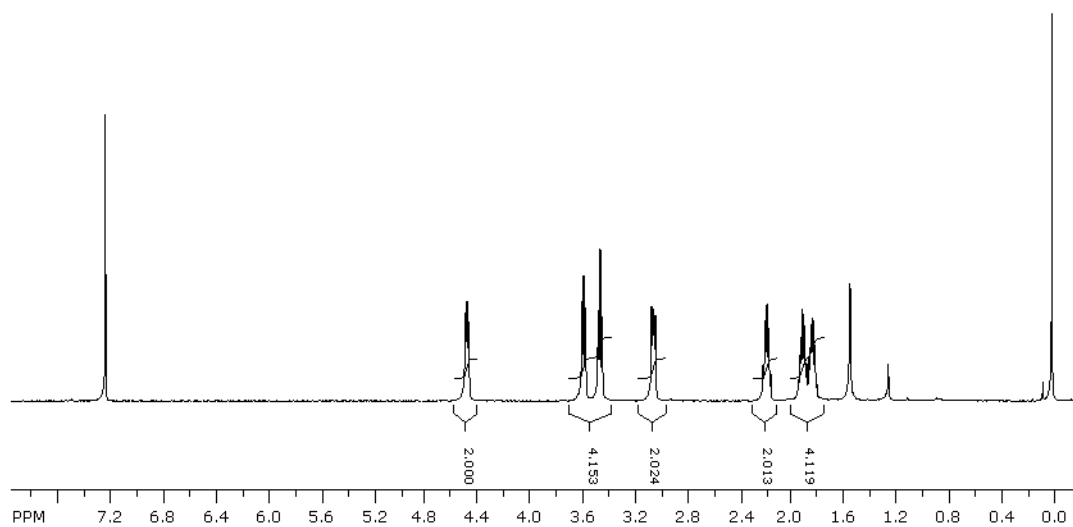
¹³ C	1	2	3	4	5	6	7	8
a	45.4	--	57.9	27.9	50.5	--	36.5	--
b	44.8	--	56.7	25.1	47.2	--	34.0	161.1

B.2. NMR Data for Nitrogen-Sulfur Compounds

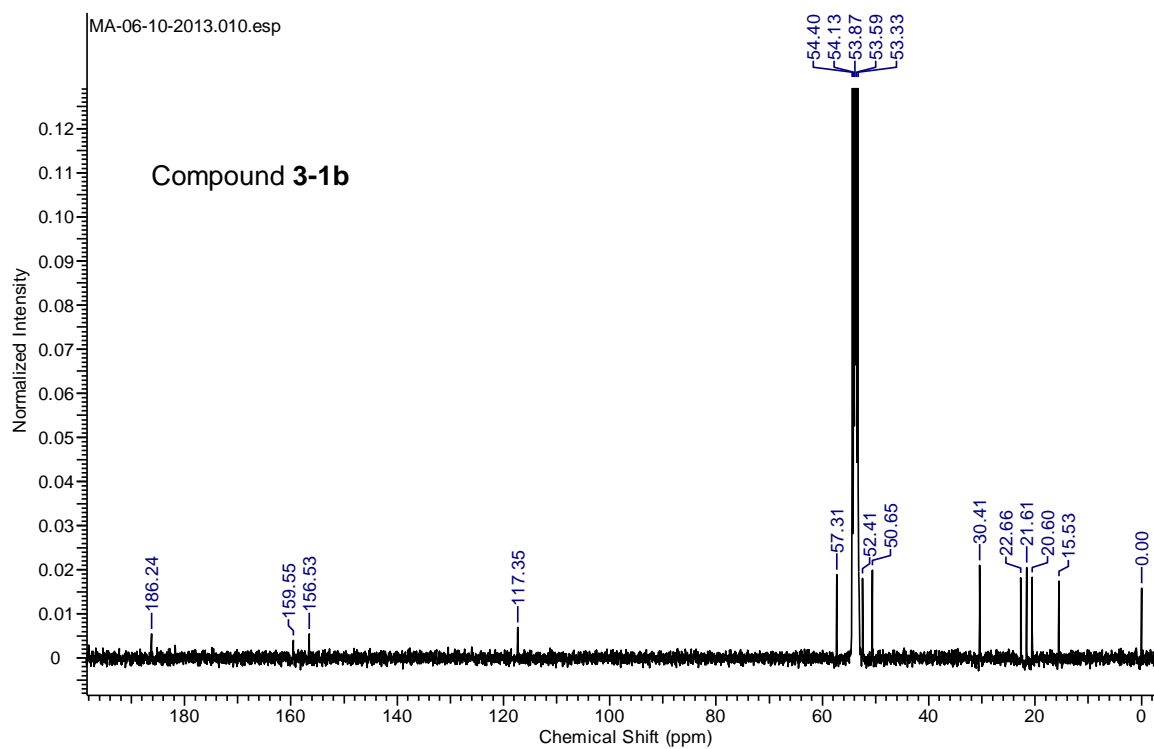
^{13}C $\{^1\text{H}\}$ NMR spectrum of compound **3-1a** (400 MHz, CDCl_3)



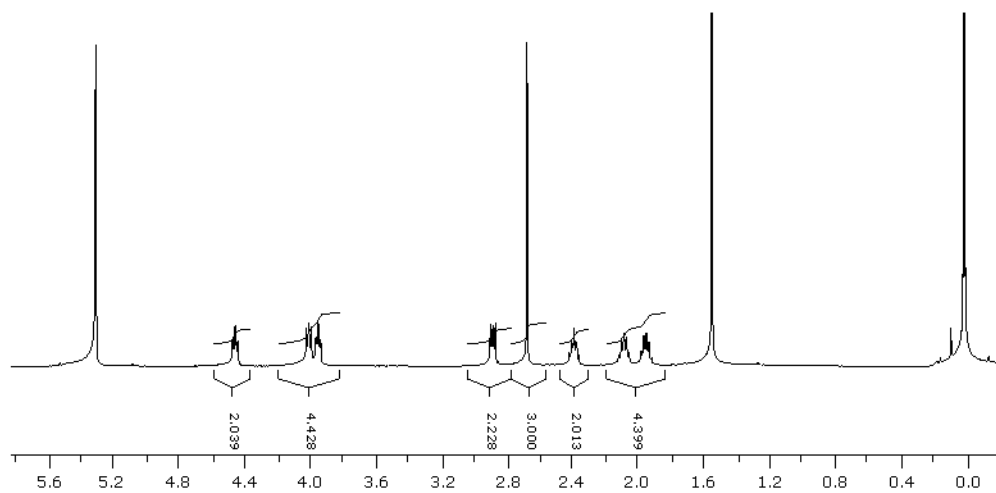
^1H NMR spectrum of compound **3-1a** (400 MHz, CDCl_3)



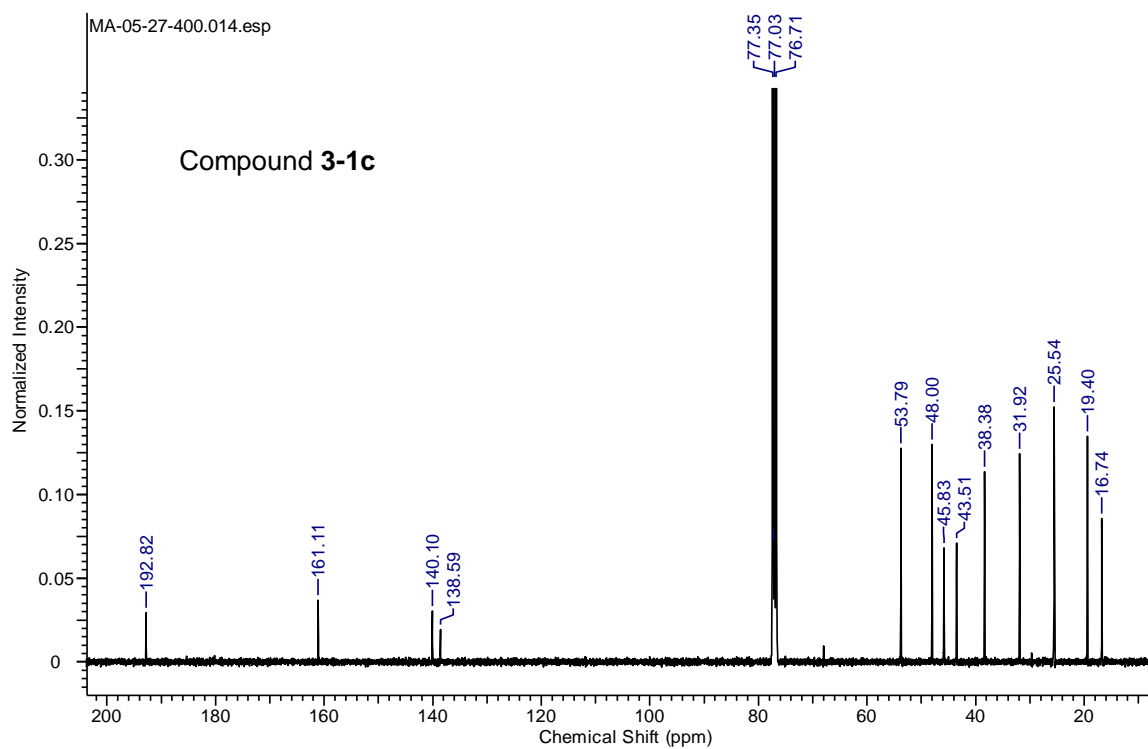
^{13}C $\{^1\text{H}\}$ NMR spectrum of compound **3-1b** (400 MHz, CD_2Cl_2)



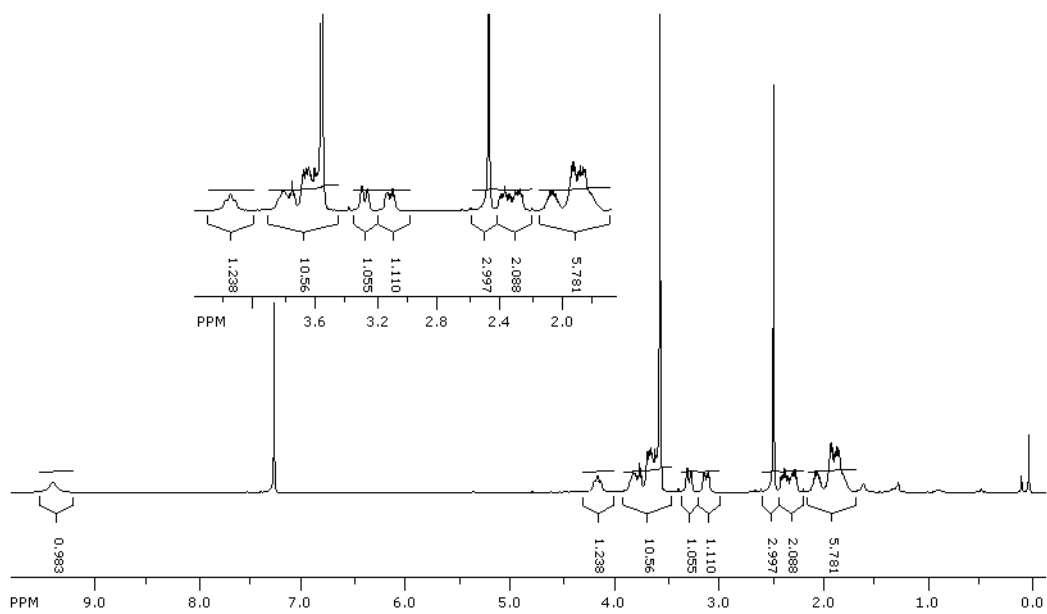
^1H NMR spectrum of compound **3-1b** (400 MHz, CD_2Cl_2)



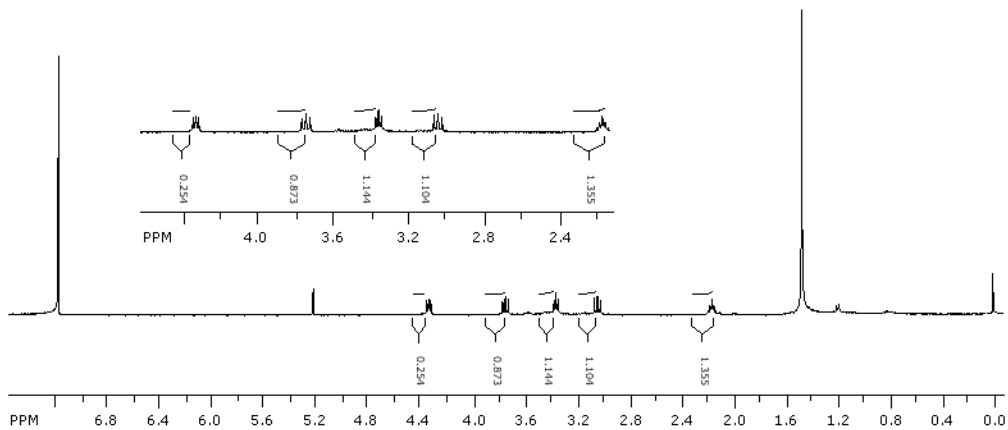
^{13}C $\{^1\text{H}\}$ NMR spectrum of compound **3-1c** (400 MHz, CDCl_3)



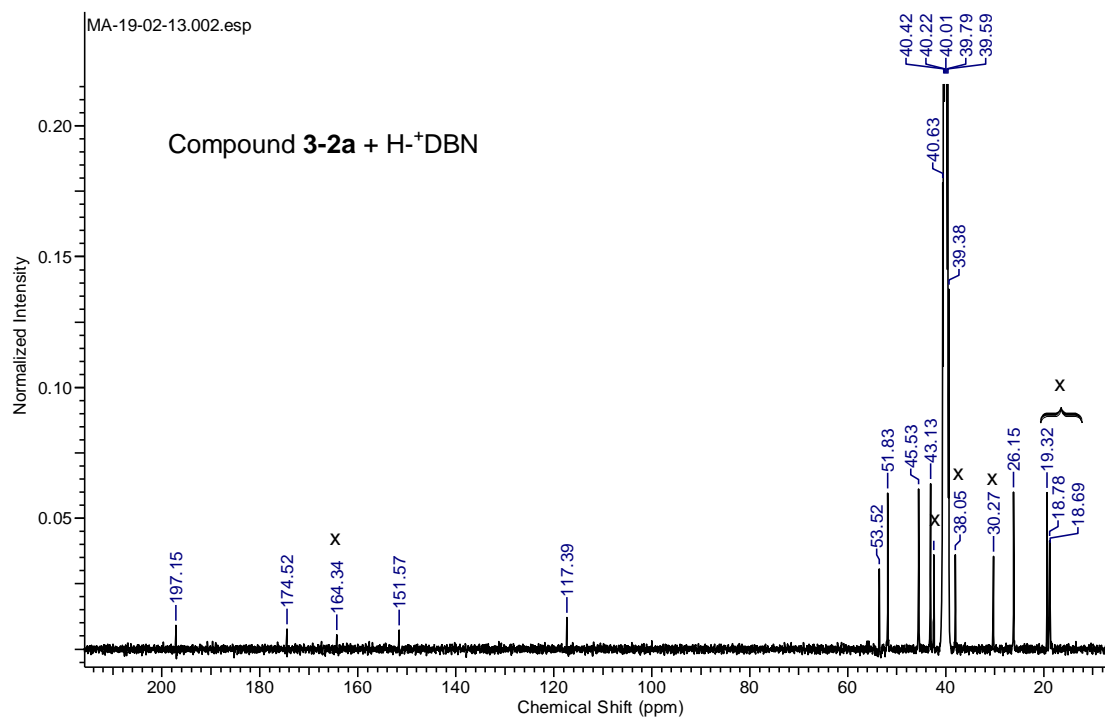
^1H NMR spectrum of compound **3-1c** (400 MHz, CDCl_3)



^1H NMR spectrum of compound **3-2a** (400 MHz, CDCl_3)

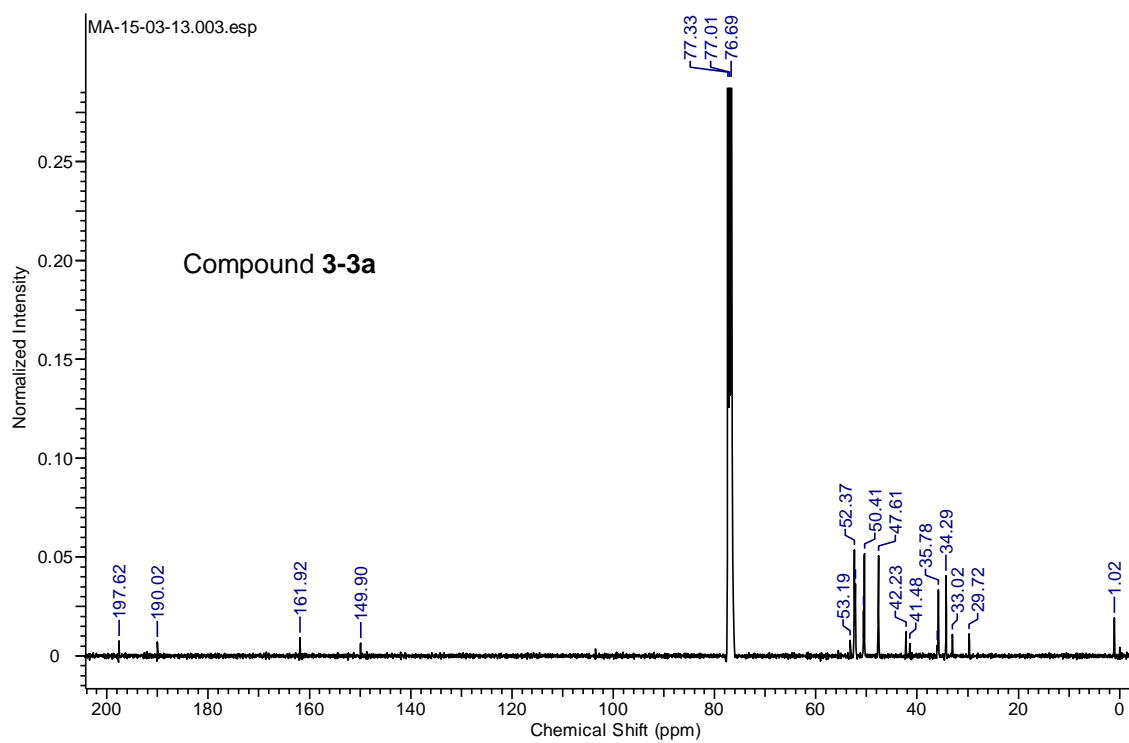


^{13}C $\{^1\text{H}\}$ NMR spectrum of compound **3-2a** and protonated DBN (400 MHz, $(\text{CD}_3)_2\text{SO}$)

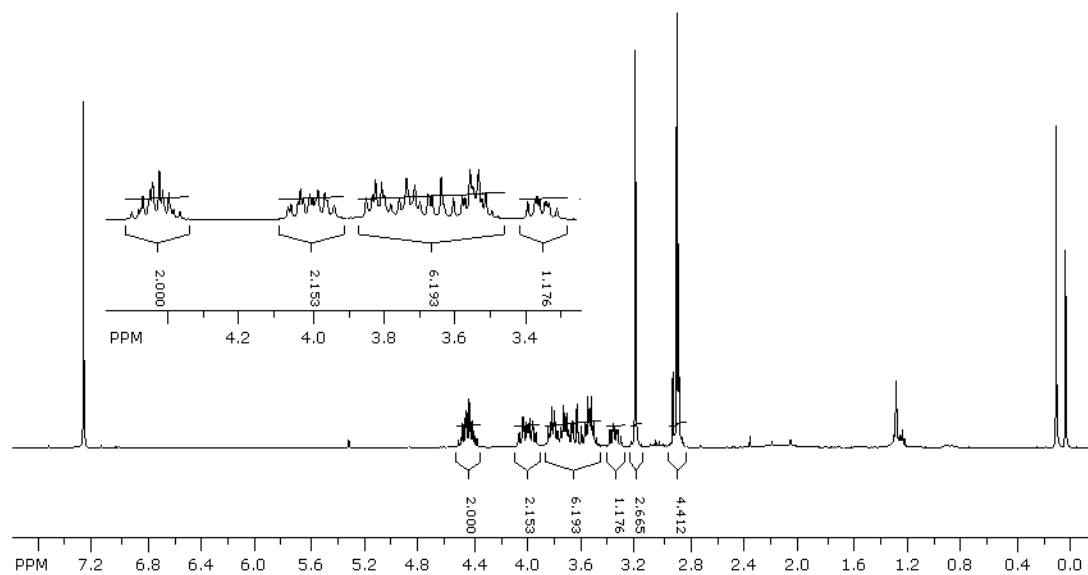


x = protonated DBN

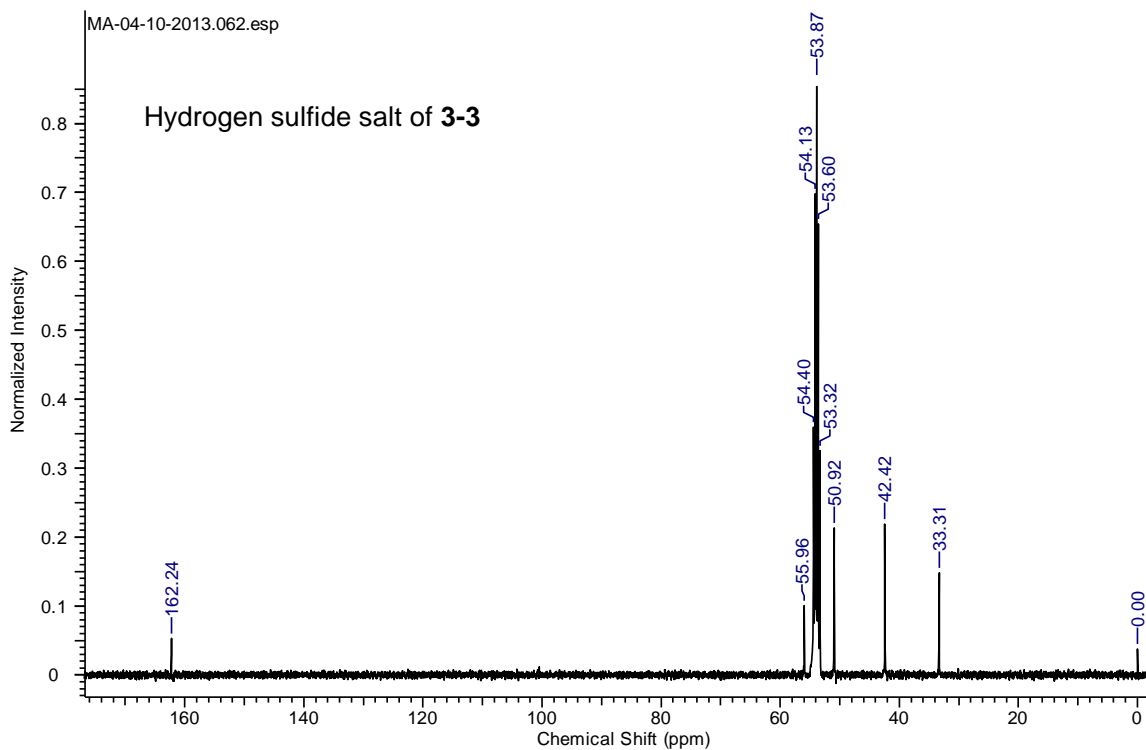
^{13}C $\{^1\text{H}\}$ NMR spectrum of compound **3-3a** (400 MHz, CDCl_3)



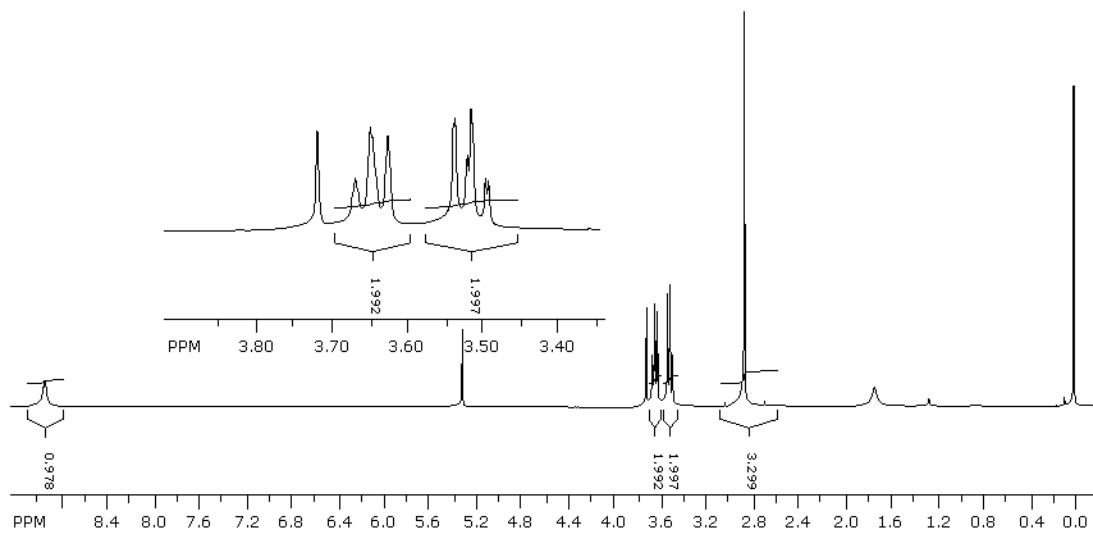
^1H NMR spectrum of compound **3-3a** (400 MHz, CDCl_3)



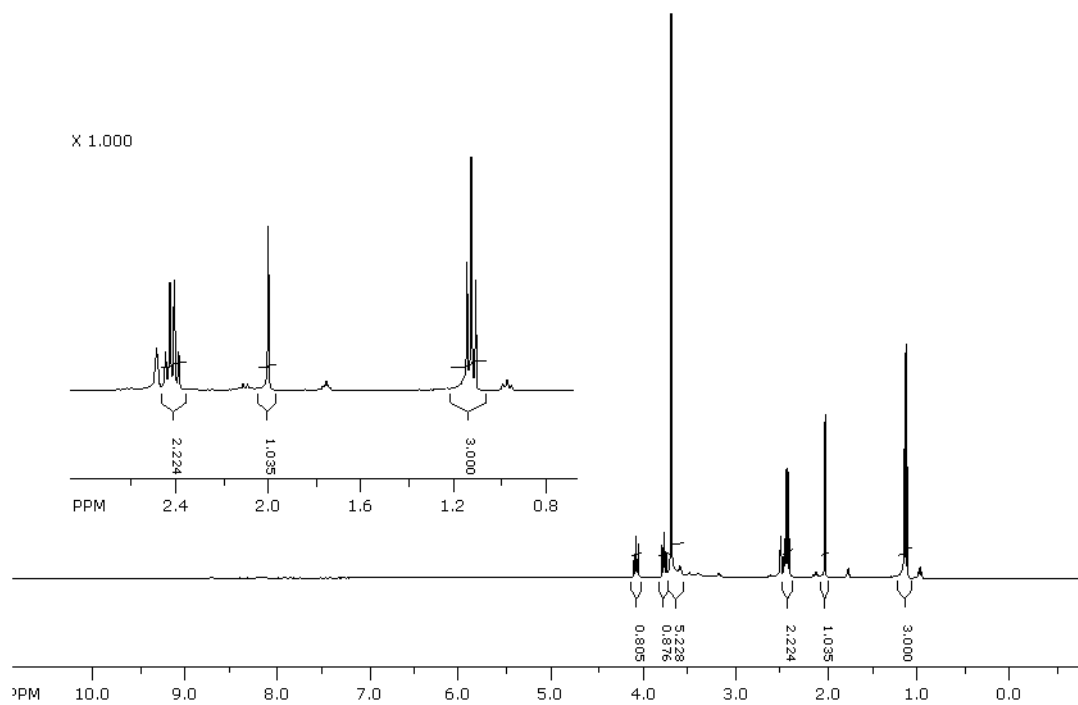
^{13}C { ^1H } NMR spectrum of hydrogen sulfide salt of **3-3** (400 MHz, CD_2Cl_2)



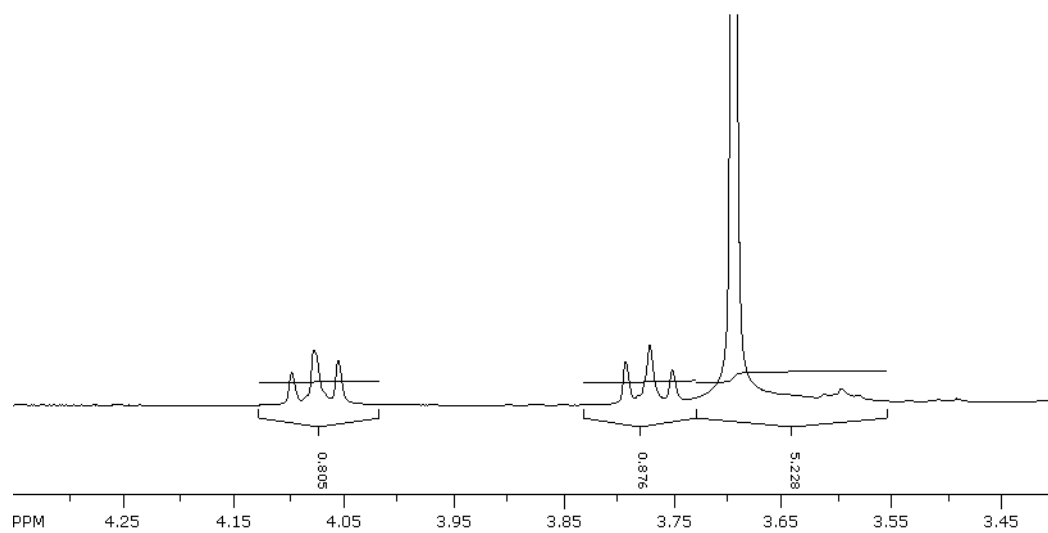
^1H NMR spectrum of hydrogen sulfide salt of **3-3** (400 MHz, CD_2Cl_2)



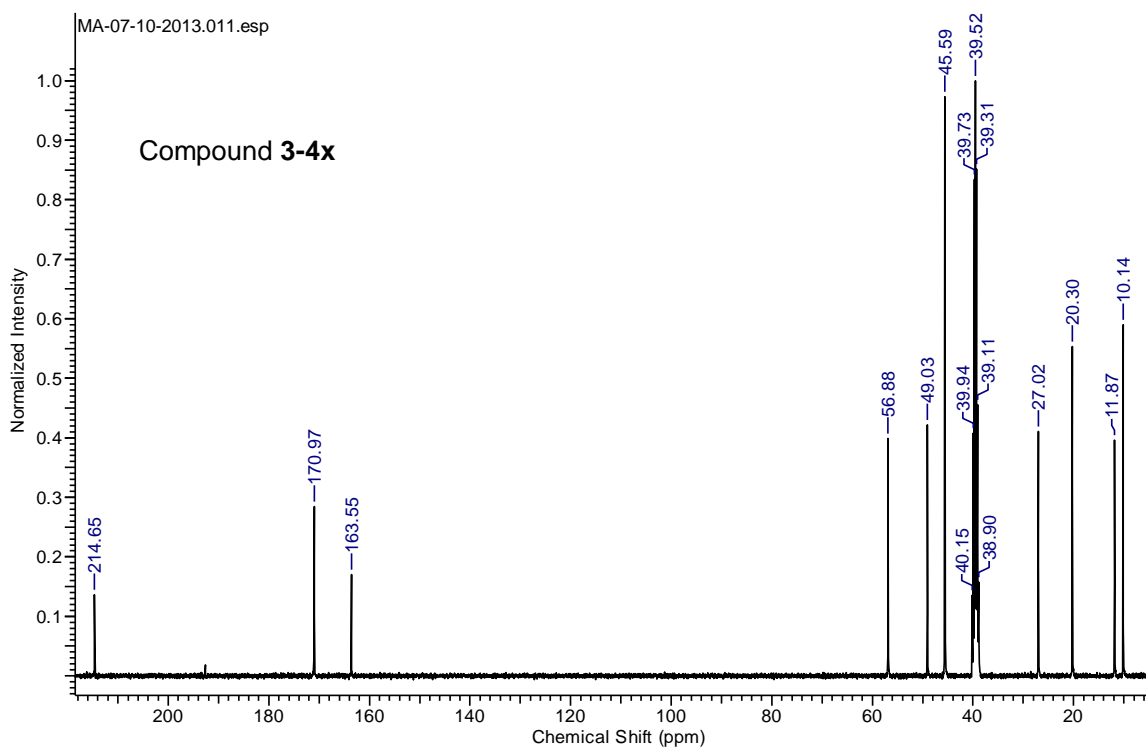
^1H NMR spectrum of compound **3-4a** (400 MHz, $(\text{CD}_3)_2\text{SO}$)



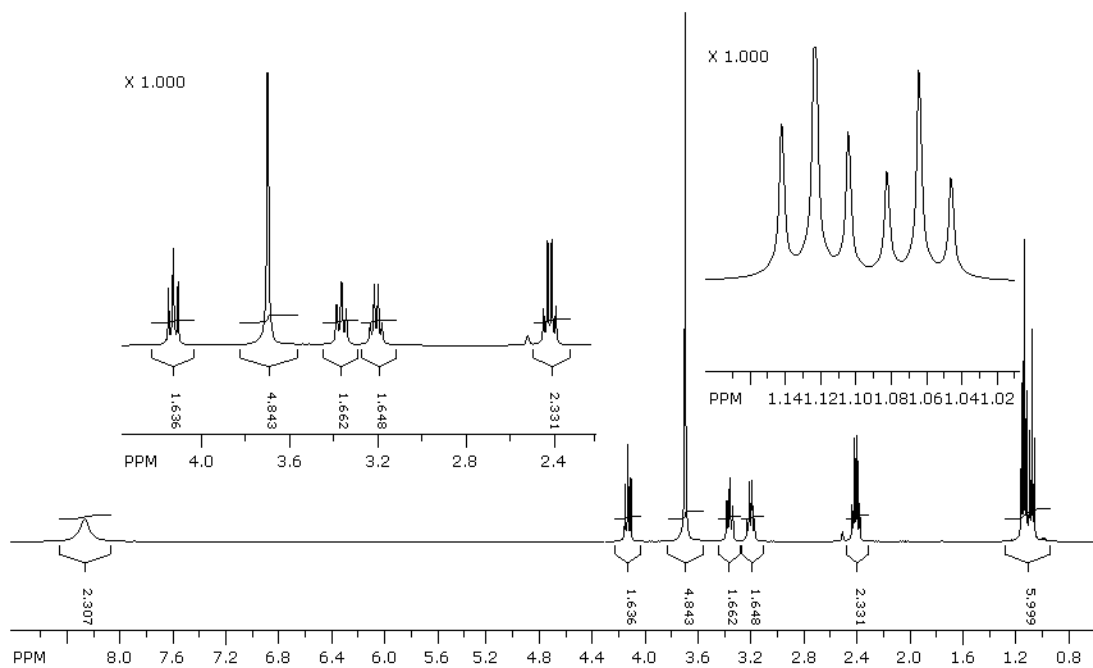
Expanded portion of ^1H NMR spectrum of compound **3-4a** (400 MHz, $(\text{CD}_3)_2\text{SO}$)



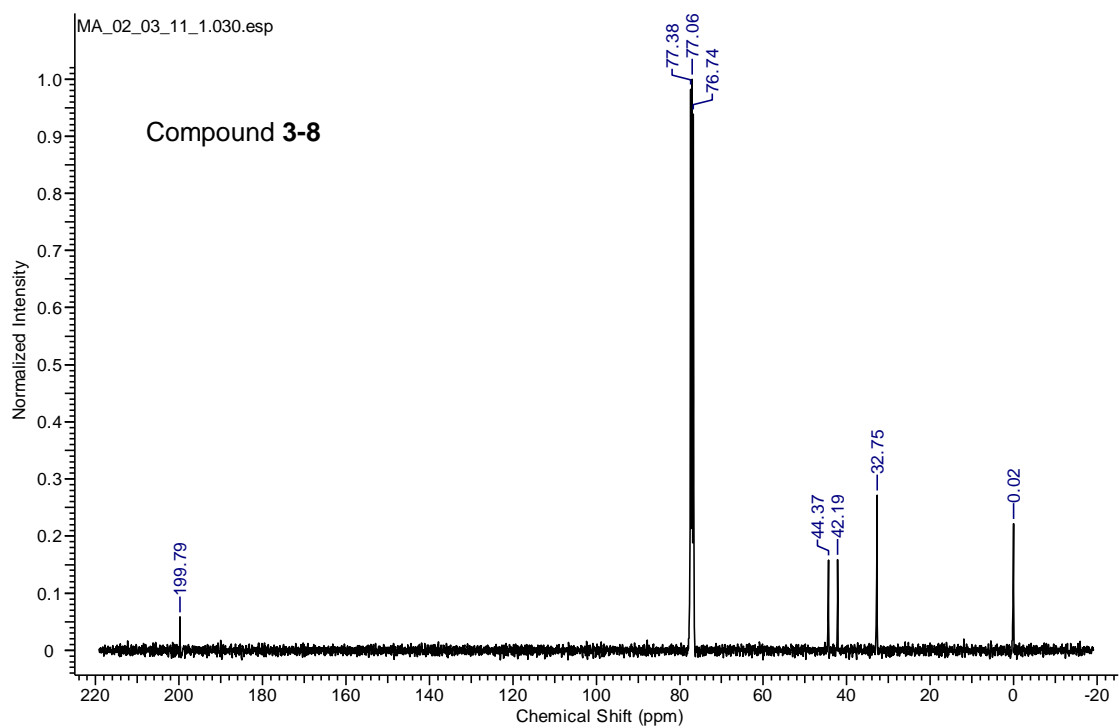
^{13}C { ^1H } NMR spectrum of compound **3-4x** (400 MHz, $(\text{CD}_3)_2\text{SO}$)



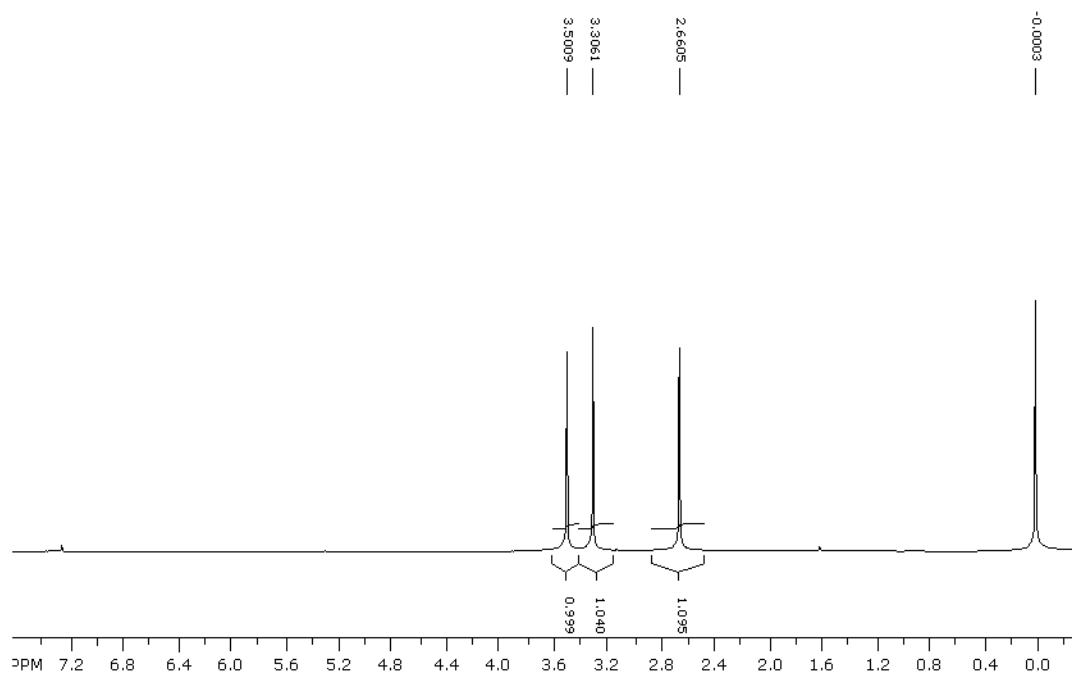
^1H NMR spectrum of compound **3-4x** (400 MHz, $(\text{CD}_3)_2\text{SO}$)



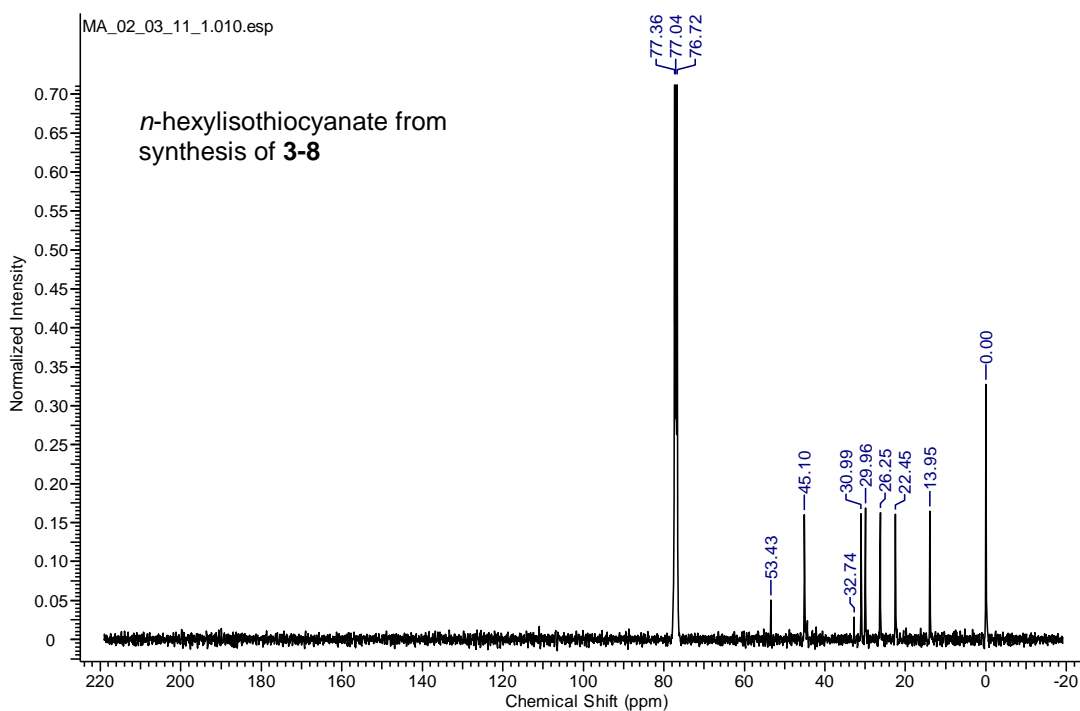
^{13}C $\{^1\text{H}\}$ NMR spectrum of compound **3-8** (400 MHz, CDCl_3)



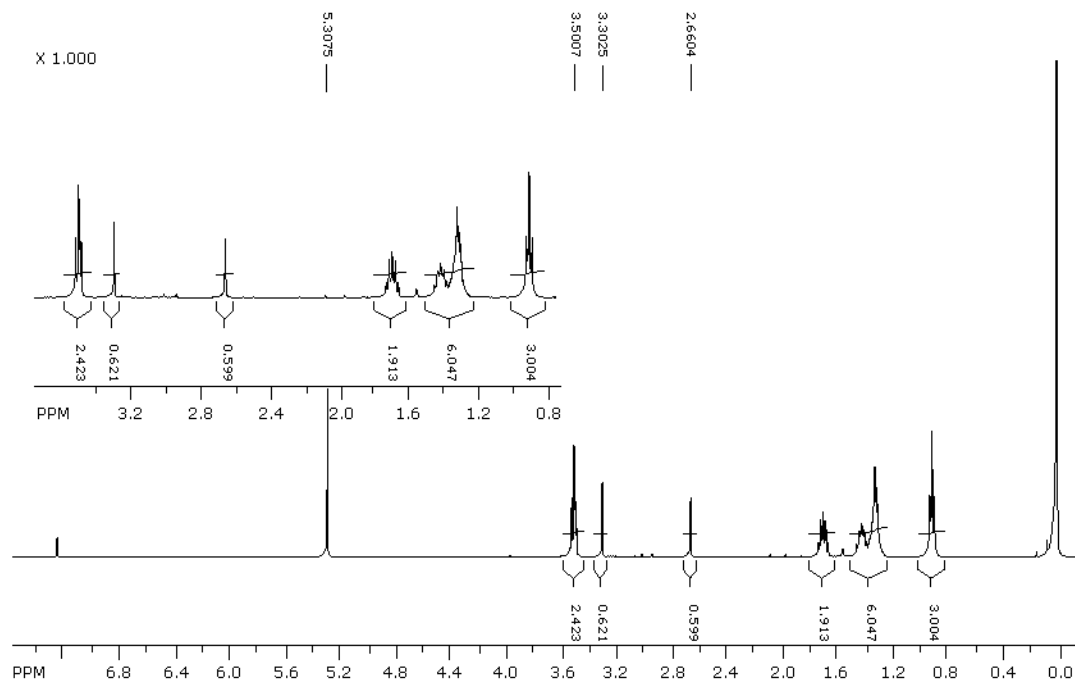
^1H NMR spectrum of compound **3-8** (400 MHz, CDCl_3)



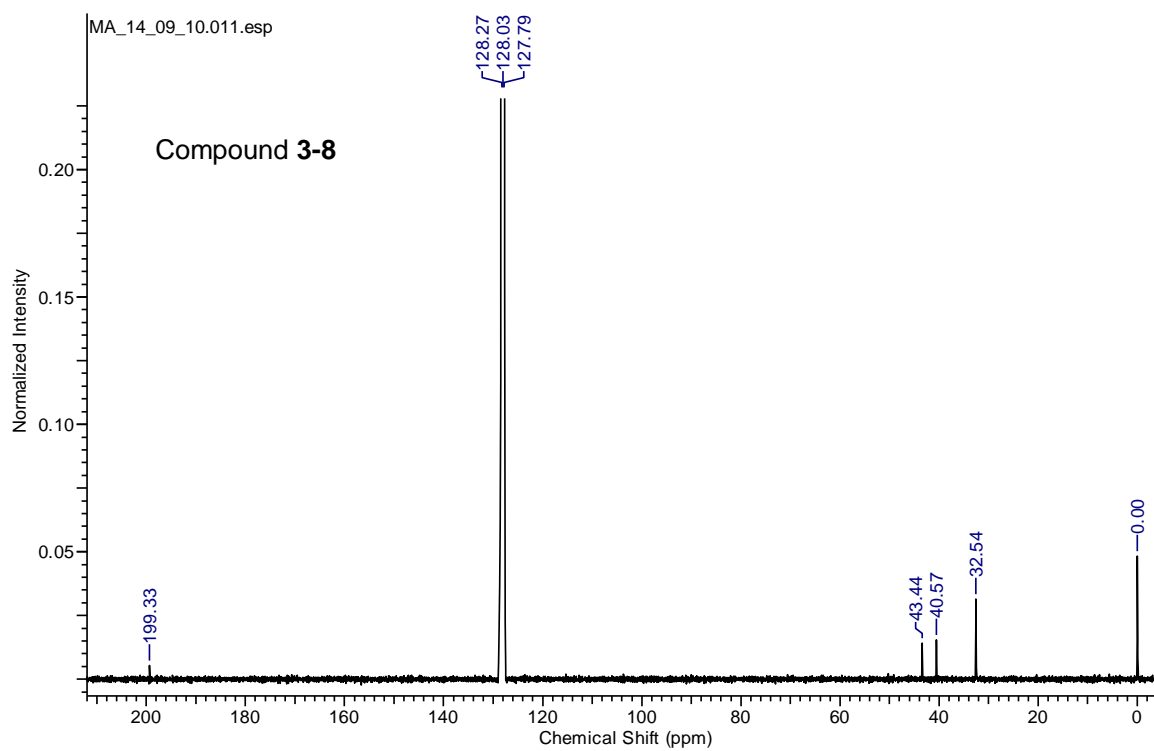
^{13}C $\{^1\text{H}\}$ NMR spectrum of *n*-hexylisothiocyanate from synthesis of **3-8** (400 MHz, CDCl_3)



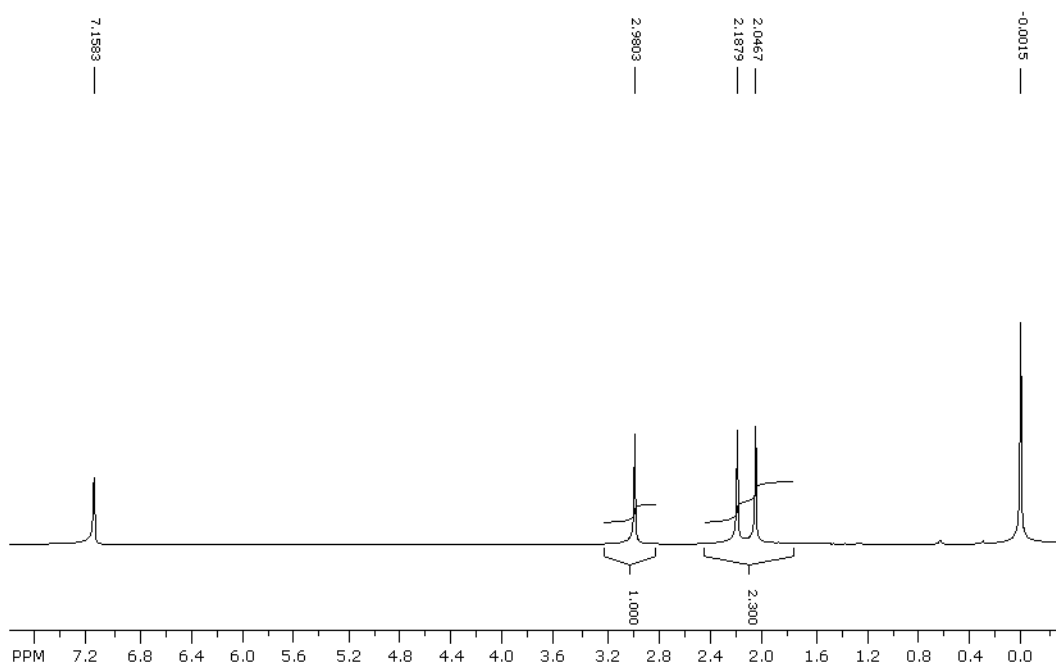
^1H NMR spectrum of *n*-hexylisothiocyanate from synthesis of **3-8** (400 MHz, CDCl_3)



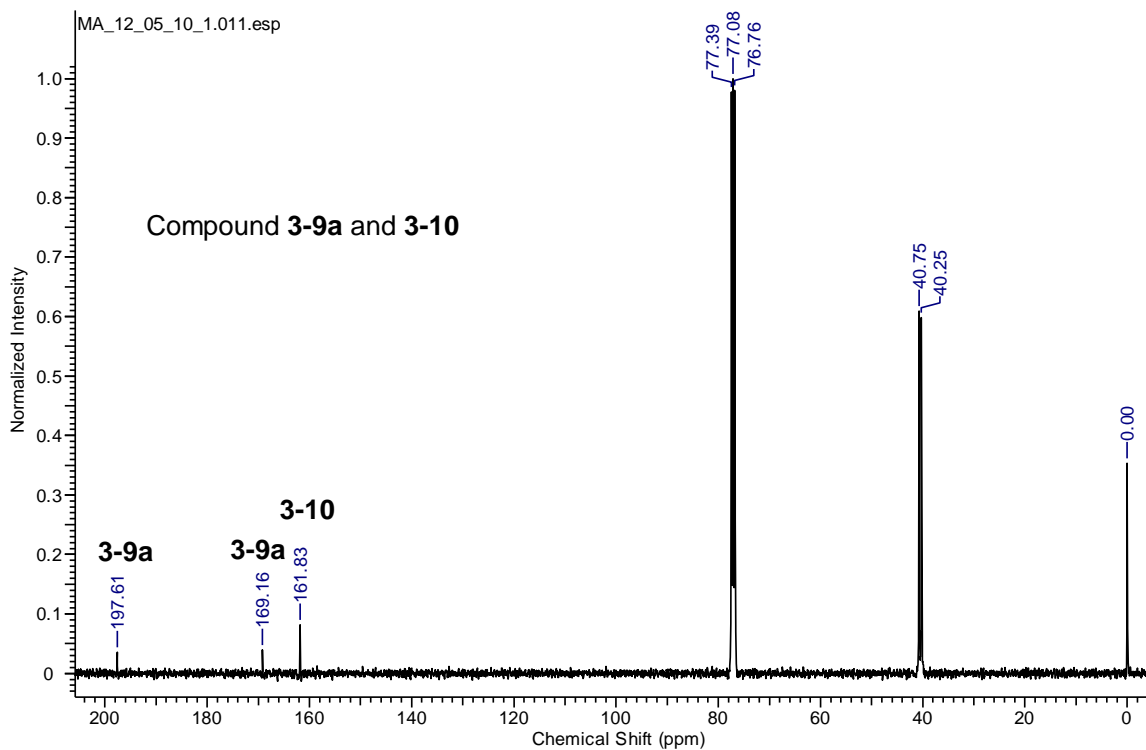
^{13}C { ^1H } NMR spectrum of compound **3-8** (400 MHz, C_6D_6)



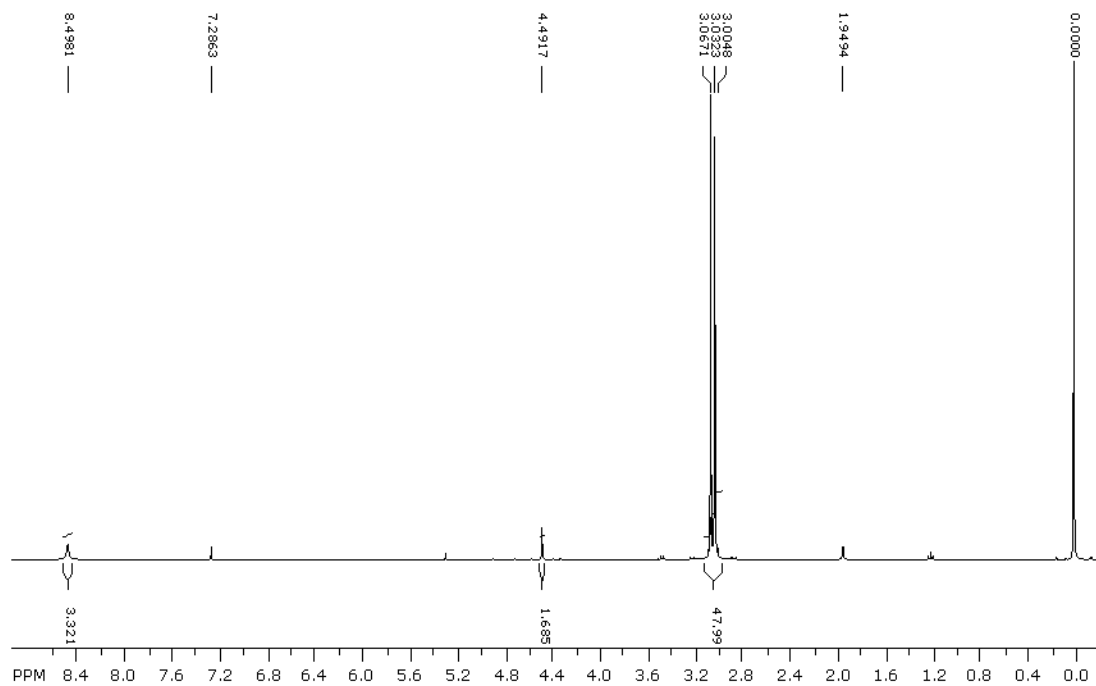
^1H NMR spectrum of compound **3-8** (400 MHz, C_6D_6)



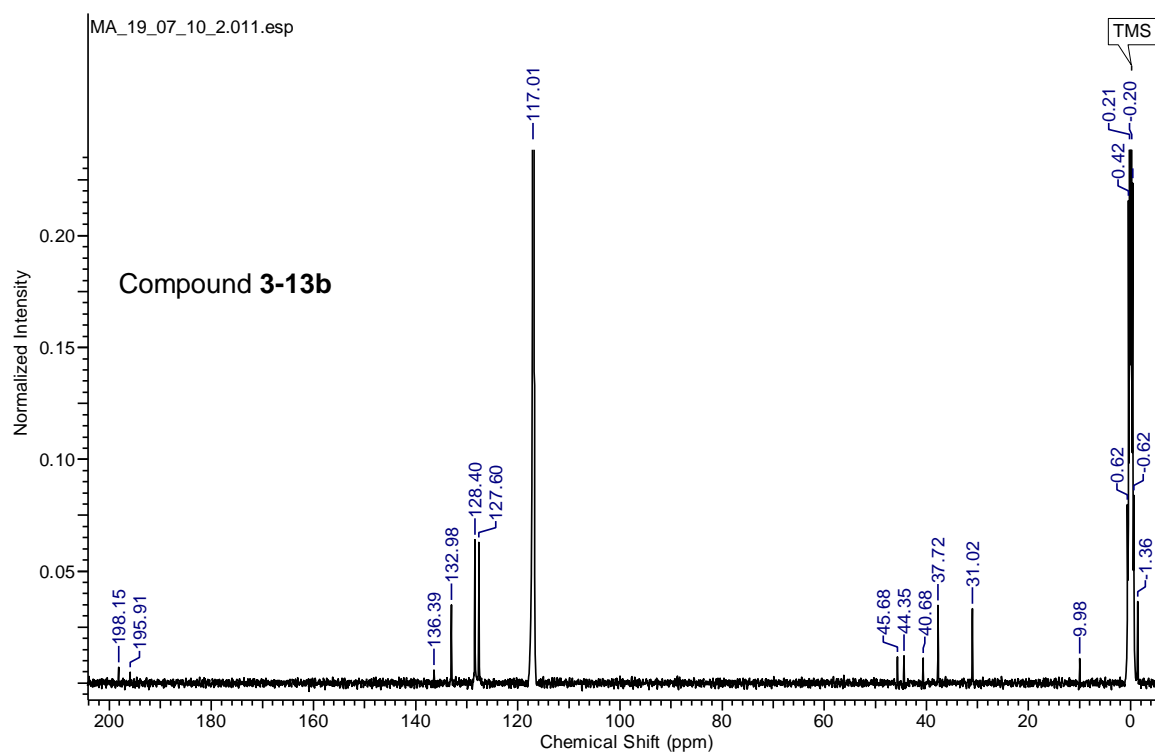
^{13}C $\{^1\text{H}\}$ NMR spectrum of compound **3-9a** and **3-10** (400 MHz, CDCl_3)



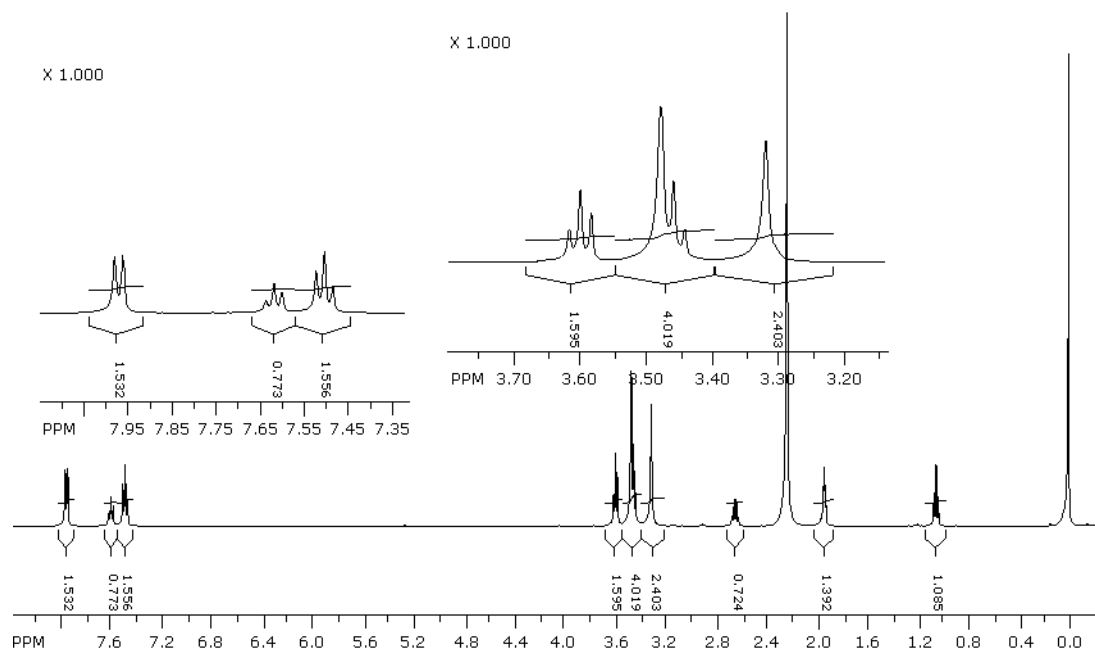
^1H NMR spectrum of compound **3-9a** and **3-10** (400 MHz, CDCl_3)



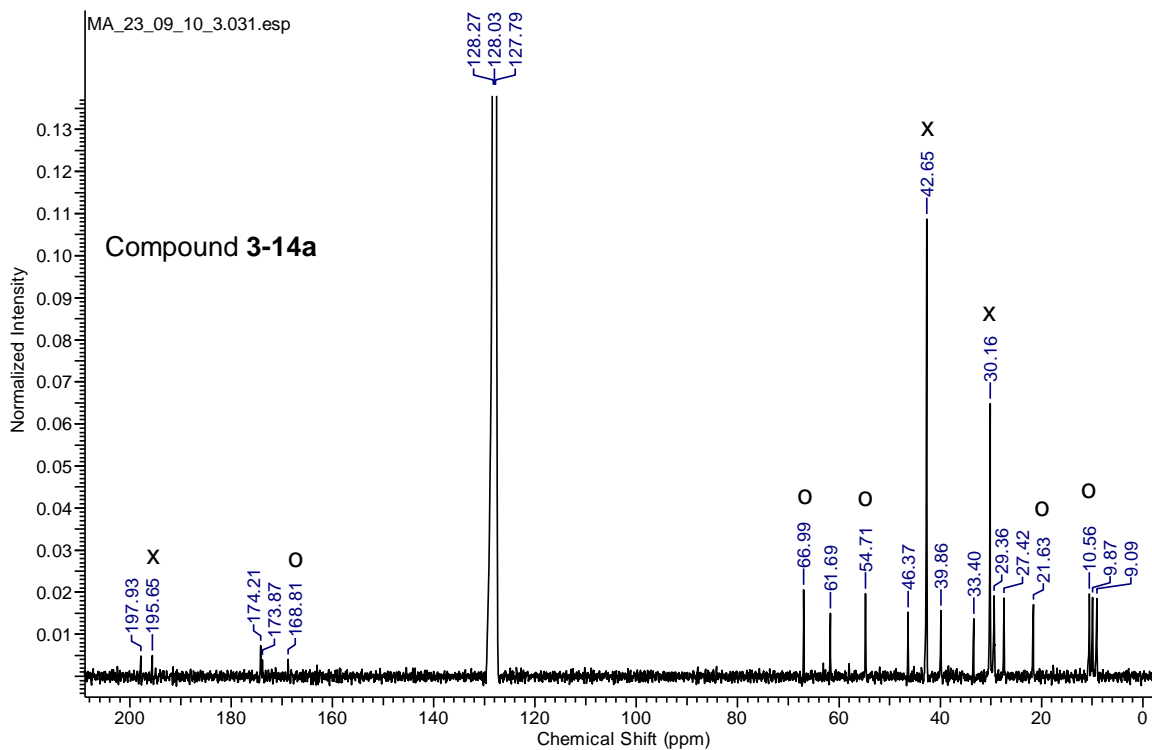
^{13}C $\{^1\text{H}\}$ NMR spectrum of compound **3-13b** (400 MHz, CD_3CN)



^1H NMR spectrum of compound **3-13b** (400 MHz, CD_3CN)

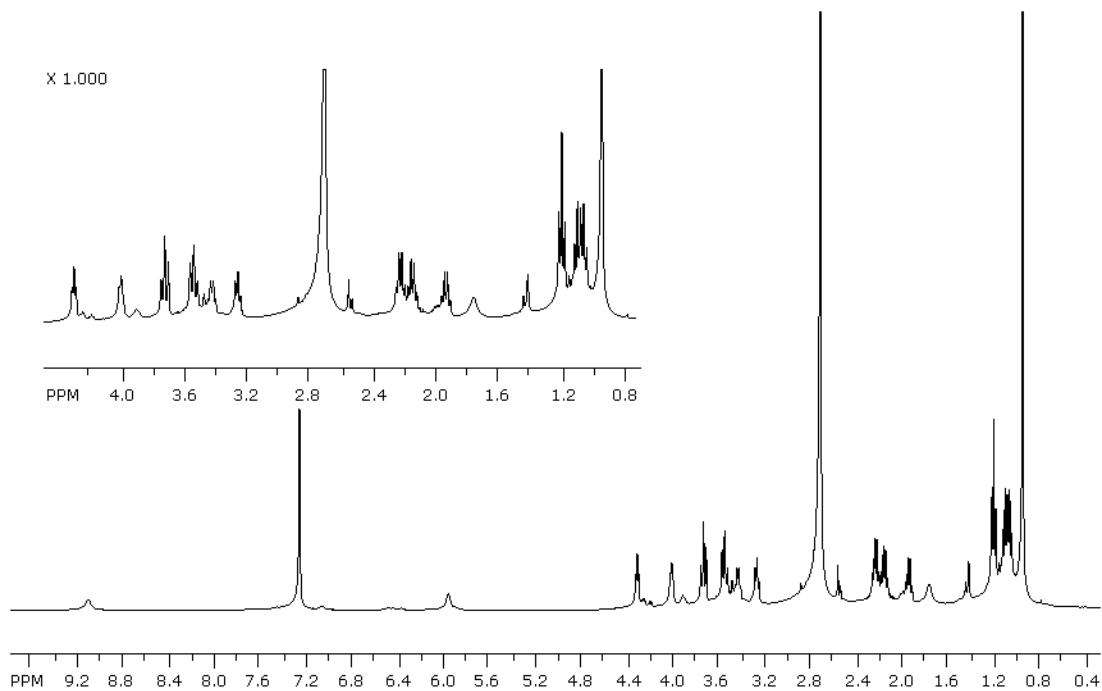


^{13}C $\{^1\text{H}\}$ NMR spectrum of proposed compound **3-14a** crude (400 MHz, C_6D_6)



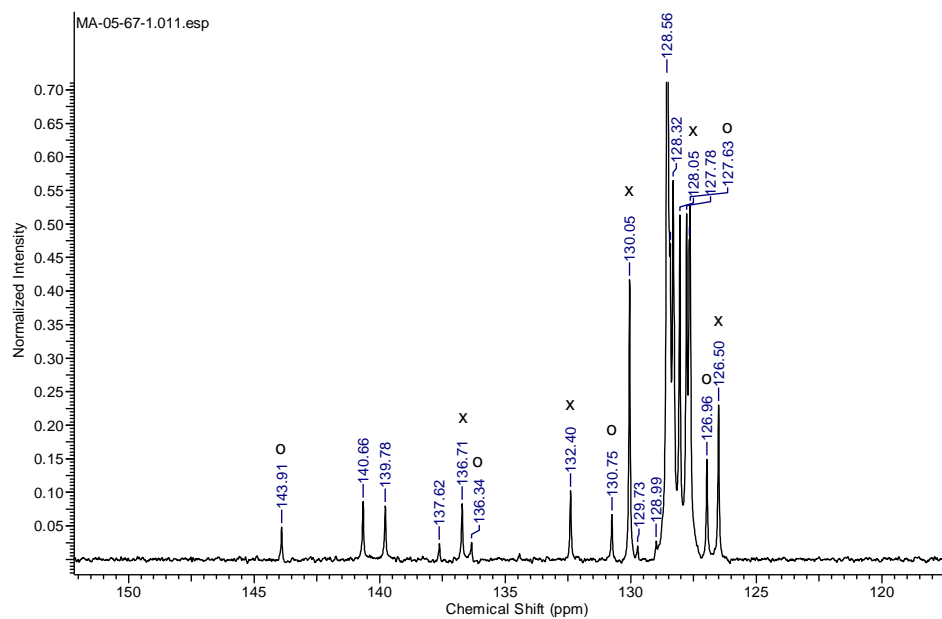
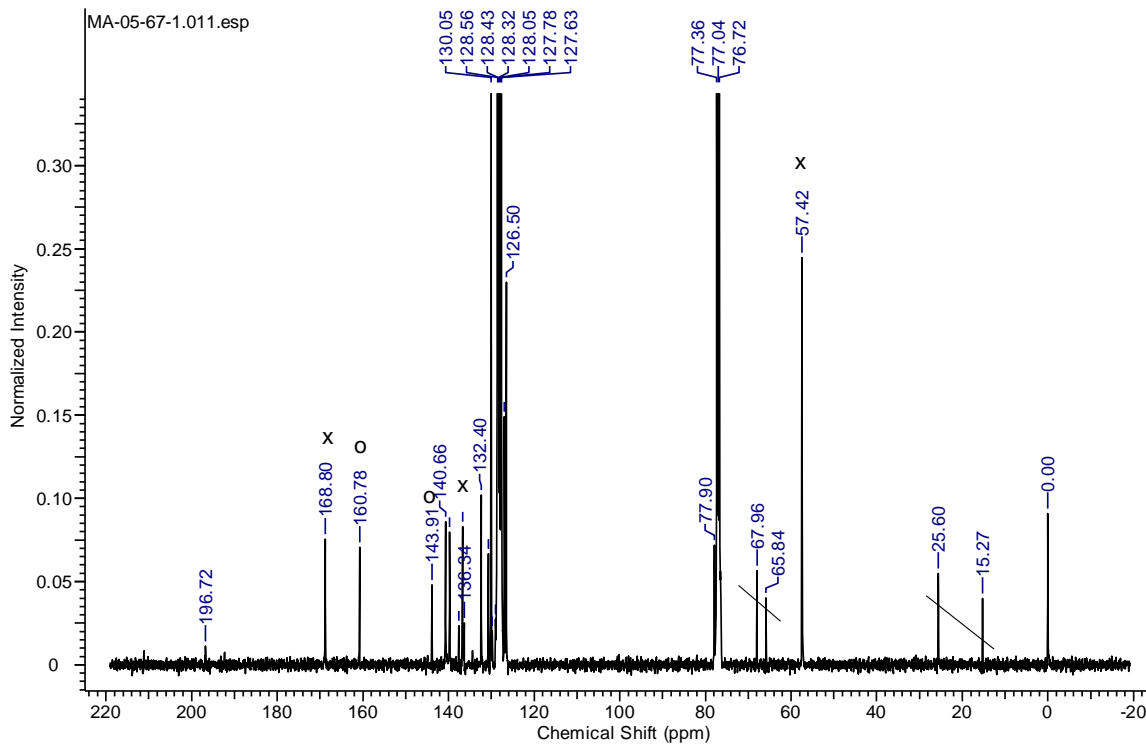
x = tetramethylthiourea, o = 2-ethyl-2-oxazoline **3-14**

^1H NMR spectrum of proposed compound **3-14a** crude (400 MHz, C_6D_6)



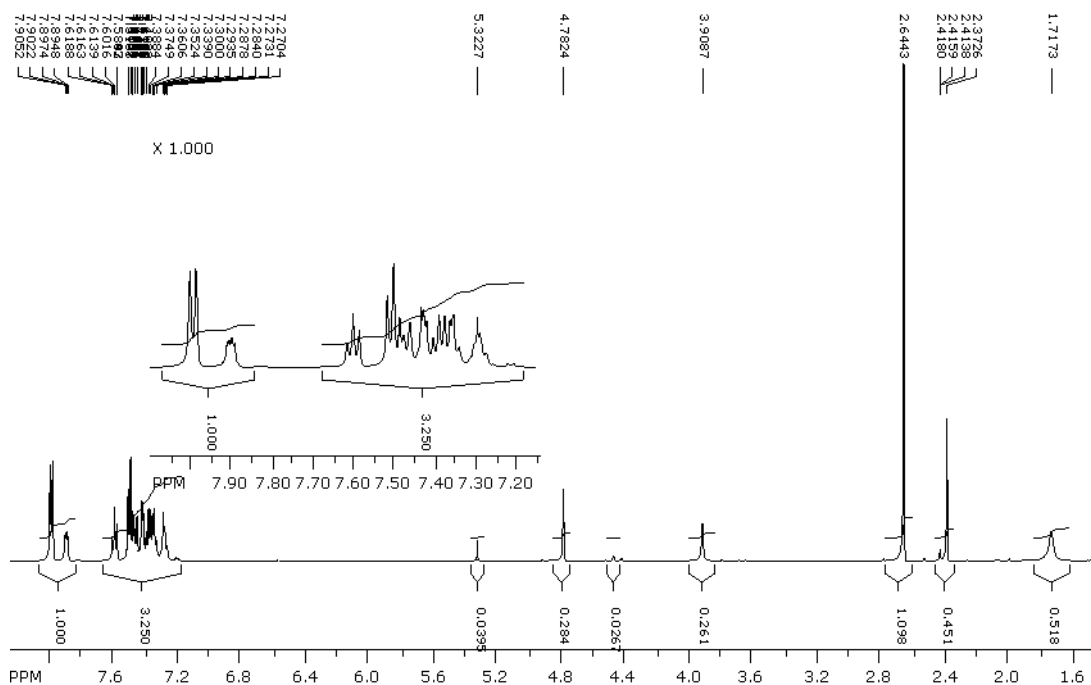
B.3. NMR Spectra of Crude Product Reaction Mixtures for Chapter 4

^{13}C $\{^1\text{H}\}$ NMR spectrum of crude reaction mixture **4-10** and **4-17**, 50 bar CO_2 , and 2 eq DBU in 1 mL of THF (400 MHz, CDCl_3)

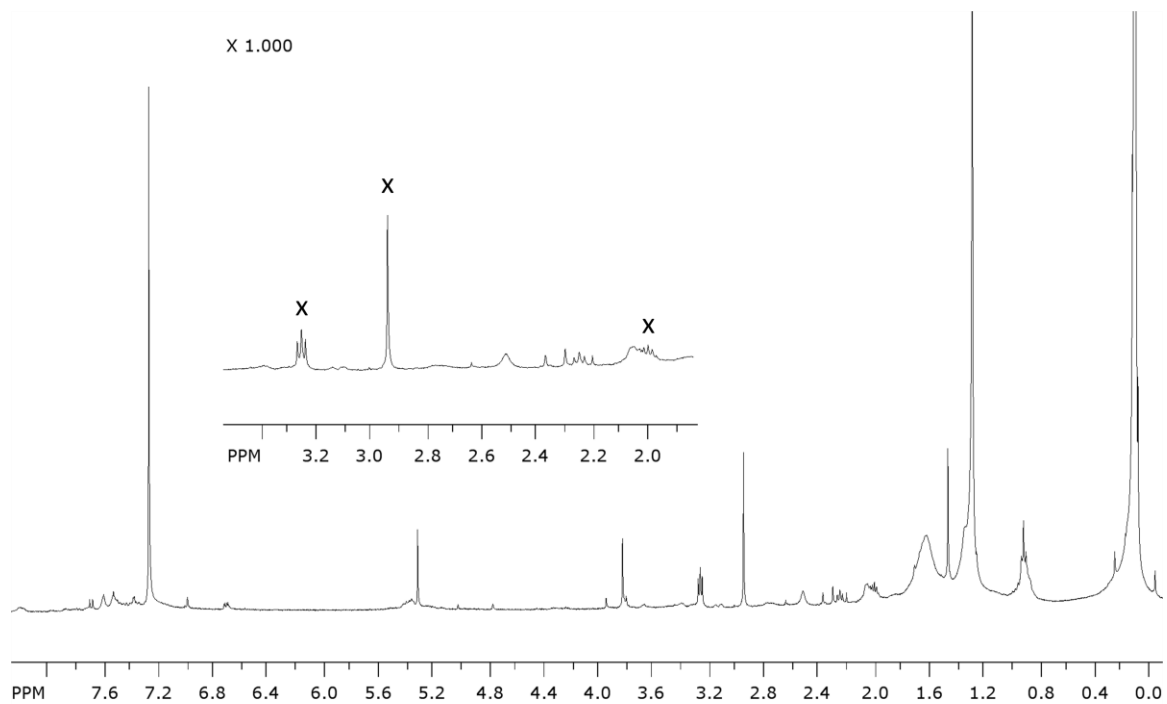


x = compound **4-10**, o = compound **4-17**

^1H NMR spectrum of crude reaction mixture from attempted amidation of benzoylacetic acid, MIBA, and benzylamine, and benzoylacetic acid (500 MHz, CDCl_3)



^1H NMR spectrum (400 MHz, CDCl_3) of crude reaction mixture from formation of cyclic urea with **2-11**, MIBA, 1 atm CO_2 and 4 Å M.S. in THF



x= cyclic urea